

DX 243786

**University Library**



Author/Filing Title ..... KOTZE, J .....

Class Mark ..... T .....

Please note that fines are charged on ALL  
overdue items.

**FOR REFERENCE ONLY**

0403177200







# Tennis Racket Performance Studies and the Design of a Novel Test Machine

by

Johan Kotze

A Doctoral thesis

Submitted in partial fulfillment of the requirements

for award of


Doctor of Philosophy

of

Loughborough University

31 July, 2005

© by J. Kotze, 2005

 <b>Loughborough University</b> Pilkington Library
Date JAN 2006
Class T
Acc No. 0403177200

## Abstract

The investigation was instigated by a growing concern from the International Tennis Federation (ITF) that the contribution of racket technology in the modern game of tennis might be changing the nature of the game by making it too fast. The serve was earmarked as the most critical stroke influencing the speed of the game, resulting in the decision to build a test machine, which would investigate racket performance under realistic serve conditions. In order to determine the design specifications for the machine the following studies were performed.

A thorough study of the current literature on racket performance revealed critical issues which needed to be resolved through testing, resulting in a series of laboratory tests which included measuring rebound characteristics of modern rackets at realistic impact speeds and under different gripping conditions. During the tests, balls were fired with a ball cannon onto a carefully selected set of test rackets, generating data to be used as a benchmark against which to compare the performance of the test machine. Likewise, vibration measurements on the same set of rackets were performed to as a reference for machine performance.

The tests were followed by a series of player tests including the measurement of racket motion profiles during a high-speed serve while simultaneously measuring the ball impact location on the strings. This would establish a realistic motion to be achieved by the test machine and reveal the influence of important racket properties on human performance.

Subsequently, a novel rotational machine was built according to the specifications and found to be an effective tool for investigating racket performance rebound characteristics, with the aim of developing a test standard for limiting racket 'power'.

## Acknowledgements

The research yet again taught me that everything in life is easier with the help and the support of the ones around you. Singling out everyone who contributed in some way to me finishing this research, would need a thesis in itself but I will do my best to do you all justice.

I would like start by thanking God, who once again proved that with his help all things are possible.

During various stages the course of my research I have had the privilege of the most knowledgeable guidance one could ask for: Roy Jones, who was always available for help and encouragement; Sean Mitchell, who provided me with very insightful direction during the research stages and Steve Rothberg, for his extraordinary assistance with the write-up.

Next, I would like to warmly mention all the Wolfson School staff and especially our Sports Technology Research Group, who made a contribution, even if it was just words of encouragement while passing by. A special thanks to Steve Carr and the rest of the staff in the Mechanical and Electrical workshops for helping to build the machine. Also, a great thank you to the Loughborough tennis squad and coach for their great help during the player tests.

Special thanks also to Robert Cottey and Simon Goodwill, for kindly allowing me to use some of their test data for this research, as well as the ITF for sponsoring the work, and all the staff who provided me with constant support.

Last but certainly not the least, a great thank you to all my friends and family, who keep on influencing my life in ways I cannot describe and never stopped encouraging me.

*"... he (God) does not play dice." - Albert Einstein*

# Contents

Certificate of originality .....	i
Abstract.....	ii
Acknowledgements .....	iii
Contents.....	v
Nomenclature .....	x
Introduction .....	1
1.1 History of tennis and tennis rackets .....	1
1.2 The need for a racket power regulation.....	3
1.3 Background study defining the problem .....	5
1.4 Equipment power regulations in other sports .....	7
1.5 Thesis outline.....	8
Modern racket technology .....	11
2.1 Tennis racket regulations .....	11
2.2 The influence of technology on racket performance.....	12
2.2.1 Overview .....	12
2.2.2 Racket materials .....	13
2.2.3 Oversized heads and peripheral weighting .....	16
2.2.4 Head shapes .....	18
2.2.5 Racket mass, balance and swingweight .....	19
2.2.6 Racket stiffness.....	22
2.2.7 Racket length.....	23

2.2.8 String/frame interface.....	24
2.2.9 String technology .....	25
2.3 Sweet spot definitions .....	29
2.3.1 Centre of Percussion (minimum shock) .....	30
2.3.2 Node (minimum vibrations) .....	32
2.3.3 Area of maximum rebound ball speed. ....	33
2.3.4 'Dead spot' (maximum serve speed) .....	33
2.4 Implications for the PDS.....	34
Racket performance indicators .....	36
3.1 Coefficient of restitution (COR) .....	36
3.1.1 Definition.....	36
3.1.2 Representative gripping conditions.....	40
3.1.3 Research related to the COR .....	45
3.2 Alternative performance indicators .....	56
3.2.1 Max ball speed under constant test conditions. ....	56
3.2.2 ACOR with power input.....	57
3.2.3 Kinetic energy definitions .....	57
3.2.4 Babolat RDC power definition .....	57
3.2.5 Mathematical models .....	58
3.3 Influence on further testing and the PDS.....	60
Racket Performance Testing .....	62
4.1 Test set-up and equipment.....	64
4.1.1 Rebound test set-up.....	64
4.1.2 Ball-cannon .....	65
4.1.3 Light-gates.....	66

4.1.4 High-speed camera .....	66
4.2 Ball rebound testing .....	67
4.3 Racket rebound testing .....	72
4.3.1 Freely suspended racket test set-up .....	72
4.3.2 Freely suspended data analysis .....	78
4.3.3 Freely suspended test data .....	82
4.3.4 Handle clamped racket testing .....	88
4.3.5 Head clamped racket testing .....	92
4.3.6 Implications for the PDS and further research .....	94
4.4 Modal analysis .....	96
Player Motion Testing .....	100
5.1 Human motion studies .....	101
5.2 Pilot player testing .....	109
5.3 Extensive player testing .....	117
5.4 Ball impact location .....	132
5.5 Implications for the PDS .....	138
Service simulation machine design .....	141
6.1 Test machines in golf .....	141
6.2 Existing tennis robots .....	145
6.3 Product design specification .....	146
6.3.1 Racket motion replication .....	146
6.3.2 Racket gripping/constraint at impact .....	148
6.3.3 Structural stability .....	149
6.3.4 Ball presentation for impact .....	149
6.3.5 Data capture .....	150



6.3.6	Safety .....	150
6.3.7	Control .....	151
6.4	Machine design .....	152
6.4.1	Concept design method .....	152
6.4.2	Racket motion replication assemblies .....	156
6.4.3	Racket gripping assemblies .....	166
6.4.4	Structural stability .....	167
6.4.5	Ball presentation assembly .....	170
6.4.6	Data capture systems .....	174
6.4.7	Safety systems .....	176
6.4.8	Control systems .....	178
6.5	Summary .....	189
	Machine commissioning and evaluation .....	192
7.1	Ball systems .....	192
7.1.1	Ball timing and consistency .....	192
7.1.2	Ball speed measurement .....	200
7.2	Racket systems .....	203
7.2.1	Racket speed prediction .....	203
7.2.2	Maximum racket speed .....	205
7.2.3	Minimum racket speed .....	206
7.2.4	Control loops .....	206
7.2.5	Influence of the gripping condition .....	209
7.3	Initial racket performance testing .....	212
7.4	Machine modifications .....	219
7.5	Proposed machine improvements .....	220

Conclusions and Recommendations ..... 260

8.1 Ball cannon tests .....260

8.1.1 Racket rebound measurements for modern rackets .....260

8.1.2 Grip compliance.....261

8.2 Player motion tests.....262

8.2.1 Racket head speed .....262

8.2.2 Location of the ICR.....263

8.2.3 Impact location .....264

8.3 Developed machine .....264

8.3.1 Proposed machine alterations .....265

8.4 Proposed machine test protocol .....267

## Nomenclature

$\rho_{cb}$	=	Crossbar density
$\sigma_{cb}$	=	Maximum bending stress in the crossbar
$\sigma'_{cb}$	=	Maximum von Mises stress in the crossbar
$\tau_{cb}$	=	Maximum tensile stress in the crossbar
$\delta_{cb}$	=	Maximum deflection in the crossbar
$\omega_i$	=	Angular frequency for a particular vibration mode
$\omega_{da}$	=	Drive arm angular speed
$A_i$	=	Amplitude constant for a particular vibration mode
$ACOR$	=	Apparent coefficient of restitution
$ACOR'$	=	Apparent coefficient of restitution for moving ball/stationary racket
$ACOR''$	=	Apparent coefficient of restitution for stationary ball/ moving racket
$b$	=	Racket balance point measured from the grip location
$c$	=	Slope constant for a linear regression
$C$	=	Constant indicating the stiffness to weight ratio of the racket beam
$COP$	=	Centre of percussion
$COR$	=	Coefficient of restitution
$CG$	=	Centre of gravity
$d$	=	Distance from the impact location to the CG
$d_i$	=	Crossbar inner diameter
$d_o$	=	Crossbar outer diameter

$E_i$	=	Vibration energy for a particular vibration mode
$E_{cb}$	=	Young's modulus for the crossbar
$f$	=	Subscript describing the freely suspended gripping condition
$f_m$	=	Frequency of the particular vibration mode
$F_d$	=	Deformation force during impact
$F_{rs}$	=	Restoration force during impact
$F_r$	=	Force applied by the racket
$F_{IC}$	=	Force applied by the instantaneous centre unit
$F_{cb}$	=	Force applied by the crossbar
$F_{da}$	=	Force applied by the drive arm
$F_{cb}$	=	Force in machine crossbar
$g$	=	gravitational acceleration
$G_r$	=	Vibration mode shape constant
$GC$	=	Geometric face centre
$gc$	=	Subscript describing the grip clamped gripping condition
$gp$	=	Subscript describing the grip pivoted gripping condition
$h$	=	Predicted distance travelled from the location laser
$hc$	=	Subscript describing the head clamped gripping condition
$hs$	=	Racket head size
$h_r$	=	Ball rebound height during drop test
$h_c$	=	Ball drop height during drop test
$h'$	=	Calibration drop distance
$ICR$	=	Instantaneous centre of rotation
$I_{cg}$	=	Racket inertia about centre of gravity

$I_{sw}$	=	Swingweight
$k_l$	=	Constant representing player strength for a linear regression
$k_p$	=	Constant representing player strength in a power regression
$K.E.$	=	Kinetic energy
$\Delta K.E.$	=	Change in kinetic energy
$l_{da}$	=	Drive arm length
$l_{cb}$	=	Crossbar length
$L$	=	Beam length
$li$	=	Racket length indicator
$m_b$	=	Ball mass
$m_{cb}$	=	Crossbar mass
$M_{cb}$	=	Maximum moment in the crossbar
$M_{ds}$	=	Maximum moment in the drive shaft
$MOI$	=	Moment of inertia (general reference)
$m_r$	=	Racket mass
$n$	=	Power constant for a power regression
$RDC$	=	Racket Diagnostic Centre
$ps$	=	Subscript describing the player simulated gripping condition
$ph$	=	Subscript describing the player or hand held gripping condition
$RA$	=	Frame flexibility for a strung racket
$s$	=	Distance for the location of the COP to the CG
$S_{head}$	=	Racket head length
$S_{clear}$	=	Dropper clear height above racket tip
$t$	=	Contact time

$t_0$	=	Deformation time
$t_1$	=	Time measured from the ball drop to the calibration laser
$t_2$	=	Time measured from the calibration laser to the location laser
$t_3$	=	Time measured between two ball speed lasers after impact
$t_4$	=	Time measured from the location laser to the predicted impact
$t_{imp}'$	=	Calibration drop time
$t_{rev}$	=	Duration of a machine rotation at the maximum impact speed
$u_b$	=	Ball inbound (impact) velocity
$u_r$	=	Racket inbound (impact) velocity
$v_b$	=	Ball rebound velocity
$v_r$	=	Racket recoil velocity
$W_{cb}$	=	Distributed load applied to the crossbar

# Chapter 1

## Introduction

### 1.1 History of tennis and tennis rackets

According to records dating back as far as the 12<sup>th</sup> century in France, tennis was first played with the palm of the bare hand. Hence the French name for the game 'le jeu de paume', meaning 'the game of the palm'. There are different theories as to where the more modern name, 'tennis' was derived and up to 1870 the game was played very differently from its modern version. It was played indoors on a hard surface with walls, much like 'real tennis', a game currently only played in a few locations around the world. After 1870 the game developed into 'lawn tennis', which was played on grass, without walls and later into the game we now know as 'tennis', played on different surfaces all around the world. It is interesting to note that originally the first stroke of the game was never intended to win the point. In fact, the ball was set in motion by a servant and not the players (who were mostly royals in the early days), hence it being called the 'service' (Clerici 1976, Robertson 1974).

Replacing the palm were various gloves, bats and paddles, until the first wooden construction with strings was introduced in the 16<sup>th</sup> century. Initially these rackets had fairly short handles, more representative of racquetball rackets today. Strings were made of natural gut, often tied or wrapped around crossing strings. Over time, racket handles gradually became longer, while head sizes remained more or less the same.

## CHAPTER 1 INTRODUCTION

Up to the mid 1900's, wood remained the dominant racket material, with the main experimentation being different kinds of woods and later the combination of different layers. With the ever-increasing development of new materials, layers of wood were also later combined with various natural and synthetic materials. Combining improved manufacturing techniques with skilled craftsmanship produced elegant rackets with stronger frames less prone to warping.

In the meantime, manufacturers were also experimenting with various metals; initially steel and later predominantly aluminium. Metals provided an easy solution to the weak throat area, which was critical in wooden rackets. It also allowed for hollow profiles, with especially aluminium resulting in lighter and much stiffer frames, ultimately revolutionising the designs forever in the 1970's. The stronger frame allowed for the development of much larger head sizes, increasing the power, the size of the sweet spot and the rotational stability of the rackets. This was also the time of the 'tennis boom', with inventors giving free reign to their imaginations. A major factor for recreational players was that these new rackets did not warp.

Not long after, composite materials were introduced, reducing weight and increasing stiffness even more, especially with the development of wide-body frames. Experimentation with various fibres eventually led to frames consisting mainly of carbon and glass fibre layers cured in an optimum resin. Optimum location of fibres combined with fine-tuned manufacturing processes now produce rackets with almost half the weight and double the stiffness of their wooden ancestors produced only 20 years previously (Kuebler 2000, Robertson 1974).

It is obvious to see that racket technology has changed over the last century into something significantly different from its predecessors and it is feared by many that this radical change in design is responsible for a significant increase in racket performance. Even more so, it is believed the influence of



## CHAPTER 1 INTRODUCTION

future technologies might change the nature of the game forever and lead to a damaging decrease in popularity. On the other hand, considering the ancient and traditional nature of the sport, one can also comprehend the anxiety of others towards any rule changes as well as the political issues involved, which had a considerable impact on the research.

### 1.2 The need for a racket power regulation

The research presented in this thesis formed part of a project prompted by the International Tennis Federation (ITF) in the light of their concern for the dominance of speed and power in the current men's game. This research resulted in a number of refereed publications; Kotze *et al.* (2000), Haake *et al.* (2000), Kotze & Mitchell (2002).

Like other sports governing bodies, the ITF's main purpose is to protect the long-term interests as well as the basic nature of its sport. During the time preceding the project there were growing concerns by the ITF and other interested parties that the men's game was getting too fast, which could result in a decline in the sport's popularity. Research was performed to substantiate these claims and areas were earmarked for possible regulation. Possible solutions proposed by researchers (Brody 1996a, 1996b, 1997) at the time included:

- Tightening restrictions on racket specifications
- Allowing professionals to only play with wooden rackets
- Shortening the service box
- Change court dimensions – serve from far behind the baseline
- Abandon the second serve
- Eliminate grass court tournaments

## CHAPTER 1 INTRODUCTION

- Use larger or lighter balls
- Make the ball deader

The two main solutions chosen by them were using larger balls and regulating the racket technology, which resulted in two areas of research.

The research related to the larger ball was aimed at determining its influence on player performance and fatigue (Bowyer, 2002). Controlled match-play tests were performed with both a standard size ball and a 6% larger diameter ball. Results indicated longer rallies played per point, less dominance of the serve and fewer return errors with the larger ball but no significant difference in muscle soreness or grip strength. This positive outcome resulted in the implementation of a new rule, proposing different types of balls to be used on different court surfaces for a two year trial period.

In parallel, the research described in this thesis was initiated, which was concerned with the contribution of modern racket technology on the speed of the game, with the ultimate goal of implementation of a new regulation. This decision was influenced to a large extent by a general trend from other sports governing bodies to use realistic dynamic tests for equipment regulation. Consequently the thesis aspires to answer the following research question; *Can a tennis serve simulation machine be developed that adequately and repeatably mimics human performance in order to investigate, define and enforce an upper limit on the racket's contribution to high serve speeds?*

The research method adopted for achieving this goal included:

- Reviewing the literature
- Lab tests on rackets
- Human player tests
- Machine design and manufacture
- Machine calibration and testing

## *CHAPTER 1 INTRODUCTION*

### **1.3 Background study defining the problem**

The increasing apprehension regarding the speed of the game of tennis prompted the ITF to launch an investigation in 1997 to estimate the magnitude of the problem. Results of the investigation were presented by Coe (2000), the head of the ITF's technical committee.

According to Coe, research based on global sales figures from manufacturers indicated a worldwide decline in recreational participation since 1990, especially in mature tennis playing nations such as Germany, France, the U.S., Japan and Spain. After interviewing over 3500 tennis playing households in 13 countries, 49% agreed with the statement that the men's professional game was too fast, while 32% disagreed. Players from countries playing predominantly on clay were more likely to disagree with the statement, since the game is much slower on clay than grass. Various comments from professionals and experts are quoted, with most agreeing that the professional men's game has become a game of power and speed and is probably getting too fast and boring. Alarming statistics are listed, such as those from the 1994 Wimbledon final between Sampras and Ivanisevic, where, of the 206 points played, only three lasted more than four shots. Fred Perry called it "... one of the most boring finals in history." The conclusion can be drawn that spectators would like to see games with longer rallies, as in previous years.

The serve is the fastest and most controlled stroke in the game, initiating each point and, therefore, having the greatest potential to influence the outcome, resulting in shorter rallies. Subsequently, priority was given to the serve by the ITF for further investigations.

In an attempt to substantiate claims with evidence based on game statistics, Coe assumed the number of tie-breaks in a match provided a fair indication of the influence of a player's serve. If both players have a very strong serve, they would both tend to hold serve, making it likely for the set to end in a

## CHAPTER 1 INTRODUCTION

tiebreak. Hence, tiebreak data from all the Grand Slams for the Open period (1968-1998) were analysed, indicating a definite increase in the influence of the serve, with the smallest change being on grass, which has always been faster with more tie breaks. The research also compares a number of individual players' tiebreak data with serve speed, revealing most of the fastest servers also have the highest tie-break percentages.

A further investigation into service speed trends reveals that in 1990 (when serve speeds were recorded for the first time) only five players on the professional men's game were recorded to serve over 200kph, whereas in 2000, the majority of the top 200 players on the Association for Tennis Professionals (ATP) tour are believed to be capable of doing it. At the time the research was proposed the fastest serve was 239.7kph ( $66.6\text{m.s}^{-1}$ ), achieved by Rusedski in 1998.

Ball-cannon tests were also performed on a wide range of old and new rackets comparing their rebound characteristics. Using the ratio of the outbound velocity to the inbound velocity (the apparent coefficient of restitution or ACOR) as an indication of power, the results were used to estimate the influence of new technology on racket power. For an average groundstroke, at  $25\text{m.s}^{-1}$ , the average racket in 2000 was estimated to have a 28.5% higher ACOR than a typical racket 20 years older and, for a serve at  $40\text{m.s}^{-1}$ , the increase in ACOR is estimated at 18.2%. These "ballpark" figures were used by the ITF to justify their consideration of racket capabilities in relation to the perceived undesirable service speed increase.

Coe further postulated that current rackets decrease the available reaction time by more than 30%, which was substantiated in later tests performed by Haake *et al.* (2000a, 2000b). These tests revealed that with an increase in serve speed, receivers reach a threshold where it is impossible to return the serve. For the players tested (university team players) the limit was at approximately 160

## CHAPTER 1 INTRODUCTION

kph, which is considerably lower than the 200 kph capability of the ATP players.

Coe concluded that the modern men's game has reached a point where the serve is becoming too dominant, resulting in shorter rallies and more tie-breaks. Matches on grass courts have been compared to a 'shoot-out' and spectators often find this serving contest boring and lose interest. This might lead to sponsors withdrawing support, reduced prize money and ultimately a decrease in popularity of the sport amongst both players and spectators. Coe's views were echoed later by Miller (2003), the new technical director of the ITF, and Haake (2000), who both described the ITF's role as investigating equipment in order to fully understand its effect on the game. Miller further cautions that the long-term effects of any rule changes should be carefully discussed with all interested parties before implementation.

Whilst it is realised that there are many other factors influencing the speed of the game, the research presented here has focussed on investigating the contribution of racket power. The full capacity of the most powerful rackets has yet to be experienced because most of the top players usually opt for a less powerful racket with more control. This is partly because they are used to playing with the older rackets and because current designs still provide a trade-off between control and power, in which case professionals opt for more control. For the next generation of rackets and players this might not be the case, making the problem more acute.

### 1.4 Equipment power regulations in other sports

Tennis is not the only sport implementing regulations limiting sports equipment, in particular power. In fact tennis rules have been very lenient, hence the current apprehension towards restrictions. Classic examples of similar regulations limiting equipment power in other sports are the banning of

## CHAPTER 1 INTRODUCTION

aluminium baseball and cricket bats in the 1970's. The bats have always been banned from the American professional league but were made legal in the American college league, where their superior power caused a great danger to fielders, eventually leading to restrictions in the rules. The aluminium bat in cricket, introduced by Lilley, was banned after one match (Elliot, 1982). A more recent example was the introduction of rules by the golf regulatory bodies, specifying maximum driving distances for balls and maximum ACOR for driver heads. The tests are performed by a robot, the 'Iron Byron', consistently hitting balls under specific test conditions by realistically mimicking the human golf swing. The objective of the rule was to protect current course records from becoming obsolete (May 2000, Kramer 1999).

It is not surprising then that, in tennis, the regulating bodies are considering a similar course of action. Consequently this investigation was initiated aiming to develop a tool, for testing the influence of various racket properties on racket power and possibly as a regulation method. The main aim of the thesis is to answer the research question posed through this investigation.

### 1.5 Thesis outline

*INTRODUCTION:* The thesis has started with a short history of the game of tennis, highlighting some of the main breakthroughs leading to an increasing racket performance over the years. The combined increase from the different technologies was believed to have given excessive influence to the importance of the ball speed and the serve in the modern game, hence calling for the need for a new regulation to limit racket 'power'. Spurred by similar regulations introduced by other sports for related reasons the development of a test machine to investigate and implement such a regulations was proposed.

*MODERN RACKET TECHNOLOGY:* Elaborating on the foregoing chapter, a thorough investigation of the available literature related to racket

## CHAPTER 1 INTRODUCTION

performance is presented to establish up-to-date knowledge on the subject and determine area for further investigation. The chapter concludes with a summary of the 'sweet spot' definitions, which form the important link between a racket's on-court performance and laboratory measurements.

*RACKET PERFORMANCE DEFINITIONS:* In this chapter the common definitions used in the literature to describe a racket's performance are presented in order to define the measurements needed for developing a test machine.

*RACKET PERFORMANCE TESTING:* In order to determine the fundamental design parameters of the test machine, basic racket performance tests were performed in the laboratory on a wide range of modern rackets, which also assisted in developing an unbiased understanding of the results from the literature.

*TENNIS SERVE PLAYER MOTION TESTING:* The remaining machine parameters related to player performance were determined through player tests. During these tests, stroke characteristics of skilled players were recorded and analysed in order to determine characteristics of a realistic serve motion to be mimicked by the developed machine.

*SERVICE SIMULATION MACHINE DESIGN:* Combining the foregoing knowledge gained, an adaptive research machine is developed. The machine incorporated the desired balance between functionality, realistic presentation, complexity and adaptability to allow for it to be used as both a research tool and a test standard.

*MACHINE EVALUATION:* In order to validate the use of the machine as an adequate test device, critical components were subjected to consistency tests. Results of these tests are presented and evaluated against the machine's product design specifications and other acceptable standards.

## *CHAPTER 1 INTRODUCTION*

*CONCLUSIONS AND RECOMMENDATIONS:* The thesis is concluded with a summary of the results and deductions drawn from them, followed by recommendations for further work needed to investigate and implement a sensible racket power standard.



## Chapter 2

### Modern racket technology

Tennis is a relatively old sport, with a huge volume of literature produced over the years, but since sport was traditionally more a subject of leisure than technology, technical information is scattered between numerous diverse publications. Very few attempts have been made to consolidate this information and especially to resolve the conflicting reports.

#### 2.1 Tennis racket regulations

The first known rules for the game date back as far as 1592 and for centuries after that rules on the tennis racket were very lenient, allowing the racket to be of almost any material, shape, size or mass. It was only with the introduction of oversize rackets in the 1970's that tennis officials became concerned about racket designs, resulting in the ITF's limit on the size of the racket head in 1980. Soon after, the 'Spaghetti' racket, designed with a double string layer, caused major upsets in large tournaments by allowing the player to impart far more spin to the ball than before. This innovation threatened to drastically change the nature of the game, so it was banned soon after. Ever since, rules on the design of the racket have become more stringent with a trend towards more realistic dynamic tests rather than traditional static tests (Robertson 1974, Arthur 1992, Brody 1995, May 2000, Goodwill and Haake 2002b).

## CHAPTER 2 MODERN RACKET TECHNOLOGY

The current ITF regulations on rackets specify that it should be characterised by (ITF 2004):

- A flat hitting surface consisting of a uniform pattern of crossed strings. Strings must be free from attached objects.
- Dimensions not exceeding:  
736.6mm in length and 327.5mm in width for the frame and  
393.7mm in length and 292.1mm in width for the string surface.
- The frame should be free of any objects not reducing wear and tear or vibration.
- The frame should be free of any device that will allow it to change the shape of the racket or the swing weight of the racket during the playing of a point.
- Should not make use of external energy sources to change, or affect playing characteristics.

## 2.2 The influence of technology on racket performance

### 2.2.1 Overview

To provide a perspective on the extent of modern technology and its influence on racket power, an overview of current and recent technology developments is presented in this section.

As mentioned before, most rackets currently on the market consist mainly of lightweight carbon fibre composites. The high stiffness-to-weight ratio, in conjunction with improved manufacturing processes, enables manufacturers to incorporate more effective racket designs with better control, power and vibration characteristics.

## *CHAPTER 2 MODERN RACKET TECHNOLOGY*

These are mostly achieved by a combination of the characteristics discussed in the following subsections:

- Racket materials
- Oversized heads and peripheral weighting
- Racket mass and balance
- Racket stiffness
- Racket length
- String/frame interface
- String technology

### **2.2.2 Racket materials**

A review of racket history soon reveals some interesting and radical designs of which very few are still incorporated in current models; most changes with a lasting effect have been a result of improvements in materials. Since power has always been one of the most desired racket characteristics, materials which promote this factor have been the main contributor to its increase. This can usually be attributed to the higher strength-to-weight ratios of the newer materials. These materials have also made larger head sizes and optimal frame and head profiles possible. The direct influence of these properties on racket power is described in the subsequent sections. When considering the influence of racket power on tennis, one is mainly concerned with the changes occurring during the modern era of the game during which rackets have changed from wood or metals to advanced composites.

For most of the 1900's, rackets were made of wood, with different types and combinations dominating changes. At first, the frames were made from a single solid piece of ash wood, which was soaked in cold water and then boiled

## *CHAPTER 2 MODERN RACKET TECHNOLOGY*

to make it pliable and bent into the desired shape while still hot. These rackets were very heavy, by today's standards, with small head sizes.

Initially wooden rackets were very weak in the throat but failures were reduced by wrapping canvas, vellum and bindings around the critical areas. Another problem was warping of the frame when exposed to wet conditions. Consequently hickory, as well as strips of metal reinforcement in the racket throat, were introduced. The next advance was in the 1930's, with the development of laminated frames consisting of an arrangement of the layers at different angles, achieving 'directional stiffness'. Synthetic cements and formaldehyde were used to bond the layered frames. The introduction of a single leather laminate between two layers of wood allowed more geometric freedom and increased strength but was soon replaced in the 1960's with Black Walnut, Vulcan fibre (a resin impregnated in paper) or plastic such as Bakelite, which was easier to machine. Later glass and graphite fibre laminations were also introduced, increasing frame strength. (Easterling 1993, Kuebler 2000)

Meanwhile, metals had also been making headway in different forms. The first rackets, recorded in the 1920's, had solid extruded aluminium frames, which were substituted with cast magnesium alloys about five years later. From the mid 1960's, until the late 1980's, hollow extruded profiles made it to the market, for both aluminium and magnesium alloys. This opened new opportunities for designers like increased head sizes, which led to the revolutionary oversized rackets developed in the early 1970's. Subsequently, aluminium was used as a cold drawn tube up to the late 1980's and is currently used for low price rackets and some junior rackets (Kuebler 2000, Polich 1995).

During the 1970's, composites of glass fibre in epoxy were entering the market and this paved the way for what was probably the greatest revolution in tennis rackets to date. Initially glass fibres were combined with varied percentages of carbon fibres but this later evolved into rackets with carbon fibres as the main component. Rackets were hollow, or filled with foam, and the

## *CHAPTER 2 MODERN RACKET TECHNOLOGY*

carbon fibres made it possible to obtain stiffer, lighter and longer lasting rackets. From 1980 till the mid 1990's polyamide was used in frames, either as a thermoplastic injection with carbon fibre reinforcements, or as braided filaments combined with carbon fibres (Haines 1983).

Currently composite rackets consist predominantly of carbon fibres as the main component, complemented with anything from glass, boron, ceramics and Kevlar® to titanium, copper and piezo fibres, applied in strategic areas in an attempt to provide the optimal combination of their properties (Table 2.1). The core carbon fibre matrix has a five times higher tensile strength than aluminium and 20 times more than wood (Arthur 1992). Even more impressive is the stiffness of carbon fibres, best expressed as its specific modulus (stiffness-to-weight ratio), which is roughly six times that of steel, aluminium and wood, allowing for extremely lightweight frame constructions. In addition, the nature of the composite lay-up process allows for each layer to be placed in any direction and since the highest strength of the composite is achieved in the direction of the fibres, placing in line with the expected load results in the use of minimal material. Research into newer forms of carbon fibre is ongoing, with even stronger fibres recently manufactured at higher temperatures. Another improvement has been the production of layers in the form of woven or braided fibre groups, which is stronger than individual layers with the same fibre directions. It also has the advantage that other materials can be woven into the mesh to combine the strengths of the different fibres, as is the case with titanium fibres included in some rackets. The fibres are claimed to increase the directional stiffness of the combined mesh. Weaves have also been shown to be stronger and directionally more stable than the same fibres simply stacked on top of each other (Easterling 1993, Brody 1995, Polich 1995, Lammer & Kotze 2003).

Recently, Head has incorporated piezo fibres as a composite layer. The fibres are applied in the high bending areas, with or without a connection to an

## CHAPTER 2 MODERN RACKET TECHNOLOGY

electronic chip system. The fibres dynamically stiffen the racket during impact by converting the mechanical energy into electrical energy, which is returned to the fibres and again converted into mechanical energy to apply force in the opposite direction (Lindsey 2000b, Lammer & Kotze 2003, Kotze *et al.* 2003, Head brochure 2001).

At present it appears that material developments have more or less reached a plateau, with manufacturers experimenting with different variations of carbon fibre or the introduction of small quantities of other exotic materials to impress consumers. Table 2.1 provides a summary of the material properties of the most common materials used in tennis.

Material	Density, $\rho$ kg.m <sup>-3</sup>	Young's modulus, $E$ GPa	Tensile strength, $\sigma_y$ MPa	Specific modulus $E/\rho$
Wood	500	14	100	28,000
Steel	7,800	210	1,000	26,923
Aluminium alloy	2,800	75	500	26,071
Titanium alloy	4,500	110	1,000	26,667
Magnesium alloy	1,700	42	255	24,705
E-glass fibre	2,540	72	3,450	30,416
Carbon fibre	1,800	220	2,070	18,6000
Boron	2,630	420	3,400	16,0000
Aramid	1,440	124	2,760	86,100
Ceramic	1,800	40	4,830	22,000
Polyethylene	970	1.4	27	1,443
Polyamide (Nylon)	1,130	1.2	64	1,062

Table 2.1: Material properties of materials commonly used in tennis rackets (Easterling 1993, Jenkins 2003, Shigley & Mischke 1989, Domininghaus 1992).

### 2.2.3 Oversized heads and peripheral weighting

In order to assist explanations for the remainder of the document a diagram indicating important terminology, including a definitions of the axes, is presented in Figure 2.1 and unless specified differently, this view is the default plane for all definitions. The introduction of the first patented oversized head racket by Prince in the late 1970's initiated the revolution in racket designs of the modern era. The obvious result of the 25% wider than usual head was that it made it much easier to hit the ball. Less obvious, but more important,

*CHAPTER 2    MODERN RACKET TECHNOLOGY*

was the almost 50% increase in resistance to polar rotation, which is more related to control but also has a component influencing power. More relevant to this research was that the longer strings increased the racket's ability to generate ball speed by two mechanisms. First, the increased string deformation resulted in a phenomenon often referred to as the 'trampoline' effect. Since the strings are more effective at returning deformation energy than the ball, any attribute resulting in more string deformation and less ball deformation increases the ball speed.

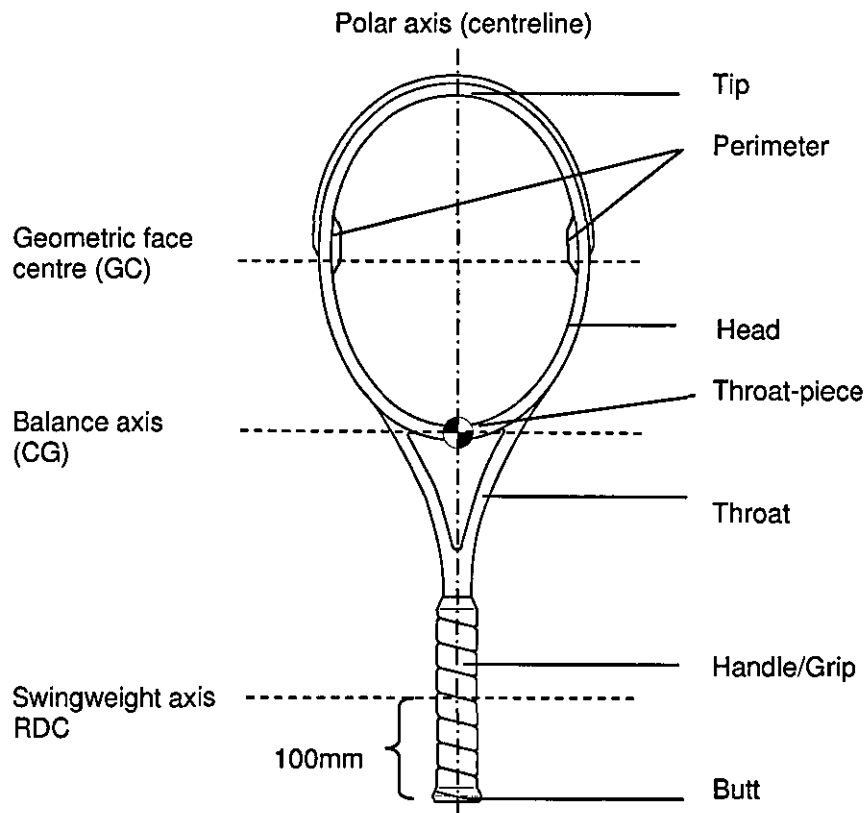


Figure 2.1: Diagram illustrating the default plane for definitions with important terminology and axis.

Another result of the longer strings was a 50% increase in the string area, which was claimed to result in a 'sweet spot' almost four times larger than before providing higher ball speeds during off-centre hits (Head 1976, Fisher 1977, Arthur 1992, Brody 1995).

## CHAPTER 2 MODERN RACKET TECHNOLOGY

According to Polich (1996), current rackets are available in the following sizes:

- Traditional: up to 516 cm<sup>2</sup> (80 sq. inch)
- Midsize: 517-581 cm<sup>2</sup> (81-90 sq. inch)
- Super midsize: 582-645 cm<sup>2</sup> (91-100 sq. inch)
- Oversize: 646-710 cm<sup>2</sup> (101-110 sq. inch)
- Super oversize: 711 cm<sup>2</sup> (110 sq. inch) and above

In 1992, Wilson introduced a new way of achieving rotational stability, by adding peripheral weights to 3 and 9 o'clock positions of the racket head, as illustrated in Figure 2.1 (Brody 1995, Wilson brochure 1992). This principle is currently the most popular amongst better players, since the smaller heads provide a better balance between ball speed and control, than the large heads.

### 2.2.4 Head shapes

The earlier use of wood limited the head to a structurally stable oval shape, but various head shapes have been tried since, particularly after the introduction of composite materials. The main motivations behind different head shapes are to increase the maximum ball speed, as well as the size of the 'power region' (the region on the strings generating the highest ball speeds) by increasing the string length on the periphery. In the traditional oval shapes, the strings at the stringbed's periphery are much shorter than the strings in the centre, but new materials allowed manufacturers to produce more box-like shapes. Some of these designs exploiting this are shown in Figure 2.2 and include the "isometric" (or square) head developed by Yonex in 1980 and later also used by Snauwaert and Völkl. The inverted throat-pieces developed by Rossignol in 1984 were virtually parallel to the curvature of the racket tip, allowing more longitudinal strings of the same length and resulting in a more consistent power region. The power region for conventional oval shaped



rackets is located close to the throat of the racket but studies have shown that most players hit the ball higher in the upper half of the racket, especially during the serve. The distal area of the racket is also the region with the highest head velocity (Yonex website 1999, Völkl website 1999, Kuebler 2000).

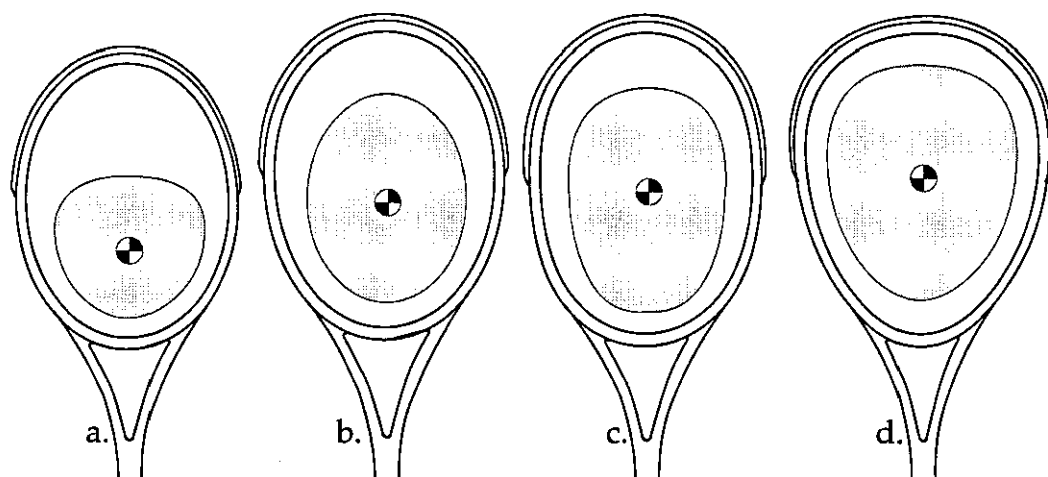


Figure 2.2: Different racket shapes and their 'power regions'. (a) Traditional; (b) Oversize; (c) Isometric; (d) Teardrop.

The isometric and teardrop shapes, address this problem by shifting the head mass as well as string distribution (and therefore the power region) higher up the racket face (Head brochure 1995, Wilson website 1999). Less common designs include FTM Sports' 10-sided head, developed in the mid 80's to resist distortion or torque during impact. Since the strings do not need to stabilise the head, lower tension can be used, increasing control and racket power (Beercheck 1991). Interestingly, most manufacturers today have returned to the traditional oval shapes, mainly because players find them more aesthetically pleasing.

### 2.2.5 Racket mass, balance and swingweight

Racket mass is an important factor when considering the racket's ability to generate ball speed. A heavier racket moving at the same speed as a lighter one should result in a higher ball speed but moving the heavy racket requires more

## *CHAPTER 2 MODERN RACKET TECHNOLOGY*

effort. According to Brody (1987), the increase in ball speed resulting from an increase in racket mass is not significant. Brody argues the difference between the mass of the ball (~60g) and the racket (~300g) is so large that a change in racket mass will not have a considerable effect on the ball speed. Based on his tests he claimed a 33% increase in racket mass would only lead to a 6% increase in ball velocity. The question is whether 6% is significant and is his argument still valid for a modern 240g racket? Cross (1998b) attempted to provide mathematical solutions by calculating the energy in an average serve and a groundstroke and assuming it to be equivalent to the player's effort. Hence, the effect of various parameters on ball speed, including racket mass were estimated for the same effort by the player. He found variance in ball speed similar to Brody's 6% but indicated an optimum mass for a serve at about 200g and about 300g for a ground stroke. Brody and Cross postulated that it is likely that an increase in racket speed due to a lighter mass would have a significant effect on ball speed but this cannot be proved until the relationship between the mass of the racket and the speed at which it can be swung is known.

Theoretically, an optimum racket mass for each player should exist, which would provide them with the highest ball speeds. The optimum mass for the highest ball speed is also different for different strokes, since they are not all played at the same velocity, which means the optimum for a whole game is dependent on the individual's style of play and surface played upon. It is common knowledge that beginners prefer lighter rackets, since they lack the strength and power to continuously swing the heavier rackets at high speeds. Professionals often play with rackets almost twice as heavy as those favoured by beginners. Many professional players are known to add lead tape to their rackets for additional weight but, since professionals don't represent the average consumer, the drive over the last few years has been to develop ever-lighter rackets, as low as 240g, compared with the wooden rackets of about 380g. The reduction in weight has mainly been made possible by the introduction of carbon fibre composites, which allow for hollow thin-walled

## *CHAPTER 2 MODERN RACKET TECHNOLOGY*

profiles. Interestingly, it seems the super-light rackets actually reached the point where they became 'unplayable'. Initially they were very popular due to what is known as the 'pick-up' effect, where players are just amazed by how light the racket is when they pick it up for the first time. Over recent years, however, manufacturers have been returning to slightly heavier rackets, which seems to be an indication they were getting too light for the average player. The super-lightweight rackets do not provide high inertial stability, therefore sacrificing control on off-centre impacts. Players also comment that the rackets are so light that they do not get the desired force feedback on some precision strokes.

Closely linked to the mass are the racket's balance and swingweight, which both refer to the distribution of the racket mass in relation to a specific axis. The balance is the distance from the butt to the centre of gravity (CG) while swingweight is the definition in the tennis world used for the racket's moment of inertia (MOI) about the gripping location, generally defined about an axis 100mm from the butt (Figure 2.1). These two quantities tend to be related; balance is an indication of the static moment applied to the hand only influencing the player's perception when holding the racket still, while swingweight refers to the racket's ability to resist rotation about the grip, influencing the racket's performance under dynamic conditions. During the remainder of the document, MOI refers to the racket's industry standard inertia measurement, unless another axis is specified. Rackets with a high balance and MOI are referred to as 'head heavy', as opposed to 'head light' rackets. Since the racket is usually swung through an arc, the further away the mass is from the arc centre the more effort is required to increase the racket's angular rotation and head speed. The principles mentioned for an increase in mass are therefore very similar to that for an increase in MOI i.e. higher ball speed at the same head speed. Many manufacturers have therefore attempted to move the racket balance towards the head by either changing the lay-up, adding special materials or adding perimeter weighting systems or having a deeper (wider) frame profile towards the tip of the head (Cross 1998b, Kuebler 2000).

### 2.2.6 Racket stiffness

Carbon fibre composites have also allowed for the development of much stiffer rackets. In principle, stiffer rackets mean less of the impact energy is lost during deformation of the frame. The frame is less efficient than the strings in returning energy to the ball, hence reduced frame deformation should increase the ball speed.

Based mainly on results from player tests, manufacturers have long been implementing the theory in various forms to create more power. One such attempt with considerable success was Kuebler's introduction of the first wide-bodied racket in 1984. This racket frame had a deeper cross-section, which made it considerably stiffer than before (Figure 2.3b). A license for the technology was obtained by Wilson and used in their very successful Profile rackets introduced in 1987. The concept was later refined into the dual-taper profile (Figure 2.3d), which meant the profile was deeper in the middle of the racket than at the tip and the handle, providing stiffness in the region under the highest bending moment (Kuebler 2000).

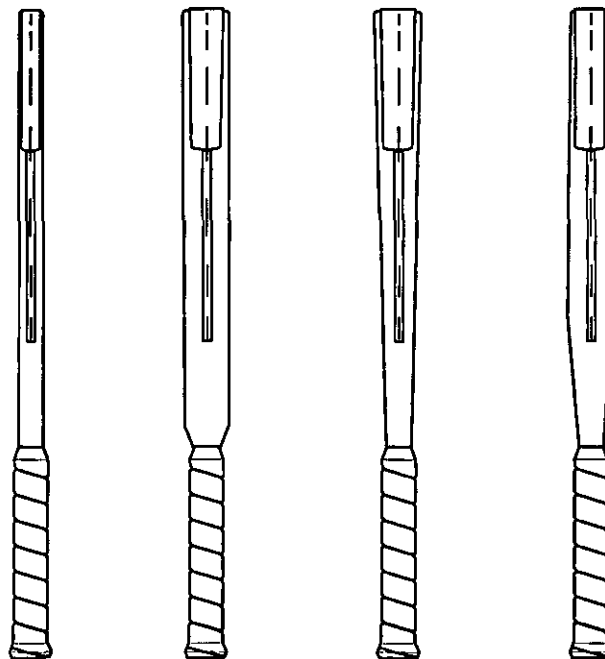


Figure 2.3: Wide-bodied rackets increase stiffness and power. (a) Traditional thin beam; (b) Constant beam; (c) Taper; (d) Dual taper.

This common belief in the industry has recently been contradicted by calculations by Cross (1998b), claiming the increase in 'power' should be almost negligible. There seems to be discrepancy between the power perceived by players and that determined via current theoretical performance definitions and this is exactly what the developed machine must be able to investigate.

### 2.2.7 Racket length

Extra-long racket designs (to the ITF maximum of 736.6mm, ITF 2004) were introduced in the mid 90's and currently most manufacturers still have a longer racket as part of their range. These rackets provide the player with more reach for playing strokes away from the body and a larger arc to the contact point, which increases head speed. During the serve, longer rackets have an additional advantage in allowing the player to hit the ball at a greater height, which increases the 'visibility' of the service box, allowing for higher serve speeds (Brody 1987, 1998).

There are various claims as to the impact location on the racket during play, with only Hennig & Schnabel (1998) providing experimental data. Unfortunately extensive tests were only performed on a single instrumented racket, which does not necessarily extend to other racket designs. Völkl website (1999) claims to have scientific proof that 80% of all players, regardless of their ability or style of play, hit the ball ~560mm from the end of the racket grip, which is above a normal racket's power region. Making the racket longer therefore could place the power region in the area where the ball is hit. Cross (1998b) and Brody (1981, 1987) both postulate that players would hit the ball in the 'sweet spot' for a ground stroke but that it would be better to hit the ball further away from the handle during the serve. However, this has not been verified by player tests and since the generated ball speed varies drastically down its face (Brody 1997), it is important to determine the most likely location

of the impact. This would assist in understanding why players hit the ball in a specific location.

### **2.2.8 String/frame interface**

Historically, the string/frame interface consisted of holes drilled through the solid wooden racket frame for weaving the strings. With development of hollow metal frames though, it became necessary to protect the strings from abrasion against sharper and harder hole edges. This was achieved with grommets, which are small tubes fitting tight in the hole drilled through the inner and outer frame wall. The grommets were, and still are, made out of a tough polymer and are flanged on the outside of the frame to prevent string contact with the frame around the hole edges. The string fits snugly into the grommet, not allowing much movement in the frame during impact. Grommets also assisted in the stringing process by providing a guide through the hollow frame (Kuebler 2000).

Later, with the introduction of thin-walled composite frames, it became even more important to have grommets, to prevent the strings from cutting through the thin carbon walls, under the high tension. Further functionality was added by extending the grommets (mostly on the racket tip) in to bumper guards to protect the frame against abrasions when contact is made with the ground. More recently, in an attempt to enlarge the string surface, hence increasing the power without increasing the head size, various manufacturers have adopted grommets with a larger hole diameter on the inside of the frame. This effectively shifts the string's point of deflection during the impact from the edge of the inner frame almost to the edge of the outer wall, theoretically achieving a greater effective string length (Lindsey 2000b, Lindsey 2001b, Wilson brochure 2002). Although no scientific data has been published proving this effect, it is still employed by various manufacturers. Following the trend of using the string/racket interface to increase power, two other noteworthy

technologies were developed; Wilson's "Roller system" and Völkl's Catapult system. The cross strings of the Roller system were strung around miniature pulleys instead of grommets in the 3 and 9 o'clock locations, which were pinned into a slot in the racket's symmetry axis. The rollers were claimed to distribute the load between adjacent strings and in so doing increase the racket power region (Lindsey, 2000b). The Catapult system consists of a carbon fibre spring plate on the outside of the frame. The plate doubles up as a second outer wall with holes through which the grommets are mounted and the central cross strings are strung. The front and back plate edges fitted into grooves in the frame, creating two slide joints, which allowed the plate to be mechanically loaded under the string and impact tension, which is released during the second impact phase (Lindsey, 2001).

### 2.2.9 String technology

Strings are the most energy efficient part of the racket and therefore the major contributor to ball speed off the racket face. Due to their high elasticity, strings are extremely effective in returning deformation energy, stored during the impact, back to the ball. Modern strings are made from natural or synthetic materials.

Traditionally strings were made from varnished natural gut, consisting of twisted strands from the inner lining of animal intestines. Gut strings are still believed to be the most 'powerful' on the market, mainly because gut is an almost perfectly elastic material, more so than synthetic polymers. Manufacturers continue to attempt to mimic gut by producing synthetic strings made from polyester, but most elite players still prefer the feel of natural gut. Gut exhibits an initial relaxation when strung, after which it has a much lower creep rate than synthetic strings, preventing tension loss. Unfortunately gut strings are very expensive and wear easily, especially under extreme

## CHAPTER 2 MODERN RACKET TECHNOLOGY

environmental conditions. Consequently, they are mostly used by professionals who can afford to restring their rackets after every match.

Synthetic strings are mainly extruded from nylon and are more durable than gut but produce less 'power'. Nylon also has the tendency to creep continuously, hence constantly losing tension.

Currently, there are numerous synthetic string constructions available on the market. Figure 2.4 highlights the main categories followed by their main characteristics:

- **Mono-filament:** Strings are made from polyester and are stiffer than nylon but softer than Kevlar® and very durable.
- **Solid core/single wrap (a):** Strings are durable with good tension retention properties. The outer wrap retains the tension and protects the core.
- **Solid core/multi-wrap (b):** Strings are used for wide-body rackets because they play 'softer'.
- **Multi-core/single wrap (c,d):** String provides soft play with reduced stretching.
- **Geometric (e,f):** Strings consist of different cross-sectional shapes and allegedly improve spin.
- **Multi-filament (g,h,i):** A core-less string with very soft, playable characteristics due to high elasticity, excellent for wide-body rackets. Strings have a tendency to stretch and lose tension.
- **Multi-core/multi-wrap (j):** Strings has two wraps with good durability.
- **Textured (k,l):** Strings have added outer wraps or increased diameter wraps to provide rough surface texture.



- **Composites:** These strings combine different materials such as nylon and Kevlar®, providing a combination of both longer life and softer feel.
- **Aramid fibre hybrids:** This stringing pattern combines strong Aramid fibre (Kevlar®, Technora®) main strings, with soft gut or nylon cross strings. Kevlar® strings are extremely durable and yield good control but are not very elastic.

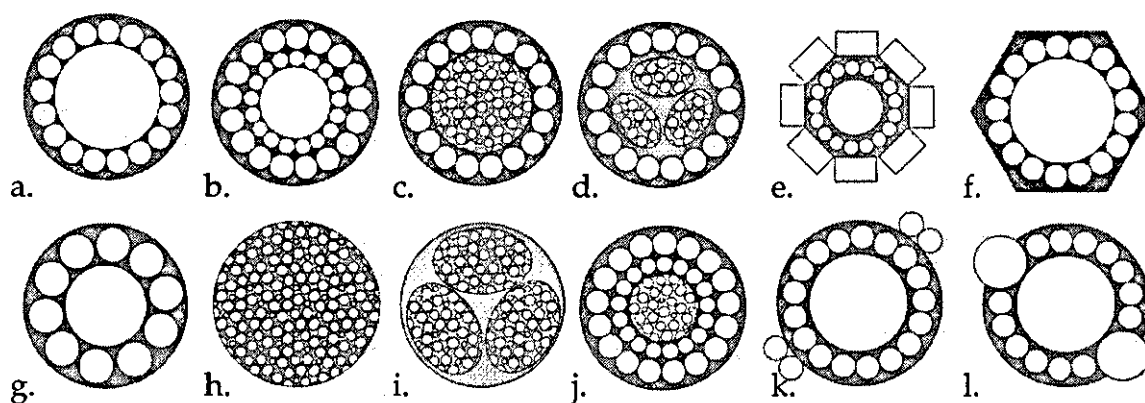


Figure 2.4: The main categories of strings types. (a) Solid core/single wrap; (b) Solid core/multi-wrap; (c), (d), (i), (j); Multi-core/multi-wrap; (e), (f) Geometric; (g), (h) Multi-filament; (k), (l) Textured.

The effect of most string parameters on rebound ball speed is known as the 'trampoline effect', whereby maximising the string deformation during the impact, rather than the ball deformation, results in an increase in ball speed. This is because the ball behaves as an imperfectly elastic material, as specified by the ITF, while strings are designed to be more perfectly elastic. A ball bouncing on a solid surface rebounds at 75% of its impact speed, while a steel ball impacting on a clamped stringbed rebounds at about 95% of its impact speed (Cross 2000b). Hence, a decrease in ball deformation and an increase in string deformation during impact, results in an increase in kinetic energy returned to the ball. This could be achieved by increasing the string length and reducing the string tension, gauge and pattern density (Brody 1987).

## *CHAPTER 2 MODERN RACKET TECHNOLOGY*

Increasing the string length is mainly achieved by enlarging the racket head as described in §2.2.4, with the limiting factor being the maximum dimension specified for the racket head by the ITF. From experience and empirical studies, players and coaches know that lower string tensions enable more powerful shots, while higher tensions promote accuracy, spin and control but the phenomena were not fully understood until the early 1980's. Brannigan and Adali (1981) mathematically linked the increase in power to the longer impact time. Shortly after, Elliott (1982b) experimentally determined an optimum string tension at 245N, which was later confirmed by Thornhill (1993). The power increases with a decrease in tension, to a point where the tension is so low that the strings start to move relative to each other, losing energy to friction.

The gauge is the common indication of string thickness, with a higher gauge indicating a thinner string (15-gauge = 1.45mm, 16-gauge = 1.28mm, 17-gauge = 1.15mm). Thinner strings are less stiff than thicker strings, hence producing more power, but are more fragile. Likewise, a denser string pattern also leads to less string, and more ball deformation, hence a decrease in power (Brody 1987).

Although most researchers agree on these principles, Cross (2000b) made an interesting discovery when he tested various modern rackets and strings. Rackets were compared during player tests and strings were subjected to laboratory tests. His results confirm most common string theories but show the effect is so small it is almost negligible during play. He explains that most strings, although performing very differently under laboratory test conditions, all return more or less the same percentage of energy stored. Since the strings return considerably more energy to the ball than the racket frame, this percentage is almost the same for all rackets. Cross emphasises that this is only valid under the same test conditions, which again raises the question of how

players react to differently configured rackets during real play conditions and hence the need for accurate motion studies.

Strings and stringing patterns also have large influence on ball spin, with tour players achieving spin rates of up to 3000rpm for the first and 5000rpm for the second serve (Pallis, 1999). Applying top-spin to the ball makes it dip towards the end of its trajectory allowing it to bounce closer to the server for the same launch height and speed, while still clearing the net. The server can therefore increase their serve speed and still land the ball in front of the service line. Researchers have found racket angular rotation, ball toss height, pattern density, string gauge and friction to be the main factors contributing to ball spin during the serve (Elliott 1983, Cottey 2002). Cross (2000c) demonstrated with a model based on impact test results, that strings needed a sliding coefficient of larger than 0.3 to be effective. This was confirmed later by Nakagawa (2002), who determined the important factor for spin generation to be the extent of deceleration during the sliding phase, which is closely linked to the sliding friction, with a decrease in the sliding and an increase in rolling increasing the spin.

### 2.3 Sweet spot definitions

The 'sweet spot' is a term commonly used by players and manufacturers to indicate the optimum ball impact zone on the racket face. Players mostly refer to the sweet spot as the zone with optimum racket performance and minimum discomfort, which is often linked to the racket's 'forgiveness' i.e. the size of the contact area where the player can still achieve optimal performance. The exact location of the sweet spot, the perception of which varies between players, is not entirely resolved but is believed to be a combination of the universal impact definitions. The challenge therefore towards understanding the mechanism behind on-court racket performance for research lies in finding

a definition or measurement in the laboratory which correlates with the on-court 'sweet spot' location.

The research related to the sweet spot was well summarised by Brody (1987), Cross (1998a) and Brody *et al.* (2002), in which they concluded there are four definable regions related to a racket's sweet spot; the maximum COR area; COP region, the node and the 'dead spot'. Figure 2.5 indicates the approximate relative distribution of these regions for most common rackets.

2.3.1 Centre of Percussion (minimum shock)

For each impact location there is a coupled location, where the velocity due to the translation and rotation motion components caused by the impact cancel each other, resulting in no net reaction force at the grip (Figure 2.6).

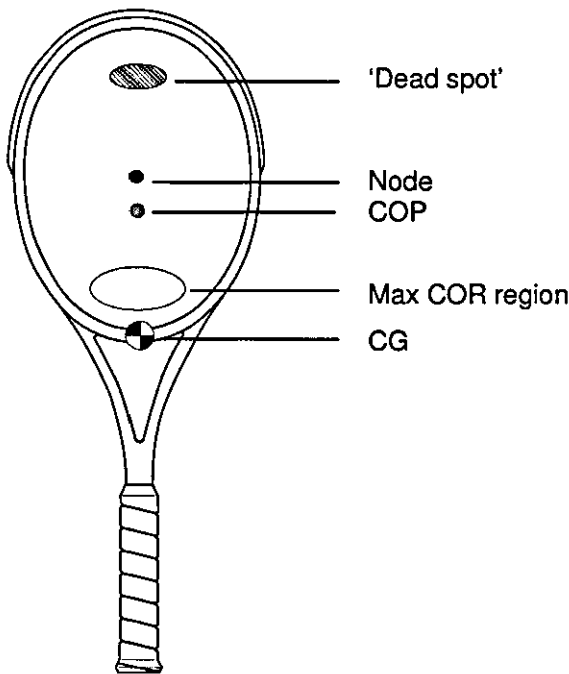


Figure 2.5: Distribution of a racket's 'sweet spots'.

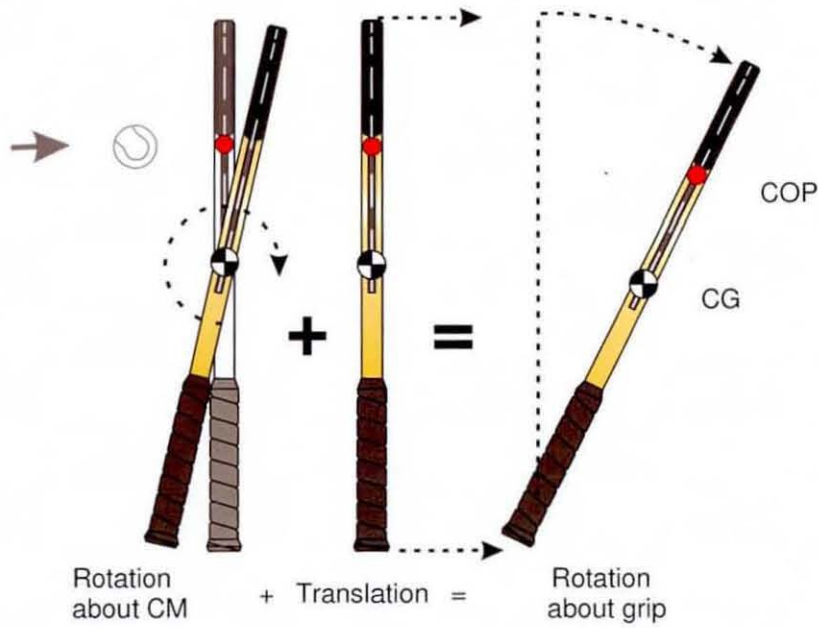


Figure 2.6: Schematic explaining a racket's COP.

The centre of percussion (COP) is therefore the impact location causing the racket to rotate about the location of the hand, hence considerably reducing the shock on the hand and improving the player's perception of the stroke. By definition this is an explicit point, rather than a region, and is a function of the particular hand gripping location, the racket mass ( $m_r$ ), balance point and MOI ( $I_{cg}$ ):

$$s = \frac{I_{cg}}{m_r \cdot b} \quad (2.1)$$

where the  $s$  is the location of the COP measured from the CG,  $I_{cg}$  is the MOI about the CG and  $b$  is the racket balance point measured from the grip location. The COP is usually closer to the middle of the racket than the peak ball speed location but has virtually no relationship to ball rebound speed except in persuading the player, through negative feedback, to hit the ball in this location rather than the area of maximum power in order to reduce discomfort.

2.3.2 Node (minimum vibrations)

Basic vibration theory states that, when excited, an object will vibrate at its natural frequencies and in corresponding mode shapes, as determined by the boundary conditions. When excited by an external impulse load the mode shapes of the racket have at least one point of no oscillation, known as a node, while the highest vibration amplitude occurs at the antinodes. Conversely, an impulse load at a node will not excite the corresponding mode, while a load at the antinode will cause the biggest excitation of that mode. The most important mode shapes for a racket is shown in Figure 2.7.

The grip-clamped condition has a first mode frequency of about 20-30 Hz, while its second mode and the first mode of the free racket are both in the range 100-150Hz. Both the latter modes are of interest to the research, since their nodes are located close to each other and both are located near the centre of the racket face and are therefore likely locations to be impacted by the players in order to minimise unwanted racket vibrations.

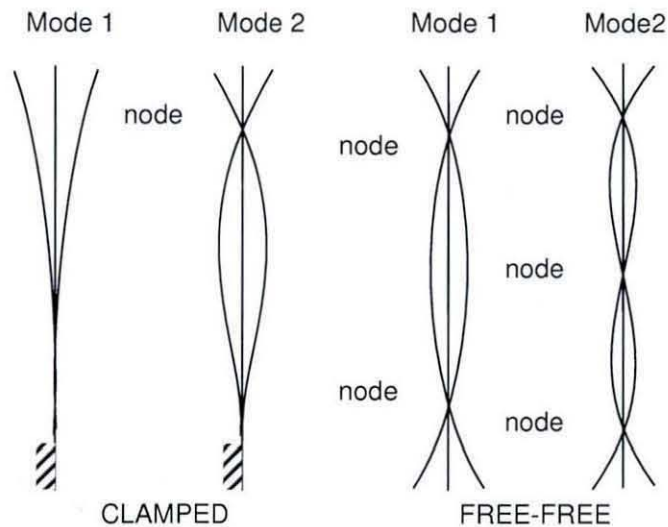


Figure 2.7: Schematic representation of a racket’s natural vibration modes under clamped and freely suspended gripping conditions.

For the racket, the node ‘sweet spot’ is therefore the impact location exciting minimal frame vibration at the grip, resulting in a better perception of



the stroke. Each mode shape has modes in different locations but according to researchers such as Cross (2000d), the fundamental mode is the only mode absorbing significant energy during the impact. Therefore minimising these vibrations should theoretically result in the most kinetic energy being returned to the ball and therefore higher rebound ball speeds. For modern rackets, this contribution is believed to be relatively small but it needs further investigation.

### 2.3.3 Area of maximum rebound ball speed.

This is the area of highest rebound ball speed on the racket face, mostly described in terms of the racket's coefficient of restitution (COR), which is the most relevant definition to the research, hence a more detailed discussion of the research related to the COR is presented in §3.1. The COR sweet spot is the area on the racket where the racket returns maximum impact energy, thus resulting in the highest ball speeds. The location of the maximum is a region rather than a point, hence it is often referred to as an 'area'. Since players are not likely to hit the ball in the perfect location every time, the size of the region to them is almost as important as the maximum value.

### 2.3.4 'Dead spot' (maximum serve speed)

Cross (1997) defined another location on the strings related to racket performance, the 'dead spot'. This is the point near the tip of a free stationary racket, where the rebound ball velocity is almost zero during impact tests, but with a very high recoil racket speed. During a serve the effect is reversed however, since it involves a moving racket impacting a stationary ball, resulting in a high ball speed at the location. With the ICR suspected to be near the racket butt, the effective mass (defined in §3.1.1) of the racket at the dead spot approaches that of the ball, which is the optimum condition for momentum transfer between perfectly elastic objects, resulting in the moving object stopping dead and transferring all momentum to the second object. The impact however, is not perfectly elastic resulting in increased energy losses so near to

the tip in the form of racket vibrations, but the net effect of the two counteracting mechanisms results in a higher ball speed at the tip than might otherwise be expected. Although players pay a penalty in terms of increased discomfort and fatigue caused by the increased racket vibrations and reaction forces at the hand, the dead spot has a higher speed at impact than the COP or linear maximum COR regions, since it is further removed from the ICR during the rotation. This could reward the player with higher ball velocities, especially during the serve, which has the highest racket head speeds.

Since the node, COR and 'dead spot' are the expected impact locations providing players with the highest ball speeds, their exact locations should be determined and their influence on performance investigated in order to reveal the relation between on-court and laboratory measurements.

### 2.4 Implications for the PDS

The test machine should be able to test all senior rackets conforming to the existing ITF regulations specified in §2.1 and all possible variations thereof within the expected boundaries of other properties such as mass and MOI.

A strict test protocol should also be implemented for testing in order to minimise the changes in variables which could affect test results during investigation. These would include a strict logging or the consistent use of test parameters such as, string type, string tension and the time passed between stringing and testing.

The test machine needs to enable mapping down the polar axis of the racket face in order to investigate the locations and the effect of the different 'sweet spot' definitions.



## *CHAPTER 2   MODERN RACKET TECHNOLOGY*

The relatively high spin generation during high-speed serves justifies the need for a realistic simulation device including a rotating racket and a ball impacting the racket face on a downward trajectory.

## Chapter 3

### Racket performance indicators

In order to develop a machine, which would be able to investigate racket performance, it is imperative to know which parameters are important to measure. These parameters would constitute the core of the PDS around which other minor specifications will be built. To describe power, various definitions are currently in use in different areas of tennis and other sports, which can mostly be divided into scientific and commercial definitions. Scientific definitions originated from the research community and are usually technically more accurate, while commercial definitions are simpler with the focus on determining and relating measures familiar to the public, and in particular tennis players.

#### 3.1 Coefficient of restitution (COR)

##### 3.1.1 Definition

As mentioned in the previous chapter, the COR is one of the most common racket performance indicators, since it relates well to on-court play, as well as laboratory measurements. The COR is a ratio often used in impact mechanics to indicate the capacity of two colliding body pairs to recover from the impact. The COR is defined as the ratio of the restoration impulse magnitude to the deformation impulse magnitude between the two bodies:

$$COR = \frac{\int_{t_0}^t F_{rs} dt}{\int_0^{t_0} F_d dt} \quad (3.1)$$

where  $F_{rs}$  and  $F_d$  are the contact forces during restoration and deformation respectively,  $t_0$  is the deformation time and  $t$  the contact time. Under idealised conditions the COR is a constant for the pair of colliding bodies, measured along the line of impact for any discrete impact location, which reduces Equation 3.1 to the ratio of relative velocity between the bodies after impact, to the relative velocity before impact (Meriam & Kraige, 1989). Adapting this equation for the tennis, as shown in Appendix A, impact yields:

$$COR = \frac{v_b - v_r}{u_r - u_b} \quad (3.2)$$

where  $u_b$  and  $v_b$  are the ball speeds before and after impact, while  $u_r$  and  $v_r$  are the racket speeds along the line of impact, before and after impact respectively as indicated in (Figure 3.1).

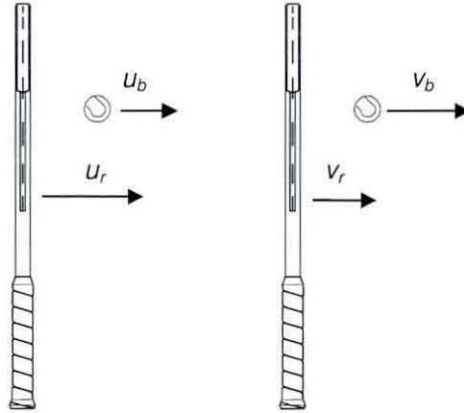


Figure 3.1: Diagram indicating impact velocities for the racket impact.

Equation 3.1 is the definition most often used to predict velocities resulting from sports ball impacts. In reality though, most impacts involve materials exhibiting strain rate dependent behaviour, hence complicating its application and leading to variations in its definition (Daish 1972, Missavage *et al.* 1984, Stronge 2000).

### CHAPTER 3 RACKET PERFORMANCE INDICATORS

The focus of the research is on the racket performance during a serve during which the pre-impact ball speed is effectively zero, simplifying the equation to:

$$COR = \frac{v_b - v_r}{u_r} \quad (3.3)$$

Another definition introduced by Hatze in 1976 for the moving ball/stationary racket test, was the apparent coefficient of restitution (ACOR), which neglects the racket's recoil speed from the definition:

$$ACOR = \frac{v_b}{u_b} \quad (3.4)$$

This definition has been employed by many researchers as a means of characterising tennis ball/racket collisions, mainly due to its simplicity and the fact that racket velocity after the impact is of no importance to the player nor does it have any influence on the game (Hatzé, 1976, 1993). The relationship between the ACOR and COR can be presented as a function of the respective racket and ball masses,  $m_r$  and  $m_b$ , as shown in Appendix A:

$$ACOR = \frac{m_r \cdot COR - m_b}{m_r + m_b} \quad (3.5)$$

This indicates that the ACOR includes the masses of the racket and ball, which enables it to distinguish between different racket masses if used as a performance indicator. Equation 3.5 assumes the impact occurs at the racket's CG, which is not the case for most impacts. Therefore, to calculate the ACOR at any impact location, the racket mass in the equation is substituted with the effective racket mass ( $m_e$ ) at the discrete impact location, together with the COR measured for that impact location. Brody *et al.* (2002) defined the effective mass along the polar axis as (derived in Appendix A):



$$m_e = \frac{m_r}{1 + \frac{m_r d^2}{I_{cg}}} \quad (3.6)$$

where  $d$  is the distance from the impact location to the CG and the  $I_{cg}$  the MOI in the impact plane about the CG. Due to the inherently empirical nature of the ACOR definition, care must be taken when comparing results measured under different impact conditions, such as relating the  $ACOR'$  measured for a moving ball/stationary racket to the  $ACOR''$  under serve conditions. The  $ACOR''$  is derived mathematically by transferring the court's frame of reference to that of the moving racket, as indicated in Appendix A (Brody *et al.*, 2002):

$$ACOR'' = ACOR' - 1 \quad (3.7)$$

Although no experimental measurements were found, most researchers in the literature concluded that an increase in impact velocity would cause a decrease in COR and ACOR. Instead, claims were mainly based on mathematical models, using COR measurements from head clamped rackets (Brody 1997, Goodwill & Haake 2000), or measurement of the racket's ACOR (Hatze 1993, Watanabe 1997). Goodwill & Haake (2004) did measure and publish racket ball speeds with a freely suspended racket for a range of impact velocities but did not calculate the COR or the ACOR. Converting the published results yields a drop of ~13% in COR and of ~11% in ACOR for an increase in impact speed from 10m.s<sup>-1</sup> to 35m.s<sup>-1</sup>. This means both definitions, especially the COR, are rather sensitive to the racket impact speed, and would therefore also be sensitive to inaccuracies in impact speed measurements of any test method or machine, which is important in order to define the machine's PDS.

One of the main disadvantage of the COR versus the ACOR concerning a test method is the difficulty in measuring it, since the velocities of the racket and ball have to be measured before and after the impact. Determining the racket velocity after impact is by no means a simple task, especially when test

automation providing instant results is considered, since it usually involves manual digitizing of the racket frame after impact.

### 3.1.2 Representative gripping conditions

It is evident from both experimental and computational studies of racket performance that COR and ACOR tests require careful consideration of the imposed constraints and initial conditions. Perhaps one of the most controversial issues in this regard has been to establish a representative gripping condition, which will produce repeatable test results and still be representative of 'real play' performance. Clearly real play conditions, with a human hand gripping the racket, would produce the most representative results but the complications with instrumentation, the effects of player fatigue, the variability between individual players and consequent lack of repeatability pose serious obstacles. Consequently, researchers have resorted to a variety of experimental gripping conditions, which can be reproduced in the laboratory with a degree of repeatability, ranging from simple to very complex mechanisms. To make matters more complex, players are believed to have different swing styles, with dynamic gripping conditions, which would not be trivial to reproduce.

Consequently, most experiments reported in literature use the following gripping conditions, with the abbreviations in brackets indicating the subscripts used in future sections to indicate these conditions:

- *Player or hand held (ph)*: a racket held by a human hand but not necessarily executing a shot, hence not necessarily representative of play.
- *Player simulated (ps)*: a complex gripping device is implemented closely mimicking the real play conditions.
- *Free (f)*: a racket supported by some means, which contributes negligible resistance to the racket motion during impact.



- *Grip-pivoted (gp)*: a racket supported by some kind of pivot at the butt of the handle, allowing free rotation about the pivot during impact.
- *Grip-clamped (gc)*: a racket clamped at the grip, such that virtually no rotation or translation in the gripped area is allowed.
- *Head-clamped (hc)*: a racket with the head clamped to a solid object, eliminating any contribution due to deformation of the remaining unconstrained racket frame.

These different test and calculation methods often lead to discrepancies and confusing results, demonstrating the need for an industry standard to be developed, which should be possible using the machine developed through this research. Of the various gripping methods utilised, the most common and probably most useful are the freely suspended, handle-clamped and head-clamped conditions, due to their simplicity and repeatability. Free and handle-clamped rackets result in very similar COR results, with a maximum COR value of 0.40-0.65 close to the throat, while head-clamped rackets results in a maximum COR of 0.65-0.85 closer to the middle of the racket. The lower COR in the handle-clamped condition is a result of some energy being absorbed by the deformation of the racket frame and not being returned to the ball. The maximum COR location for handle clamped is nearer to the throat than that for the free racket due to less bending of the frame towards the grip under the first bending mode, which decreases the energy losses in this area. Although useful for particular applications, the head clamped condition is less representative of play conditions, leading to the preference towards handle clamped and free tests. Furthermore, many light-weight handle-clamped rackets cannot withstand realistic impact at high velocities, swinging the scales in favour of the freely suspended condition but there are still debates amongst researchers regarding the most representative condition.

In summary, the published work can be broadly divided into two categories; those which claim the gripping condition does not affect impact

results and those that do. However, the division is perhaps not as wide as it appears. Although there seem to be obvious differences between published results, it is believed these are most likely attributed to different methods and variables used. Some test variables include:

- different rackets, strings and balls
- dimensions and placing of instruments, such as accelerometers and force sensors
- location of the impact point
- impact speed
- string tensions
- definition of test measures (e.g. COR, ACOR)

A typical example of tests not performed using the same variables, are the contradictory conclusions drawn by Hatze (1976) and Baker and Putnam (1979), as presented in more detail in the following section. Hatze measured impulse using strain gauges on the racket, while Baker and Putnam calculated the impulse from the measured ball velocities, while measurements were performed at different impact speeds, racket models, string tensions and gripping conditions. It is therefore not surprising that Baker and Putnam disagreed with Hatze's conclusion that the gripping condition does influence the impulse and, hence, the ball speed.

A further cause for differing opinions is the definition of 'significance'. For example, Elliott found a 17% reduction in reaction impulse, which compares well with the 10-15% found by Hatze. Hatze, however, concluded the change in impulse will lead to an increase in the "power of the stroke" even though rebound velocity and COR were not measured. Elliott on the other hand, who measured COR, found changes in reaction impulse caused an "insignificant increase in rebound velocity".



For impacts off the centreline there is only one claim, made by Grabiner (1983), to indicate that the gripping has no influence on off-centre impacts. The “free-rotating” experimental arrangement Grabiner describes includes an artificial lateral constraint introduced by the two non-compliant suspension cords that, perhaps, explains his unexpected conclusions.

A popular approach to investigate the gripping condition’s influence is to estimate the propagation time of a transverse wave through the racket. Authors state that for the grip condition to have an effect on the rebound velocity the transverse pulse caused by the impact needs to travel from the point of impact to the handle and back to the impact point. If the ball is still in contact with the strings at this moment, the grip will affect the rebound velocity otherwise it will have no effect.

The wave speed ( $v_w$ ) can also be calculated by (Brody *et al.*, 2002):

$$v_w = C \sqrt{f_m} \quad (3.8)$$

where  $C$  is a constant indicating the stiffness to weight ratio of the racket frame and  $f_m$  is the frequency of the particular vibration mode. The frequency can be determined by:

$$f_m = (G_r \cdot C / (2\pi L))^2 \quad (3.9)$$

with  $L$  the beam (racket) length and  $G_r$  is a constant depending on the gripping condition and particular vibration mode, increasing with an increase in mode (freely suspended;  $G_r=4.730, 7.853, 10.996$ , clamped;  $G_r=1.875, 4.694, 7.853$ ). Since the speed of the wave is calculated by dividing the distance between two adjacent nodes by the time the wave needs to travel between them, it can be determined during laboratory tests by multiplying double the distance (equal to a wavelength) by the frequency. Cross (1998a) experimentally measured the wave speed by attaching piezoelectric discs to different locations on the racket. He found the wave speed for a hand held racket with a

fundamental mode of 102Hz to be  $80\text{m.s}^{-1}$ , which meant it needed 6.5ms to reach the hand, while the second mode of 276Hz, had a wave speed of  $143\text{m.s}^{-1}$  and needed 3.6ms. According to the general reasoning, the impulse of the first mode only gets to handle after the ball has left the strings, for a 5ms impact duration. Cross measured an impulse at the hand 1.5ms after the impact though and attributed it to the higher string mode of about 500Hz, which travels faster through the frame and therefore is able to excite the fundamental frequency. Cross therefore concluded that the hand had a strong influence on the racket behaviour while the ball is still on the strings, but did not publish results indicating if this had any influence on the rebound ball speed, which still leaves the question unanswered.

Cross also concluded that the vibration response of the hand-held racket is closer to that of the free gripping condition but not exactly replicated by it. For the free condition, the mode shapes are essentially the same as for the hand-held condition except for a slight shift in the two nodes towards the end-points of the racket and approximately a 10% decrease in vibration frequency results, due to the added constraint of the hand. Hence, if tests on vibration aspects of racket impact are performed, the free condition will produce the most representative results.

Combining different measurements from the literature (Brody 1981, Cross 1998b, Brody *et al.* 2002) revealed racket vibration frequencies under the different gripping conditions of:

- Grip-clamped: 23 to 35Hz (first mode), 125Hz (second mode)
- Pivoted: 85Hz (first mode)
- Hand-held: 100 to 150Hz (first mode)
- Free: 125 to 200Hz (first mode)
- Strings: 500Hz (under all grip conditions)

Without much evidence to prove the contrary, the argument regarding the effect of gripping on the ball rebound speed is in favour of it having less, if any, significant influence for less stiff rackets but, for the modern lighter and stiffer rackets, there might be some measurable effect depending on the test criteria. More tests on newer rackets are needed for more conclusive results. The effect on ball speed is also very likely to be influenced by the relative pre-impact speed, since it affects impact times and impact forces. Most tests in the literature are done at relatively low speeds of about  $\sim 30\text{m.s}^{-1}$ , which represents an average groundstroke. In contrast, this study investigates the effect of serves up to  $\sim 67\text{m.s}^{-1}$ , stressing the need for tests to be performed at higher impact speeds.

### 3.1.3 Research related to the COR

The following section provides a summary of all the literature relating racket performance to some form of COR measurements or gripping condition in order to establish gaps for further investigation. This is summarised in Table 3.1.

Initial investigations into the importance of grip firmness revealed a major influence on rebound velocity (Bunn 1955, Plagenhoef 1970, Broer 1973, Tilmanis 1975). They agreed that a firm grip would prevent the energy lost to racket rotation and therefore return more energy to the ball.

The first noteworthy introduction of ACOR to the tennis public was when Head (1976) performed a series of ACOR tests on his oversized Prince racket, to substantiate the revolutionary improvement claimed for the racket. Balls were fired at stationary rackets at up to  $27\text{m.s}^{-1}$ , while measuring inbound and outbound ball velocities using a high-speed camera. Tests were performed under grip-clamped, player-held and freely suspended conditions but only values for the grip clamped conditions were disclosed. The  $\text{ACOR}_{\text{gc}}$  measurements were plotted for various points over the string surface and



contour maps of  $ACOR_{gc}$  were used to compare the racket to its predecessors. Figure 3.2 shows the comparison, with  $ACOR_{gc}$  values for the oversized racket increasing from 0.3 measured at the tip of the head to more than 0.6, close to the throat.

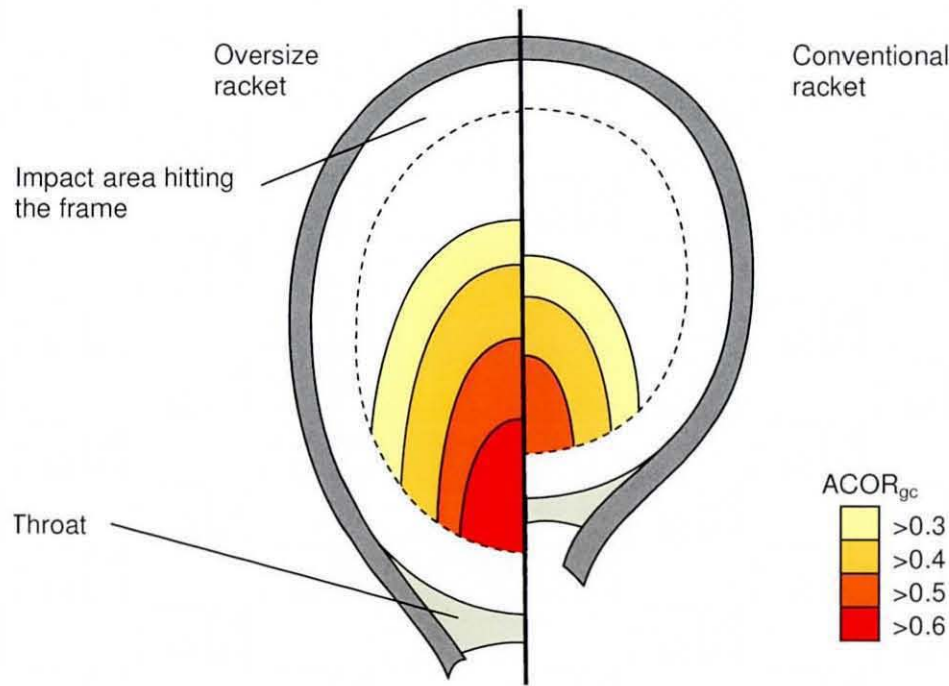


Figure 3.2: The difference between the  $ACOR$  mapped for a normal racket and oversized racket (taken from the patent by Fisher, 1977)

Hatze (1976) developed a mathematical model of the racket impact. Tests were performed on a wooden racket (strung at 250N tension), with ball speeds of up to  $34.1\text{m.s}^{-1}$ , under grip-pivoted, hand-held and real play conditions. One set of strain gauges was fixed to the frame, at the level of the impact point, which quantifies the impulse, while another set was placed just above the handle grip, measuring transverse vibrations. Substituting the test values into his model, Hatze concluded an increase in incident velocity would cause a decrease in contact time and an increase in the amplitude of the racket vibrations. The loose grip during the real play tests revealed a 10-15% decrease in the reaction impulse imparted on the ball at the impact location and a reduction in unpleasant vibrations to the hand. Hatze considered this reduction

in reaction impulse and its assumed influence on racket performance as significant, which led to much debate amongst some of his contemporaries.

Baker and Putnam (1979) fired balls at rackets (strung at 178-267N tension) under grip-clamped and free conditions. The first part of the experiment was performed at ball impact speeds of  $28.2\text{m.s}^{-1}$  on different rackets. Pre- and post-impact velocities were recorded with a high-speed camera and were used to determine the impulse imparted on the ball. Contrary to earlier findings by Hatze (1976), no significant difference in impulse between the free and head-clamped conditions was found for any of the rackets. The second part of the experiment entailed high-speed recording of a single impact at a ball impact speed of  $26.5\text{m.s}^{-1}$ . The contact times for both clamping conditions were 4 ms and resultant deflections along the racket were found to be virtually the same during ball contact. After contact, the deflections for the different conditions differ dramatically but this is deemed too late to have an effect on the ball speed. Notwithstanding, a difference of note between the two conditions is the clear disparity in the frame's visible mode shape, indicating an effect on vibration response. Unfortunately, the impact was only recorded for a single impact location and the relationship of this point to the racket's COP was not noted, which will have significant influence on the impulse at the grip.

Watanabe *et al.* (1979) measured  $\text{ACOR}_f$ ,  $\text{ACOR}_{gc}$  and  $\text{ACOR}_{ph}$  for wooden rackets (strung at 267N tension), at impact velocities ranging roughly from  $5\text{m.s}^{-1}$  to  $25\text{m.s}^{-1}$ . The tests revealed the ACOR values for these rackets decreased with impact velocities and were independent of grip condition. Maximum ACOR values for all gripping conditions were approximately 0.43.

In 1979, Brody compared the maximum COR of different rackets. His results emphasized the matter of properly defining testing conditions for COR measurements. Brody's tests were performed with a ball dropped from a height of 3.7m onto a racket, with its head clamped in a vice. The peak  $\text{COR}_{hc}$  values of approximately 0.85 were considerably higher than those measured by Head



(1976) under different clamping conditions. Constraining the racket's head eliminates energy losses to the racket frame, resulting in a considerably higher COR. Brody also measured the contact time of a tennis ball on the racket strings, as well as the racket oscillation characteristics. The contact time was found to be 4.5ms and the half-period of the fundamental frequency for different rackets measured not lower than 15.3ms. Brody concluded that most of the energy absorbed by the racket frame is not returned to the ball because the ball leaves the strings before the racket can snap back.

In 1980, Elliot performed  $ACOR_{gc}$  measurements at discrete points along the longitudinal and transverse axes of conventional wooden and oversized rackets at  $21\text{m.s}^{-1}$  (strung at 245N tension). These tests revealed a similar map across the racket surface to that found by Head (1976). Along the longitudinal axis the values increased from close to zero at the tip up to a maximum, approximately 20mm before the throat, and then decreased slightly towards the throat. Measurements along the transverse axis increased from almost zero at the extremity to a maximum at the longitudinal axis. The  $ACOR_{gc}$  values measured for the oversized rackets confirmed those performed by Head (1976) with a maximum of approximately 0.50 compared with 0.45 for the wooden rackets. The difference between the rackets was even larger for off-centre impacts. Elliot's justification for performing hand-held tests was the difference in frequency response, amplitude and duration of vibrations measured for the other gripping conditions but no data were presented to support these claims.

In 1982a, Elliott projected balls at  $22.7\text{m.s}^{-1}$  towards a linearly moving racket (strung at 245N tension). The racket was actuated pneumatically and mounted with adjustable grip tightness. The racket speed for a location 5 cm from the racket tip ranged between  $6.4\text{--}7.4\text{m.s}^{-1}$  for different rackets producing relative incident impact velocities of  $29.4\text{--}30.1\text{m.s}^{-1}$ . Force transducers located in the racket arm measured reaction force at the grip and velocities were measured with stroboscopic photography. Impacts along the centre line in the

longitudinal and transverse directions were performed, with the largest  $ACOR_s$  measured at the centre of the racket head. These measurements yielded peak  $ACOR_s$  values of approximately 0.65, which is significantly higher than his  $ACOR_{gc}$  measured in 1980 and believed to be a result of neglecting the transferring of reference frames during the calculation. Comparing results from the force transducer at this location for the largest difference in gripping conditions, revealed a relatively small increase of 7% in the rebound velocity, and 17% in reaction impulse. The grip tightness had a more pronounced effect on the off-centre impacts, resulting in a reduction in ACOR of approximately 15% between the racket centre and tip.

In contrast, Grabiner *et al.* (1983) dropped balls at low speeds ( $10.62\text{m.s}^{-1}$ ) onto a 'freely-rotating' and a handle-clamped racket (267N tension). Rebound velocities were measured using high-speed cameras. Employing a multivariate regression analysis, they observed no difference between the rebound velocities for the different clamping conditions, even on off-centre hits. The researchers noted that the ball inbound velocity used is low but failed to note the effect on transverse racket motion imposed by their 'freely-rotating' clamping method. The method entails a racket suspended horizontally from two wires, attached at the neck and grip respectively, which is likely to resist the impact not allowing completely free motion.

In the same year, Liu (1983) addressed the issue of relative velocities by developing a rigid body model of a static racket and moving ball impact. Substituting constants from Baker and Putnam (1979) and Hatze (1976) yields the same ACOR ratios for both the freely suspended and handle clamped conditions. Further substitution of the experimental ACOR values measured by Watanabe *et al.* (1979) into his equations yielded maximum  $COR_{gc}$  and  $COR_f$  values ranging from 0.80 to 0.95 for an increase in impact speed from  $5\text{m.s}^{-1}$  to  $25\text{m.s}^{-1}$ . The biggest difference between the two clamping conditions was found at lowest impact speeds.



In 1984, Missavage *et al.* developed a similar mathematical model to Liu but solved it using a numerical finite difference method. They found zero moment at the handle of the racket during the time of contact, indicating that the ball has already left the racket before the impulse reached the handle. This implied that the gripping condition does not influence the coefficient of restitution. Notwithstanding, the model predicted that for a drastically stiffened or shortened racket, the grip firmness would affect the coefficient of restitution. Practical tests were performed on a racket stiffened by the researchers, increasing the maximum ACOR from 0.36 to 0.42 from the free and grip-clamped conditions. Similarly, for a shortened racket, the maximum ACOR increased from 0.50 to 0.59. This increase in ACOR is argued to be a result of the increase in stiffness or shorter racket lowering the time needed for the impulse to travel towards the handle, hence producing a positive moment integral i.e. a moment at the hand during impact. This raised the matter of the contribution of frame stiffness and gripping conditions on racket performance, especially with modern rackets being much stiffer than their predecessors.

In 1989 Knudson and White mounted two force-sensing resistors on the handle of a tennis racket (strung at 245N tension) during player tests. The resistors measured the forces in key areas on the hand, while an accelerometer, mounted at the racket's centre of gravity (CG), measured the frame vibration. Players were instructed to return balls, with incident ball velocities of approximately  $12\text{m.s}^{-1}$ , using a natural forehand drive. Comparing the accelerations and force measurements revealed a 2ms delay in impulse, travelling from the racket CG to the handle, which is in the same order of magnitude as the impact duration if it needs the same time to travel back to the impact location.

In the same year, Brody measured the damping characteristics of a free and hand-held racket, using a vibration sensor situated at the throat of the racket. The damping time for free rackets was found to be between 180-750ms,



compared with that of a hand held racket measured as 20-30ms. Furthermore, results indicated a tight grip dampens the vibrations considerably faster than the loose grip and that players perceived the free racket's first non-zero mode, in the range of 120-200 Hz, to be the most uncomfortable (Brody, 1989).

Later, Hatze (1992b) utilised his unique 'manusimulator' in an attempt to reproduce player-testing conditions. The machine incorporated an intricate passive linkage mechanism in order to simulate a forehand drive, with representative gripping conditions. Balls were fired onto a gripped racket at  $16\text{--}26\text{m.s}^{-1}$ , yielding peak  $\text{COR}_s$  measurements of between 0.76-0.88, similar to real play test results of 0.75-0.89, previously recorded by Groppel *et al.* (1987).

In 1992 Leigh and Liu published a model constructed from a combination of springs and dampers, representing the ball, strings and frame. Results indicated the impulse returning from the handle reaches the racket head at 1.7 and 1.2 times the impact time for clamped and free rackets respectively, implying that the gripping conditions would not affect ball rebound speeds. However, the results revealed that a decrease in racket vibration energy would increase the ball rebound velocity. It also showed that the gripping condition has a considerable influence on the vibration modes, hence the location of the node, where the impact excites the least vibrations.

Hatze (1993) developed and published a theoretical model, based on the energy losses in the ball, strings, racket and grip.  $\text{COR}$  measurements were obtained from 'manusimulator' held, rigidly clamped and head clamped rackets. Hatze reported further  $\text{COR}_s$  and  $\text{ACOR}_s$  results for the manusimulator, as well as the  $\text{COR}_{hc}$  for different rackets at  $22.7\text{--}30\text{m.s}^{-1}$ . Only the inbound and outbound ball velocities were measured, providing a direct measure of  $\text{ACOR}$  from which the  $\text{COR}$  was calculated using derived energy balance equations. Typical peak values obtained were:  $\text{COR}_s = 0.83$ ;  $\text{ACOR}_s = 0.43$ ;  $\text{COR}_{hc} = 0.85$ . His results also confirmed a decrease in all  $\text{ACOR}$  and  $\text{COR}$  measures of approximately 3-8% with an increase in incident velocity and that

### CHAPTER 3 RACKET PERFORMANCE INDICATORS

ACOR increases with an increase in the gripping constraint. Another outcome of interest is the good correlation between results from the respective static and moving racket tests, proving that either configuration could be used for testing. Energy losses to the different components were calculated as: strings 2-4%; hand 2%; ball 15% and frame 58-64% with approximately 20% of the original kinetic energy returned to the ball. This substantiated that a decrease in frame deformation could noticeably increase the energy returned to the ball.

In 1993, Kawazoe published an energy model for predicting COR. The model predicted  $ACOR_f$  values at  $30\text{m.s}^{-1}$ , which was compared with real test data at  $26.4\text{m.s}^{-1}$ . Kawazoe found maximum  $ACOR_f$  values of approximately 0.5 and confirmed the variation of COR along the longitudinal axis of the racket reported earlier by Head (1976) and Elliott *et al.* (1980).

Wilson (1995) measured the  $ACOR_{gc}$  over the entire surface of rackets at speeds up to  $19\text{m.s}^{-1}$ . The  $ACOR_{gc}$  map across the entire strung surface was typical, with maximum values of approximately 0.6 at the throat of the racket, except for a second peak located near the tip of the racket. Even though similar studies had been performed previously by Grabiner (1983) and others, this second peak had not been reported before and was not explained during this study.

Later, Brody (1987), and then Cross (1997), confirmed and explained Wilson's findings. For low velocity impacts at the racket tip, the ball impacts at the 'dead spot', as defined by Cross. Initially the ball stops dead at impact while the racket flexes. Before the ball is displaced by gravity, the racket returns to hit the ball for the second time, approximately 15ms later. The net result is a local increase in COR. This phenomenon depends on a match between the racket frequencies and the ball's contact time on the strings, which might explain why it has not been recorded by all researchers.

In 1997, Brody published a rigid-body model based on energy and momentum conservation equations. This model incorporated a single  $COR_{hc}$



value measured for the specific racket, and provided an equation for  $ACOR_f$ . Using the equation, values were calculated for various locations along the racket's longitudinal axis and compared with experimental results. The calculated values ranged from 0.27 at the tip to 0.52 at the throat, while the experimental values ranged from 0.17 at the tip, to a maximum of 0.49 close to the throat, decreasing again to 0.485 at the throat. Brody concluded that controlling service speed purely by limiting  $ACOR_f$  is likely to be inadequate, since the relation between the initial racket velocity and final ball velocity for a serve can be calculated as:

$$v_b = (1 + ACOR_f) \cdot u_r \quad (3.10)$$

which indicates  $ACOR_f$  has a small influence on the ball speed compared with the influence of the racket speed. However, racket speed is dependent on racket inertia, which in turn influences the  $ACOR_f$  and the combined effect of the two opposing influences had not been determined. Brody also calculated the time it takes for the transverse wave to travel from the impact point to the handle and back. Estimating the wave velocity as  $120\text{m.s}^{-1}$ , the time was calculated as approximately 8ms, implying that for an average impact lasting about 4ms, the ball leaves the strings before the impulse returns to the handle. His tests revealed frequencies for the racket's fundamental vibration modes as 23-35Hz for the first grip clamped mode and between 125-200Hz for both the second grip clamped as well as the first free mode. The first mode for the hand-held conditions was found at approximately 150Hz, hence the conclusion that the free condition is the best approximation of real play results.

In the same year, Cross (1997) measured and published the forces, deflections and  $ACOR_{gc}$  values for a ball bouncing on a wooden ruler and an aluminium beam at discrete locations along their length. Cross discovered the beam (i.e. racket) has a well-defined 'dead spot', the point of minimum rebound velocity near the tip of a stationary racket. However, he agreed with Brody

(1997) that this spot acts as the point of maximum rebound velocity for a moving racket. Cross verified his results with an analytical mass-spring model, which indicated a double impact with the mass of the ball almost equal to the mass of the beam. During the same study, Cross also investigated the gripping condition's influence in terms of the impact pulse's speed of propagation in a real racket. Piezoelectric crystals were attached to a static racket, measuring its vibration characteristics under different clamping conditions. The speed of the transverse wave through the racket was estimated to be  $100\text{m.s}^{-1}$  and it therefore travels about 500mm during a contact time of  $\sim 5\text{ms}$ . Since this is shorter than the distance to the handle and back, the ball would have left the strings and gripping has no effect. The fundamental frequency at  $\sim 23\text{Hz}$  for the clamped condition was not present in the hand held racket, indicating the clamped racket does not truly represent the hand held racket. On the contrary, the fundamental frequency of 100Hz which was present corresponded better with the fundamental frequency of the free racket. Furthermore, two vibration nodes were present in the hand held racket; one at the middle of the strings and the other near the thumb, corresponding to the nodes of the free condition. The handle clamped and hand held conditions similarly damp the high frequency modes by a factor of 10 and the hand held condition reduces the fundamental frequency of the free racket from 110 to 100Hz. Cross concluded that the hand-held racket vibrations are better simulated by the free condition.

In the following year, Cross (1998b) reported further racket vibration experiments, by attaching a piezoelectric element and capacitance plates to the racket tip. The respective fundamental frequencies measured for grip pivoted, hand held and free conditions were 85Hz, 102Hz and 109Hz. The fundamental vibration modes for the freely suspended and gripped rackets were found to be very similar with the node at the tip having virtually the same location, while the node at the handle was shifted further towards the butt, at the location of the hand. Similar to Brody (1995), the decrease in frequency from the freely suspended to the gripped racket was proven to be the equivalent of adding a



40g mass to the end of the racket. Adding the mass did not result in the shift in node location though, and he concluded that this is not achievable with any mass.

Another series of tests were performed with a hand held racket, with piezoelectric cells fitted at discrete positions from the tip to handle. Cross observed that the pulse propagation is faster than the analysis of the fundamental mode implies ( $143\text{m.s}^{-1}$  rather than  $80\text{m.s}^{-1}$ ), since the impact excites higher vibration modes as well. Using a kinematic model for the upper arm, forearm and racket chain, he further concludes that the hand plays an important part in racket performance for impacts away from the COP (Cross, 1998a).

In 1999, Cross was the first to publish a flexible beam model. Cross used experimental measurements from a ball impacting an aluminium beam at  $1\text{m.s}^{-1}$  to determine model parameters and verify its accuracy. The model was further refined for a graphite racket and results compared with previous rigid body models. Comparing the rebound characteristics and mode shapes indicated that the model provided a more realistic representation of the impact. The model predicted significant differences in ACOR values measured close to the racket throat for the clamped, pivoted and freely suspended conditions. Peak COR values of about 0.4 were measured at about 200mm from the tip for the pinned and freely suspended conditions, while the COR continued to increase towards the handle.

According to recent work published by Cross (2003a), the development of modern racket technology might eliminate the effect of the node on perception altogether. Through vibration measurements on a rackets, Cross proved common impact theory, which states that an impact will only excite the frequency lower than the inverse of the contact time. Hence, if manufacturers manage to increase the stiffness and decrease the weight of rackets to result in a fundamental natural frequency of more than 200Hz the duration of the

excitation ( $5\text{m.s}^{-1}$ ) due to impact will be too long to significantly excite any of the important vibration modes, since they would all be above 200Hz.

A summary of all the COR results gathered by the various researchers under particular grip conditions is presented in Table 3.1:

Year	Researcher	COR /ACOR <sup>†</sup>					Ball speed ( $\text{m.s}^{-1}$ )
		hc	gc	f	ph	ps	
1976	Head	-	0.6	-	-	-	27
1993	Kawazoe	-	-	0.5 <sup>†</sup>	-	-	26.4
1984	†Missavage <i>et al.</i>	-	-	0.36 <sup>†</sup>	-	-	25.3
		-	0.42 <sup>†</sup>	-	-	-	25.3
1982	Elliott.	-	-	-	-	0.65 <sup>†</sup>	22.7
1993	Hatze	-	-	-	-	0.83	21.2
		-	-	-	-	0.43 <sup>†</sup>	21.2
		0.80	-	-	-	-	21.1
1980	Elliott <i>et al.</i>	-	0.5 <sup>†</sup>	-	-	-	21
1992	Hatze	-	-	-	-	0.89	20
1997	Brody	-	-	0.49 <sup>†</sup>	-	-	20
1979	Watanabe <i>et al.</i>	-	0.44 <sup>†</sup>	-	-	-	19.3
		-	-	-	0.43 <sup>†</sup>	-	19.6
		-	-	0.43 <sup>†</sup>	-	-	16.5
1995	Wilson	-	0.6 <sup>†</sup>	-	-	-	19
1979	Brody	0.85 <sup>†</sup>	-	-	-	-	8.5

† Performed on artificially stiffened racket  
Subscripts: hc = head clamped; gc = grip clamped; f = freely suspended; ph = player held; ps = simulated play

Table 3.1: Summary of maximum COR and ACOR (indicated with <sup>†</sup>) results from the literature.

3.2 Alternative performance indicators

3.2.1 Max ball speed under constant test conditions.

Another ‘simplification’ to the COR definition would be to keep the relative velocity before impact constant and simply measure the ball velocity after impact as an indication of the racket power (Elliott 1983; Elliott *et al.*, 1995). This is, in effect, the ACOR but a direct measure rather than a calculated ratio.

A velocity is a simple entity for players to relate to, making it an appealing as a racket performance indicator.

### 3.2.2 ACOR with power input

Brody *et al.* (2002), defined racket 'power' as the ACOR of the racket. Due to the interdependence between racket mass, racket speed and the ACOR, it was proposed to be the power needed to get the racket up to speed into consideration when determining the racket speed at which to test the ACOR. It was estimated that during a serve a 10% drop in racket mass should result in a 3.3% increase in racket head speed.

### 3.2.3 Kinetic energy definitions

Various kinetic energy (K.E.) ratios might be used as 'power' indicators, such as:

$$Power = \frac{K.E._{ball}^{post-impact}}{K.E._{racket}^{pre-impact}} \quad (3.11)$$

or the change in kinetic energy ( $\Delta K.E.$ ):

$$Power = \frac{\Delta K.E._{ball}}{-\Delta K.E._{racket}} \quad (3.12)$$

In order to measure the kinetic energy of the racket and ball all translational and rotational components need to be measured and mass/MOI properties need to be known.

### 3.2.4 Babolat RDC power definition

Babolat's Racket Diagnostic Centre (RDC) has long been used as an industry standard to provide an assessment of racket 'power' for players, coaches and distributors. The RDC is a machine developed to measure racket



### CHAPTER 3 RACKET PERFORMANCE INDICATORS

characteristics including mass, balance, stringbed stiffness and frame flexibility. Power is calculated by:

$$Power = (li.hs.RA)/10 \quad (3.13)$$

where  $li$  is the length indicator (26" = 0.9, 27" = 1, 28" = 1.1, 28.5" = 1.15, 29" = 1.2),  $hs$  the head size (in sq. in.) and  $RA$  is the frame flexibility measured with the RDC for a strung racket, simulating a 3-point bending test (Babolat manual 1999, Lindsey 1997). In 2000, the United States Racquet Stringing Association (USRSA) adapted the definition in order to correlate better with their player test results:

$$Power = (li.hs.RA.I_{sw})/1000 \quad (14)$$

where  $I_{sw}$  is swing weight in kg.cm<sup>2</sup>, measured with the RDC (Lindsey, 2000a). The definition has been shown to provide a useful tool for comparing subjective racket performance but is unlikely to be acceptable as an international tennis regulation. Although most parameters have been linked to power in the literature, the formula was not derived scientifically, undermining its validity.

#### 3.2.5 Mathematical models

In 1997, Brody proposed using a formula to calculate the velocity ratios for a general impact. The racket is assumed to be a rigid body and by combining the conservation of linear and angular momentum theory, the solution simplifies to a formula consisting of standard measurable racket properties, except for the  $COR_{hc}$ , which needs to be determined experimentally across the centreline of the racket face. Simplifying the equation for a serve calculates the ACOR:

$$ACOR = \frac{1 + COR_{hc}}{\frac{m_r \cdot d^2}{I_{cg}} + 1 + \frac{m_b}{m_r}} \quad (3.15)$$



where  $I_{cg}$  is the racket's MOI about the CG,  $d$  the distance from the impact point to the CG and  $m_b$  and  $m_r$  the respective ball and racket masses.

Goodwill and Haake (2000) advanced Brody's formula by including calculation of the racket recoil and ball velocity after impact. During the same time, Cross (1997) had been developing a model similar to that of Leigh & Lu (1992), where both the ball and racket were modelled as mass/spring units connected in series. The model was improved soon after (Cross, 1999) by replacing the simple beam mass with a two dimensional flexible beam model, and then again by Cross (2000d) to include off-centre impacts. The model consisted of a segmental solution derived from the free-free beam deflection equation in Graff (1975), with spring models for the ball and strings. Goodwill & Haake (2002b, 2003) enhanced the model once more by adding dampers to the springs for the ball and strings. Instead of applying the force as a point load like Cross, it was improved by applying it as a non-linear distributed load. This is more realistic since the force in the racket is applied to the frame through the stringbed, which distributes the load to all the points of contact with the frame. Frame displacements calculated by the model appear to be very accurate for impacts at and below the GC (geometric centre), compared to the experimental data, while the rebound ball velocities correlated very well across the entire racket face. Comparing the results of the flexible models with the simpler rigid body model, revealed similar rebound speeds for impacts at the nodes, since no energy is lost to frame vibrations but the difference increases for impacts away from the node, especially for impacts below the node. There is a clear trade-off between the accuracy of the models and the development and computation effort involved in producing the results.

Quantifying the racket 'power' using any of these models, rather than a real racket test could have the advantage of less effort and smaller investment in test equipment. Although most models require considerable testing in order to obtain the necessary parameters for them to be accurate. A foreseeable

limitation of the use of models would be their application to new racket technologies. A simple example would be the inclusion of active piezo fibres in the racket beam, as introduced by Head in 2000 (Lindsey 2000c, Kotze *et al.* 2003, Lammer & Kotze 2003). This technology is claimed to increase racket 'power' but these mathematical models have no component simulating the effect of this enhancement.

Researchers have also developed other analytical and finite element models (Brannigan and Adali 1981, Missavage *et al.* 1984, Leigh and Lu 1992, Kawazoe 1993). In general, to more accurately model real systems using numerical methods (e.g. finite element analysis), model complexity and computational time increase as does the difficulty and number of tests required to prove validity. These models can only ever embody known racket design behaviour, and as such cause problems for establishing an enduring assessment method when compared to testing under controlled real-play simulated conditions. Thus they are useful as design optimisation and research tools but not as credible quantitative racket performance indicators.

### 3.3 Influence on further testing and the PDS

Considering trends in other sports such as golf, the optimal balance needs to be found in the design, to satisfy the demands in test accuracy and repeatability, as well as the desire for a realistic stroke production and since the serve is believed to be the most critical stroke influencing the speed of the modern game, the machine will need to mimic expected serve conditions achievable by the top tennis men's tour players.

In order for the test machine to measure all the considered definitions described in the section it would need accurate measurements of the ball and racket speeds before and after impact and with an expected contact time of



about 5ms the minimum sample rate of the measurements should be in the order of 1ms or 1kHz.

The maximum performance for all the definitions is located somewhere on the racket centreline, requiring measurements only along the centreline. For a comprehensive investigation of racket performance, the test machine should be able to test impacts along virtually the entire racket face, without the ball touching the racket frame.

Other racket properties such as the mass, balance, MOI, length, frame stiffness and stringbed stiffness should also be measured in order to calculate some of the desired definitions but these could be measured on other industry standard machines such as the RDC. Similarly, the properties of machine components such as the gripping device, which might contribute to the racket's performance should be known and included in calculations if needed.

Tests in the literature have been performed at relatively low impact speeds of up to  $30\text{m.s}^{-1}$ , which are not believed to be representative of serve speeds of up to  $66.6\text{m.s}^{-1}$  recorded for professional players at the time. These results from the literature would therefore need validation at higher impact speeds in order to correlate the final design for the test machine. The maximum head speed which needs to be achievable during future testing is calculated in Chapter 6 by combining the maximum ball speed which needs be achieved with the maximum ACOR measured for all tested rackets.

The literature revealed that, for the more modern stiffer rackets, the speed of the impulse propagation thorough the racket frame is increasing to an extent where the influence of the gripping condition is increasing and would have to be investigated for the latest racket designs at realistic impact conditions.

## Chapter 4

### Racket Performance Testing

From a thorough study of existing research on racket performance and test methods, shortcomings in that research were established for further investigation in order to generate the PDS for the test machine. This chapter highlights these shortfalls then devises and executes the necessary tests to provide the required information.

*Ball rebound characteristics:* The literature revealed concerns regarding the variability of tennis ball properties. Since all studies in this research would involve racket/ball impacts, one of the major concerns was the change in ball rebound performance over time and with number of impacts.

*Modern racket properties:* Most of the laboratory tests investigating racket rebound characteristics were performed on relatively old equipment. In contrast, the research question is mainly concerned with the speed of the game as influenced by modern rackets. Further, in order to establish a reference for comparing the test machine's accuracies once it is built, the comparative tests had to be performed on the same set of tests rackets using current test methods, such as the ball-cannon tests.

*Impact speeds:* Tests reported in the literature were performed at relatively low speeds, not higher than  $\sim 30\text{m.s}^{-1}$ , which is representative of a good forehand stroke but not of a professional first serve. The research question, which demands the development of a realistic high-speed test machine to assist

## CHAPTER 4 RACKET PERFORMANCE TESTING

in researching and imposing test standards for regulating the speed of the game, calls for test results at higher impacts speeds.

*Gripping conditions:* One of the most controversial issues in the literature involves the effect of the gripping condition on racket rebound characteristics. Several investigations conducted to determine the most representative condition to be used during laboratory tests have produced no clear agreement. It is obvious that it is neither of the two extreme conditions; the freely-suspended and the rigidly-clamped conditions, most commonly used. These conditions are the easiest to produce accurately and repeatably though, compelling researchers to use them and spurring the debate on which is the most representative, or which intermediate solution should be adopted. The results have been inconclusive with tests being performed on relatively old and considerably different equipment, subjected to dissimilar impact conditions.

*Impact location:* No recorded tests have provided tangible evidence indicating the optimum impact location during play. Four sweet spot definitions had been identified (COP, vibration node, area of max ball speed and the dead spot) and various theories had been put forward as possible locations for the impact for different strokes, although this has never been confirmed with real measurements, especially for the serve. The impact location for the serve is claimed to be higher up the racket face due to the higher head speed towards the racket tip, resulting from the racket rotation. Given that the research objective is concerned with the maximum ball speed a player can generate with a racket, the impact location during a real serve and the relation to the sweet spots could provide the optimum impact location to be measured for investigating racket performance.

Consequently, laboratory tests were devised to further investigate these uncertainties. A set of ball rebound tests performed via multiple impacts of a ball over time would address the consistency of existing tennis balls. Next, racket rebound tests on the control group of modern rackets used throughout



the research would be performed at more representative serve speeds. This would yield the rebound characteristics of modern rackets under realistic serve conditions and simultaneously provide data for later comparison between ball-cannon tests and tests with the developed machine. In addition, these tests would be performed under different gripping conditions in an attempt to resolve the most representative gripping condition. Finally, in order to explain the real impact location during a serve, which would be measured in Chapter 5, the set of control rackets would be subjected to a modal analysis. This would provide the location of the vibration nodes for each racket, which is one of the sweet spots linked to the optimum impact location.

## 4.1 Test set-up and equipment

### 4.1.1 Rebound test set-up

The test set-up for all the racket rebound tests is illustrated in Figure 4.1

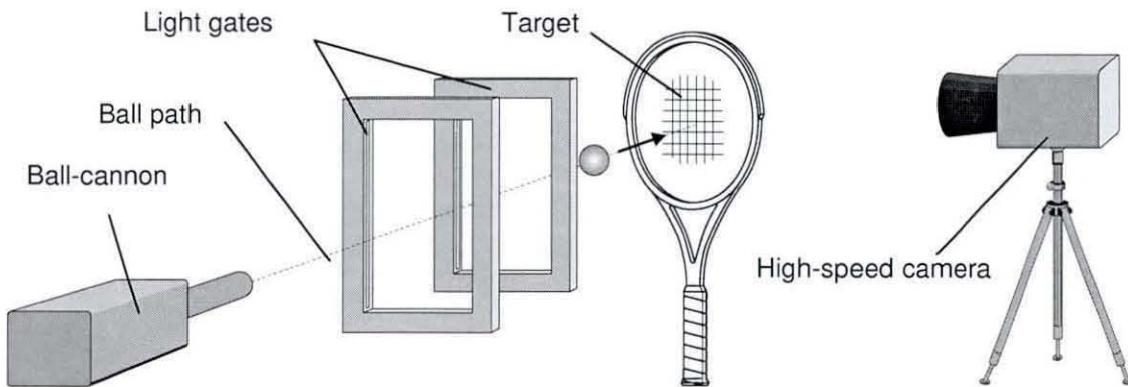


Figure 4.1: The setup used during the ball cannon rebound tests.

A ball-cannon was used to fire balls at a target mounted normal to the ball path. The ball passes through a set of light-gates, which measures inbound ball speed before impacting with the target. Depending on the target's boundary conditions and COR, the ball could return in the opposite direction, in which

case its speed can be measured when the ball moves in the opposite direction through the same light gates. If the COR of the target is low or the boundary constraints are weak, the ball may continue in the same direction as before the impact and an additional system is needed to measure the speed. For the latter case, a high-speed camera recorded a side view of the entire impact, which was digitised to determine the speed of ball and/or the target after the impact.

### 4.1.2 Ball-cannon

The main piece of equipment used for the testing was a pneumatic ball-cannon, which consisted of a ball chamber in which a ball is loaded and sealed manually and fired at the target through the release of the pressure valve. The ball is propelled through a 1m barrel (70mm internal diameter) towards the target, which is about 0.8m removed. The cannon, including the light-gates, is enclosed in a durable extruded aluminum profile cage to which the target is attached. The cage is fitted with transparent polycarbonate panels, which contain all moving objects, thus protecting the operator and the equipment, as well as eliminating environmental influences, while still providing sufficient visibility to allow video recording of the impact.

At the onset of this research the ball cannon could achieve ball speeds of up to  $39\text{m.s}^{-1}$ , which is representative of a relatively high serve-speed but not up to the desired  $50\text{m.s}^{-1}$ . Ultimately, for the final head-clamped tests, a mechanical booster was added to the pressure system, which increased the reservoir pressure from about 380kPa to 550kPa and the line supplying the air to the ball chamber was rerouted to feed directly from the reservoir instead of the old pressure system as before. This increased the maximum possible impact speed from  $39\text{--}52\text{m.s}^{-1}$  (Cotter, 2002).

Other commonly used machines incorporating wheel mechanisms were also considered as alternatives to the ball-cannon. One such machine is the Bola, which consists of two spinning wheels separated at a distance considerably less

than a ball's diameter apart and accelerates the ball by squeezing it through wheels rotating in opposite directions. The authors experience with the machine revealed that the maximum achievable impact speeds with these machines are relatively high, at the expense of impact location and ball speed accuracies. Furthermore, the machines considerably increase ball deterioration due to the extreme deformation and surface abrasion caused by the wheels as well as introducing spin to the ball, resulting from the differences in wheel angular velocities (Haake *et al.* 2000a).

### 4.1.3 Light-gates

Two ballistic light-gates, 195mm apart, are positioned between the barrel and the target measuring the normal pre- and post-impact ball speeds. The light-gates were calibrated against an electronic timer/counter as part of concurrent research and found to have a linear relationship ( $R^2=0.85$ ) with the electronic timer measurement. It was also calibrated against measurements from a Kodak Ektapro HS 4540 high-speed camera (described in the next section) at 4,500fps for the range 25-40m.s<sup>-1</sup> and found to have an accuracy of <4% (Cottey, 2002).

### 4.1.4 High-speed camera

During the racket rebound tests, a high-speed camera was used to determine the racket post-impact velocity. The camera had a maximum recording rate of 40,500fps, and could record up to 3,072 full frames in its onboard solid-state memory, which was downloaded after the recording. The camera was placed normal to the ball path, about a metre away from the impact, with the optimum lens and highest frame rate providing a clear enough image of the ball path and the racket. The optimum set-up resulting in the highest accuracy is a trade-off between the image pixel resolution, recording frame rate and zoom. Lower frame rates allow a higher pixel resolution, which increases the accuracy of the digitising process, while an increased frame rate



increases the measurement accuracy via the smaller time intervals. Similarly, an increased zoom results in a higher image quality, hence improving digitising accuracy, while zooming out increases the field of view, thus allowing digitising over increased object movement during the same time interval. An optimum was found with a frame rate of 9,000fps, recording a landscape image of 768x384 pixels. The landscape view had the advantage of increasing the field of view for movement in the ball path, without sacrificing image quality or frame rate but the disadvantage is that it clipped the racket's tip and butt. The lack of an entire racket image meant some rotational racket parameters, which could otherwise be measured, could not be digitised accurately from these images.

### 4.2 Ball rebound testing

The research sets out to develop a repeatable test machine, therefore the first stage of the racket testing was to eliminate, or understand, the effect of other variables, which might influence the repeatability of results. One variable in most racket impact tests is the ball, justifying some investigation of its consistency. Information from the ITF (Coe, 2000) at the onset of the research implied a significant inconsistency in balls available on the market, in spite of the ball being one of the most strictly regulated pieces of equipment.

One of the most important ball specifications is the 'drop test', which states that if a ball is dropped from 100" (2.540m) onto a hard concrete surface the ball should rebound between 53" (1.346m) and 58" (1.473m). Calculating the COR from the rebound height, yields:

$$COR = \sqrt{\frac{h_r}{h_d}} \quad (4.1)$$

## CHAPTER 4 RACKET PERFORMANCE TESTING

which neglects drag and contains  $h_r$  as the rebound height and  $h_d$  the drop height of the ball from the bottom of the ball to the bounce surface, resulting in a COR of 0.73 - 0.76. The balls intended for use during the research were specially selected by the manufacturer for tournament play and should therefore all conform to this specification. Nevertheless, the drop test is performed at a very low speed ( $\sim 7\text{m.s}^{-1}$ ) compared to the racket speed during a serve, which caused some concern as to how they would perform at representative speeds.

In order to avoid a full scale testing of all ball brands and types, which is not the focus of the research and very unlikely to happen during real testing, a common tournament ball type was selected and subjected to ball-cannon COR testing to investigate the behaviour and consistency at higher speeds and in so doing assess their suitability for use throughout the research.

Three Dunlop Max TP tennis balls, fresh from the same can were fired with the ball-cannon at a rigid concrete slab using the set-up described in §4.1. Inbound and rebound ball speeds were measured using light-gates, with inbound speeds varying between  $35.2\text{--}38.5\text{m.s}^{-1}$  due to inconsistency of the cannon. The COR was calculated for 100 impacts, which was the longest expected usage of a ball during future testing. The tests were performed in two sets of 50 impacts, carried out over two consecutive days in an attempt to determine how the rebound characteristics change over time after being taken out of the can. The impacts were performed at about three minute intervals to eliminate the effect of the rubber heating as a result of the deformation.

The coefficients of restitution for the balls were measured as 0.458 ( $\sigma=0.006$ ) for ball A, 0.443 ( $\sigma=0.005$ ) for ball B and 0.448 ( $\sigma=0.005$ ) for ball C, which indicated the standard deviation for each ball was insignificant, while variations between the balls were significant. Ball A had an appreciably higher COR (3%) than ball B and ball C, substantiating the ITF's claim regarding inconsistencies between balls. The average COR for all three balls was 0.449

( $\sigma=0.008$ ), which was much lower than the 0.73 - 0.76 specified by the ITF's standard drop test, where the ball is dropped from a height of 2.5m, resulting in a much lower ball speed of  $\sim 7\text{m.s}^{-1}$ . During the high-speed impact much more energy is lost to the ball due to the increased ball deformation, reiterating the need to perform all ball/racket impact tests at representative speeds. A linear trend fitted through the data (Figure 4.2) indicated an average drop in COR for all three balls of  $\sim 1\%$  over the 100 impacts, which were believed to be acceptable for using the balls in future.

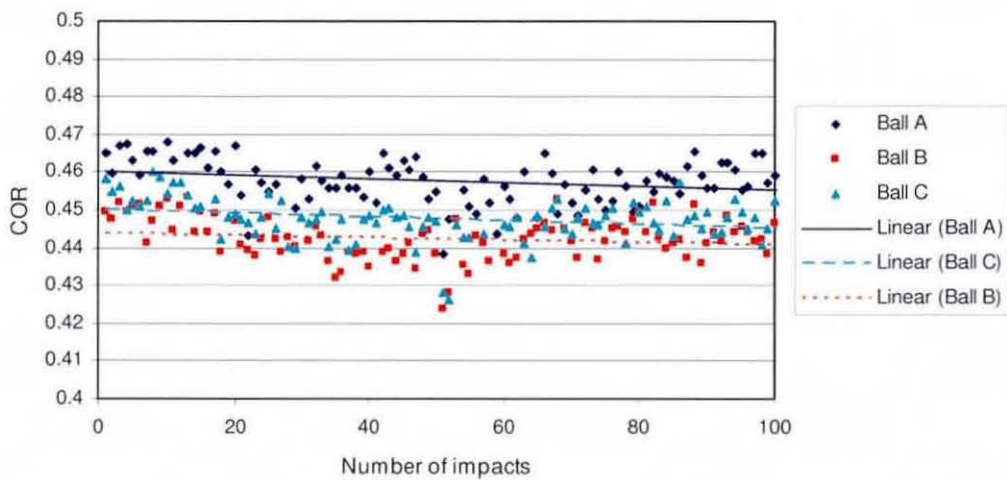


Figure 4.2: The COR measurements for three new Dunlop Max TP balls fitted with a linear regression.

Interestingly, fitting a second order polynomial through the data (Figure 4.3) revealed an initial decrease in COR in the central region of the tested impact range.



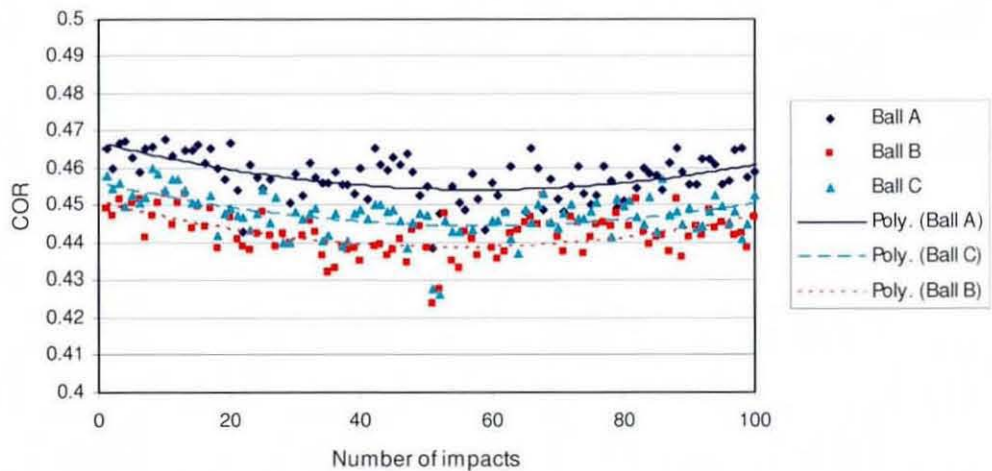


Figure 4.3: The COR measurements for three new Dunlop Max TP balls fitted with a second order polynomial.

To locate the minimum, the total impact test range was subdivided into groups of ten impacts, and T-test used to compare each section with the first ten impacts. The most significant difference for all three balls ( $p=0.001$ ) was consistently found between 40 and 60 impacts for all three balls. This was only explained when compared with the impact speeds, which revealed a peak for the same impacts (Figure 4.4).

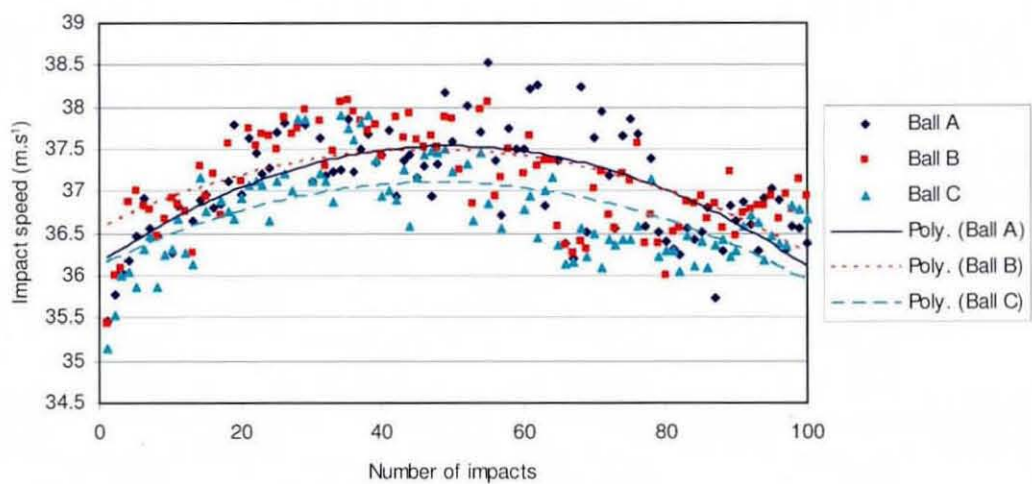


Figure 4.4: The impact speed for three new Dunlop Max TP balls fitted with a second order polynomial.

## *CHAPTER 4 RACKET PERFORMANCE TESTING*

According to the literature an increase in impact speed would cause a decrease in ball COR (Bernstein 1977, Goodwill & Haake 2004). This was confirmed by fitting a second order polynomial through the impact speeds, indicating a peak in impact speed towards the 40-60 impact zone where the COR was the lowest. This change in impact speed ( $\sim 3\text{m.s}^{-1}$ ) caused by the inconsistency of the ball-cannon appeared to have a more significant effect on the ball COR than the number of impacts, which flagged the consistency of the impact speed as an important parameter to control during the development of the test machine.

It is concluded that for impact speeds varying between  $35.2\text{--}38.5\text{m.s}^{-1}$ , fresh Dunlop Max TP would have a COR of about 0.45. Each ball performed consistently without a significant change in COR over the first 100 impacts and after a reasonable time outside the can but COR varied up to  $\sim 3\%$  between balls from the same can. It is therefore proposed that for rebound testing new balls are used, for not more than 100 impacts, to be safe not for longer than 24hrs and to improve test consistency balls with similar COR could be pre-selected after a small set of impact tests.

Although the COR did not change considerably over the impact range the balls did show some signs of external deterioration in the form of hair loss, small cracks in the seam glue and loosening of the felt but it did not seem to affect their COR. This suggested that less consistency might be found for angular impacts, since the deterioration in surface condition might cause the ball to slide more on the string surface, affecting the rebound angle and possibly the rebound speed. This should not cause any problems during the current research, since it is only concerned with impacts normal to the racket face. Moreover, impacts on the concrete surface should be considerably more abrasive than those on a racket string bed. Another factor diminishing the influence of the variance in ball properties during ball/racket impacts is the

decreased ball deformation, resulting from more energy being absorbed by the string deformation.

The tests raised a concern about the accuracy of the ball-cannon's impact speed regulation, which appeared to have a considerable influence on the COR. Initially it was not clear what caused this variance; hence different solutions were investigated during later testing.

### 4.3 Racket rebound testing

Three sets of racket rebound tests were performed on the same rackets under different extreme gripping conditions to enable comparison between the three extreme gripping conditions in order to include the widest range of conditions possible. The entire face needed to be tested to enable a comparison with the distribution profiles from the literature as well as to define the optimum impact location to be used later during machine testing. Varying the impact horizontally across the racket face, as well, would demonstrate the rackets' sensitivity to off-centre impacts, which would reveal the influence of the impact accuracy on the machine's repeatability. Further statistical analysis of the variance in test results would provide a preliminary indication of the number of parameters (i.e. impacts, impact locations or the density of the impact grid) needed to achieve statistically significant results when performing tests with the intended test machine. In addition, since the ball-cannon is a commonly used test machine, its repeatability would serve as a benchmark for the developed machine.

#### 4.3.1 Freely suspended racket test set-up

The same test set-up described in §4.1 was used to fire balls at a racket suspended freely from a pin as indicated in Figure 4.5. This presented the racket



in its natural freely suspended condition, believed by many to be the most representative and functional test condition.

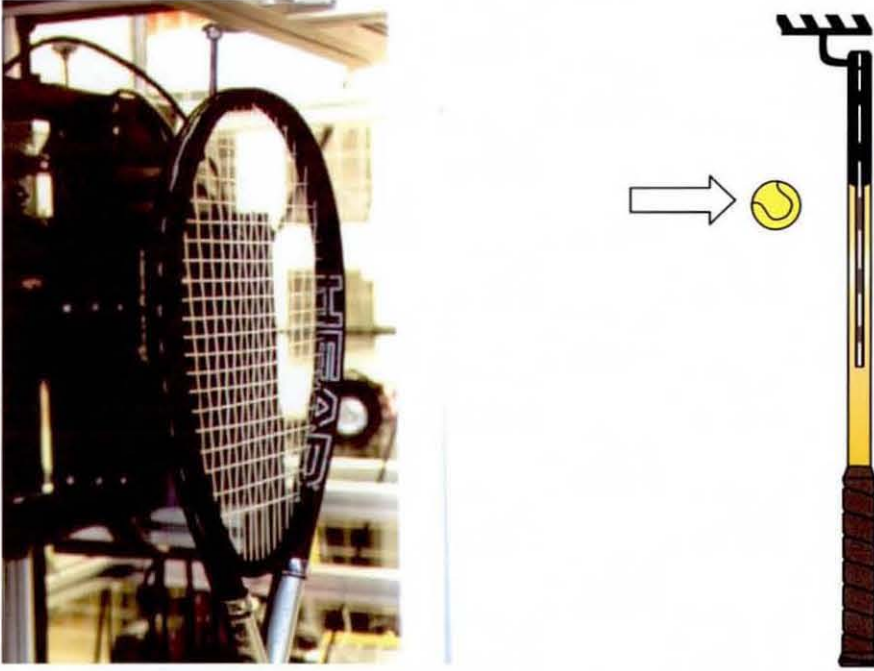


Figure 4.5: The test set-up for the freely-suspended racket rebound tests.

A side-view of the impact was recorded with a KODAK EktaPro high-speed camera, at 9,000fps for determining the post-impact racket speed, while the inbound and rebound ball speeds were measured via paired light-gates. The racket was caught after the impact with soft feather padding and had to be carefully repositioned on the pin and normal to the ball path after each impact.

A set of eight trial rackets with a large spread of important properties such as length, mass and MOI were selected to represent the contemporary spectrum of 'playable' rackets. The extremes ranged from the lightest oversized rackets, to the heavier small sized tour player rackets.

The selection included four Head Titanium Ti.S6 rackets (rackets A-D), selected because they were the lightest rackets available on the market at the onset of the project. The mass and MOI of these rackets were modified, to provide a control group of identical rackets, apart from their mass distribution. The lightest racket (racket A) was kept with its original properties, while lead

tape was applied to the throat area of rackets B-D, to produce a range of mass and MOI (swing weight) properties incrementally increasing from the lowest to the highest available on the market (Table 4.1).

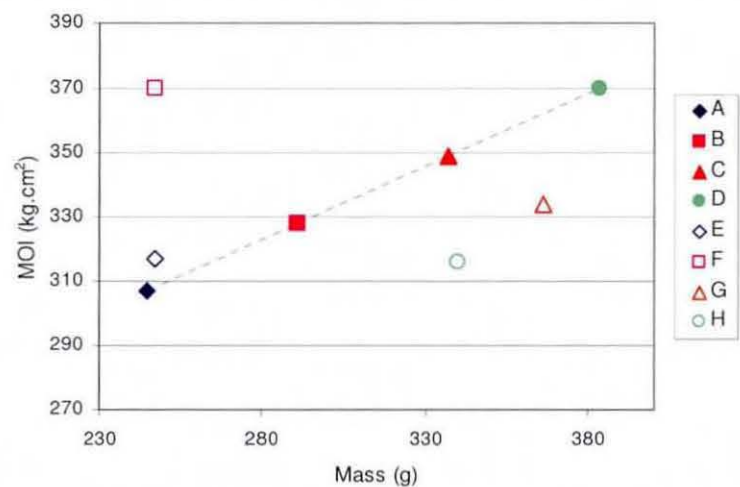


Figure 4.6: Showing the MOI vs. mass of the eight selected test rackets, with a linear trend designating the incremental increase from Rackets A-D.

The remaining four rackets were chosen to represent other mass/MOI combinations within this envelope and simultaneously introduce other extreme parameters into the control group. Racket E is a Head Titanium TiS7, which does not have a throat piece and therefore its main strings are longer than allowed by the ITF rules. This racket represents a very ‘powerful’ lightweight construction. Racket F is a Dunlop MAX Super Long +2.00, which is 49mm longer than the standard racket, hence increasing the inertia of the racket and the possible impact distance from the handle. Combined with the oversized head and the inverted pear-shaped racket face, the racket should generate high ball speeds, especially at distal impact locations. Racket G is a Wilson Pro Staff 6.1 Tour Edition 95 and Racket H a Dunlop Revelation Max 200G, both representing the more common handle heavy tour rackets used by more experienced and professional players for whom ball control is more important.





Figure 4.7: The control group of test rackets. A-D: Weighted Head Ti.S6, E: Head Ti.S7, F: Dunlop Max Superlong 2.00+, G: Wilson Pro Staff 6.1, H: Dunlop Revelation Max 200G.

All rackets were strung with the same strings at 245N (55 lbs) and their properties measured on the Babolat RDC. Figure 4.7 shows all the rackets used and Table 4.1 their individual measured properties.

Nr.	Model	Mass [g]	MOI [kgcm <sup>2</sup> ]	Balance [mm]
A.	Head Ti.S6	245	307	384
B.	Head Ti.S6 (weighted)	291	328	386
C.	Head Ti.S6 (weighted)	337	349	378
D.	Head Ti.S6 (weighted)	383	370	379
E.	Head Ti.S7	247	317	387
F.	Dunlop Max Superlong 2.00+	273	370	382
G.	Wilson Pro Staff 6.1	366	334	313
H.	Dunlop Revelation Max 200G	340	316	310

Table 4.1: The properties measured for each test racket on the Babolat RDC.

Impacts were measured for 10 different locations as shown in Figure 4.8, seven on the centreline and three off-centre.

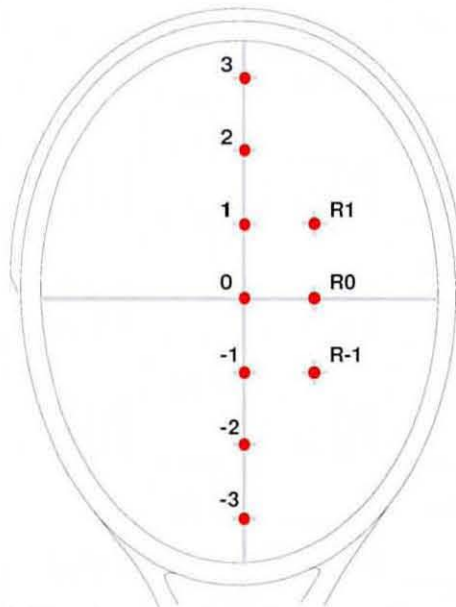


Figure 4.8: The impact locations on the racket face.

Location 0 is at the geometric centre (GC) of the racket head, with the Locations 1 and 2 at 50mm intervals towards the racket's tip, while Locations -1 and -2 are similarly towards the throat. Locations 3 and -3 were as close as possible to the tip and throat of the racket respectively, without touching the racket frame during impact. Locations R1, R0, R-1 are 50mm removed from the centreline, positioned on the same height as their centreline counterparts. New Dunlop Max TP tennis balls, the same type tested in the ball rebound tests, were fired at the racket at a mean speed of  $37.2\text{m.s}^{-1}$  ( $\sigma=1.8\text{m.s}^{-1}$ ). This was lower than was hoped for but this was the highest possible speed at the time and adaptation of the cannon to achieve higher speeds was still under investigation. Initial experimentation indicated that performing three impacts per impact location provides statistically significant results.

During the data analysis, it became apparent that the light-gates recorded several unrealistic values for the rebound ball speed, compelling the manual digitisation of all measurements from the high-speed camera footage. These malfunctions occurred at extreme locations such as side impacts and impacts close to the racket tip, where the ball had such low rebound speeds that it is almost stationary after impact and does not travel all the way to the light-gates

or was significantly affected by gravity. Furthermore, during side impacts the ball often hit the side of the light-gates, since it does not return on its incoming ball path. The inbound light-gate speeds, which were believed to be accurate, were nevertheless compared with the digitised values to calibrate them for future use and to ensure no errors were made during the digitisation. A maximum difference of  $2.96\text{m.s}^{-1}$  ( $\sigma=0.48\text{m.s}^{-1}$ ) was measured between the light-gates and the digitised values, which indicated both systems are sufficiently accurate but problems that could occur if light-gates were used particularly with stationary racket/moving ball tests to measure rebound ball speeds for light-weight rackets, which generate the lowest ball speeds.

In order to determine the pixel to distance ratio for digitisation of the impacts, a distance calibration sheet, with a 50mm grid, was placed in the vertical plane through the inbound ball path and digitised afterwards. To minimise disc space and download times from the camera to the pc, only five images needed for calculating ball incident, ball rebound and racket rebound speeds were downloaded from the camera memory for analysis (Figure 4.9). Images (a) and (b) determines the ball impact speed, (c) and (d) the post-impact racket speed and (c) and (e) the post-impact ball speed.

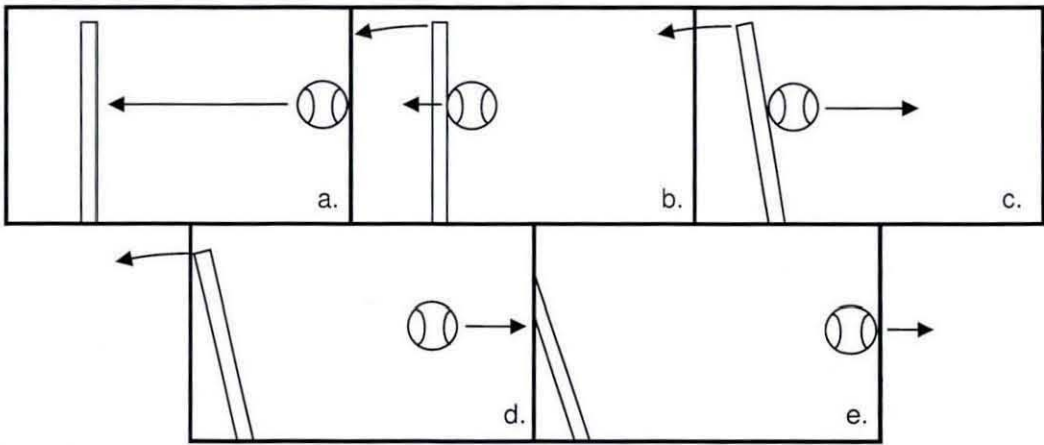


Figure 4.9: The orthographic image sequence needed to calculate the impact speeds.

The images were digitised in a specific software program (Flightpath), developed by Loughborough University. The software was developed to



facilitate digitising still images of moving sports balls, taken under fixed period stroboscopic/multiple flash lighting conditions. It was therefore limited to digitising moving objects overlaid on a single image, with particular dimensions and in the Windows Bitmap (BMP) format. Hence all downloaded images had to be resized, enhanced and converted from JPEG into BMP format and then overlaid so that the two instances of the object to be digitised appeared on the same image. This was programmed in Corel Photo-Paint and performed in an automated batch conversion.

### 4.3.2 Freely suspended data analysis

The Flightpath software was later found to be insufficient for accurately digitising the racket speed after impact. The software was originally developed for round golf balls, incorporating an elliptical selection function for the discrete ball images, to calculate their geometrical centres and the distance between them. Combined with the time intervals between balls and conversion ratios from the calibration image, the ball velocities between images were determined. Therefore, in order to digitise the moving racket, which included a degree of racket polar rotation for misaligned impacts, the rotation resulted in a perspective view of the racket (Figure 4.10) instead of a simple 2-dimensional side view (Figure 4.9), which was needed to accurately digitise the racket. In addition, the racket is not a sphere or an ellipse, which is expected by the software, instead it consisted of a 'virtual' impact location, whose exact position needed to be derived from 'landmarks' such as the string holes, which are visible on both images.

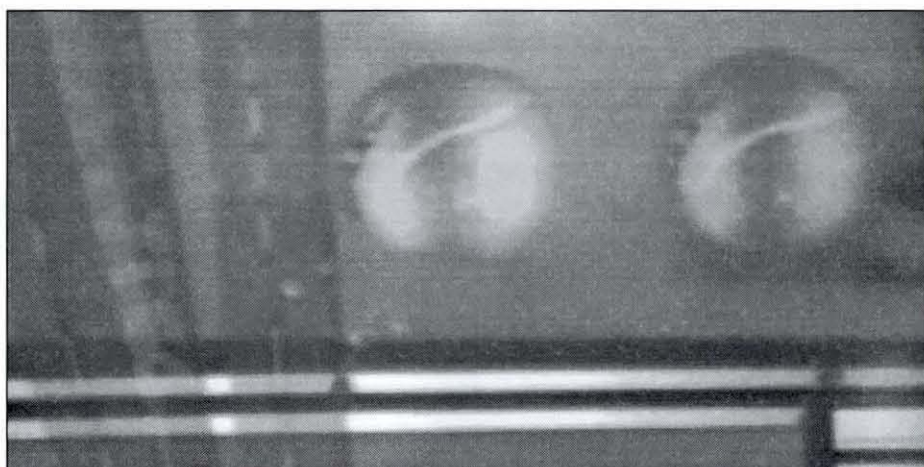


Figure 4.10: A typical overlaid image for determining the racket velocity after impact.

This dictated the development of a special program in Visual Basic, dedicated to digitising the rackets. Similar to the Flightpath software, the program opens the captured images and provides a construction method for determining the impact point on the strings. In addition to the new functionality, the developed software can also open the raw JPEG images captured, without the need for overlaying or enhancing, which resulted in a clearer digitised image and higher accuracy.

Due to the racket rotation and the position of the camera, the digitised image (d) is a perspective view of the racket face, as indicated in Figure 4.10, instead of an orthographic side view, as illustrated in Figure 4.9. The software therefore constructs the perspective guide lines from visible landmarks (manually selected by the user) to the image's vanishing point, which was the same for all images, since the camera's position and zoom was never changed. Using basic geometry, the real impact location on the perspective view can be determined from its relative location to other distinguishable landmarks in the planar view of the impact, provided by image (c). The location of the vanishing point is established empirically; with its horizontal location assumed to be in the centre on the image since the camera was set up to be level, while the vertical location was determined by extrapolating a line through the racket's cross strings on various images to intersect with the horizontal centreline at the

vanishing point. Figure 4.11 depicts the basic selection sequence for image (c) and (d) to construct the lines [A] to [D] in order to determine the best estimation of the impact location [5]. Three visible points are selected; a reference string hole [1], its complementing hole on the opposite side of the stringbed [2] and the horizontal height of the ball centre intersecting with the centre of the racket frame's centreline [4].

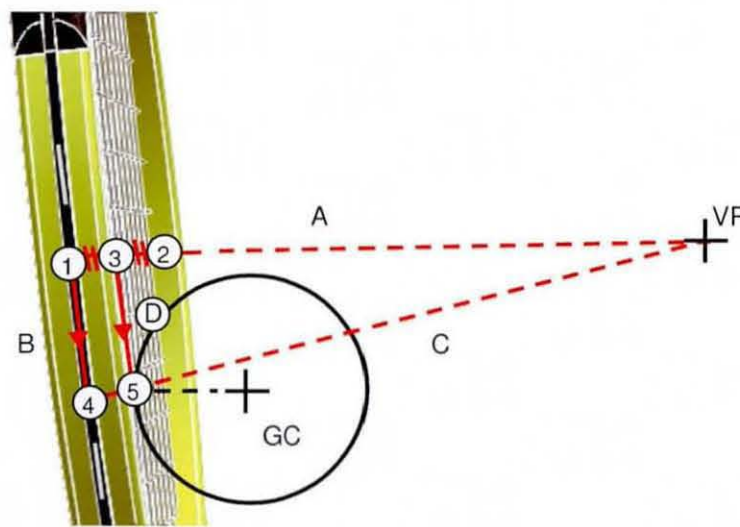


Figure 4.11: Diagram illustrating the digitising of the impact location on the centre of the strings for the last impact frame (c).

Image (c) with the ball just leaving the stringbed is digitised first, followed by image (d) in which the racket has travelled to the furthest end of the image. This provided the longest time difference between the two images in order to calculate the most accurate average speed of the impact point between the images. Digitisation of the first image commences by selecting a reference string hole [1] visible in both images (c and d) as a distinguishable marking on the frame. The software then draws a perspective line [A] from this point to the vanishing point (VP), the location of which has already been determined. The user then selects the intersection point [2] of line [A] and the complementary hole on the inside of the frame on the face's opposing perimeter and the software calculates the midpoint [3] between points [1] and [2], which should



lie on the face's centreline. The impact height [4] on the side of the frame is then selected on the same horizontal line as the ball's geometric centre (GC) and connected with line [B] to point [1] by the software, and with line [C] to the vanishing point. The software then constructs line [D] parallel to line [B], and calculates the intersection with line [C], which is the real impact point [5] on the stringbed's centreline. A similar construction (Figure 4.12) sequence was performed on image (d), in which the racket has rotated about the polar axis as well as the swing axis.

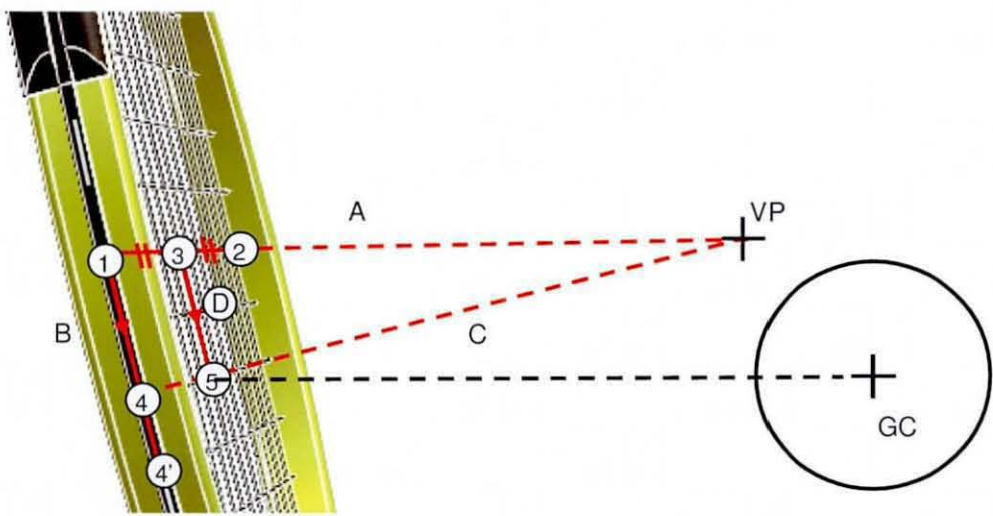


Figure 4.12: Diagram illustrating the digitising of the impact location on the centre of the strings for the first impact frame (d).

The new location of point [4] is undefined since it had no distinct marking on the frame and the racket has rotated too much to use the ball's vertical position as for image (c). Therefore point [4] is determined using the string hole [1] selected as a reference point in image (c) and assuming the distance [B] between the two points did not change significantly between the two images. Hence the main difference in procedure used for image (c) is the software calculating the location of point [4] instead of the user selecting it. This is performed after determining points [1] to [3] as before, then a temporary point [4'] is estimated and selected anywhere on the frame's symmetry line to form line [B']. The real point [4] is then calculated on line [B'], with the length of line

[B'] equal in length to line [B] determined from image (c) and the software concludes by constructing the location of the impact point [5] as before. Dividing the horizontal distance between the locations of the impact point [5] calculated for both images by the time difference between them produces the average racket post-impact speed. Combining this with the pre- and post-impact ball speeds results from the Flightpath software, the rebound ball speed,  $ACOR_f$  and  $COR_f$  for all the impacts were calculated, as defined in §3.1.

4.3.3 Freely suspended test data

For the racket comparison only centreline impacts were analysed, while the off-centre impacts were investigated later in order to determine the rackets' sensitivity to impact inaccuracies.

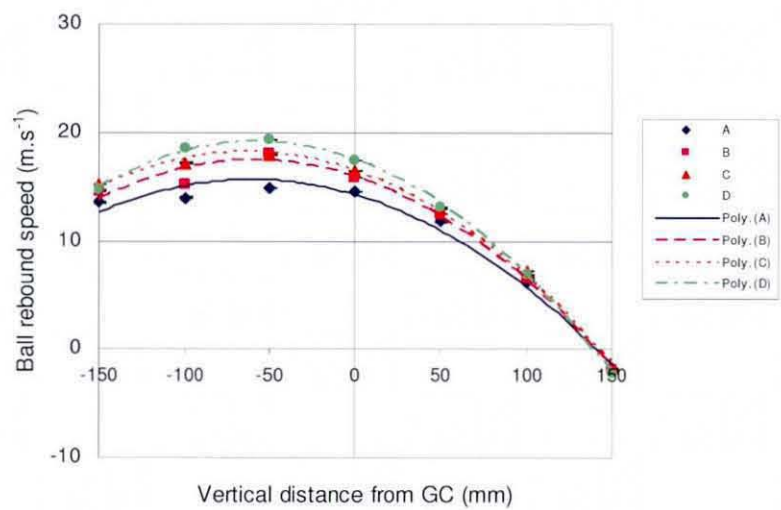


Figure 4.13: The rebound ball speed measured along the vertical racket face centreline for Rackets A to D.



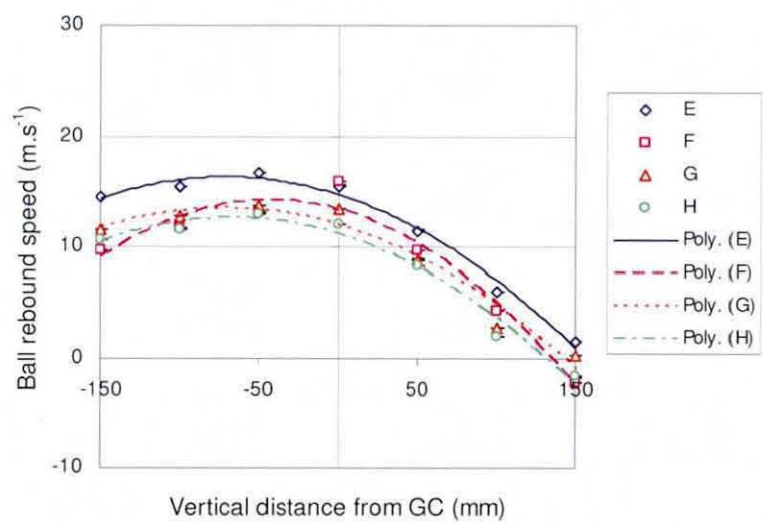


Figure 4.14: The rebound ball speed measured along the vertical racket face centreline for Rackets E to H.

The rebound ball speeds are presented in Figure 4.13 and Figure 4.14, with the highest speed achieved by Racket D ( $19.3\text{m.s}^{-1}$ ,  $\sigma=0.35\text{m.s}^{-1}$ ) and the lowest with Racket H. The peaks for the measurements are located between 58-72mm below the GC.

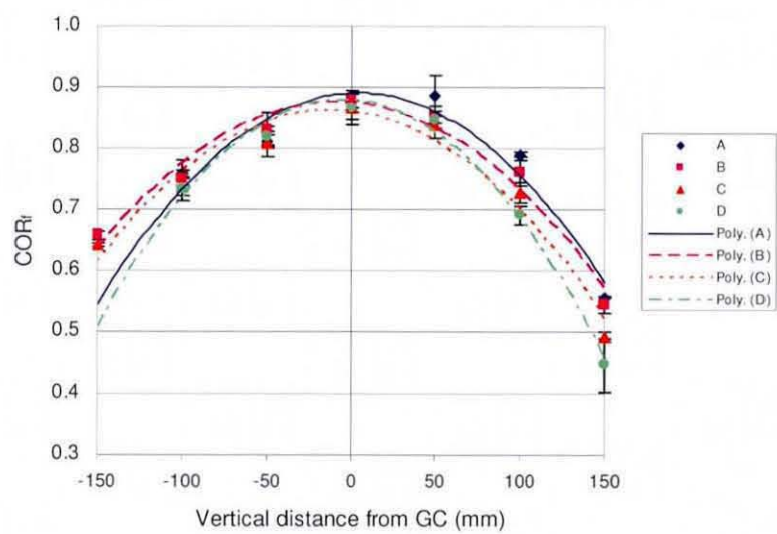


Figure 4.15: The COR<sub>f</sub> values measured along the vertical racket face centreline for Rackets A to D.

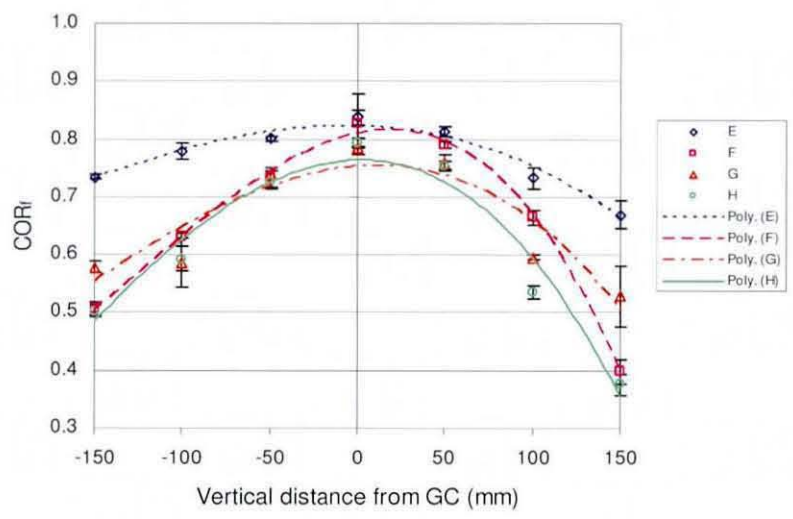


Figure 4.16: The  $COR_f$  values measured along the vertical racket face centreline for Rackets E to H.

The  $COR_f$  measurements confirmed the characteristic profile for all rackets (Figure 4.15 and Figure 4.16), yielding the lowest value at the tip, increasing to a maximum about 10mm above the GC and then decreasing again towards the throat. The maximum value measured ranged from 0.80-0.90 ( $\sigma=0.024$ ) for all the measured rackets, which corresponds to values reported by researchers such as Hatze (1992b, 1993), Liu (1983) and Watanabe (1979). The highest maximum was measured for the modern Head Ti.S6 rackets, while the lowest were obtained for the older tour rackets, the Wilson Pro Staff 6.1 and the Dunlop Revelation Max 200G. Thus the  $COR_f$  seems to support the common belief, that tour rackets and older rackets generate lower ball speeds than the new 'beginner' rackets. Another interesting observation is that the  $COR_f$  is virtually the same for all four weighted Ti.S6 rackets, confirming the basic COR definition for two colliding objects being independent of their mass and MOI.

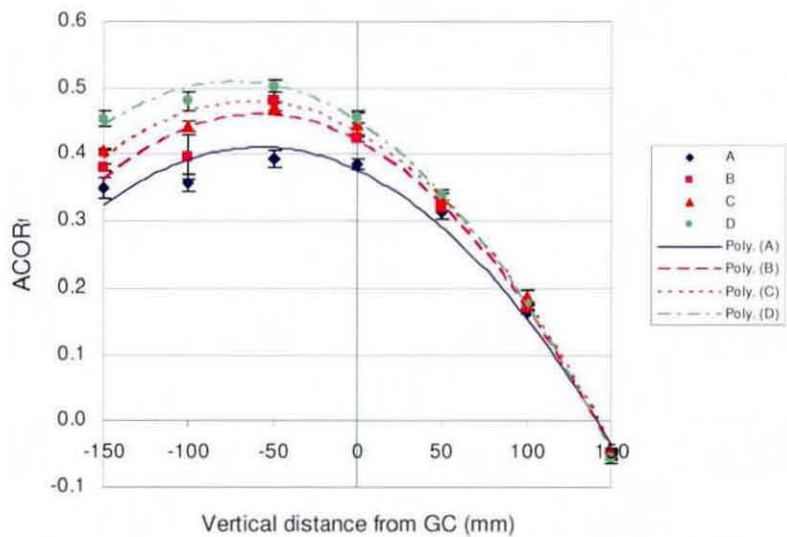


Figure 4.17: The ACOR<sub>f</sub> values measured along the vertical racket face centreline for Rackets A to D.

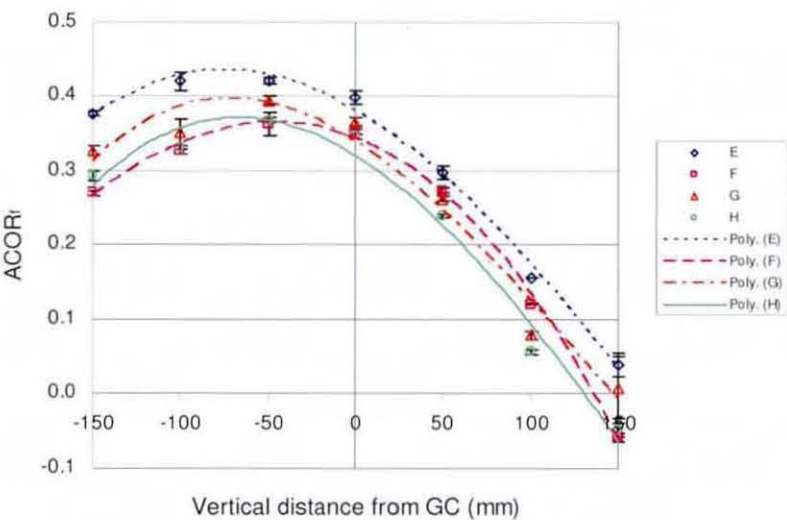


Figure 4.18: The ACOR<sub>f</sub> values measured along the vertical racket face centreline for Rackets E to H.

As with the COR<sub>f</sub>, the ACOR<sub>f</sub> values (Figure 4.17 and Figure 4.18) follow a similar trend for all rackets, with the lowest values measured as virtually zero at the racket tip, then increasing to a maximum about 70mm below the geometrical face centre and dropping off slightly towards the throat. The maximum values ranging between 0.36-0.50 ( $\sigma=0.011$ ) are again similar to

previous reports by Brody (1997), Watanabe *et al.* (1979) and Elliott *et al.* (1980). The rackets with the highest and lowest maximum  $COR_f$  also displayed the highest and lowest  $ACOR_f$  values, except for the discernable difference between the  $ACOR_f$  results for the rackets A-D, supporting general opinion that the ACOR increases with an increase in racket MOI (Brody *et al.* 2002). The maximum  $ACOR_f$  increased by about 25% from the lowest to the highest MOI.

The results from Racket A to D in particular, for which only the mass and MOI was varied for the same racket amplified the difference between the COR and the ACOR measures, confirming that the ACOR is the more sensitive measure for detecting the differences between maximum rebound racket characteristics due to changes in mass/MOI properties. Table 4.2 presents a summary of all the  $COR_f$  and  $ACOR_f$  values calculated.

	Racket identification							
	A	B	C	D	E	F	G	H
Mass [g]	245	291	337	383	247	273	366	340
MOI [kg.cm <sup>2</sup> ]	307	328	349	370	317	370	334	316
Impact location	$COR_f$							
150	0.56	0.54	0.49	0.45	0.67	0.40	0.53	0.38
100	0.79	0.76	0.73	0.69	0.73	0.66	0.60	0.54
50	0.89	0.85	0.84	0.85	0.81	0.79	0.76	0.75
0	0.87	0.88	0.87	0.87	0.84	0.83	0.79	0.79
-50	0.81	0.83	0.81	0.82	0.80	0.73	0.74	0.72
-100	0.76	0.75	0.74	0.73	0.78	0.63	0.62	0.59
-150	0.50	0.66	0.64	0.76	0.73	0.51	0.58	0.50
Average	0.74	0.75	0.73	0.74	0.77	0.65	0.66	0.61
STD	0.0138	0.0163	0.0156	0.0185	0.0122	0.0180	0.0191	0.0120
Maximum	0.89	0.88	0.87	0.87	0.84	0.83	0.79	0.79
Impact location	$ACOR_f$							
150	-0.05	-0.05	-0.05	-0.06	0.04	-0.06	0.01	-0.05
100	0.16	0.17	0.19	0.18	0.16	0.12	0.08	0.06
50	0.31	0.32	0.33	0.34	0.30	0.27	0.26	0.24
0	0.39	0.43	0.45	0.46	0.40	0.35	0.37	0.35
-50	0.39	0.48	0.47	0.50	0.42	0.36	0.40	0.37
-100	0.36	0.40	0.44	0.48	0.42	0.33	0.37	0.33
-150	0.29	0.38	0.41	0.45	0.38	0.27	0.33	0.29
Average	0.26	0.30	0.32	0.34	0.30	0.24	0.26	0.23
STD	0.0090	0.0105	0.0085	0.0088	0.0079	0.0057	0.0125	0.0044
Maximum	0.39	0.48	0.47	0.50	0.42	0.36	0.40	0.37

Table 4.2: The  $COR_f$  and  $ACOR_f$  values measured for the control racket group during the racket free-free testing. The racket mass and moment of inertia, measured with the Babolat RDC, is presented for comparison.



CHAPTER 4 RACKET PERFORMANCE TESTING

As an accuracy check of measurements and confirmation of the theory relating the COR to the ACOR, the theoretical values for the COR were calculated from the ACOR results using Equations 3.5 and 3.6. The theoretical results presented in Figure 4.19 compare well with the measured values in Figure 4.15, with the largest differences appearing at the racket tip. The author therefore has sufficient confidence in the accuracy of the test procedure and the results obtained from it, and will be using it as a benchmark for determining the accuracies and performance specifications for the test machine.

To this end the standard deviation for the  $COR_f$  and  $ACOR_f$  measurements along the centreline was calculated, revealing similar values of 2.88% and 2.67% respectively.

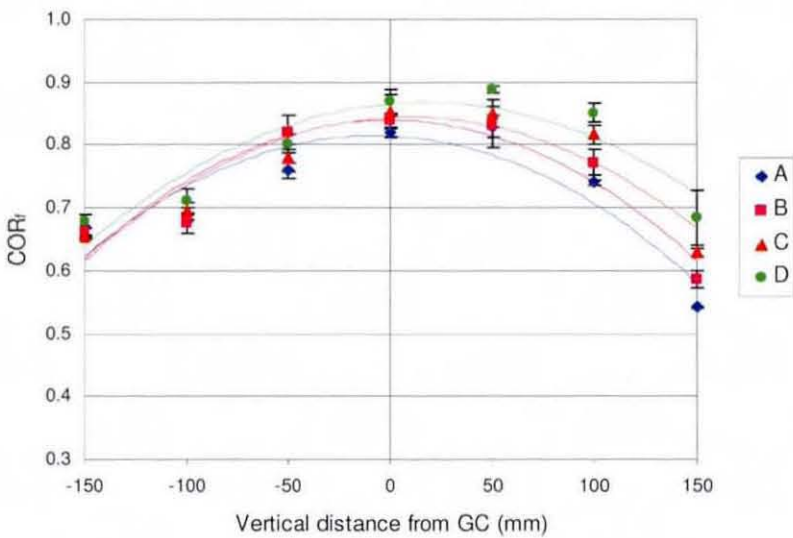


Figure 4.19: The theoretical  $COR_f$  values measured along the vertical racket face centreline for Rackets A to D.

The next step was to determine the sensitivity of both definitions to off-centre impacts, in order to establish the desired accuracy of the test machine in this regard. Hence, the results at the GC vertical location for the centreline impacts (Location 0) and 50mm away from it (Location R0) were compared. For off-centre impacts, the average decrease was 28% for the  $ACOR_f$  and 36% for the  $COR_f$ , indicating the  $COR_f$  to be significantly more sensitive to off-centre

impacts. If this decrease is assumed to be linear it relates to a maximum impact location variance of approximately  $\pm 5\text{mm}$  in order not to exceed an error of 5% in the  $\text{COR}_f$  measurement, which was used to specify the tolerance to be achieved by the test machine.

Similarly, the acceptable variance in the vertical impact location was determined by investigating the variance of a typical  $\text{ACOR}_f$  profile along the vertical axis (Figure 4.17 and Figure 4.18). This was performed at the location of the peak  $\text{ACOR}_f$ , since this would be the area of interest during performance testing. Therefore the third order polynomial fitted through the data was used to determine the location of the peak  $\text{ACOR}_f$  and the vertical offset in impact location, which would result in a 5% drop in  $\text{ACOR}_f$ . This yielded an allowable vertical tolerance of  $\pm 22\text{mm}$  to be achieved by the test machine to ensure 95% accuracy in  $\text{ACOR}_f$  measurements.

### 4.3.4 Handle clamped racket testing

In order to complement the freely suspended tests and resolve gripping issues related to the machine design, rigidly clamped tests were performed. These tests would represent the opposite extreme clamping condition, which would shed light on the debate on the influence of the gripping condition on racket performance. Combining the results from both sets of tests with those obtained from later player tests would reveal what kind of gripping method should be used to develop a representative machine. The more extreme gripping condition would also indicate the durability of the new light-weight rackets at realistic serve speeds.

Motivation for the tests arose from simplicity compared to developing a realistic gripping device for the final test machine. In contrast, the other simple extreme, the freely suspended condition revealed disadvantages, which could be critical for a functional and accurate, repeatable system. The fixation method allows for improved impact point alignment and better possibilities for a fully



automated machine, especially for a moving racket arrangement under consideration.

The test procedure was similar to that used for the freely suspended rackets, as presented in the previous section except for the gripping condition as indicated in Figure 4.20.

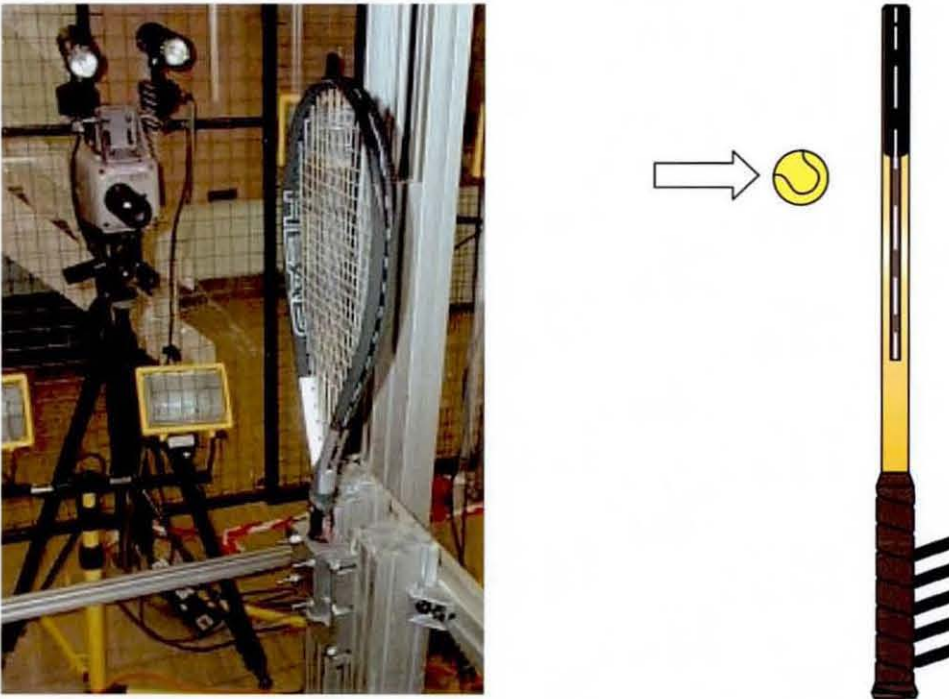


Figure 4.20: The test set-up for the handle clamped racket rebound tests.

A KODAK EktaPro high-speed camera was used to record the entire impact, from which the  $COR_{gc}$  and  $ACOR_{gc}$  would be calculated for the same rackets and impact locations as per previous tests. In contrast to freely suspending the racket off a pin as before, it was rigidly clamped in the gripping mechanism shown in Figure 4.21. The aluminium clamp distributes pressure across the racket handle, over an 80mm long surface starting from 20mm to 100mm from the butt.

The gripping pressure could be adjusted by varying the torque applied to four nuts holding the clamping plate. Torque values were estimated from the literature; Baker and Putnam (1979) torqued a similar gripping arrangement consisting of C-clamps at 13.6Nm without providing any explanation. Elliott

(1982a) measured the grip force via transducers mounted to a racket handle. Players were asked to grip the handle at different grip strength levels and the average determined. Four bolts were torqued between 0.45Nm and 0.75Nm to obtain resulting grip forces equivalent to the measured values, which were not published. Knudson and White (1989) later attempted to measure the grip force at impact during play with resistive force transducers mounted to the racket handle, finding values ranging between 5N and 71N under the hypothenar and from 4N to 309N under the index finger, which indicated the complexity of accurate grip force measurements on a racket handle, hence the decision to use the torque between that used by Baker and Putnam and that from Elliott. In order not to damage the handle by applying excessive gripping pressure, it was decided to perform trial tests at the lowest realistic torque of 2.5Nm in each bolt. This was especially critical since the grip tape was removed to eliminate the damping effect introduced by the gripping material and to ensure rigid gripping condition.

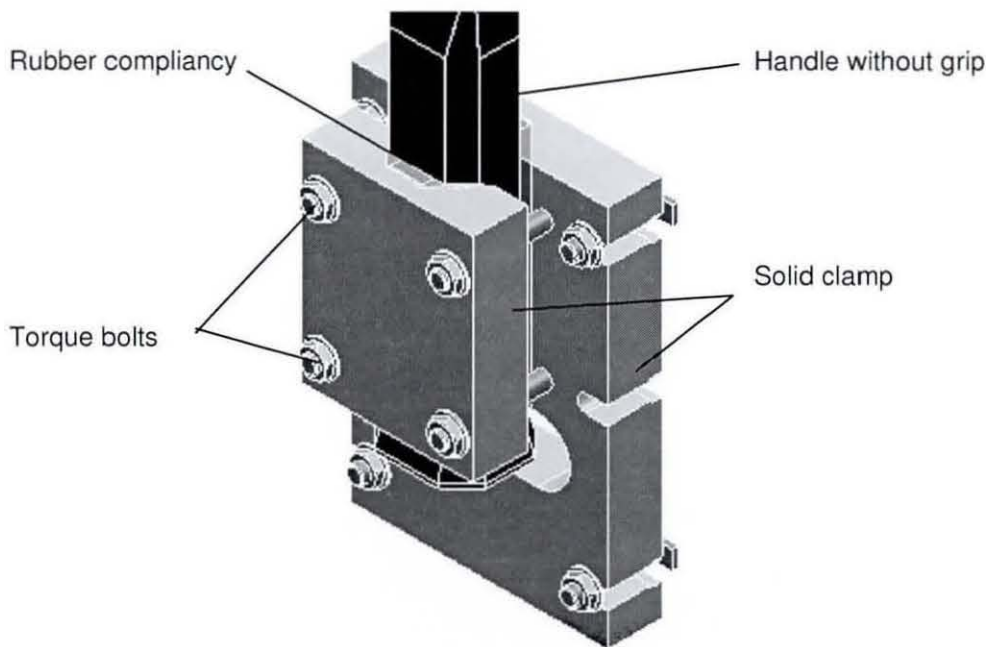


Figure 4.21: The test set-up and handle clamp used in the rigid clamped COR tests.

After only a few trial impacts performed at  $34\text{m.s}^{-1}$  on Racket E (Head Ti.S7), the racket handle failed. The failure occurred above the clamp on the side of the racket facing away from the ball, as shown in Figure 4.22.

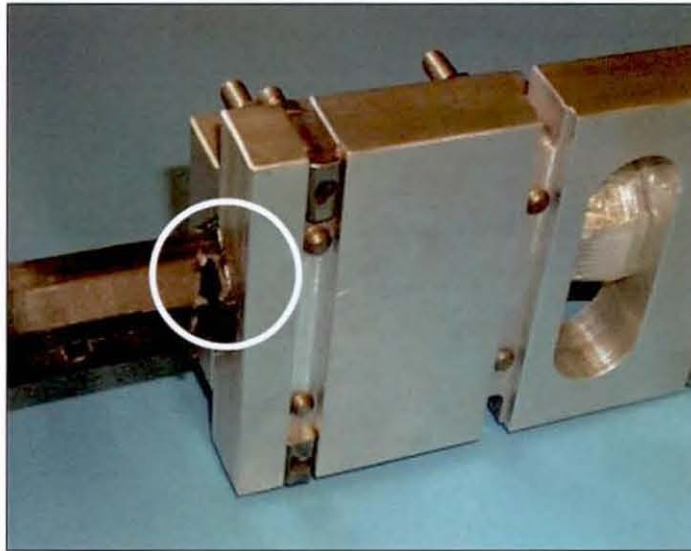


Figure 4.22: Failure of the Head TiS7 racket handle during the rigid clamped rebound tests.

It was clear that even at this relatively low impact speed the magnitude of impact is too high for the racket to withstand. This was not surprising, since the thin-walled hollow handles in modern rackets are not designed to withstand the contact pressures induced under these special gripping conditions. Wooden rackets tested in the past have more robust solid handles, which performed better under these conditions but by chance rather than conscious design intent, since there was no way to produce hollow handles at the time. Communicating this to the ITF revealed their researchers had experienced similar failures under such extreme conditions. At the time the tests were performed this was not yet documented and similar tests in the literature had also been performed at lower speeds:

- Baker and Putnam (1979):  $\sim 28.2\text{m.s}^{-1}$
- Watanabe *et al.* (1979):  $\sim 20\text{m.s}^{-1}$
- Elliott *et al.* (1980):  $\sim 21\text{m.s}^{-1}$



- Elliott (1982a):  $\sim 30\text{m.s}^{-1}$

It was concluded that that racket failure could only be prevented by one of the following methods:

- Decreasing the incident ball velocity.
- Introducing damping material around the handle.
- Decreasing the gripping force on the handle.
- Increasing the radius of the grip edge.

All of the above would defeat the objective of the testing, which was comparing the rebound characteristics of the two extreme gripping conditions. Decreasing the incident velocity would prevent a comparison with the freely suspended rebound tests, since the COR is dependent on incident ball speed and lower speeds are not representative of a high-speed serve and would provide disputable results. Introducing damping materials and decreasing the gripping force will mean the racket is not rigidly clamped, which defeats the main objective of the testing. Consequently, since it was considered advantageous to perform all racket tests for the project with the same rackets, a decision was taken not to continue with the rigidly clamped tests but rather use the developed machine to experiment with the gripping conditions.

### 4.3.5 Head clamped racket testing

Another extreme gripping condition often used for testing racket rebound characteristics is the head clamped condition, to the point where researchers such as Brody (1997) have included these results in mathematical racket models. Brody measured the COR for a head clamped racket and then derived an equation to predict the racket COR for a racket in the freely suspended condition. It was therefore decided to perform these tests on the control rackets, in order to compare and evaluate such models at a later stage of the research.

The test would also isolate the performance of the stringbed by eliminating the contribution of the frame. The sensitivity of the performance to the string performance would significantly affect the method specified for a standard test, defining which strings, string tension and stringing method should be used for testing and how long after the rackets have been strung test should be performed. Since strings are an easily replaceable component, this could be a loophole in a standard test if the parameters are not properly defined.

Balls were launched with the same system described for the other rebound tests at a racket clamped by the head in the device shown in Figure 4.23. The device securely holds the racket head in place, while still allowing some frame deformations radial to the GC. For these tests, changes to the ball-cannon to increase the achievable impact speed had been made as described in §4.1.2. The racket was mounted with the stringbed normal to the ball direction and balls fired at locations on the centreline at approximately  $50\text{m.s}^{-1}$ .

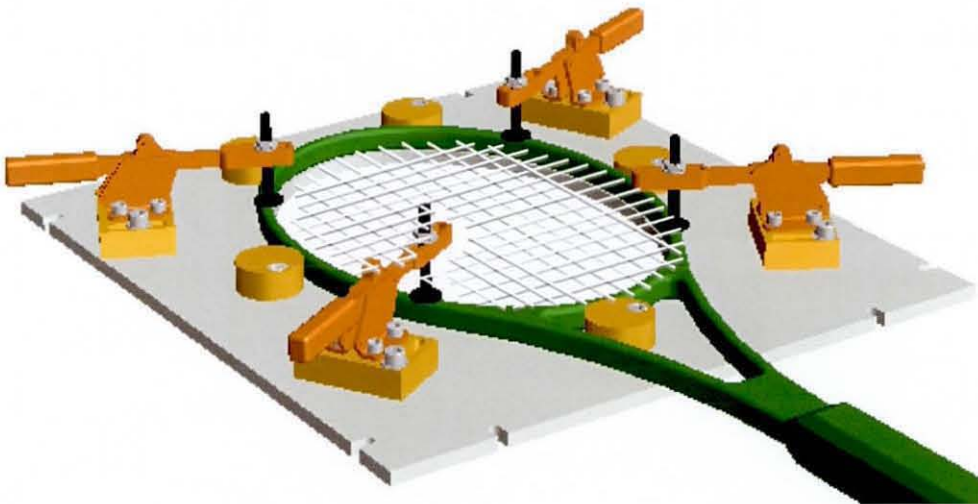


Figure 4.23: Head clamp device for ball-cannon tests.

The first racket (Racket B) which was tested failed unexpectedly during the initial test set-up. The failure occurred at the tip of the racket (12 o'clock position) as indicated in Figure 4.24.



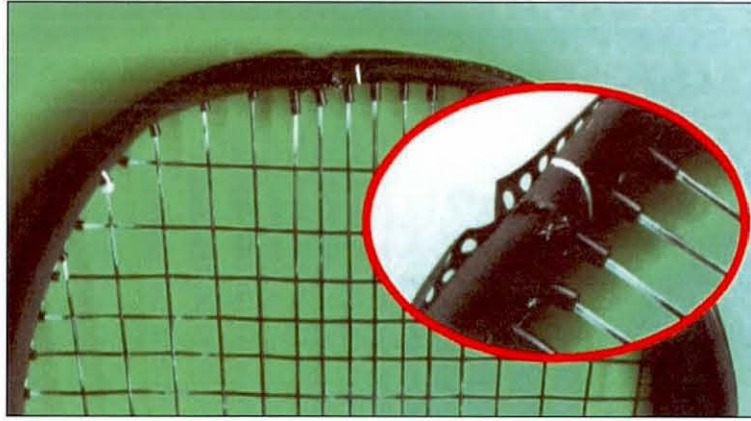


Figure 4.24: Failure of Head TiS6 under high-speed head clamped conditions.

The combination of lightweight construction and a discrete clamping regime introducing a varying stress distribution around the head during impact were the most likely causes of failure. Using the same set of test rackets during future tests with the test machine was given a high priority, therefore the risk of losing another racket from the set was considered too high compared to the importance of the head-clamped test in terms of the machine design and these tests were discontinued.

#### 4.3.6 Implications for the PDS and further research

The testing provided  $COR_f$  and  $ACOR_f$  profiles at realistic impact speeds for modern tennis rackets, which was not available at the time. It confirmed that although the peak values of measurements performed at higher impact speeds differ noticeably from lower impact studies in the literature, the comparative trends such as the distribution of the  $COR_f$  and the  $ACOR_f$  profiles are not significantly influenced. For most of the rackets, the maximum  $COR_f$  was located near the GC and the  $ACOR_f$  about 70mm below the GC. These locations would be compared later with real play measurements of ball impact locations in order to establish the link between racket performance in the laboratory and on court. The maximum  $COR_f$  value measured for all the rackets was almost 0.9, while minimum values achieved near the throat and racket tip were about 0.45. These measurements were used to define the limits, which needed to be

## *CHAPTER 4 RACKET PERFORMANCE TESTING*

achieved by the test machine. Combining the rebound characteristics from the modern rackets with the performance of top level tennis players presented in the next chapter would provide the expected test conditions at which the machine needed to operate.

Crucial to the machine's performance would be the repeatability of its test results but no published data was available at the time to specify accepted consistencies for such a machine. Therefore results from the ball-cannon tests were used as a benchmark to stipulate acceptable performance specifications. The standard deviations of the  $COR_f$  and  $ACOR_f$  along the centreline, and the sensitivity to off-centre impact will be used for this purpose, while the peak measurements and profiles from the set of test rackets would provide comparative data for evaluating the machine's performance during the commissioning phase.

The tests also revealed some of the advantages and disadvantages for different test methods, which would assist in the functional design of the test machine. The freely suspended ball-cannon tests were relatively simple and accurate, with the main concern being the ability to automate the test method, which would be crucial if it was to be used as a standard test method. Systems, which would need further investigation for automation, were the measurement of the post-impact racket velocity, post-impact ball velocity for lightweight racket, especially for tip impacts and repositioning of the racket. The latter slowed the test procedure considerably, since the racket had to be carefully repositioned on the pin after each impact. The accuracy of the placement on the pin could be improved by using an alignment laser beam across the racket or incorporating positioning struts in front of the racket, on either side of the racket face (3 and 9 o'clock positions).

In contrast to the freely suspended tests, the severe consequences of over constraining the racket during the handle and head clamped conditions was also high-lighted, which resulted in racket failures at representative serve



speeds. Therefore care should be taken during the design phase to develop a gripping mechanism with a realistic inertia in order to avoid racket failure during high impact speeds.

Although the testing proved the versatility of using a ball-cannon to investigate racket rebound characteristics, it also highlighted some of the major disadvantages of the system. These included difficulties in automating all mechanisms and measurements such as the reloading of the racket after impact, digitizing of racket speed after impact, mapping of the entire stringing surface. The design complexity required to achieve this could be as complex as building a 'swing robot', which is traditionally perceived as a more complex test machine. A 'swing robot' though would provide the benefit of providing a more realistic representation of a serve and therefore be more acceptable to the non-scientific community.

### 4.4 Modal analysis

The vibration node is another sweet spot mentioned in §2.3.2 influencing racket performance during play and therefore a possible impact location favoured by the players. Subsequently the exact location of the node could be of significant importance when investigating a racket performance in the laboratory if this is indeed where players obtain the optimum performance. In order to compare the node location with the maximum rebound measurements in the previous section, the same set of tests rackets utilized during these tests was used for the vibration measurements.

The vibration characteristics of freely suspended rackets were measured using an Ometron laser vibrometer. The rackets were suspended from a cord with a freely suspended shaker connected to the throat area as shown in Figure 4.25. The shaker applies vibrations consisting of a very wide frequency spectrum, known as 'white noise', to the application point, while the laser beam

was focused on a small piece of reflective tape stuck to the racket frame. The vibrometer measured the vibration response of the specific point, which was stored via the system software for further analysis. Discrete locations all along the frame length were measured to determine the natural frequencies, as well as the location of the nodes and anti-nodes for the first vibration mode. The point on the racket with the highest vibration amplitude was determined as the anti-node and the two points with the lowest amplitude as the nodes.

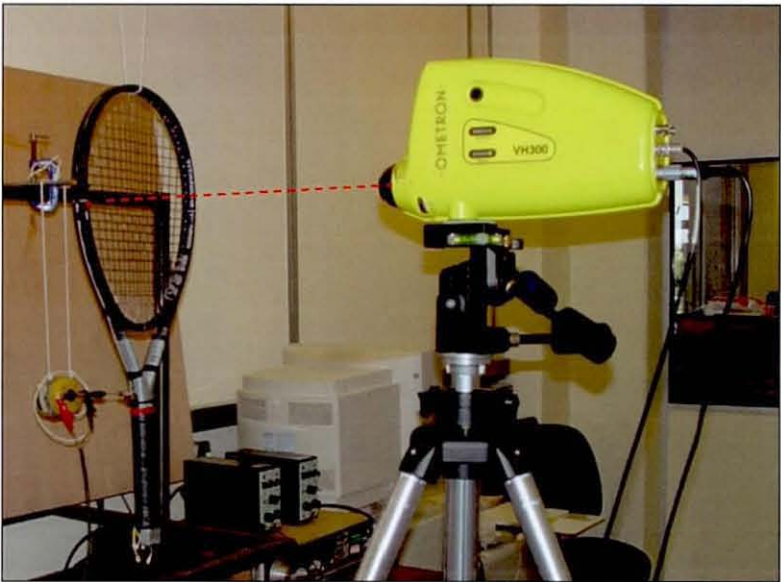


Figure 4.25: Test set-up for measuring the vibration response of the rackets.

During the analysis, the frequency, amplitude and location of the nodes for the fundamental frequency were determined. The results of the tests are represented in Table 4.3.

Property	Racket Identification							
	A	B	C	D	F	G	H	I
Frequency [Hz]	146	151	144	136	126	140	111	96
Max. Amplitude[m.s <sup>-2</sup> ]	96	84	60	40	21	17	15	11
1 <sup>st</sup> Node location [mm]	113	130	138	151	123	102	109	130
2 <sup>nd</sup> Node location [mm]	562	561	548	555	595	551	547	548
Mass [g]	245	291	337	383	273	366	340	383

Table 4.3: The vibration response measures for the control rackets with the node location measured from the butt (node locations from the butt).



## CHAPTER 4 RACKET PERFORMANCE TESTING

Racket E was not measured because it broke during the handle clamped rebound testing, while a wooden racket (Racket I) was taken as a replacement. It would serve as a comparison for the influence of modern technology on the racket's vibration characteristics, since the literature often refers to the extreme differences between wooden and composite rackets. The wooden racket was not included in the rebound tests due to a fear of breakage under the high impact speeds and these old rackets being relatively difficult to replace.

The results confirm general vibration theories, with the first vibration mode varying between about a 100Hz and 150Hz for all rackets. The highest vibration frequencies and amplitudes were measured for the stiffer Head Ti.S6 rackets and the lowest for the flexible wooden racket. It was also clear how the addition of mass to rackets B, C and D lowered the natural frequency as well as the maximum vibration amplitude. From Cross 1998b, the racket frame's vibration energy ( $E_i$ ) for a particular vibration mode is calculated as:

$$E_i = \frac{1}{2} m_r \omega_i^2 A_i^2 \quad (4.2)$$

where  $m_r$  is the racket mass, and  $\omega_i$  and  $A_i$  the angular frequency and amplitude constant for that mode. Since the energy is proportional to the mass, as well as the square of the frequency and the amplitude, which are both inversely proportional to the mass, it should mean the decrease in energy absorbed due to the decrease in racket mass should be cancelled by the simultaneous increase in frequency and amplitude. Therefore more deformation energy is absorbed by the lighter racket frames during the impact and less energy is returned to the ball, which should decrease the ball rebound speeds.

The vibration measurements completed the characterization of properties needed to define the representative control group of rackets in order to be used in future tests. During the subsequent player tests, the real impact location will be measured from a serve and the location compared to that of the node and the maximum rebound measurements in order to determine the preferred sweet



## *CHAPTER 4 RACKET PERFORMANCE TESTING*

spot used by players. This would assist in determining which impact location is of importance during machine testing, hence defining part of the PDS.

# Chapter 5

## Player Motion Testing

Although modern technology has made significant enhancements during the last few decades to racket performance, the contribution of the players should never be neglected. This was substantiated by Coe (2000), who compared the size of the male champions in the 1920's and 1930's with the top ATP Tour players in 1998, revealing a considerable increase in height and weight. Players of equivalent height exhibited an increase of up to 22% in weight when compared to their counterparts from the past, which indicated players have become stronger. This demanded further investigation in order to distinguish between the contribution of player and the racket to the increase in performance.

The player has two basic contributions to the ball speed during the serve; generating the desired racket motion in order to present it to the ball at impact and the effect of the gripping on the racket handle during the impact. Many of the effects of the gripping conditions have been well investigated and simulated successfully in laboratories or could be investigated further using a test machine but the influence of the racket properties on the serve motion could only be determined through motion studies. The chapter therefore aims to characterise the typical racket motion performed during a high-speed serve in order to derive the necessary parameters for developing a test machine, which could realistically and effectively reproduce the required motion. The influence of important racket parameters on its swing motion was also tested as a benchmark of how the machine should perform under similar conditions.

## 5.1 Human motion studies

The published research contains a number of studies of human motion while performing a tennis serve, or similar motions such as throwing, volleyball serves and golf swings. The studies provide an understanding of the contribution and coordination of different body parts to achieve the optimum execution of a tennis serve. Much can also be learned regarding typical velocities and accelerations of important points, which are essential for developing representative testing equipment.

Johnson (1957) reported results from a study into the relationship between speed and accuracy for advanced women players in 1957. Ball speeds of up to  $45\text{m.s}^{-1}$  were recorded via an 8mm film and the placement was scored with the help of a scoring grid on the far end indicating players' ability to hit a target. Johnson discovered, rather simply, that speed and accuracy were independent for her test group.

In his book, Plagenhoef (1970) documented the use of a single camera (64fps) footage and simple linear momentum theory to explain the service performance of several elite players. He concluded that the different grip firmness used by Ashe, Pilic and Laver changed the effective racket striking, which explained why Ashe and Pilic could achieve ball speeds of up to 118mph with a racket maximum head speed of 73mph while Laver only achieved 100mph from 83.5mph. He concluded the firm grip increased the striking mass and the control of the racket up to and during impact. This apparently large influence of the grip firmness is now believed to have been exaggerated by the low sampling rate used during the tests.

A few years later Johnson (1976) described the serve action based on another cinematographic analysis performed by Plagenhoef (1971) at 128fps. Three main components of upper body activity were identified:



- Cocking: the racket is positioned parallel to and pointing down the spine, with the elbow at  $\sim 90^\circ$  and upper arm pointing forwards and upwards.
- Swing: the racket is swung through  $\sim 180^\circ$ . The motion is initiated by shoulder girdle rotation followed by straightening of the flexed arm.
- Pronation: the racket is 'whipped' into the impact by a  $\sim 180^\circ$  rotation of the forearm through the impact.

Anderson (1979) published a combined electromyographic and tri-plane cinematographic study (64-100fps), comparing results for skilled athletes throwing a ball in other sports and performing a tennis serve. Although there was some similarity between the two skills, significant differences in swing motion of the two actions suggested players should not train for one by practising the other. The difference in motions was attributed to the size and weight difference between the two objects, implying a possible difference in motion when using different rackets with extreme characteristics.

A similar study performed on Japanese men using 16 mm film at 100-200fps was reported by Miyashita *et al.* The study indicated a 'silent' muscle period for the first half of the forward swing, which suggests no active drive of the system during this time (Miyashita *et al.* 1980).

Soon after, Elliott and Wood (1983) published a two camera cinematographic comparison of two different serve techniques, with both techniques exhibiting a deceleration of racket angular velocity prior to impact. That same year Elliott also published a study of topspin generation from the serves of junior and adult players. Using two cameras, one for the player (200fps) the other for the ball (300fps) he observed topspin values up to 1140rpm for the adults at service speeds of  $\sim 45\text{m.s}^{-1}$  (Elliott, 1983).

Van Gheluwe and Hebbelinck (1985) recorded the serve action for a top class male and young female using four cameras at 400fps. The results provide

typical serve velocities, especially the racket head speeds (head centre) before and after impact, respectively ranging between  $30.8\text{-}32.2\text{m.s}^{-1}$  and  $17.5\text{-}19.7\text{m.s}^{-1}$ , while the COR, as well as the ratio between the racket speed before and after the impact, was calculated as  $\sim 0.6$ . Interestingly the racket slows down just before impact, with this delay increasing for locations further down the kinematic chain, away from the racket. Furthermore 50-70% of the racket speed before impact was attributed to its angular velocity, indicating some kind of whip action. Van Gheluwe and Hebbelinck also concluded that the player applied little force to the racket during impact, since the net momentum remained the same during impact.

Elliott *et al.* (1986) presented a comparison between the serve action of four elite male and four elite female players using 3D reconstruction of two 200fps cameras. The tests provided typical serve velocities with racket speeds for the males at  $\sim 34.8\text{m.s}^{-1}$ , with the data revealing a decrease in racket angular velocity before impact. Visual interpretation of the film showed that forearm pronation and upper arm endorotation had a considerable effect on racket speed  $\sim 5\text{ms}$  prior to impact, which suggests an instantaneous centre of rotation to be in close proximity to the racket handle.

In 1987, Van Gheluwe *et al.* reported a 3D study (3 cameras, 300fps) of three skilled players. They reported an explosive endorotation of the upper arm just after maximum pronation and just before impact and conclude this is an important point of racket speed development.

In the same year, Miura *et al.* (1987) performed a serve motion analysis on Japanese players using a 16mm cine camera at 64fps. They confirmed the sequential increase in velocity towards the distal segments of the kinematic chain ending in a very fast snap of the wrist to create the high racket velocity in what they then referred to as the “cracking of the whip effect”. This does not necessarily mean that it is caused by the wrist flexor muscles but rather, as in



the case of the whip, through a deceleration of the proximal segments in the chain.

In 1988, Buckley and Kerwin published an EMG/cinematographic study of the serve for five players. Their results supported the findings of other researchers that much of the force creating the high speed elbow extension is generated via passive energy flow along the body's kinematic chain. They noted the elbow extension velocity of  $\sim 44 \text{ rad.s}^{-1}$  is beyond the  $20 \text{ rad.s}^{-1}$  limit imposed by the maximum contractile velocity of human skeletal muscle. In any case, the force that can be generated at such high speed would be minimal. The triceps' contribution, peaking just before impact, is a powerful stabilising co-contraction, rather than a dominant muscle torque.

In 1989, Bahamonde published joint forces and torques based on an inverse dynamics analysis of 3D cinematographic data. Most torque was generated by the shoulder (internal rotation and horizontal adduction) and elbow (arm extension), with a large torque throughout the swing up to the impact. The pronation/supination torque was negligible, suggesting that this is a guiding or releasing action rather than a racket driving one.

Several years later, Springings *et al.* (1994) published mathematical equations to determine contributions for the kinematic chain segments to the racket velocity. They employed a cinematographic analysis of a high quality player achieving a maximum racket head speed of  $\sim 27 \text{ m.s}^{-1}$ , which revealed a slight deceleration just before impact. Springings *et al.* noted that the magnitude of a segment's angular velocity is insufficient to judge its contribution to racket speed. For example, the lower horizontal cross-flexion speed of the upper arm was 1/3 of forearm pronation but 'contributed'  $6.5 \text{ m.s}^{-1}$  as opposed to  $4 \text{ m.s}^{-1}$  to the head speed. However, they failed to establish conclusively that segment velocity is not the cause of head speed but the condition required not to impede it further.

In the same year, Cohen *et al.* (1994) correlated and published anthropometric data and serve velocities measured from 40 tournament players with a handheld camera, a radar gun and upper extremity strength and usability measuring equipment. The measurements were linked to the achieved serve velocities, indicating the highest correlation for the flexibility of the dominant wrist and shoulder (forward) flexion and internal rotation in the dominant shoulder at 0° of abduction and all strength measures related to shoulder torque production.

Another study performed by Bartlett *et al.* (1994) on 26 British national and county players, using two cine cameras at 200Hz, confirmed the increasing speed of distal segments in the kinematic chain. They also observed that all segments reached a maximum velocity just before impact with the most distal segment being the closest to the time of impact.

In the next year, Elliott *et al.* (1995) presented a cinematographic study using three cameras (200fps) to compare the service action of 11 elite players. Internal rotation of the upper arm reached its peak ~5ms before impact. Segment contributions to the 31.1m.s<sup>-1</sup> horizontal racket head speed were calculated as:

- internal rotation of upper arm (54.2%)
- hand flexion (31.0%)
- horizontal flexion and abduction of upper arm (12.9%)
- linear shoulder velocity (9.7%)
- forearm pronation (5.2%)
- forearm extension (14.4%)

In 2000, van der Meer presented a summary of the literature on stroke biomechanics, which concluded, contrary to the general opinion, that during a

serve the forearm drove the racket through the impact. However, no references were presented to justify this opinion.

In the same year, Papadopoulos *et al.* published results from a study performed on the best four female players at an international tournament, using two 60 Hz video cameras. Maximum racket head speeds recorded ranged from 18.54-21.66m.s<sup>-1</sup> and balls speeds between 38.11-49.04m.s<sup>-1</sup>. They concluded that the proximal-to-distal joint speeds increased sequentially during the strokes, but the maximum racket head speed only coincided with the impact for two of the players (Papadopoulos *et al.*, 2000).

Still in the same year, Wang *et al.* presented results from another motion study. The serves of eight Taiwanese international players were recorded with six cameras at 250Hz. Excluding the shoulder joint, angular velocity graphs of all upper extremity joints indicate that they reach a maximum angular velocity before the impact, most likely indicating very little acceleration of the entire arm during impact (Wang *et al.*, 2000).

Lo *et al.* (2003) performed a motion analysis of the upper extremity segments during a flat tennis serve. Three-dimensional displacement markers placed on the strategic joints were recorded at 240Hz. Unfortunately, only one player was analysed and although markers on the racket are visible, no racket data was reported. Nevertheless, results confirm a deceleration in linear and angular momentum for all arm members and joints, except for upper arm angular momentum.

Two studies investigating the relationship between racket properties and player performance for children were performed on two large control groups during two training camps (Stanbridge *et al.* 2003, Stanbridge 2004). Players were divided into different skill levels and given rackets with different properties to perform the same set of practice drills, while the location of the ball was recorded. The court was divided into zones and the ball placement used to score each hit. The location of the first bounce was used as an indication



of the control while the second bounce indicated the 'power'. The tests revealed that the racket length, head size and MOI had a considerable influence on the player's power and control. It is conceivable that these test results would also apply to adults, probably to a lesser extent.

Koenig *et al.* (2004) performed similar studies for baseball bats, determining the relation between the bat's MOI and swing speed. In two separate studies, male baseball and female softball players swung 13 configurations of production bats, aluminium rods and modified production bats at flexible targets, balls on a tee and balls pitched via a machine. Sensors were sampled from above via three light sensor arrays sampling at 250kHz, measuring bat speeds ranging from 22-23m.s<sup>-1</sup>. Unfortunately, conclusions from the researchers were inspecific, only claiming a significant decrease in swing speed with an increase in MOI and mass.

In summary, there appears to be lack of agreement over the source of speed generation during the service action. This is perhaps due to the large position measurement errors in most cases causing the inverse dynamics calculations to be difficult and inconclusive. Most studies were performed at about 100 Hz, and employed large markers, thus introducing considerable errors during digitisation. Only the studies performed at the highest frame rates (200-400Hz) reveal a peak racket velocity slightly before impact, suggesting lower frame rates are not accurate enough for a detailed characterisation of a tennis swing, thus identifying the need for more accurate player testing using a method with higher frame rates. If the peak in head speed occurring before the impact would be confirmed by these tests, it would suggest that service impact simulations can be adequately achieved in the laboratory under constant velocity conditions, which would result in a simplified test mechanism. Buckley and Kerwin's (1988) paper perhaps provided the key to understanding the combined results of so many researchers. The force/contraction speed limitations for human skeletal muscle suggest the service energy is generated

early in the action by contraction of the larger muscles at low speed. This is transferred in a 'whiplash' action through the kinematic chain with consequent sequential angular velocity magnification. Distal segment rotation and muscular activity during this period serve only to guide the release and not impede the energy transfer. This phenomenon is most likely analogous to the wrist deceleration for the typical golf swing, which is well documented by a number of researchers (Cochran & Stobbs 1999, Jorgenson 1999, Miura 1999). The passive wrist action through most of the down swing, known as the "uncocking" of the wrist, has been shown to produce maximum club head speeds. The highest head speed is reached just before impact through a whipping action from the wound-up shaft, believed to guide the downward motion for a more consistent swing. Further investigation is needed to verify the same phenomenon for the tennis serve.

Following on from the literature, the following goals were earmarked for a series of player tests as part of the research:

- Obtaining a high-resolution motion profile of the racket before and after impact in order to set a benchmark for the test machine to achieve and propose justifiable design simplifications.
- Investigate extreme racket parameters and the influence on racket performance, such as racket and ball speeds in order to lay down the boundaries for the test machine's PDS.
- Determine the relationship between head speed and the racket's MOI, which should be incorporated by the test machine to determine the impact speeds for testing various rackets.
- Investigate the locations of real play ball impact on the racket face in relation to the racket's 'sweet spots'.



## 5.2 Pilot player testing

As a validation of equipment and possible acquisition configurations to be used, a pilot motion study was performed on university team level players using a high-speed video camera and a newly developed motion capturing system. The latter was still under development with frequent alterations being made to the hardware and software during the research in order to improve its performance.

As a first approach, a Kodak Ektapro high-speed video camera was used to record the serve motion at 4500fps. The players were required to serve centreline serves as fast as they were able to, in an attempt to reproduce conditions most often used by players to perform the fastest recorded serves. This also confined the racket motion just before and after impact to a plane almost perpendicular to the camera viewing direction. The camera viewing direction was aligned parallel to the baseline and focused with a field of view suitable to capture racket motion through a  $180^\circ$  arc from the horizontal before impact to the horizontal after impact. Lightweight polystyrene markers were attached to the tip and heel of each racket and these positions were manually digitised afterwards from the recorded video sequence. Five frames from the video data, spanning  $\sim 90^\circ$  of the swing and spaced at roughly equal intervals with the last just before impact, together with five similarly spaced frames starting from just after impact were used to establish the racket's planar position, velocity and acceleration profiles.

The second method utilized the CODA (Cartesian Optoelectronic Dynamic Anthropometer) system, selected due to its high sample rate and marker resolution, which made it the most accurate system commercially available at the time. Moreover, it was a real-time motion analysis system, utilizing active markers as opposed to the passive markers used by traditional systems, which required a very time-consuming digitisation process at a relatively low

resolution. Instead, the active markers consisted of infrared light emitting diodes (LEDs), which burst in sequence while being detected by three special cameras, each consisting of a fine light-sensitive grid for locating a single axis position of each marker. A CODA scanning unit (Figure 5.1) combined the information from three such cameras in combination with a calibration set-up matrix in order to calculate the three dimensional location of each marker. The set-up matrix is determined by initialising the CODA with a set of three markers arranged in a specified orientation at the desired origin chosen for the measurements. The markers burst sequentially, synchronised by the CODA units via the receiver boxes, which can drive a pair of markers. The CODA units utilise the flash sequence to distinguish between the different markers. The maximum sample rate of the system depended on the number of markers used, with a maximum of 800Hz when sampling up to six markers, which was at least double the highest sample rate previously measured in the literature (Charnwood, 2003). Previous methods also utilised relatively large markers, about 20mm in diameter, while the CODA LEDs are only 7.5mm in diameter with a 1mm light emitting core, resulting in a significantly better spatial resolution.

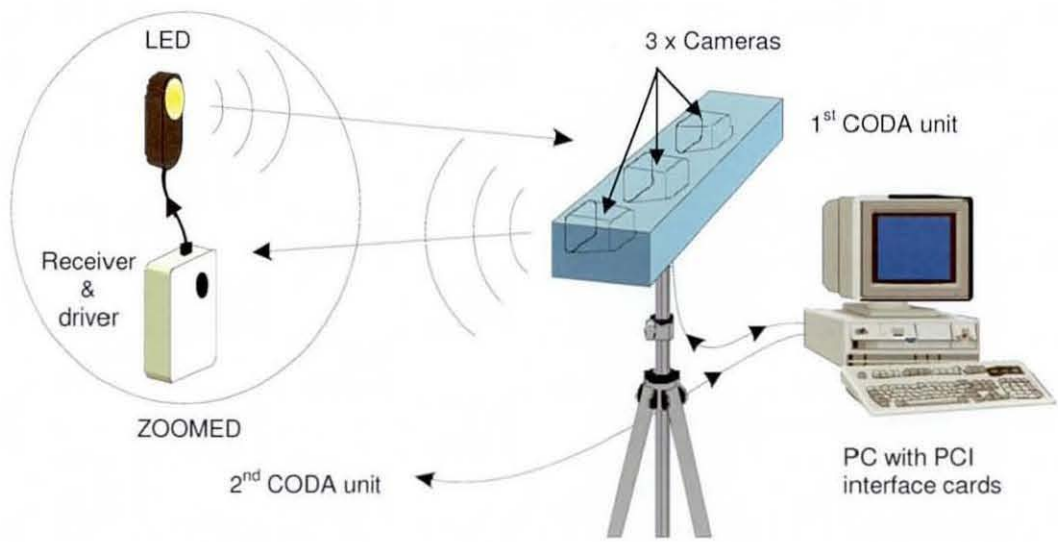


Figure 5.1: A diagrammatic representation of the CODA system.

The optimum test set-up was established with two CODA mpx30 scanning units placed on either side of the baseline, given that the accuracy for movement parallel to the scanning units ( $\pm 0.1\text{mm}$ ) is higher than movement normal to it ( $\pm 0.6\text{mm}$ ). A scanning unit was placed on either side of the court, with the main racket motion parallel to the units (Figure 5.2).

Four markers were placed on either side of the racket, with two facing each scanning unit during the impact. One pair of these markers was attached close to the middle of the racket face and the other in the throat area, as illustrated in Figure 5.3. The two receiver units driving the markers were also attached to the throat area, just above the two lower markers.

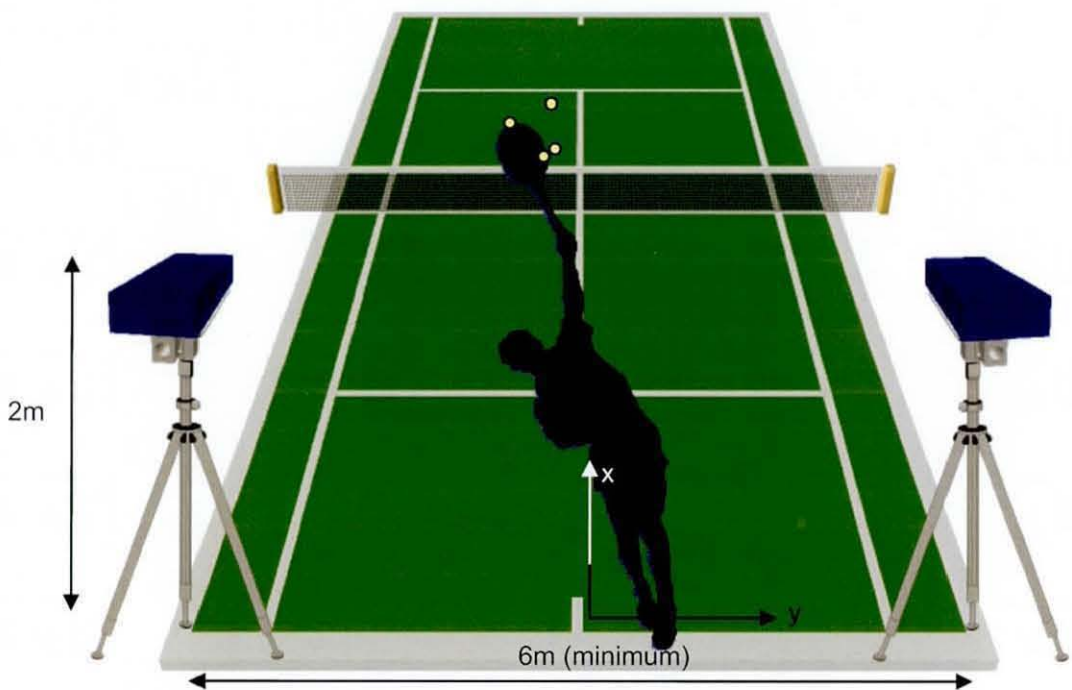


Figure 5.2: The general CODA set-up during the player testing.



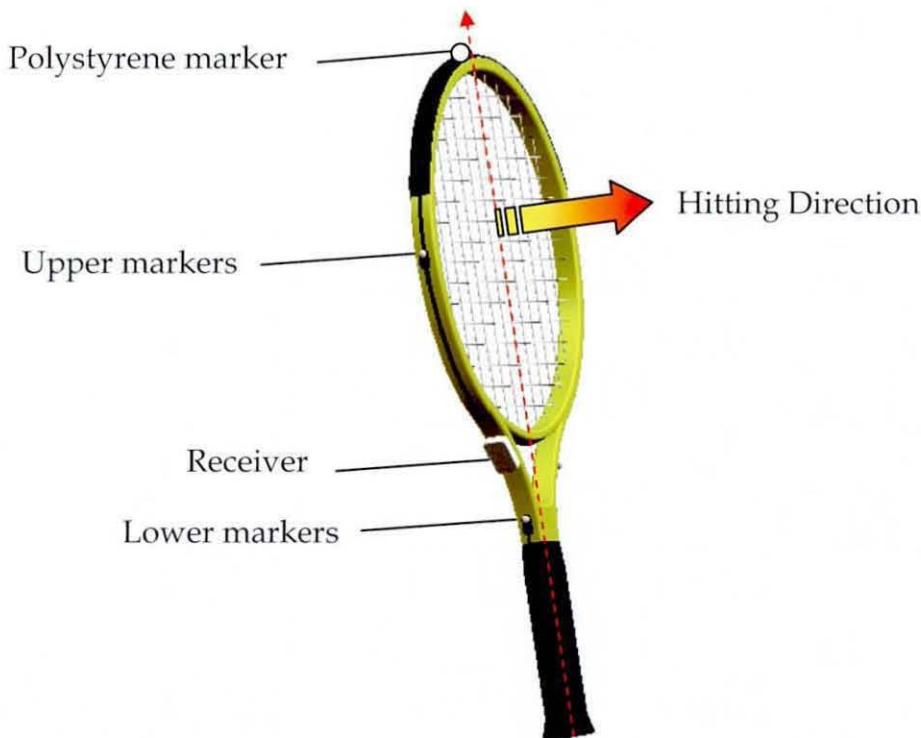


Figure 5.3: The marker and receiver locations of the racket during the initial testing.

Players were instructed to serve six ‘good’ first serves with three pre-prepared rackets. They were continuously motivated verbally to perform at their peak and the only serves recorded were those landing inside the service box and with the players’ confirmation that it was a good representation of their optimum technique.

The rackets used for the tests were an original Head Ti.S6 (representing the lightest racket available at the time), a weighted Dunlop 200G (representing the notional acceptable maximum mass/MOI for a modern racket) and a weighted Ti.S6 (representing the balance of an old wooden racket). The rackets were selected to represent the entire racket inertia range available on the market (Table 5.1). In addition, each player also performed the test with their own racket, which was used to normalise the data from the other rackets.

Racket	Length [m]	Mass [kg]	Balance [m from butt]	MOI [kg.cm <sup>2</sup> ]
Head Ti.S6	0.705	0.291	0.374	331
Dunlop 200G	0.684	0.392	0.302	340
Head Ti.S6 (weighted)	0.705	0.426	0.338	371

Table 5.1: The properties for test rackets used for the CODA analysis.



The CODA scanning units recorded the coordinates of four markers during the serve, while the PC based software calculated the coordinates of virtual markers, which were defined in relation to the real markers in order to represent other landmarks of interest on the racket. The software uses a curve-fitting algorithm to interpolate missing marker coordinates due to bad ambient conditions and invisibility of the markers or receiver boxes to the CODA units. The coordinates are then differentiated to determine additional parameters, such as velocity and acceleration, for both real and virtual markers. During this pilot study, the CODA software was still under development and did not accommodate for sequential sampling of the markers. This meant the last marker in the sequence was sampled at a discrete time ( $172\mu\text{s}$  at  $400\text{Hz}$ ) after the first and therefore, the data was not a true representation of the marker positions at a single specific instance. The data therefore had to be deskewed externally in order to determine the true location of the markers by means of interpolation. The deskewed data was imported back into the software, which was used for further manipulation.

The recalculated data is exported again to a spreadsheet where the final detailed analyses were performed. The racket face before the impact was selected as the plane for determining the coordinate system for calculating desired parameters. Hence, the head speed was calculated normal to the racket face and the instantaneous centre of rotation (ICR) was located in the plane normal to the face and intersecting the longitudinal axis.

For the high-speed tests, the polystyrene markers at the racket tip and butt as well as the ball itself were digitised throughout the impact. Figure 5.4 represents a typical captured side view of a racket and ball reconstructed in MS Excel. The results revealed a changing in racket length (the distance between the tip and butt markers), which indicated the racket was subjected to a significant rotation of up to  $\sim 30^\circ$  out of the global X-Z plane during the impact.

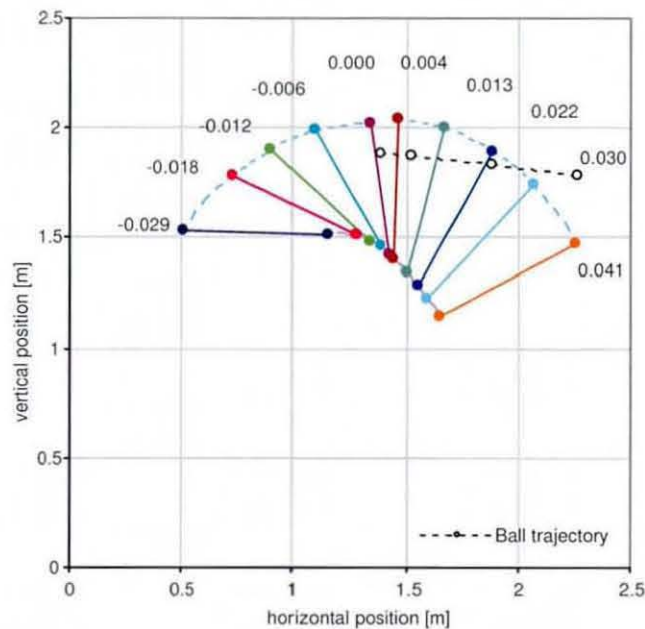


Figure 5.4: A reconstructed representation of the racket motions measured with the high-speed camera.

Calculation of the velocity profiles from the high-speed camera was performed by interpolating the 2D position data with two polynomial curves, which were then differentiated to give the velocity of each marker location versus time. Typical velocity profiles of important locations on the racket are plotted in Figure 5.5 and it is evident that the profiles were much smoother than those calculated by the CODA software in Figure 5.6, which was the first indication that its digitising resolution with the high-speed camera was not high enough to produce an accurate representation of the impact. The next indication was the order of magnitude of the peak racket velocities, which were similar to those measured with the CODA, but had a greater degree of variability of  $\sim 20\%$  between different hits, as opposed to the  $\sim 3\%$  obtained from the CODA. The CODA profiles also indicated the decrease in impact speed just before the impact, which was reported in the literature, while only a constant velocity is visible on camera profiles. These results established the CODA system to be superior in accuracy, and despite the high-speed camera's advantage of also providing the ball velocity, the CODA was selected as the

preferred test method, especially because it provided 3-dimensional data from which additional parameters could be calculated.

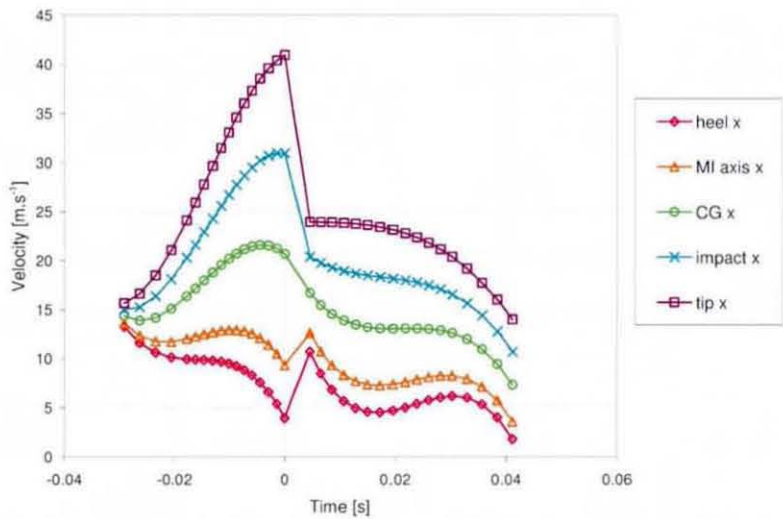


Figure 5.5: A reconstructed representation of the racket motions measured with the high-speed camera.

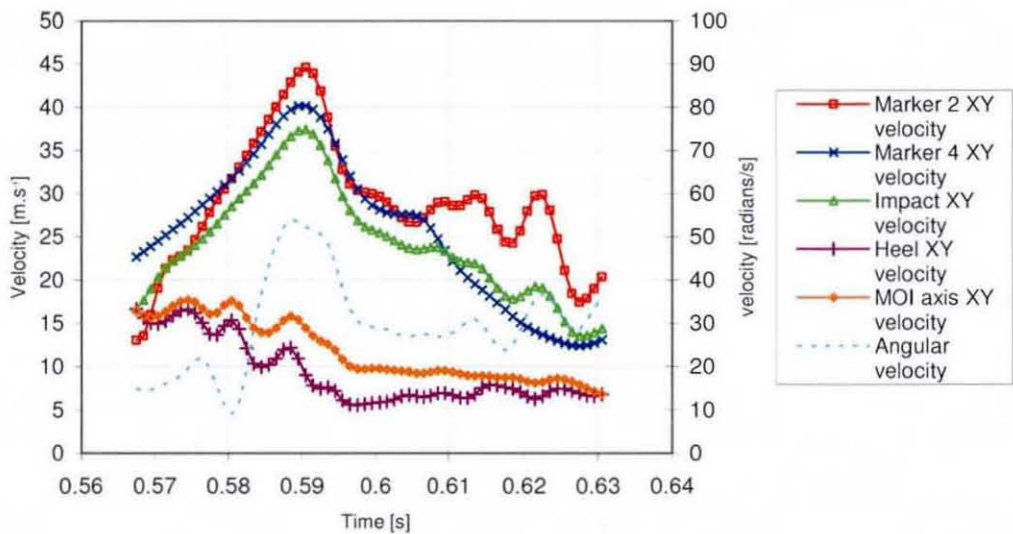


Figure 5.6: A reconstructed representation of the racket motions measured with the CODA system.

Maximum impact head speeds varying between  $27\text{--}38\text{m.s}^{-1}$  were measured for the different players, which appeared to be related to each racket's MOI, as expected. In order to develop test procedures for racket performance, which would not discriminate against heavier rackets, the relation between the



racket's MOI and the head speed needed to be determined. The average maximum head speed achieved with each racket was therefore calculated for all players from the CODA data and is presented in Figure 5.7.

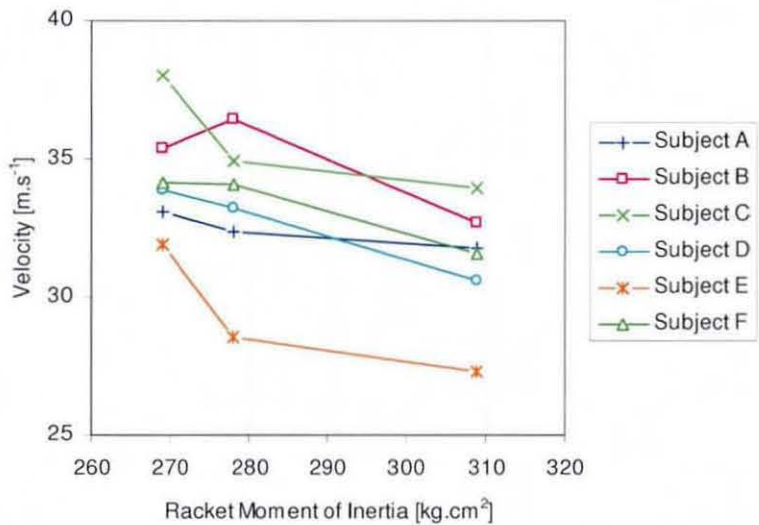


Figure 5.7: The head speed achieved by players with each racket.

Results indicated that Subjects E and C were less skilled players, with a more erratic swing style and they were therefore omitted from the control group for further analysis. The results for the remaining subjects indicated an  $8\pm2.5\%$  decrease in head speed for a  $12\%$  ( $\sim 40\text{kg.cm}^2$ ) increase in racket MOI.

The drive of a realistic machine, swinging a racket at a stationary ball raised the question of the ICR location. The ICR location in the racket's frame of reference was calculated in relation to the racket butt. Excluding subjects E and C once more, the ICR locations were reasonably consistent for the remaining players, located vertically between 127-227mm below the racket butt and horizontally between 86-183mm behind the butt (Figure 5.8).



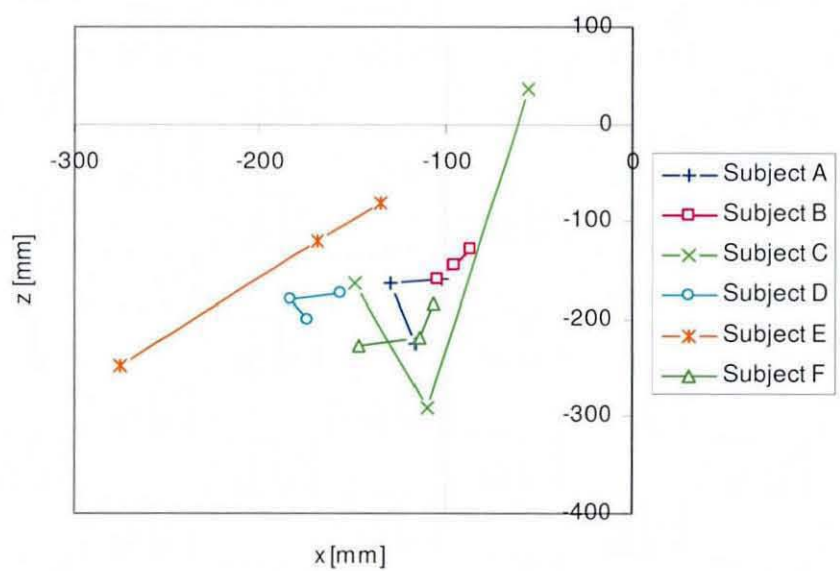


Figure 5.8: The ICR location achieved by players with each racket.

The results clearly indicate that for the detailed analysis required of the racket’s motion during impact, the CODA was the preferred system above the high-speed camera due to its higher spatial resolution. These initial tests were performed on a relatively small group of only six people and although these tests provided good initial data, it was necessary to increase the data pool. For these extended tests, care hat to be taken to increase the sample rate of the system to its maximum of 800Hz and to improve on the pilot set-up where possible to increase measurement accuracies.

5.3    Extensive player testing

For the extended player testing, an upgraded CODA system was used, which could sample at the desired 800Hz and automatically deskewed the acquired data without having to export it. After experimenting with various test configurations, a test protocol similar to that used during the pilot testing described in the previous section was adopted. The only exception was the placement of the receiver/driver units, which were relocated below the butt, instead of the throat area (Figure 5.9).

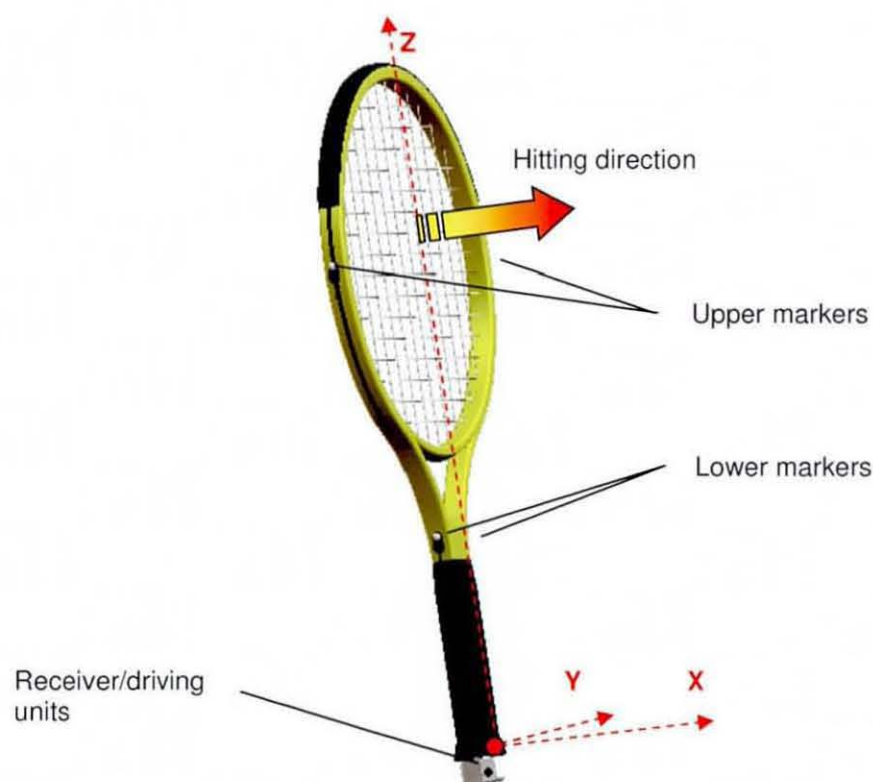


Figure 5.9: The marker and receiver locations of the racket during the final player testing.

In this position their contribution to the racket's MOI would be minimized and it would reduce the vibration amplitude, which caused them to malfunction during pilot testing due to mechanical fatigue of the electronic components. The flat bottom end of the butt-end cap also provides a better surface for mounting the receivers. Both receivers were fixed via a very lightweight aluminum bracket, which allowed for them to be removed easily and swapped between rackets during testing. Since court bookings and players' personal schedules only allowed for relatively few and short testing windows, considerable effort was made to streamline the test set-up and procedure. The same four weighted Head TiS6 rackets, which formed part of the initial control group of the rackets used during the COR testing (§4.3), were used. As described before, these rackets were incrementally weighted with lead tape, from the lowest to the highest MOI available on the market at the time. Players were given all four rackets to play with in a random order, in order to cancel

the effect of the test sequence on the results. The basic test procedure was the same as used in §5.2, with each subject allowed a sufficient warm up with the test racket after which they were instructed to perform 10 'good' serves. Players were asked to perform their fastest first serve down the centreline, applying as little spin as possible to the ball. Nine players were tested, ranging from male and female university team players to male junior ATP tour players (junior ATP rankings 13-20).

The CODA software allowed for virtual markers to be constructed, which represent points on the racket for which the position and velocity could be automatically calculated. Virtual markers were created at the midpoints between the two upper markers and the two lower markers, which were connected to represent the racket's centreline or Z-axis for the internal reference frame. The centreline was extended to locate further virtual markers for landmarks of interest, such as the butt, the centre of mass (CM), the impact point and the racket tip. The X-axis was normal to the face surface with its origin at the racket butt in order to determine the relative location of the ICR. For calculating the latter, the relevant marker position coordinates and velocities for each impact were exported into a MS Excel spreadsheet, which was used in combination with Mathcad to perform the vector analyses, while the results were exported back into MS Excel for further statistical analysis.

Figure 5.10 and Figure 5.11, respectively, represent typical side and plan views (in relation to the CODA's global reference frame) of the racket motion from about 5ms before to about 5ms after contact with the ball commenced. The stick figure was constructed by connecting the discrete markers only for every second sample for better visualisation.

Initial calculations indicated a relatively small deviation angle of  $\sim 6^\circ$  between the racket velocity vector of the impact point and the vertical global x-z plane just before impact, and an angle of  $\sim 3^\circ$  with the x-y plane, which was significantly smaller than the  $30^\circ$  angle measured during the pilot. It is believed



to be a result of the more accurate measurement, which made the location of the impact point more exact. It also makes sense for a player to hit a centre-line shot with the racket virtually in the planar position to ensure the ball is hit straight. The small  $\sim 6^\circ$  degree angle evident before the impact is needed for the ball to leave the racket face in the planar position, since the ball stays on the strings for about 5ms as represented by the last stick figure in Figure 5.11. The angle was calculated to result in an insignificant error of  $\sim 1\%$  in impact velocity due to the smaller component measured in the global x-axis, justifying using the global coordinate system to calculate the racket head speed. Also, only velocity components in the x-direction would contribute to the ball speed down the centreline, which is the main concern of the research and implies that a single axis rotation test machine could sufficiently replicate the serve motion. The head speed was therefore calculated directly from the CODA software as the horizontal speed of the upper middle virtual marker. The marker location was in fact  $\sim 3\text{mm}$  below the average impact location measured for most players (as described later in §5.4) but was regarded as a sufficiently accurate estimation, since the location could only be measured for each set of impacts rather than every impact.



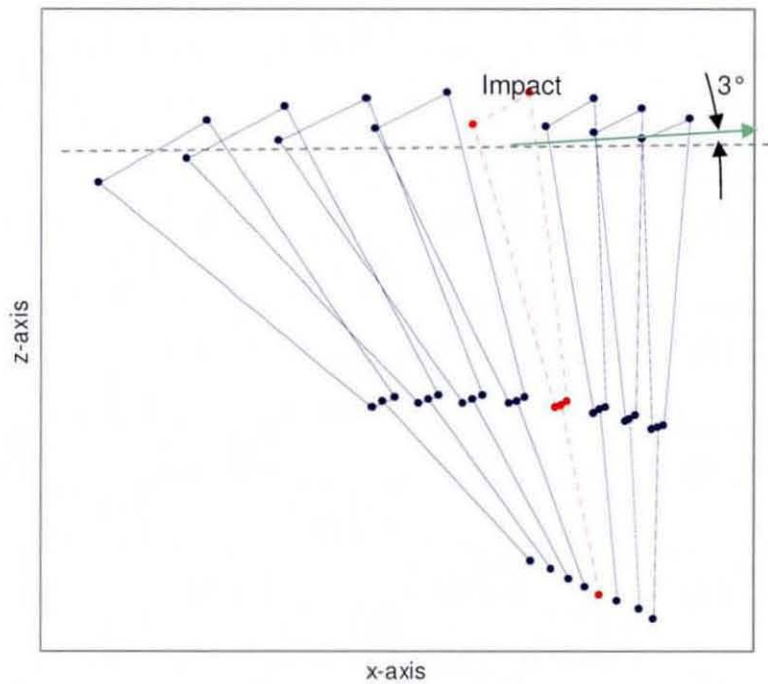


Figure 5.10: The global x-z plane (side view) of the racket during the serve indicating the impact point (red dotted).

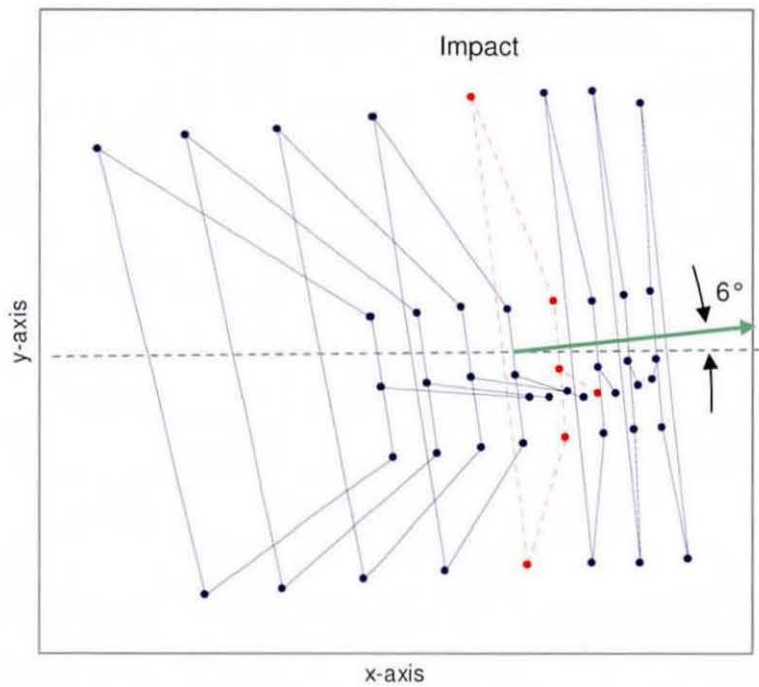


Figure 5.11: The global x-y plane (plan view) of the racket during the serve indicating the impact point (red dotted) and velocity vector

A typical velocity trace for the markers is shown in Figure 5.12. During upswing, the head speed increases until it reaches a maximum just before the impact. During impact the racket slows down by a maximum of ~50% of the impact speed, which compares well with the ~60% calculated from measurements by van Gheluwe and Hebbelinck (1985) The impact lasted for about four sample points (i.e. ~5ms at 800Hz), which also substantiated values obtained from the literature (§3.1.2). As a result of the frame deformation caused by the impact, the signal after the impact is a sinusoidal vibration rather than a smooth curve, which complicated the calculation of post-impact velocities.

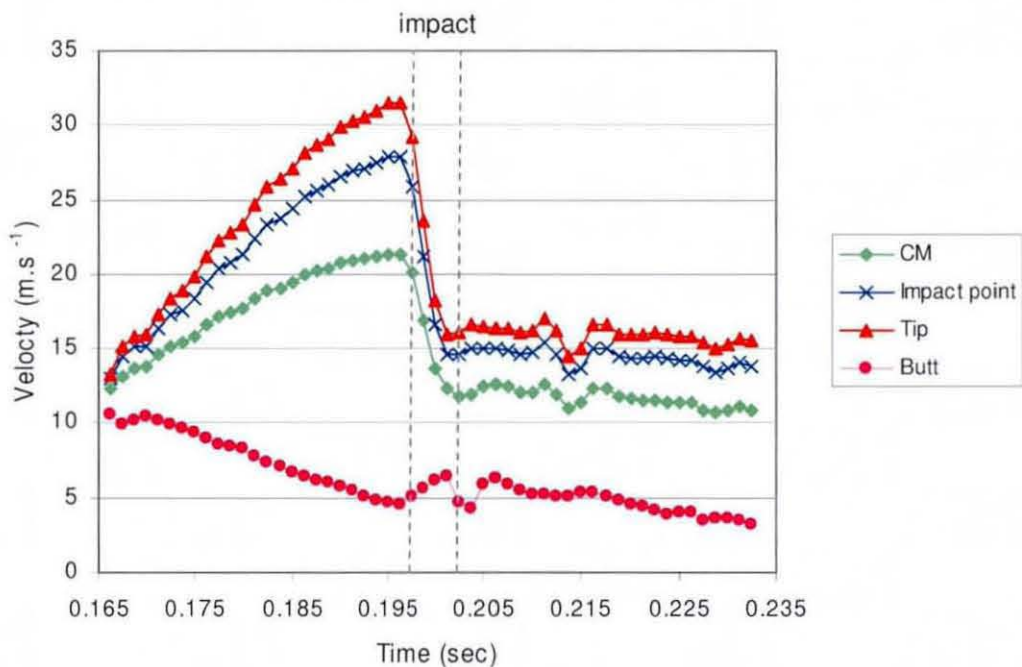


Figure 5.12: The typical velocity profile for important landmarks on the racket (measured in the x-direction of the global axis).

The maximum head speed achieved by players would provide an indication of the upper limit to be achieved by the test machine. Tests revealed racket average maximum head speeds for the men to vary between 31-42m.s<sup>-1</sup> and between 27-31m.s<sup>-1</sup> for the woman, with a standard deviation of 0.6m.s<sup>-1</sup> (1.64%) for all players with each racket. The maximum speeds are in the same

range as those from the pilot study and significantly higher than those measured by Elliot (1986), who measured an average of  $34.8\text{m.s}^{-1}$  for the men and  $31.8\text{m.s}^{-1}$  for the woman. The speed traces from the pilot study and especially those from Elliot look significantly different to Figure 5.12. With the pilot study sampled at 400Hz and Elliot's tests only sampled at 200Hz, compared to 800Hz in the extended tests, the resulting speed profiles are smoother and do not indicate the sudden drop in head speed during the impact. Instead of the decrease in head speed found shortly before impact in the earlier tests, the current test indicates a short period of constant head speed just before impact, followed by a dramatic drop in speed during the impact. It is suggested that, during the previous tests, the sampling resolution was not high enough, thus smoothing the real peak so that it appears to be earlier. The consistency of the players and accuracy of the test set-up should serve to set specifications for the test machine.

The highest head speeds for the group were achieved by the two junior players (subjects F, G) on the ATP tour, which should be most representative of the desired operation speed for the test machine. In order to obtain the maximum limit to be achieved, the ideal situation would be to measure the fastest head speed achieved by any player on the ATP tour. This was not possible, therefore Equation 3.10 was used to estimate the head speed as  $\sim 48\text{m.s}^{-1}$ , using the fastest recorded serve at the time ( $66.6\text{m.s}^{-1}$ ).

In order to relate the head speed to the other parameters like the racket MOI and the ball speed, the location of the racket's ICR at impact was needed. This would provide a realistic ICR location for the racket when swung in the test machine. Since the machine will only rotate the racket in a single plane, only the horizontal and vertical components of the ICR location had to be found. The first stage of the analysis was to ensure the quality of all data sets by only analysing data with all markers continuously visible up to the impact and by comparing a measured gauge length with its known length. The scalar

distance used for the latter was taken as the distance from the upper middle (*um*) to the lower middle (*lm*) marker (Figure 5.13). First the relative position vector ( $\vec{R}_{rel}$ ) between the upper marker ( $\vec{R}_{um}$ ) and the lower marker ( $\vec{R}_{lm}$ ) position vectors was calculated:

$$\vec{R}_{rel} = \vec{R}_{um} - \vec{R}_{lm} \tag{5.1}$$

The scalar distance  $|\vec{R}_{rel}|$  was measured as 327mm and the allowable tolerance set as  $\pm 4$ mm.

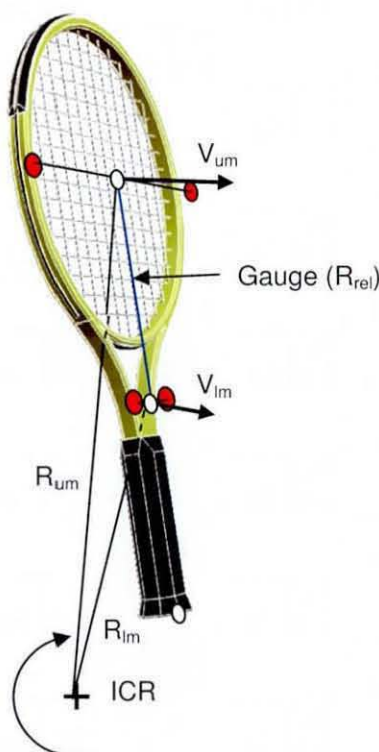


Figure 5.13: A diagram for calculating the racket parameters.

In order to determine the ICR location the angular velocity vector ( $\vec{\omega}$ ) was determined by calculating the relative velocity vector ( $\vec{V}_{rel}$ ) from the upper ( $\vec{V}_{um}$ ) and the lower marker velocity ( $\vec{V}_{lm}$ ):

$$\vec{V}_{rel} = \vec{V}_{um} - \vec{V}_{lm} \tag{5.2}$$



The angular velocity of the racket was then given by:

$$\vec{\omega} = \frac{\vec{R}_{rel} \times \vec{V}_{rel}}{|\vec{R}_{rel}|^2} \quad (5.3)$$

Next, the scalar radius ( $|\vec{R}_{lm}|$ ) from the ICR to the lower middle marker was calculated by:

$$|\vec{R}_{lm}| = \frac{|V_{lm}|}{|\omega|} \quad (5.4)$$

while for determining the vector  $\vec{R}_{lm}$ , the unit vector perpendicular to the velocity of the lower marker was needed. First a vector ( $\vec{R}_{per}$ ) perpendicular to the velocity in the XZ-plane was calculated:

$$\vec{R}_{per} = \vec{V}_{lm} \times \vec{\omega}^{-1} \quad (5.5)$$

$$n_{lm} = \frac{\vec{R}_{per}}{|\vec{R}_{per}|} \quad (5.6)$$

Finally, the position vector ( $\vec{R}_{lm}$ ) from the ICR to the lower marker was calculated and subtracted from the lower marker position to provide the coordinates of the ICR.

So far all calculations have been performed in the global reference frame, but the position of the ICR is more functional when expressed relative to the racket butt in the racket's frame of reference as shown in Figure 5.14. The vertical and horizontal distances ( $|\vec{R}_{ver}|$ ,  $|\vec{R}_{hor}|$ ) from the IC to the butt are calculated as:

$$|\vec{R}_{ver}| = |\vec{R}_{ICR}| \cdot \cos(\alpha + \beta) \quad (5.7)$$

$$\left|\vec{R}_{hor}\right|=\left|\vec{R}_{ICR}\right| \cdot \sin (\alpha+\beta) \tag{5.8}$$

with the angles  $\alpha$  and  $\beta$  calculated using the locations of the upper and lower markers. The ICR locations for all players, achieve with each racket are presented in Figure 5.15.

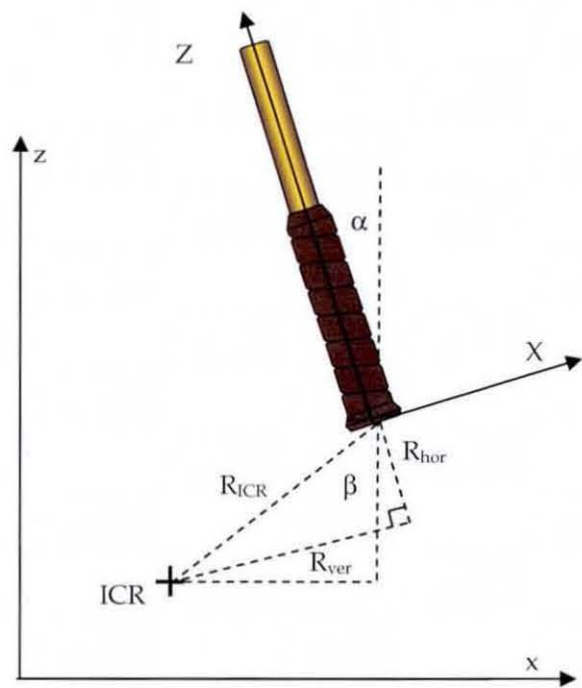


Figure 5.14: A diagram for converting racket parameters from the global frame of reference ( $x, z$ ) to the racket frame of reference ( $X, Z$ ).

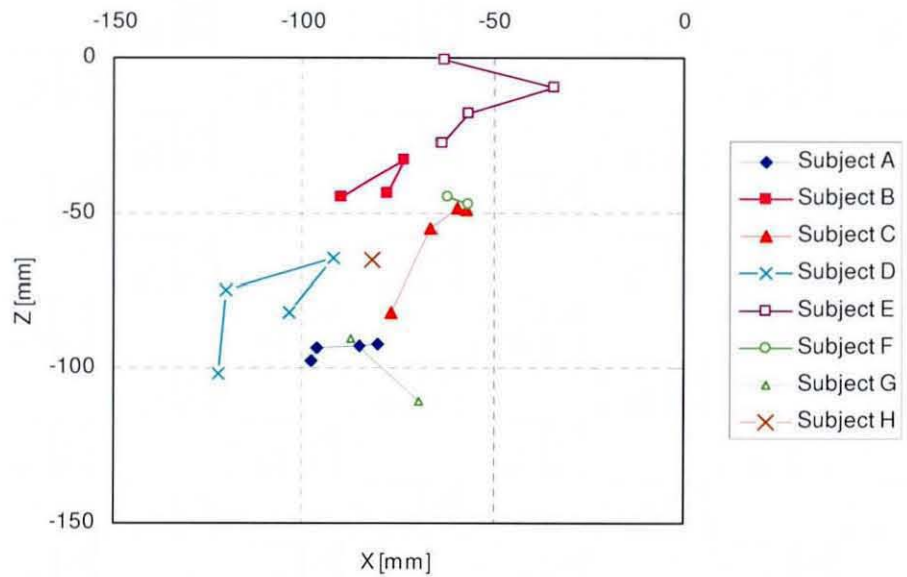


Figure 5.15: The average ICR location achieved by players with each racket.

It is interesting to notice that each player achieved a reasonably consistent ICR location with the different weighted rackets. The spread achieved by different players is also rather small considering their different swing styles. The ICR lay between 34-122mm ( $\bar{Z}=62\text{mm}$ ,  $\sigma=12\text{mm}$ ) below and 1-111mm ( $\bar{X}=80\text{mm}$ ,  $\sigma=12\text{mm}$ ) behind the racket butt. The locations are closer to the butt than those measured during the pilot study (§5.2), which yielded distances of up to ~220mm below and ~180mm behind the racket butt. This could be related to a different plane (plane normal to the racket face) used by Mitchell *et al.* (2000a, 2000b) or the higher sampling rate of the current testing, hence increasing the accuracy. It could also have something to do with the different style and quality of the control groups, since only subjects A and D were used in both studies and even they had had almost two more years of coaching which could have changed their swing styles. In order to ensure a system incorporating all expected variances the results was combined with those from Mitchell *et al.* (2000a, 2000b) to determine a representative range for the ICR to be achieved by the test machine.

It was anticipated that a player would be able to swing a racket with a lower MOI at a higher head speed, therefore if a test standard for all rackets were implemented at the same head speed, rackets with a lower MOI would appear to be less powerful since they would measure lower ball rebound speeds, but during play the increase in head speed achieved would also increase rebound ball speed. This relationship between a racket's MOI and the racket head speed during play was not known and needed further investigation. To achieve this, the average maximum head speed achieved with each racket was determined for each player and average relation between the head speed and MOI determined. In order to make the best use of the available data, since some players did not get to use all the rackets and the data for some rackets had to be dismissed, the following approach was adopted to determine this relation. Traditionally, the relationship was assumed be linear, therefore a regression was fitted through the average head speeds achieved with all the rackets by each player (Figure 5.16) and the average slope calculated for all the players. The linear equation describing the relationship between the head speed ( $v_r$ ) and the swing weight ( $I_{sw}$ ), achieved during the serve by high-level players with a standard set of rackets, is therefore in the form:

$$v_r = c \cdot I_{sw} + k_l \quad (5.9)$$

with the slope ( $c = -0.031$ ) representing the relationship between head speed and MOI and  $k_l$  and indication of the player's strength. The equation was used to calculate the average drop in head speed over the test MOI range.



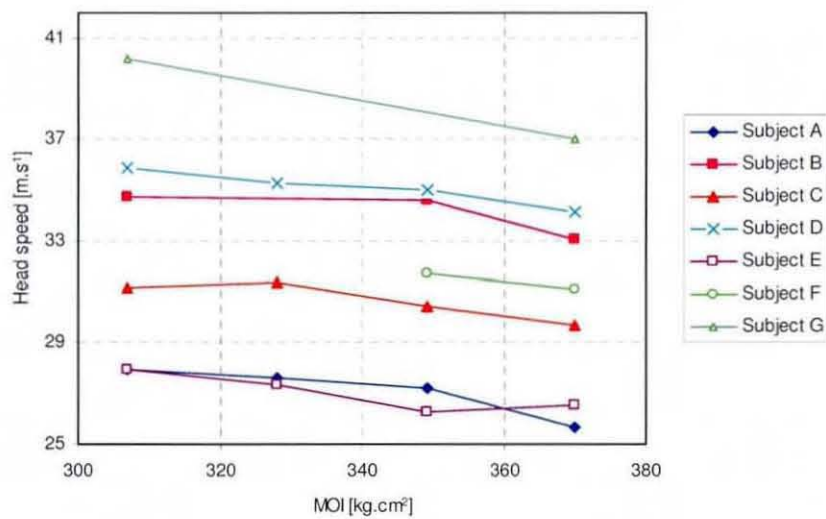


Figure 5.16: The average head speeds achieved by players with each racket.

The results for all players indicated an average decrease in head speed of  $1.93\text{m.s}^{-1}$  ( $\sigma=0.60\text{m.s}^{-1}$ ) for the  $63\text{kg.cm}^2$  increase in MOI, which firstly stressed the players' consistency and related to a 5.8% decrease in head speed for a 21% increase in MOI. This is significantly lower than the 8% drop in head speed measured for a 12% MOI increase during the pilot tests (§5.2). The different results are most probably due to the lower acquisition sampling rate, which caused more variability by missing the real head speed peaks. It could also be related to the difference in player skills but this is unlikely since the two tour players (subjects F and G) displayed no considerable difference in consistency of the head speed, or the change in head speed due to the increase in MOI.

In 2001, Cross derived the relation between the head speed and the swing weight as an inversely proportional relationship:

$$v_r = k_p / I_{sw}^n \tag{5.10}$$

where  $k_p$  is a constant representing player strength,  $n$  a constant characterising the relationship between the two parameters. The value of  $n$  was solved by fitting a power regression through the results from the four players who played

with each of the four rackets (Figure 5.17) and calculating the average power achieved by them.

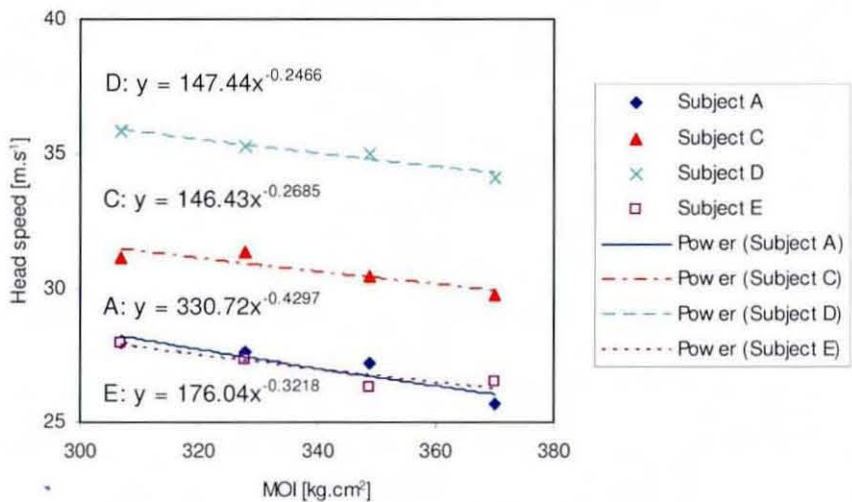


Figure 5.17: The average head speeds achieved by players used in order to determine the power constant  $n$ .

The average value of  $n$  was calculated as 0.32 ( $\sigma=0.08$ ), which is similar to the 0.2 predicted by Cross. For the range of the rackets, the power regression had almost the same average correlation to fit the test data ( $R^2=0.85$ ) as the linear regression ( $R^2=0.86$ ), meaning both accurately describe the relationship between head speed and MOI within the tested range, although the inversely proportional relationship is preferred, since it provides a better description of the physics behind the motion, which would ensure its accuracy over a wider range of rackets and players.

During the player testing, the ball speed was also measured using a JUGS radar gun but readings were found to be very unpredictable at times and were therefore not included in the full analysis. Instead, the resulting ball speeds were estimated by substituting the  $ACOR_f$  results from the freely suspended rebound testing (§4.3.3) into Equation 3.10.

The equation calculates the ball speed  $v_b$  from the  $ACOR_f$  measured at each impact location, for a maximum nominal head speed of  $42\text{m.s}^{-1}$ , which was

the highest recorded for the average impact location during the player tests. This was taken as the nominal speed of racket A, while the nominal head speeds for the remaining rackets were calculated using Equation 5.10. For each racket, in turn, the head speed of each impact location ( $u_r$ ) was calculated from its distance to the average ICR location.

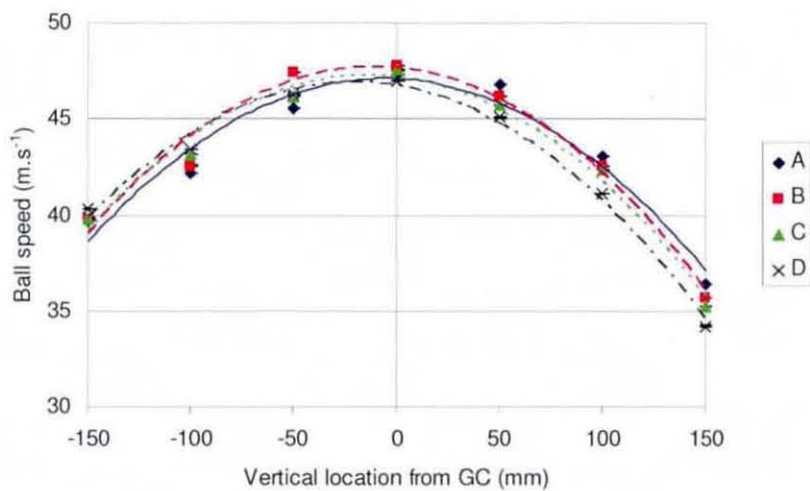


Figure 5.18: The transformed rebound ball speed measured for Rackets A to D during the freely suspended performance tests.

The results in Figure 5.18 indicated the maximum ball speed of  $47.7\text{m.s}^{-1}$  achieved with Racket B and the lowest with Racket D at  $46.9\text{m.s}^{-1}$ , which is a 1.7% decrease in ball speed over a 12% increase in MOI. Although the difference was marginal, it substantiated the theory that, during the serve, the increase in head speed due to the lower racket MOI increases the ball speed more than the decreasing effect on the  $\text{ACOR}_t$ , especially further away from the ICR e.g. closer to the racket tip. The max ball speeds measured with the JUGS radar gun for the player achieving the highest head and ball speeds were significantly lower at  $45\text{m.s}^{-1}$ . This was believed to be due to the JUGS measuring the average ball speed across the court, rather than the peak immediately after impact. The locations of the peak ball speed measurements were between 6mm and 22mm below the GC for rackets A to D respectively,



which is significantly lower than the common belief that the maximum rebound ball speed for a serve could be achieved by hitting the ball relatively higher up the racket face.

Comparing results between different test methods also emphasised the dependency of results on the boundary conditions and the importance of correct transformation of results. Since, this would not always be understood by the stakeholders considered for the machine, it strengthened the case for a test machine reproducing play conditions.

### 5.4 Ball impact location

From the performance tests in Chapter 4, it was clear that the ball's impact location has a major influence on the racket's rebound characteristics. Hence, the real impact location during play needed to be determined and investigated. Limited research had been done in this area, with most claims from researchers based more on theories than actual measurements. Amongst these were claims made by manufacturers (Völkl website 1999, Wilson website 1999), the measurements for a single racket, performed by Hennig & Schnabel (1998), and mostly theoretical speculations by researchers on where the preferred impact should be during the serve (Brody 1987, Cross 1997). The most common conclusion is that during the serve the player might tend to hit the ball closer to the tip to take advantage of its higher velocity. The additional height also gives the server a larger angle or 'window' to aim for, thus increasing the chances of getting the serve in. The ball also needs to be hit near the tip to maximise topspin.

Various methods of determining the impact point were experimented with. A simple, low cost solution was found in colouring the entire surface of the transparent strings with a black 'white board' marker. During impact the ink was rubbed off the strings by the ball, with the resulting 'white spot'



providing a fair indication of the impact location (Figure 5.19). Initial tests indicated that the players tested achieved a high level of repeatability with the 'white spot' varying only slightly in size after a number of impacts. Hence, the impact point was not measured after each serve but after a set of approximately 15 serves with each racket.

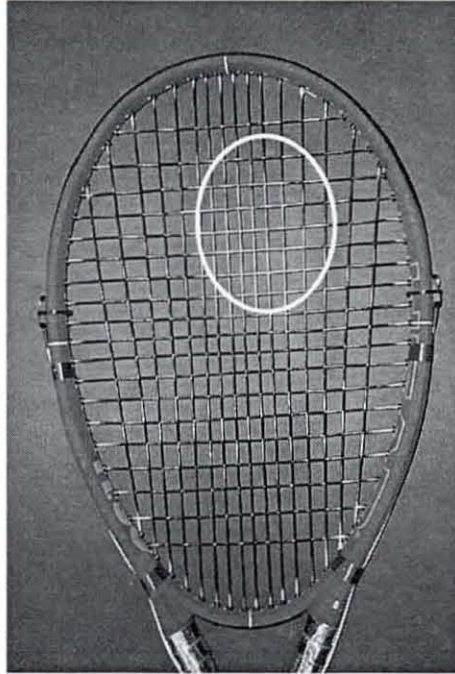


Figure 5.19: The average impact location ('white spot') resulting from a set of serves with a single racket.

All the strings, mains and crosses, were indexed into a grid, to record the centre and extremities of the 'white spot'. Measurements were later converted into x, y-coordinates in relation to the stringbed's geometric centre (GC) and the butt, to determine the representative impact location during the serve. This should shed light on which of the three 'sweet spots' mentioned in §2.3 (or others) players are aiming for and why and, in so doing, denote a better reference point to use when investigating a racket's sweet spot. The standard deviation in impact location would also assist in establishing acceptable tolerances to be achieved by the test machine. The range was measured as the width of the white spot minus the ball diameter, producing the maximum deviation of the ball's impact location as illustrated in Figure 5.20. Throughout

the analysis, it was assumed that the 'white spot' remaining after the set of impacts was the same size as the ball diameter. The effect of the ball edges not rubbing as heavily as at the impact centre would have been compensated by the ball deforming on the stringbed to the point where the contact area was approximately equal to the ball diameter.

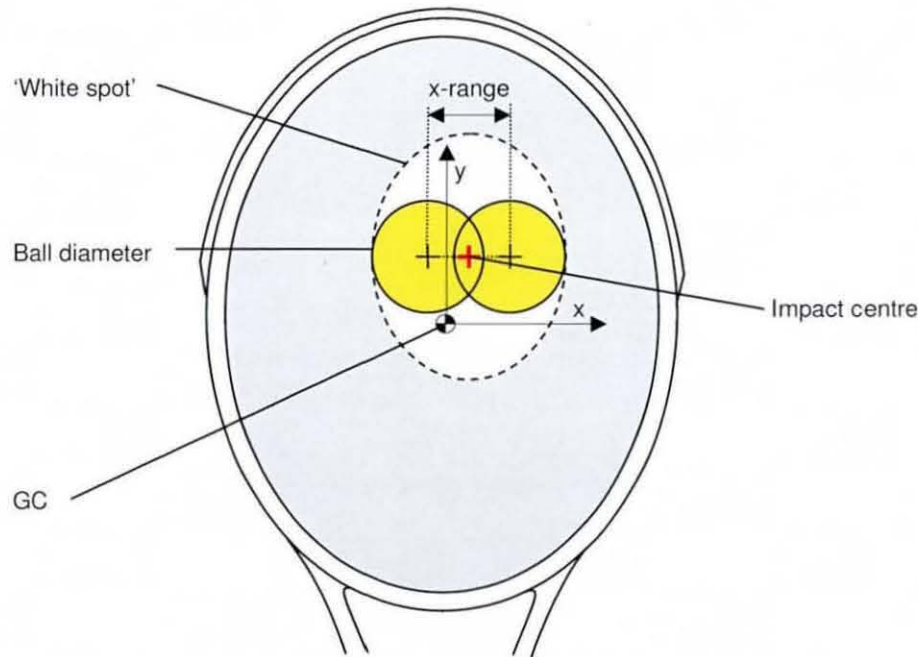


Figure 5.20: The coordinate system and method used to determine the impact location range.

The rackets used for testing were the same rackets used for the rebound testing described in Chapter 4; the four incrementally weighted Head TiS6 rackets (Rackets A-D). The measurements were taken during the player tests described in the previous section, hence the same players were used and a total of 10 players were analysed.

Of particular note was the remarkable consistency of players at this level, and one can only speculate what the accuracy of top-level tour players would be. As indicated in Table 5.2, the average range in impact location for all players and rackets was 56mm in the horizontal and 55mm in the vertical direction.

Comparing the average impact ranges for different rackets revealed that most players were more consistent with racket B, which would make sense, since its mass distribution best represented that of their own rackets. It also meant the test machine needed to achieve at least the same accuracy to be more consistent than players.

	Average	Racket A	Racket B	Racket C	Racket D	Racket G	Racket H
X range	56	57	53	57	54	42	8
X centre	10	7	20	6	5	10	15
Y range	55	54	46	53	68	54	79
Y centre	30	30	31	33	33	20	12
Y centre <sup>†</sup>	537	537	538	540	540	522	565

Table 5.2: The impact location (in mm) during the serve relative to GC (<sup>†</sup> relative to butt).

The average vertical location of the impact was approximately 30mm above the GC, which agrees well with the 17mm measured by Hennig & Schnabel (1998). This is above the location where each racket had its maximum coefficient of restitution, which was measured during the freely-suspended ball-cannon tests (§4.3.1) virtually on the GC. The average horizontal location of the impact was approximately 10mm towards the inside of the racket face (towards the player), which is also close to the 20mm measured by Hennig & Schnabel (1998). It is suggested that the ball was hit virtually on the centre line with the small offset probably attributed to rolling of the ball on the strings during impact. Although the players were instructed to perform a flat serve with no spin, the natural motion of the racket during impact includes a degree of polar rotation, which will always induce some degree of sidespin on the ball. This has been substantiated by NASA’s investigation of high-profile players (Pallis, 1999), where large amounts of spin were measured during all serves. Assuming this is mostly side spin and that these players also hit the ball virtually on the centreline, the influence on the horizontal ball speed leaving the racket face should be insignificant. Consequently, it confirmed the acceptability of excluding polar rotation from the design of the test machine.



There was an insignificant increase (~3mm) in the vertical location of the impact with an increase in racket mass, which was unexpected. If a racket with higher mass is swung with a lower head speed, the ball should be struck later than with the lighter racket, resulting in an impact lower on the racket surface. Clearly the players have adjusted the timing of their throws to compensate.

To shed more light on the vertical location of the impact, an additional set of tests were performed using two completely different rackets; a Wilson Pro Staff 95 (Racket G), only 680 mm in length and a Dunlop Super Long (Racket H), 734mm in length. These rackets represented the extremes in racket lengths available, in contrast to the Head TiS6 rackets, of a length 703mm. The results for all the rackets are presented in Table 5.2. A significant difference was found between the vertical impact locations, measured from the racket butt, which indicates that the players seem to adjust their timing to hit the ball further away from the butt with longer rackets. The range of impacts measured for the standard length rackets is 522-565mm, which agrees to an extent with a statement made by the Völkl website (1999), claiming “80% of all players, regardless of their ability or style of play, hit the ball at approximately 22inch (558mm) from the end of the grip”.

Possible explanations for the impact location were investigated by determining all the locations of each racket’s measurable ‘sweet spots’. It had been postulated by many researchers that players would adjust their swing to achieve a ball impact in the area of one of the three ‘sweet spots’ described in §2.3. The  $COR_f$  and  $ACOR_f$  and peaks were determined from the freely suspended racket tests (Figure 4.15 and Figure 4.17), while location of the maximum ball speed during play was obtained by combining these measurements with the human motion studies. These were combined with the location of the upper node from the first vibration mode from the vibration tests (§4.4) and the location of the COP for each racket in Table 5.3 and Figure 5.21. The latter was calculated as indicated in Appendix A (Brody *et al.*, 2002):



$$COP = \frac{I_{cg}}{m_r \cdot b} \tag{5.11}$$

where  $b$  is the racket balance point measured from the grip location (usually calculated from the butt). Since there seems to be no relation between the impact location and the racket butt all the locations are presented relative to each racket face’s GC instead of the racket butt.

	Racket A	Racket B	Racket C	Racket D	Racket G	Racket H
Ball impact	30	30	31	33	33	20
Max. ACOR <sub>f</sub>	-60	-70	-70	-80	-74	-67
Max. COR <sub>f</sub>	5	10	15	5	-4	-8
Max. ball speed	-6	-12	-14	-22	-6	-12
Vibration node	48	47	34	41	33	34
COP	-9	-44	-62	-81	3	2

Table 5.3: Relating the ball impact location during a serve to the various ‘sweet spot’ locations measured for the test racket (all locations are measured in relation to the GC).

Although the individual locations of all the measured ‘sweet spots’ indicated in Figure 5.21 were significantly higher than implied by the literature (Brody *et al.* 2002), their positions relative to each were correct. From the results, it is suggested that during a flat serve players most likely adapt their swing style to impact the ball at the vibration node, which is located just above the impact location. There had been some indications in the research that the effective impact node measure on the strings is slightly lower than that measured on the frame during these tests, since the load is transferred to the frame via the stringbed (Cross 2001, Goodwill & Haake 2002b). This would shift the node even closer to the impact location, although effect of the hand should have an opposing effect, moving the node towards the racket tip (Cross 1998a). This was not modelled during this work and could be simulated using the test machine. Although, more testing is needed for conclusive results, this is the first time that evidence has been presented to identify the location of the impact

during play. This has implications for future testing with the test machine and its relationship to on-court performance.

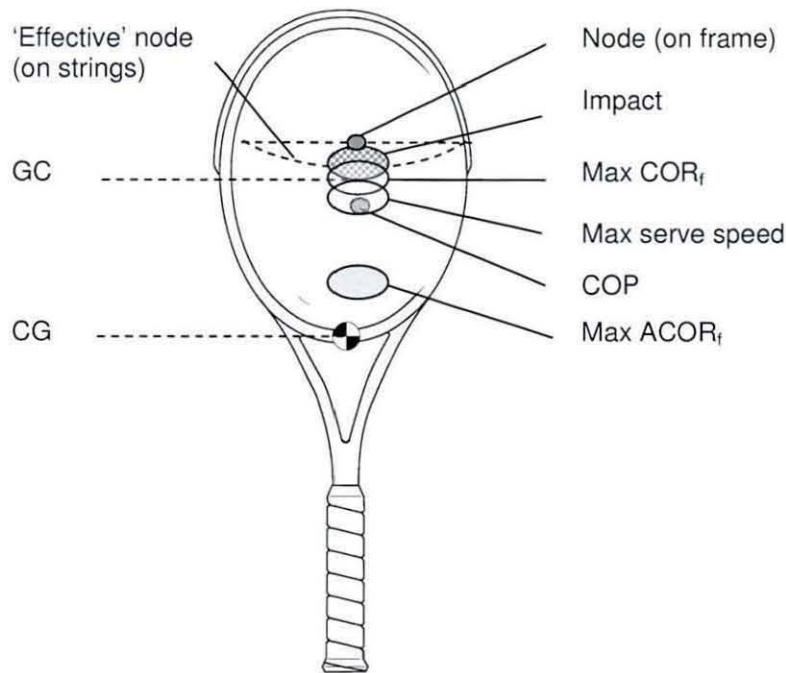


Figure 5.21: Distribution of the average test racket's 'sweet spots'.

### 5.5 Implications for the PDS

The motion studies revealed important parameters linking on-court play performance with laboratory measurements, which is crucial for realistic research into racket performance. Most of these parameters have not been measured before or testing had not been performed on an identical set of rackets or at high enough sampling rates to obtain conclusive results. The results will be used to specify the parameters for determining a comprehensive PDS for the test machine.

Peak head speeds of  $42\text{m.s}^{-1}$  were achieved, which indicated an acceptable operation speed for the test machine, while the standard deviation of  $0.6\text{m.s}^{-1}$  achieved by the players was used to determine the consistency in head speed

## CHAPTER 5 *PLAYER MOTION TESTING*

demanded from the machine. The tests indicated 800Hz as the minimum sampling rate for measuring head speed in order to distinguish the important characteristics of the racket motion for accurate measurements thereof.

The head speed profile reveals a constant speed just before the impact, implying no active drive during impact, which means a mechanism rotating the racket at a constant velocity would be representative of a real serve. The racket's ICR location during impact varies for different players and needs to be experimented with in order to determine the extent of its influence on the racket performance. The range of realistic adjustment was taken as the span of the average ICR locations obtained from the pilot and extended studies respectively.

It was also noticed that for all the rackets tested the racket never lost more than about 50% of its speed during the impact, providing the expected range for post impact racket speed measurement, which is useful as a guideline for the test machine's control parameters.

The angle of the racket face to the court centre-line during a high speed first serve was found to have an insignificant effect on the ball speed in the same direction. In addition, the average impact location on the racket face during these serves was very close to the racket's centreline, further eliminating virtually any remaining out of plane velocity components. This means the test machine does not need to include polar rotation of the racket, simplifying it to a single axis design.

In order for the test machine to be able to develop a fair performance indicator, which does not discriminate against rackets with particular MOI, a realistic relation for the racket head speed was determined. This relation had been speculated upon based on theoretical models and laboratory tests but not measured accurately during play conditions. A power regression was found to provide the best prediction of the relationship between the head speed and the MOI to be used during further testing.

## ***CHAPTER 5    PLAYER MOTION TESTING***

Comparing the measured vertical impact location with the 'sweet spots' measured for all the test rackets, for the first time provided tangible evidence that the node location is most likely to be used by players as the optimum impact location during a high-speed serve.



## Chapter 6

### Service simulation machine design

The chapter describes the design of a test machine, capable of replicating human performance in order to investigate racket performance especially for the serve. It commences with a review of current test machines used in the sporting industry, from which the knowledge of their functioning and implementation was combined with the experimental work described in earlier chapters to produce a PDS for the machine.

#### 6.1 Test machines in golf

For various reasons, the golf industry seems to be ahead of the tennis industry regarding research and test methods and therefore served as a sensible comparator for similar investigations in tennis. Club rebound performance has long been investigated in golf; initially via subjective player testing, which was later aided with the use of mathematical and finite element models and validated with experimental measurements from ball-cannon and robot testing (Cochran & Stobbs, 1999).

Most of the recent academic research performed on golf club performance testing is based on developing control models, which could closely mimic the motion of a human swing (Suzuki & Inooka 1997, 1998, 1999, Suzuki & Ozaki 2002). The swing mechanisms were predominantly modelled with a 2-dimensional analytical model, which swung the club through an angled plane at the ball. The robot mechanism was based on a double pendulum, consisting

of a joint representing the resulting centre of rotation for the arms and a wrist joint, representing wrist flexion, while the club could adequately be described by a relatively flexible shaft and a point mass as the club head. The research investigated the well-known wrist-release action promoted for the optimum golf swing (Cochran & Stobbs, 1999), with Suzuki's model confirming that this motion resulted in the highest possible club head speeds. An optimum motion was found by accelerating the arm with the wrist locked at a 90° angle during the initial swing phase, followed by release of the arm joint. Soon after, when the flexed shaft has bent back to its non-deformed shape, the wrist is released at about 0.14 seconds before impact. The motion therefore utilizes the potential energy in the flexed shaft to generate the high club head speed, which is more effective than attempting it using the driving power.

Concurrently, Ming *et al.* (1998, 2002) reported the use of a real robot based on the same model used by Suzuki. The motion was simplified by using an active arm joint and a passive wrist joint. The wrist was locked in the 90° position against a mechanical stopper during the initial phase of the downswing and released at the same time the arm joint was released.

The use of golf robots in the industry precedes their use in academia but employed the same driving mechanisms. The robots were more comprehensive and robust, similar to the one shown in Figure 6.1, mainly developed for industrial club testing (Miyamae website 2004, Golf Laboratories website 2004), but slowly making their way into academic laboratories as more funding became available.

These robots all mimic a golf swing by swinging the club at an angled plane using at least 3 DOF's; shoulder rotation, wrist flexion ('cocking') and rotation about the shaft axis, with various degrees of control over these DOF's. The *Golf Laboratories* robot has a single motor that powers the main arm while the wrist joint is completely free. The latter is latched in position at 90° to the arm prior to the swing then at the top of the backswing the latch releases, with

the centrifugal force straightening the wrist angle during the downswing. The point of wrist release is therefore controlled by the arm's torque input profile. For the *Miyame* robots (Robo Shot), all joints are actively driven allowing programming of the swing profile, while older versions drive the wrist via a geared system linked to the main drive, hence with a fixed swing profile. These robots provide a reasonable balance between achieving a realistic swing, adaptability and repeatability but are too costly for most research laboratories.

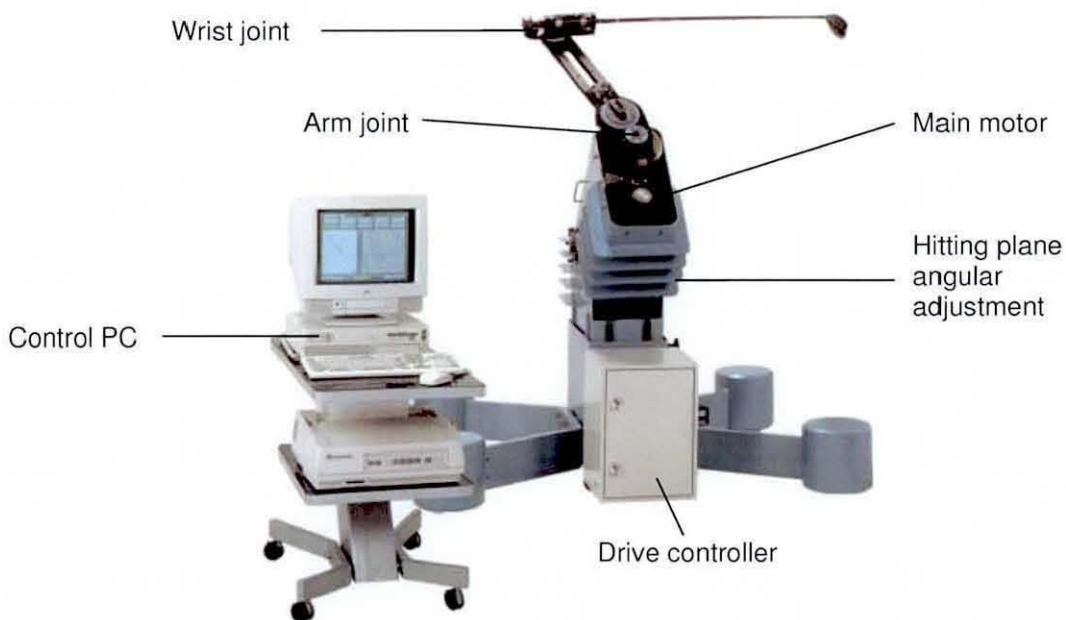


Figure 6.1: A typical golf robot (the Miyame 'Robo Shot').

Over the last decade the golf governing bodies have also started using test machines for establishing dynamic equipment regulations, developing tests to limit performance of golf clubs and balls. The aim of these regulations is to prevent players from destroying existing course records, which would force the changing of course standards and nullify historical player statistics.

The ball rule test introduced in 1976 specified a maximum driving distance (292.6m) allowed when a ball was hit by a standard non-branded titanium club, swung by a golf robot with a head speed of  $53.6\text{m.s}^{-1}$ . The robot known as the 'Iron Byron' was a pneumatically driven robot built by *True Temper*, with a

similar mechanism to that from the robots already described. The swing motion is based on the swing profile of Byron Nelson, a famous player in the 1940's, who was considered to have the "perfect swing".

The rule for regulating club performance specified that the club face should "not have the effect on impact of a spring". The effect, later referred to as the 'spring-like' effect, was defined for the first time in 1998 by the United States Golf Association (USGA) by specifying a standard 'Coefficient of Restitution Test'. The test entailed firing a standard ball (Pinnacle Gold) at  $48.8\text{m.s}^{-1}$  at a resting club head and measuring the  $\text{ACOR}_f$ . The mass of the ball (45.4g) and the club head is substituted to calculate the  $\text{COR}_f$ , for which the limit was set to below 0.830 by the USGA and 0.860 by The Royal and Ancient Golf Club of St Andrews (R&A) during the time of the research. At the beginning of 2004, the test specification was revised and replaced with the 'Pendulum Test'. The test incorporates a pendulum being released from various heights onto the club clamped at the shaft, while a 'characteristic' time is measured across the clubface. The time is claimed to be directly related to the flexibility of the clubhead and the conformance limit is set at below 0.239ms. The rationale behind the new test was that it was relatively simple, non-destructive and portable. (USGA 2004, R&A 2004)

Considering these golf regulations, it was clear that an acceptable balance between realistic representation, complexity and repeatability had to be found for a regulation to be successfully implemented. Compared to a ball-cannon test and theoretical models, the major advantage of employing a robot was its realistic replication of the hitting motion, which did not require a full understanding of the complex motion and impact dynamics for it to be credible to the public. Another advantage was that it employed the actual racket and measured the exact parameters of interest under controlled and representative conditions, leaving no loopholes for manufacturers to exploit. Since the tennis ball/racket impact is still not fully understood, manufacturers will always



retreat to player tests for a final evaluation despite results from lab tests, underlining the importance of realistic test conditions. At the time of the research, the ITF was under considerable pressure to introduce something of a similar nature to golf, hence advocating a 'robot' test incorporating a realistic racket hitting motion.

### 6.2 Existing tennis robots

Hatze (1992a, 1992b) developed the manusimulator, the first passive 'tennis robot' replicating a player's entire arm, and measured the COR<sub>s</sub> for various rackets. The simulator consisted of an upper arm, forearm and hand, connected via the shoulder, elbow and wrist joints. The shoulder joint allows three degrees of freedom (DOF), while the elbow and wrist joints both allow only two DOF. Physical properties of each component represented that of a human arm, including the length, mass and principal MOI. Miyamoto and Kawato (1998) reported the use of an extensive active robot, which incorporated a similar structure to a human arm with seven DOF. A control theory for the robot was developed, which would simulate a tennis stroke by extracting points from 3-dimensional motion data recorded at 250Hz. The use of a similar robot was reported by Kanemitsu (2003) incorporating waist twist, arm lift, arm twist, wrist flexion/extension and supination/pronation. The robot was adapted from an existing industrial robot to test the performance of different rackets during a forehand stroke. The robot could swing the racket up to 30m.s<sup>-1</sup> and impart a certain amount of spin to the ball. It utilised a pressurised grip to provide compliance with adjustable gripping pressure. Unfortunately, no further technical specifications were provided for the robot.

Although such complex robots are more realistic than other traditional test methods, they would be too complicated and potentially inconsistent to be used as a standard test method. Such machines also have high calibration and

maintenance costs and it would be difficult for others to replicate the same test conditions without making a precise copy thereof. Hence, an intermediate solution was proposed, providing the optimum balance between repeatability and realistic stroke mechanics.

### 6.3 Product design specification

The optimum solution for the test machine could be anything from a mathematical equation to a 'Steel Sampras' but the ITF indicated that the test machine should lean more toward a realistic serve simulation. This was influenced to a great extent by the trend set by the golf industry at the time. It was therefore decided to develop an adaptive machine, which could be used as both an extensive research tool and as the basis of a robust test standard. Testing the complete racket as it would be used during play would ensure that the effect of devices added to, or built into, the racket would be revealed by the test. More detailed specifications are presented in the following sections, divided under functional units.

#### 6.3.1 Racket motion replication

Basic momentum principles state that the design of an adaptive test machine should produce the same results for a static ball/moving racket test as for a moving/ball static racket test, as long as the relative movements are considered. The final decision to implement a *moving racket* approach was mainly based on the fact that it would allow more realistic, or believable, racket and ball impact conditions, which was favoured by most of the stakeholders affected by its design.

Fundamentally, the machine must reproduce a high speed human service action for any legal tennis racket design. This means the machine should be able to test *all senior tennis rackets* available on the market, consisting of various



combinations of relevant physical properties such as mass, balance, MOI and physical dimensions. The limits for most of these properties were obtained by investigating properties for all possible racket models introduced into the market up to the time of the research (Racquet Research, 2000), while the upper limits of the physical dimensions were specified by the ITF rules (§2.1). A summary of the significant properties is presented in Table 6.1.

Physical property	Minimum	Maximum
Mass [g]	213	383
Balance [mm]	303	435
MOI (RDC) [kg.cm <sup>2</sup> ]	262	412
Length [mm]	660	737
Head width [mm]	-	328
Head length [mm]	-	394
Grip size [Nr.]	1 {105 <sup>†</sup> }	7 {124 <sup>†</sup> }

Table 6.1 The physical racket properties used as design requirements (<sup>†</sup> Grip size circumference in mm).

The *maximum impact speed* at the GC to be achieved by the machine was calculated with Equation 3.10 as  $50m.s^{-1}$ , using the maximum measured  $ACOR_f$  values during testing and the velocity of the fastest recorded serve ( $66.6m.s^{-1}$ ) during a tournament at the time and rounding it up to include a sufficient tolerance.

Impact location measurements described in §5.4 indicated that for high-speed first serves, players hit the ball virtually on the racket centerline (~10mm towards the inside of the racket), implying that the racket's polar rotation should not have a big influence on the ball velocity. In addition the racket rebound tests (§4.3.6) confirmed that the maximum rebound velocities were achieved along the racket's centreline and given that the objective of the research is mainly concerned with the maximum performance achievable by a racket, it was decided to restrict the racket movement to a *single axis rotation*. This would significantly simplify the design and increase repeatability by decreasing the component complexity.

Motion study results in §5.3 revealed a constant head speed immediately before impact, which implied the racket does not need to be 'driven' through the impact but could be moving at a constant speed. Further investigations

indicated that the racket's ICR just before the impact is fairly consistent for individual players. There is a significant variability between different players though, which was highlighted as an interesting parameter for further investigation using the machine. It should therefore incorporate an ICR allowing for a reasonable degree of variation. The requirement was set as the average location from the players tested, including the adjustability as  $162 \pm 20\text{mm}$  below and  $112 \pm 20\text{mm}$  behind the racket butt.

The standard deviation in *head speed* achieved by players was  $\pm 0.54\text{m.s}^{-1}$ , which meant the machine would have to at least achieve this level of consistency. In order for any test standard to allow for different MOI, the machine should allow adaptation of the impact speed to the racket MOI. In §5.3 an inversely proportional relationship between the MOI and the *head speed* were proposed in Equation 5.10 to be used for specifying the relation between the two parameters.

### 6.3.2 Racket gripping/constraint at impact

The most representative gripping condition for lab testing was one of the most debated issues taken from the literature (§3.1.2). Researchers agree that it is closer to the freely suspended than the handle clamped condition, but the most representative compromise had not been fully defined yet. In order to resolve the issue, the machine's gripping mechanism needed to allow further investigation of the influence of the gripping on performance by incorporating *adaptable gripping* conditions such as the clamping mode, grip pressure and dexterity. In order to represent the freely suspended condition the gripping mechanism should be decoupled from the drive during the impact but have a high inertia coupled to it for the fully clamped condition. The failures occurring during the rebound testing under the clamped conditions in §4.3.4 emphasised that a degree of *compliance* would be needed in the gripping mechanism.



### 6.3.3 Structural stability

In order to prevent component failure and excessive vibration and noise, which could affect measurements, *machine components* must be *balanced* as far as possible. Where unbalanced components were unavoidable the machine should be strong, *rigid* and sufficiently massive, or the components should be isolated to reduce vibrations.

### 6.3.4 Ball presentation for impact

Although during the serve the ball has virtually no forward velocity, it has considerable vertical speed, which is known to have a significant effect on the racket performance during play due to increased top spin generation. This should not greatly affect the ball speeds measured with a test machine, since it is likely to measure the ball speed immediately after the impact, by which time the spin is not expected to have significantly affected the ball speed. Nevertheless, the vertical movement across the face during impact would affect the impact location, which in itself affects the ball speed. Hence, it would be preferable if the ball was introduced to the racket face at a *representative vertical speed*.

The studies also indicated that the impact region favoured by the players lay the closest to the racket's vibration node. Since it would be too time-consuming to measure the node location for each racket, the best way to find the maximum performance would be to *map* the entire *string surface* down the centreline. The test machine should therefore allow for impacts to be measured across the entire racket surface at all speeds. In order to ensure testing efficiency, the user needed to be able to easily change the impact location via the software as well as have the option to *automate* the mapping procedure.

Since the accuracy of the impact locations achieved in the ball-cannon rebound tests (§4.3.6) was significantly higher than that achieved by players during the motion testing (§5.5), the impact variations for the ball cannon tests

were used to set the corresponding machine's tolerances. For horizontal or *off-centre* impacts, the specification was set as  $\pm 5\text{mm}$  from the centreline and  $\pm 22\text{mm}$  for the *vertical accuracy*.

### 6.3.5 Data capture

The impact measurements to be captured by the system depended on the possible performance parameters to be investigated by the machine, as defined in Chapter 3. These included the *pre- and post-impact racket speed* as well as the *post-impact ball speed*. Physical racket properties could be measured with another machine, such as the Babolat RDC, but should be entered by the user into the machine's user interface together with other important parameters in order to incorporate them in the test procedure and processing of the captured data. The accuracy of individual measurement components should be such that the *measured* performance standard has a deviation of less than  $\pm 5\%$  at a specific impact location.

### 6.3.6 Safety

The system should be designed such that it *protects the user* in all possible test scenarios, as well as during set-up procedures. This means that the user should not be allowed access to the racket swing volume before all moving components have come to a halt and power to the drive disconnected.

In addition, the ball trajectory paths before and after the impact should be isolated to protect the user, as well as components, from possible impacts or *critical dropping errors*. To minimize such errors, all control systems and safety systems should be robust and reliable with built-in redundancy when possible.

In the event of a component or racket failure, the user and other components should be protected against any further damage or injury and *emergency buttons* should also be within reach of the user at all times.

### 6.3.7 Control

The fact that the racket does not need to be driven through the impact implies that the profile by which the racket is brought up to the desired impact speed should not affect the test results, hence the final control strategy would depend on an acceptable balance between the political and functional parameters, which would be determined during the development phase.

The machine should be able to perform various *test set-ups*, configurable by the operator with minimal effort via a *user-friendly interface*. The optimum solution would provide full *automation*, which would ideally allow a complete racket test with no user input required once the test is started but still allow the user to intervene if it is desired. The test procedure should allow single impacts and a continuous series of impacts, with the latter allowing impacts at different impact locations.

The operator should also be given the opportunity to manually operate the machine as well as *calibrate* the various systems.

A summary of all the parameters for the PDS and the sections in the thesis where they originated from is presented in Table 6.2

Specification	Criteria	Section
Machine complexity	Realistic robot	6.1
Racket range	All senior rackets	2.1
Rotation axes	Single axis in ball direction	5.3
Acceleration profile	Constant velocity	5.3
Head speed max [m.s <sup>-1</sup> ]		
Maximum	50	3.3
Accuracy	±0.54	5.3
ICR range [mm]		
Vertical	162±20	5.3
Horizontal	112±20	5.3
Adaptable gripping range	Free-free to rigid	3.3
Map entire racket face	Along centre-line	2.4
Ball presentation	Representative vertical speed	2.4
Measurement error [%]		
Ball speed	5	4.3.1
Racket speed (pre- & post-)	5	4.3.3
Impact location [mm]		
Vertical	±22	4.3.3
Horizontal	±5	4.3.3
User-friendly pc interface	-	-
Automate testing	-	-

Table 6.2 A summary of the parameters for the PDS.



## 6.4 Machine design

### 6.4.1 Concept design method

A methodical top-down design approach was implemented as indicated in Figure 6.2. The process commenced with generating various concept via brainstorming, which were then evaluated and refined in order to make a final concept selection. The concepts were then divided in the main macro units needed to achieve the functionality set by PDS, which were further divided into smaller assemblies and subassemblies and subsequently into functional mechanisms consisting of individual parts. In order to ensure an optimal design, a consistent iteration process for evaluating and refining designs from the mechanisms down to the individual parts was employed throughout the entire development process.

This refinement process was initiated through brainstorming concepts designs for the macro units and then evaluating them based on their fundamental advantages and disadvantages. The most promising solutions were selected and, where applicable, turned into analytical models for further evaluation. A 2-dimensional planar mechanism simulation software, Working Model 2D, was predominantly used for this purpose. It allowed for fast development of approximate dynamic models based on basic concepts. In the case of critical components, results were double-checked with manual calculations often performed in Mathcad or MS Excel. Subsequently, mechanisms were evaluated and refined into a component level and then compared against each other during the final selection stage.

Selecting an actuation method was fundamental to the machine design, since it would determine the functionality of most other components. The possible actuators considered for the machine, as indicated in Figure 6.3, were pneumatic or hydraulic cylinders (a), linear or rotational springs (b) and electric motor drives (c, d, e). Different solutions incorporating the different actuators



were modelled in Working Model 2D and discussed with respective vendors. Finally, the rotational concept (d, e) with an electric motor as actuator was selected, due to its high accuracy, low power requirements, affinity for continuous testing and to simplify the design by running all system components off a single and commonly available power source (Figure 6.4).

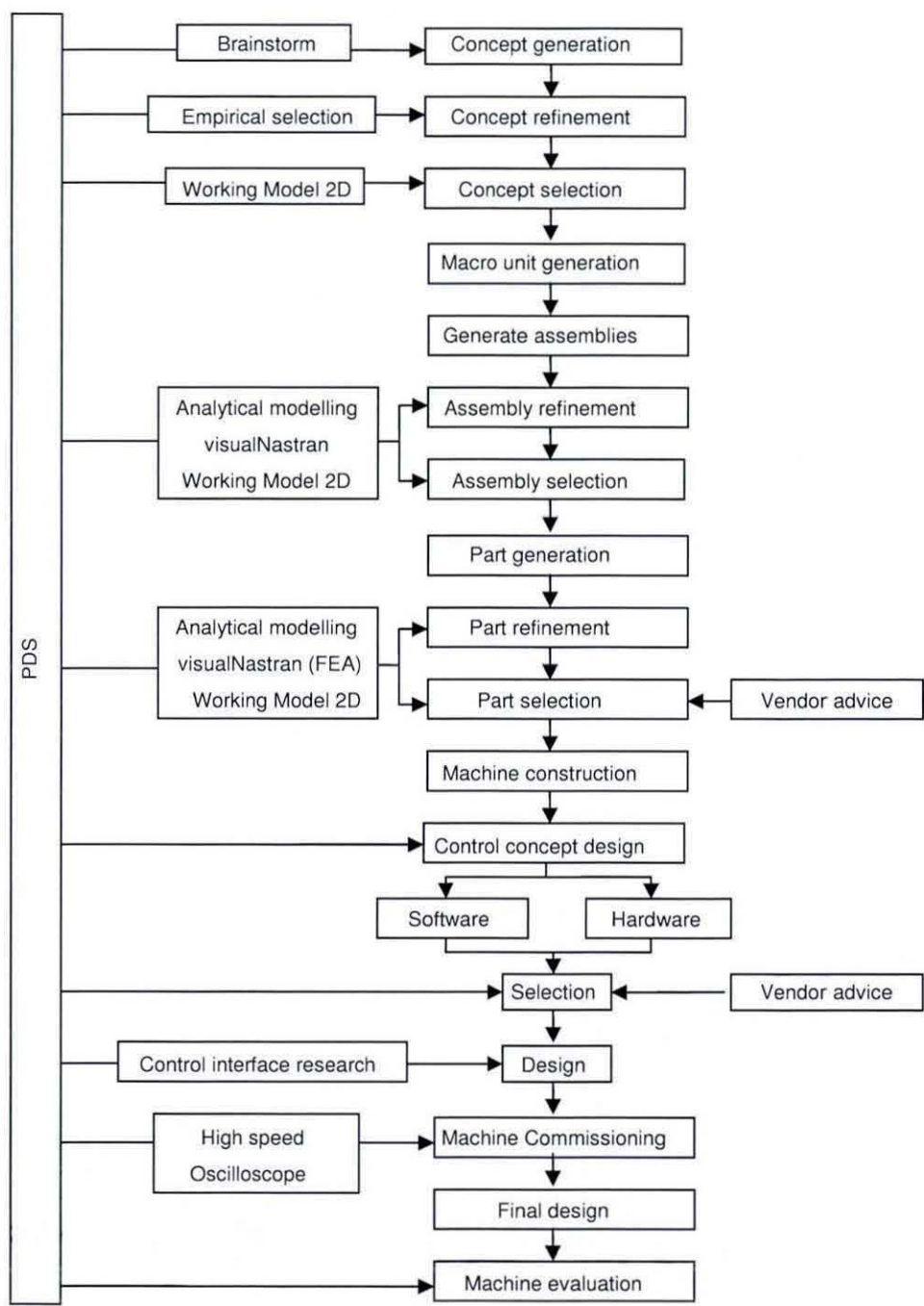


Figure 6.2: A flowchart indicating the design machine design process.

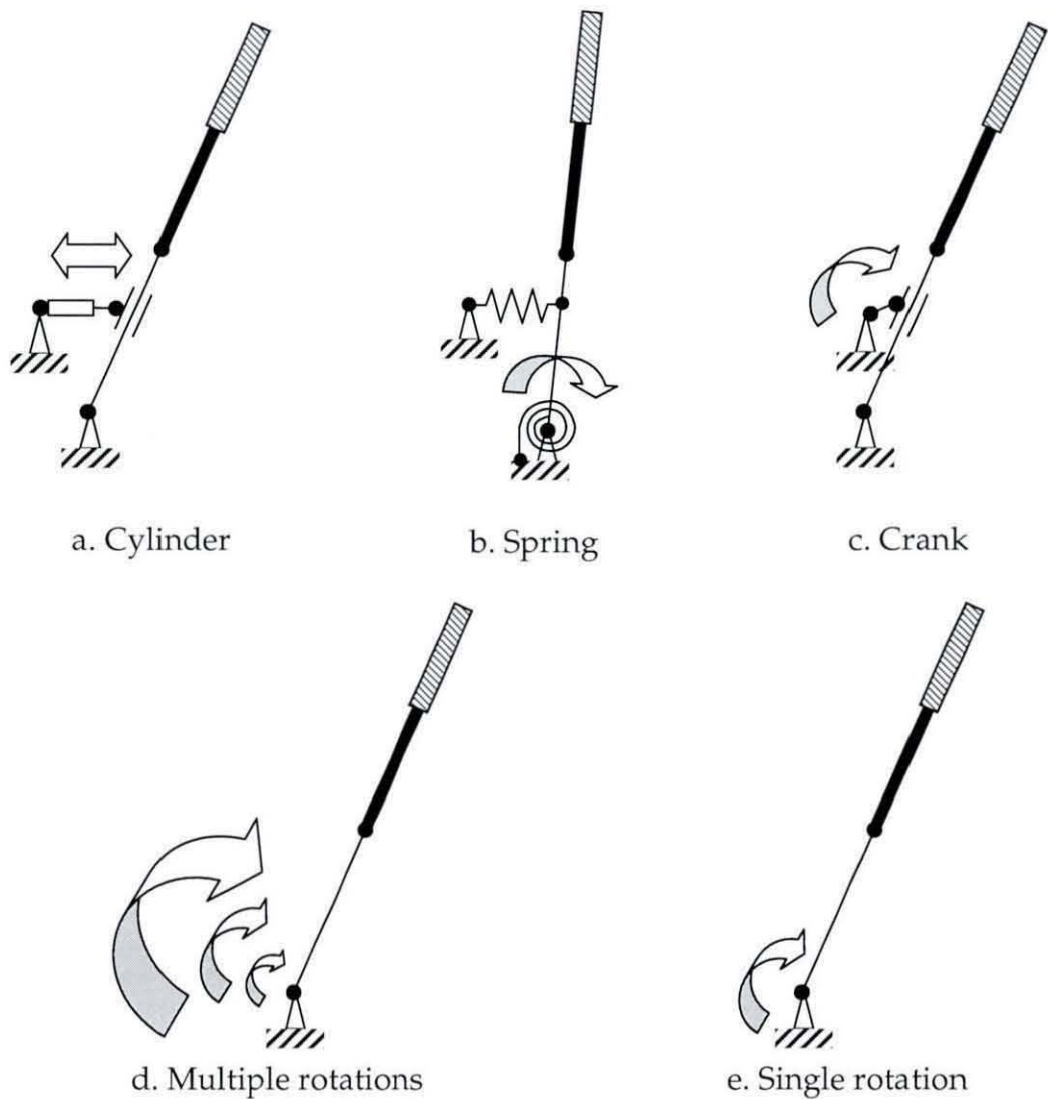


Figure 6.3: A schematic illustrating various concepts considered for the main drive mechanism.

The rotational model was developed further into a simple 3D model using Solid Edge, which was linked to visualNastran 4D in an iterative development process. In visualNastran 4D (Figure 6.5), motion constraints and material properties can be defined to calculate accurately the expected torque requirements using the 3D model dimensions. Results were double-checked with manual calculations, using the MOI values and dimensions of the major components as calculated in Solid Edge.

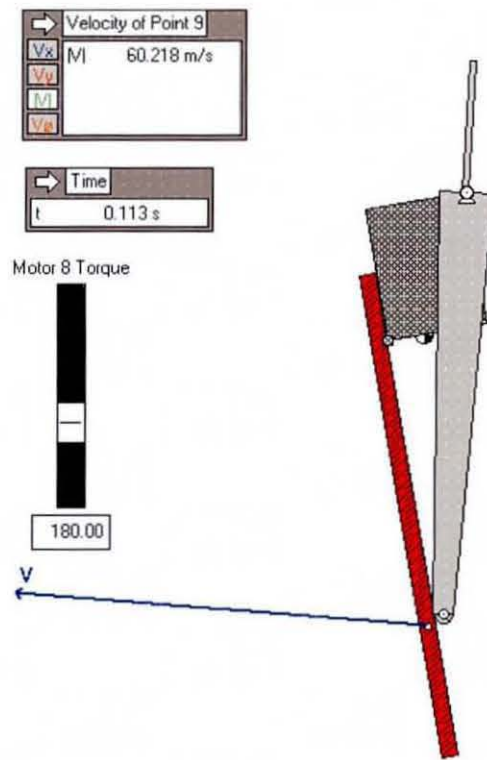


Figure 6.4: A simple Working Model 2D model of the rotational concept.

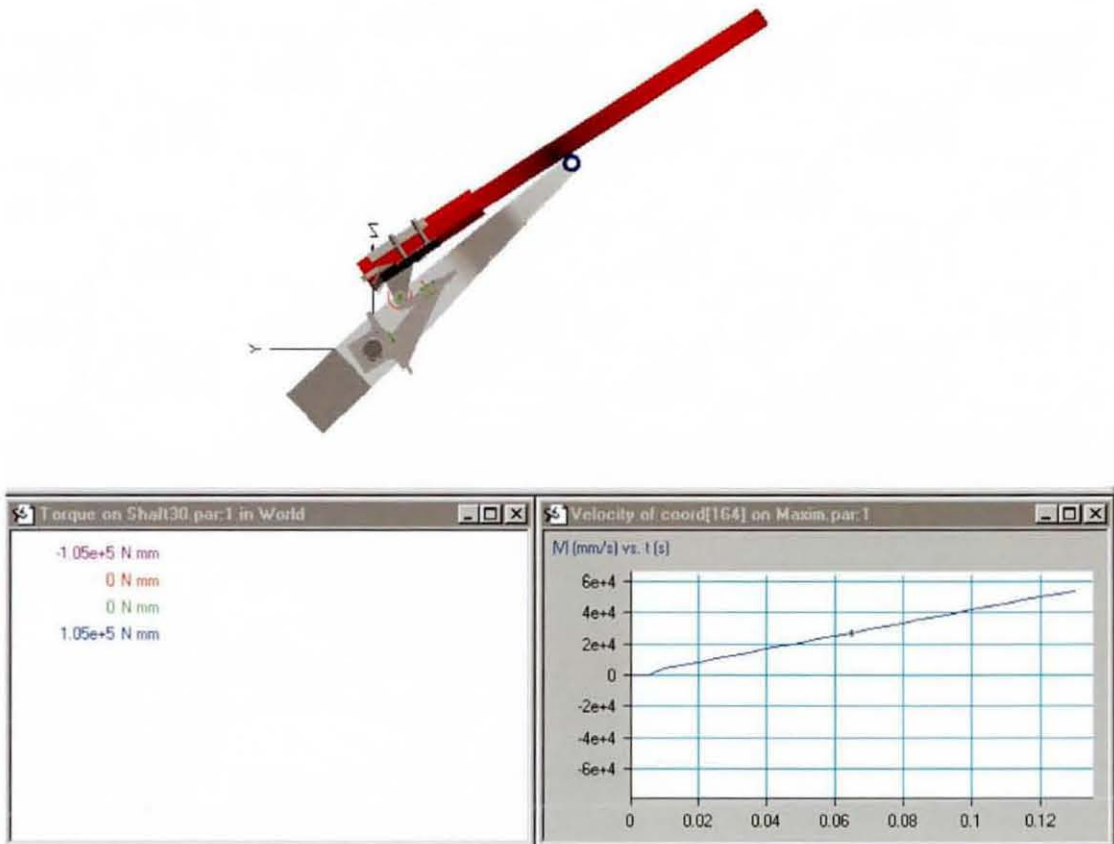


Figure 6.5: A detailed visualNastran 4D model of the rotational concept.

Using the same tools, individual machine components were refined at a more detailed level. In Solid Edge, component geometries were verified in proportion to the entire assembly and models for critical components were exported to visualNastran 4D, which provided a detailed dynamic analysis, in which materials were evaluated and finalised. The software allowed the calculation of various dynamic parameters including torque needed to achieve the required velocities, dynamic impact response and resulting loads as well as finite element analyses (FEA) of individual parts at any instant during the simulation. The combination of different tools proved to be very effective for detailed component evaluation by means of an iterative process. The final configuration is shown in Figure 6.6. Individual assemblies and controls will be discussed in more detail in subsequent sections.

### 6.4.2 Racket motion replication assemblies

One of the core assemblies specified by the PDS was the racket motion replication assembly (Figure 6.7). The objective was to realistically and repeatably replicate the condition of a human serve by presenting the racket to the ball in a planar rotation, at representative serve speeds. Traditional motion replication robots used in other sports have the motor drive directly coupled to the swung instruments, which does not truly represent the real boundary conditions imposed by the human hand and arm and does not allow for adjustability to enable further investigation thereof, as required by the PDS. In order to enable adjustment of the boundary condition, the drive would have needed to be uncoupled from the racket during the impact. Since this was not possible to achieve without adding unrealistic weight to the gripping mechanism, and thereby changing the boundary condition, the robot was fitted with a novel driving mechanism.



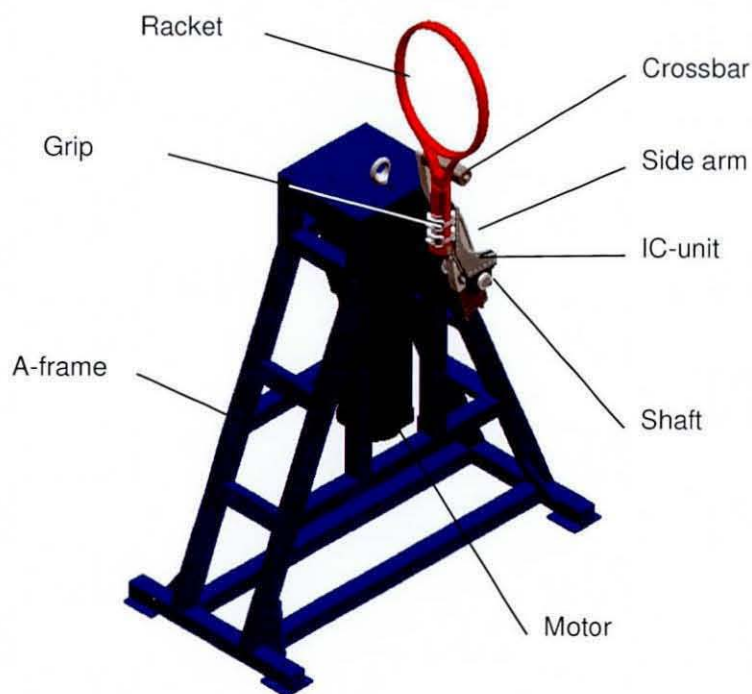


Figure 6.6: The basic machine design.

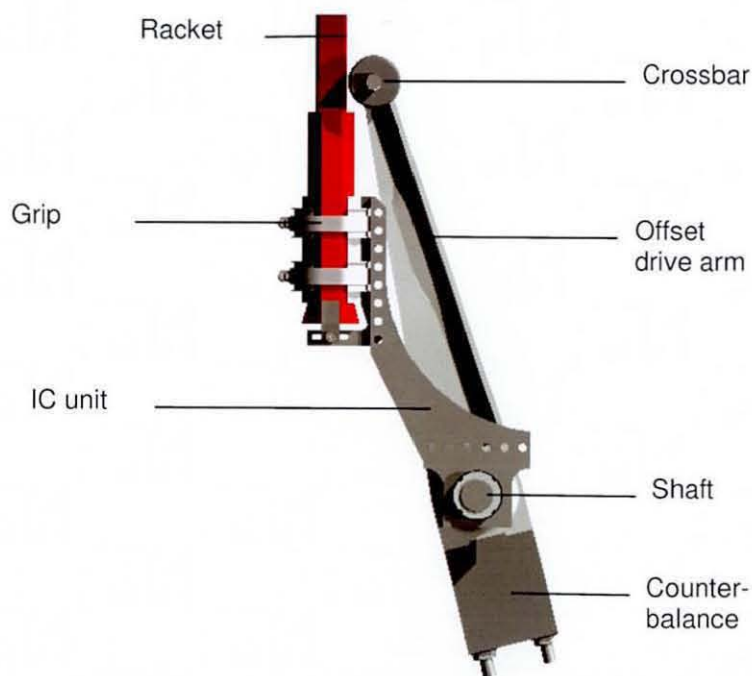


Figure 6.7: The racket motion replication assembly.

The machine comprises of a racket driven by the drive arm through the throat area instead of the grip, which ensured the lightest possible instantaneous centre unit (IC-unit), hence allowing tests to be performed under conditions varying from virtually free (restrained radially at the base of the racket) to the almost rigidly clamped (inertially restrained about the IC-unit). The latter was achieved via threaded holes underneath the base of the IC-unit through which mass could be added in order to increase its inertia and in so doing approach the rigid boundary condition.

As an example of the design process, the systematic development of the driving assembly will be discussed in detail highlighting the evolution of the mechanism and its individual components, especially that of the drive arm, (Figure 6.8 and Figure 6.14).

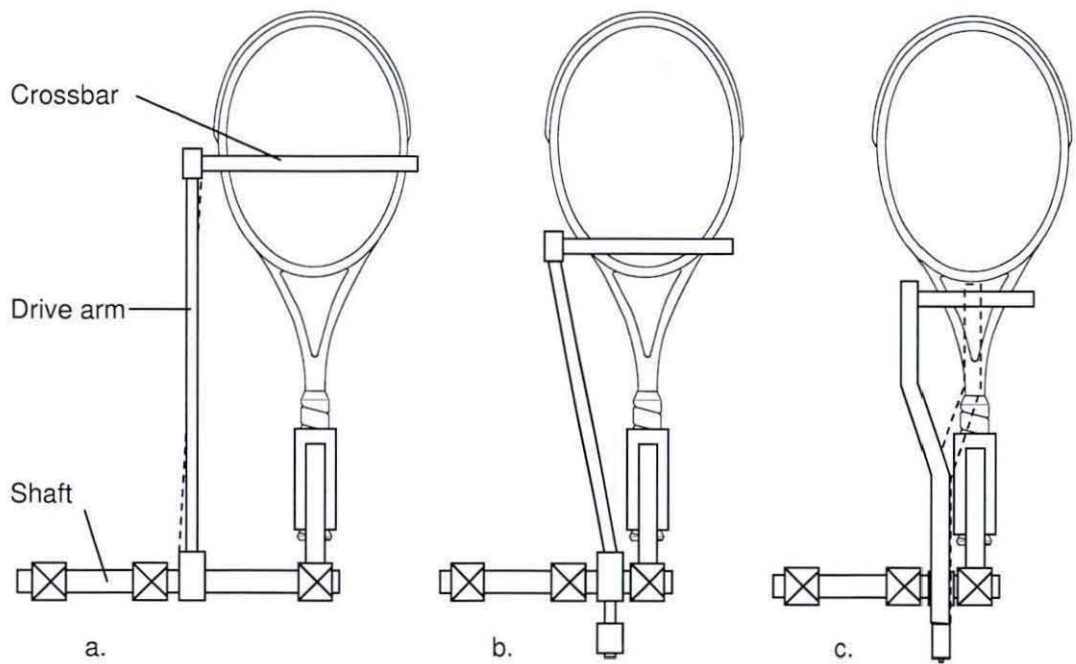


Figure 6.8: Diagram illustrating the design evolution of the driving unit.

A manual strength analysis was performed on the mechanism as indicated in Figure 6.9, which was used to identify critical parts and then continuously as a double check for the FEA performed on them.

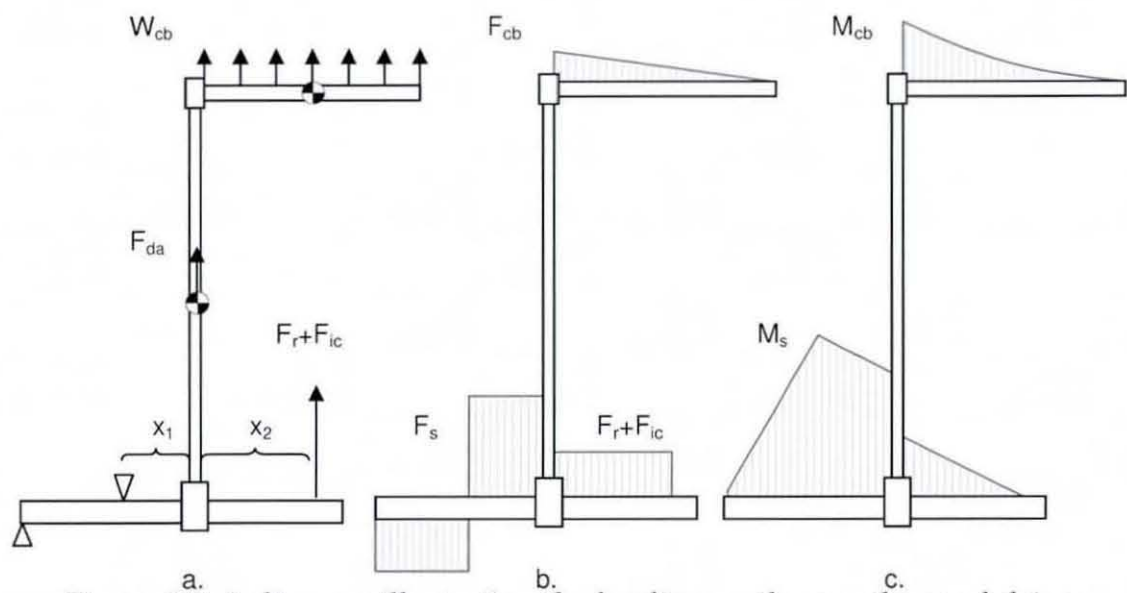


Figure 6.9: A diagram illustrating the loading on the crossbar and drive shaft: (a) applied loads and boundary conditions; (b) the resulting vertical force distribution; (c) the resulting moment distribution.

Figure 6.10 to Figure 6.13 show typical results from the FEA performed on the crossbar, drive arm, shaft and IC-unit respectively. The results shown were based on accelerating the racket up to the desired head speed of  $66.7\text{m.s}^{-1}$  (or  $87\text{rad.s}^{-1}$ ) within a single revolution, requiring a driving torque of  $\sim 110\text{Nm}$ .

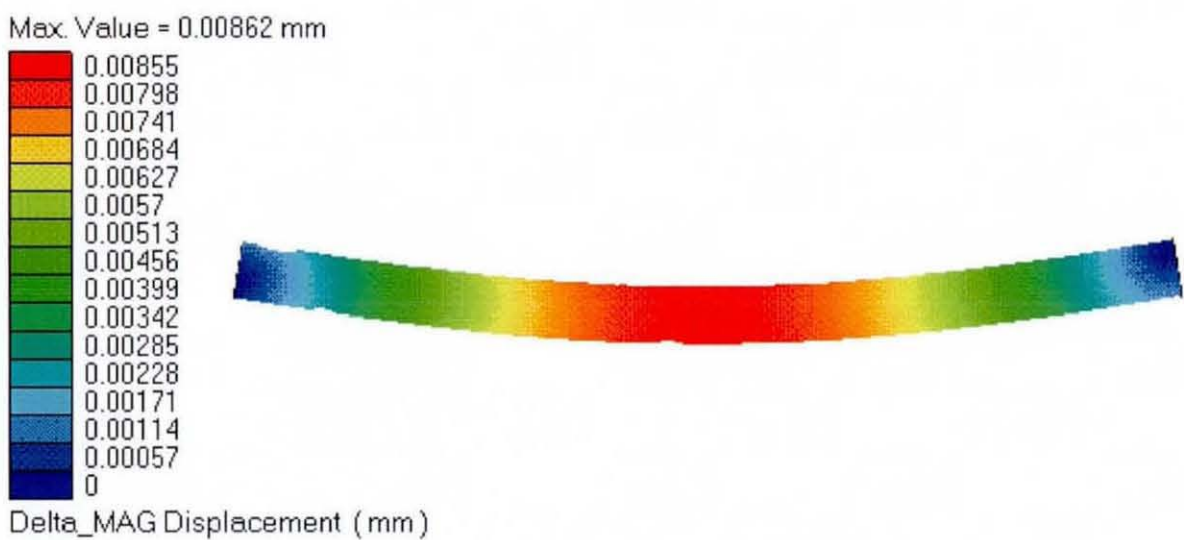


Figure 6.10: Results from a typical FEA analysis on the crossbar.

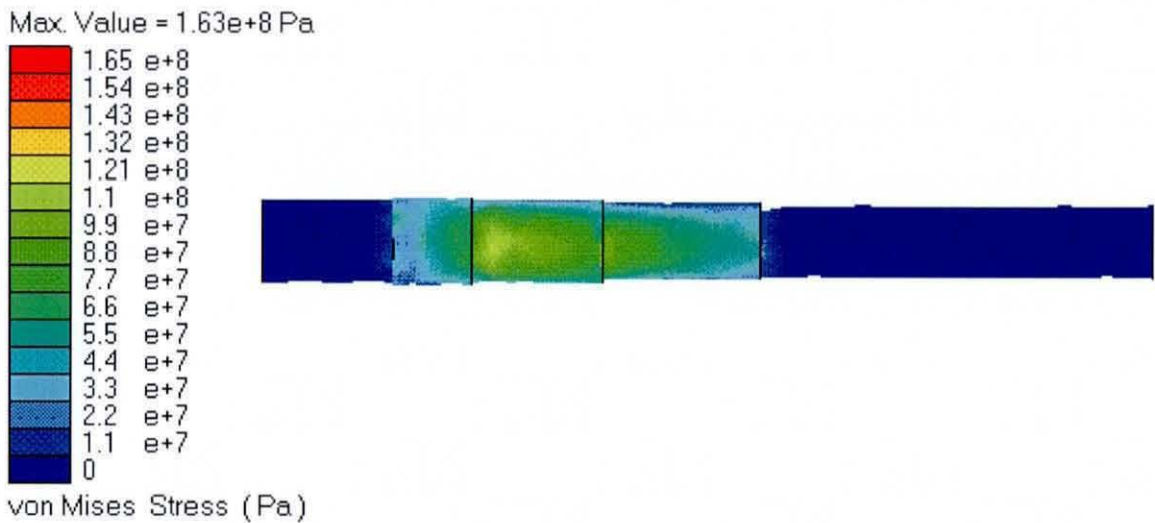


Figure 6.11: Results from a typical FEA analysis on the shaft.

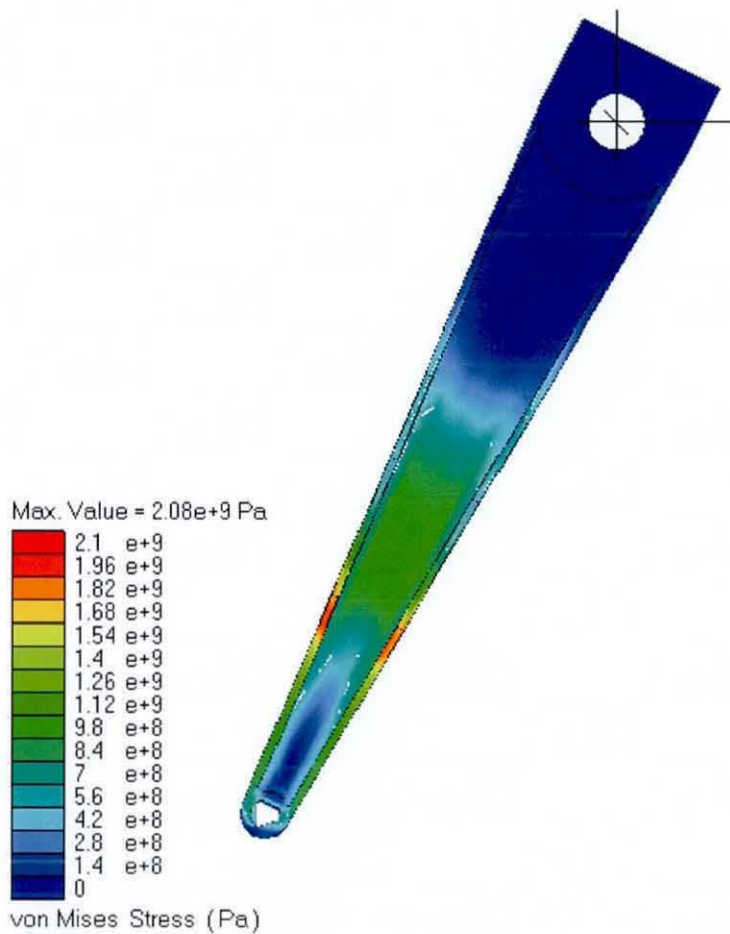


Figure 6.12: Results from a typical FEA analysis on the drive arm.



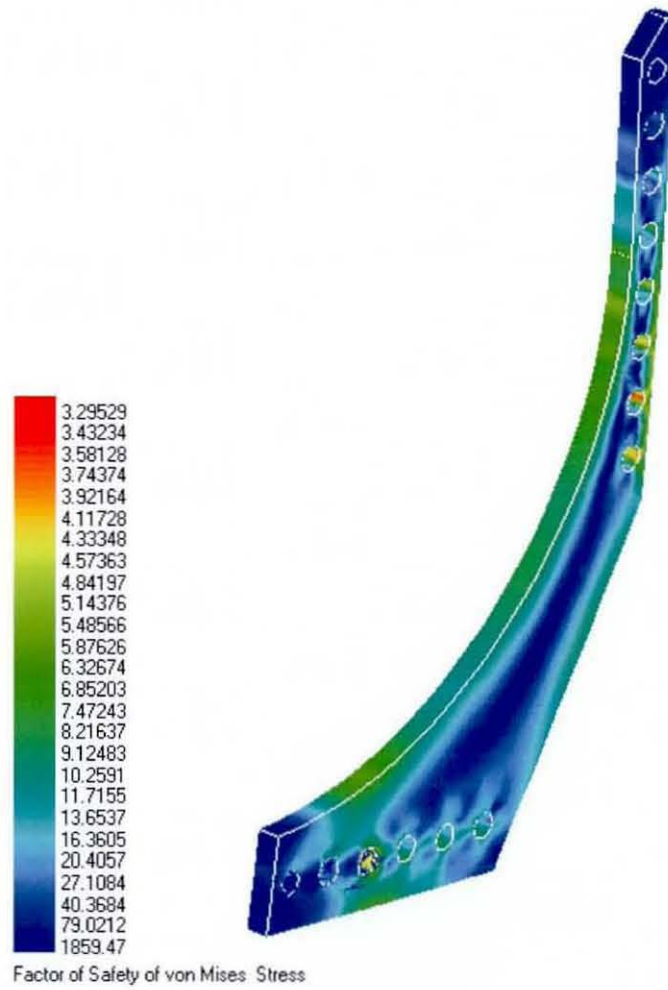


Figure 6.13: Results from a typical FEA analysis on the IC-unit.

The first iteration (Figure 6.8a) comprised of a simple straight drive arm, which pushed the racket at the GC of the face. The crossbar experienced a large distributed centrifugal force ( $W_{cb}$ ) due its rotation around the shaft, which applies a resulting load  $F_{cb}$  to the drive arm.

$$F_{cb} = m_{cb} \cdot \omega_{da}^2 l_{da} \quad (6.1)$$

where  $\omega_{da}$  is the angular velocity,  $l_{da}$  is the length of the drive arm (between the hole centrelines) and  $m_{cb}$  is the mass of the crossbar calculated as:

$$m_{cb} = \rho_{cb} \cdot l_{cb} \cdot \pi \cdot (d_o^2 - d_i^2) / 4 \quad (6.2)$$

with  $l_{cb}$ ,  $d_o$  and  $d_i$  being the crossbar length, outer and inner diameter respectively. The moment transferred from the crossbar to the drive arm ( $M_{cb}$ ) is given by:

$$M_{cb} = F_{cb} \cdot l_{da} / 2 \quad (6.3)$$

The maximum bending stress in the crossbar ( $\sigma_{cb}$ ) is calculated as:

$$\sigma_{cb} = \frac{32 \cdot M_{cb} \cdot d_o}{\pi \cdot (d_o^4 - d_i^4)} \quad (6.4)$$

and the shear stress ( $\tau_{cb}$ ) as:

$$\tau_{cb} = \frac{4 \cdot F_{cb}}{\pi \cdot (d_o^2 - d_i^2)} \quad (6.5)$$

in order to calculate the crossbar's maximum von Mises stress ( $\sigma'_{cb}$ ), which is used for the fatigue analysis:

$$\sigma'_{cb} = \sqrt{\sigma_{cb}^2 + 3 \cdot \tau_{cb}^2} \quad (6.6)$$

Several design iterations utilizing these equations refined the final version of the crossbar to have a maximum von Mises stress of 11.2Mpa. To determine if the members were sufficiently strong the von Mises stress was multiplied by a safety factor of  $\eta=1.5$  and compared with 40% of the ultimate tensile strength of the material to include fatigue of more than  $10^6$  cycles (Shighley & Mischke 1989). The maximum deflection ( $\delta_{cb}$ ) of the crossbar was also calculated from the material's Young's modulus ( $E_{cb}$ ):

$$\delta_{cb} = \frac{8 \cdot F_{cb} \cdot l_{cb}^3}{E_{cb} \cdot \pi \cdot (d_o^4 - d_i^4)} \quad (6.7)$$

in order to avoid excessive bending of the bar, which could affect accuracies during operation due to relative motion. The manual calculations indicated the

design for the final bar achieved a maximum deflection of 0.0082mm, which were found to be within 10% of the FEA analysis, providing confidence in the latter for drive arm and IC-unit with complex geometry, where no manual calculations were possible. For these components only the FEA was used to compute the maximum von Mises stresses, after which the same failure criterion was used as for the crossbar. For the drive shaft, the maximum moment ( $M_{ds}$ ) is the sum the loads applied to it through the drive arm, as well as the racket and IC-unit:

$$M_{ds} = M_{cb} + (F_{cb} + F_{da}) \cdot x_1 + (F_r + F_{IC}) \cdot (x_1 + x_2) \quad (6.8)$$

with  $F_{da}$ ,  $F_r$  and  $F_{IC}$  being the centripetal forces from the drive arm, racket and IC-unit respectively, calculated from the acceleration of their individual CG, while  $x_1$  and  $x_2$  define the distances from the location of the maximum moment on the shaft. Again the same failure criteria were used to determine the shaft strength, which was confirmed with the FEA and used to select or adjust the dimensions and materials for individual parts.

For the first iteration, the loading for all the components was excessive, regardless of the materials selected for any of the components or attempts to change the component cross-sections. Special effort was made to optimise the crossbar in order to reduce the load on it as well as the rest of the assembly. An optimum solution to reduce the mass was investigated by increasing its cross-section, decreasing the wall thickness and using stronger materials. A situation was soon reached where the larger diameter forced an increase in drive arm dimensions, thus increasing the drive arm's contribution to the overall load. Likewise the wall thickness reached a threshold where it was too weak to carry its own load and using stronger homogeneous materials would only increase its mass, pointing to the use of a thin-walled carbon fibre composite as an optimum solution due to its high strength-to-weight ratio. Although this solution provided the ultimate strength for the crossbar, during commissioning



a wooden dowel proved to be more practical for safety reasons explained in a later section. The loads on the other components were still significant and attempts were made to cut holes out of the drive arm to reduce weight and webs were introduced at both ends to strengthen it in the direction of the moment applied but it was still insufficient, requiring more comprehensive changes.

For the next iteration (Figure 6.8b), large improvements were made by reducing the drive arm length, since the centripetal force is proportional to the radius of rotation of each component's CG. Also, a counterbalance mass was added to counteract the centripetal load of the drive arm and the crossbar. By having the drive arm at an angle, the moment on the shaft was further reduced since the loads applied to it by virtually all the components were acting closer to the inner bearing. It also shortened the crossbar, therefore reducing its load on the other components.

Since the loading was still critical, it was further reduced in the final iteration (Figure 6.8c) by shortening the side arm even more and flipping horizontally (dashed lines) so that it would attach to the centre of the crossbar, thus almost halving its moment. Although, this was a favourable solution for the loading conditions, it was not practical in terms of the functioning of the machine, since it would interfere with the IC-unit during the reverse braking procedure, described in §6.4.8. The side arm was therefore flipped back for the final solution and the attaching of the counter balance was improved to decrease the loading on the beam to which the mass was attached. As an illustration of the iteration process for a specific part, the evolution of the drive arm is shown in Figure 6.14.

Further improvements to components included optimising the drive arm's I-beam cross-section and making it out of special high strength aluminium (Certal, 7022/AlZnMgCu0.5). In order to minimise the risk of failure of the drive shaft itself, or the connection to the drive arm, a friction coupling was



used to connect them rather than the traditional key with keyway approach. Keyways are renowned for causing stress concentrations and weakening of the shaft at the key location.

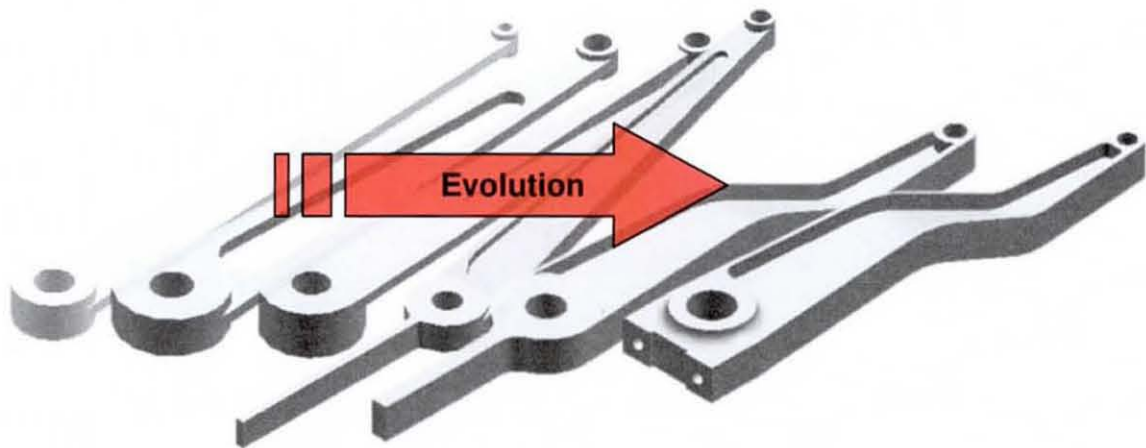


Figure 6.14: A schematic demonstrating the design evolution of critical parts.

The crossbar was designed to act as a sacrificial member in order to increase the safety of the system and protect critical machine components, as well as the racket, in the event of an overload. After initial trials with a lightweight carbon fibre shaft it was found to be too 'bouncy' with its high energy return causing the racket to bounce off it during contact, which led to control problems. Hence, the crossbar was covered with standard isolation foam to absorb the impact energy during contact with the racket. Experimentation with the crossbar indicated that it was too strong to be used as a sacrificial member and also tended to splinter during failure instead of resulting in a clean break. It was therefore replaced by a solid wooden bar, turned from inexpensive commercial dowel.

The exact location of the rotation axis with respect to the racket was designed to be adjustable within the known bounds of typical human play, which would allow the effect of different service actions to be investigated. These dimensions were determined via player testing and specified in the PDS. As a result, the IC-unit provided adjustment in the vertical and horizontal

directions, with the movements indexed via location pins and measured in the respective planes as the distance between the racket's butt and the shaft centre. The vertical range allowed by the unit is 127–197mm, while the horizontal location ranged between 95–165mm.

### 6.4.3 Racket gripping assemblies

The gripping mechanism (Figure 6.15) grips the racket handle and connects it to the IC unit. Two lightweight jubilee clamps were tightened to exert a radial force via a thin pre-shaped aluminium pressure plate onto the racket handle. The octagonal pre-shape would accommodate all standard sized grips (Nr. 1-7). The mechanism did not allow any polar rotation except for some movement resulting from the compliance in the gripping pads, which could be inserted between the pressure plates and the racket handle. The latter could be substituted with materials having different compliances for simulating the effect of different grip bands and variance in fatty tissue inside different player's hands, while adjusting the tension in the clamps would simulate different grip strengths. In order to prevent the racket from flying radially out of the grip during loose gripping conditions, a pivot clamp could be fitted to the racket butt-end cap. It is pinned through a slot in the gripping mechanism just below the butt to radially locate the pin whilst allowing transverse movement, hence forming a pivot between the gripping mechanism and the racket.

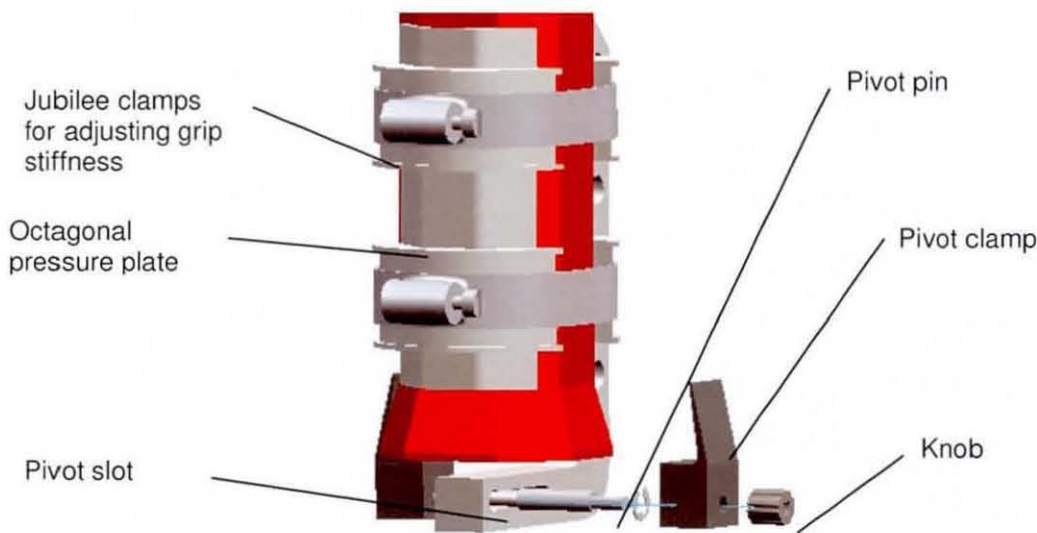


Figure 6.15: The pivot clamp fitted to the racket butt during loose gripping conditions.

6.4.4 Structural stability

The machine’s stability was vital to its repeatability, hence special care was taken to ensure all components performed consistently under the extreme operating environment as well as reducing maintenance and calibration demands. Consequently the motor was mounted vertically to an A-frame, which provided a stable 1050mm wide base in the plane of the main resulting moment, while minimising the floor space occupied by the machine. In order to have a horizontal shaft rotating the racket in a vertical plane, it was driven through a 90° gearbox, as shown in Figure 6.16.



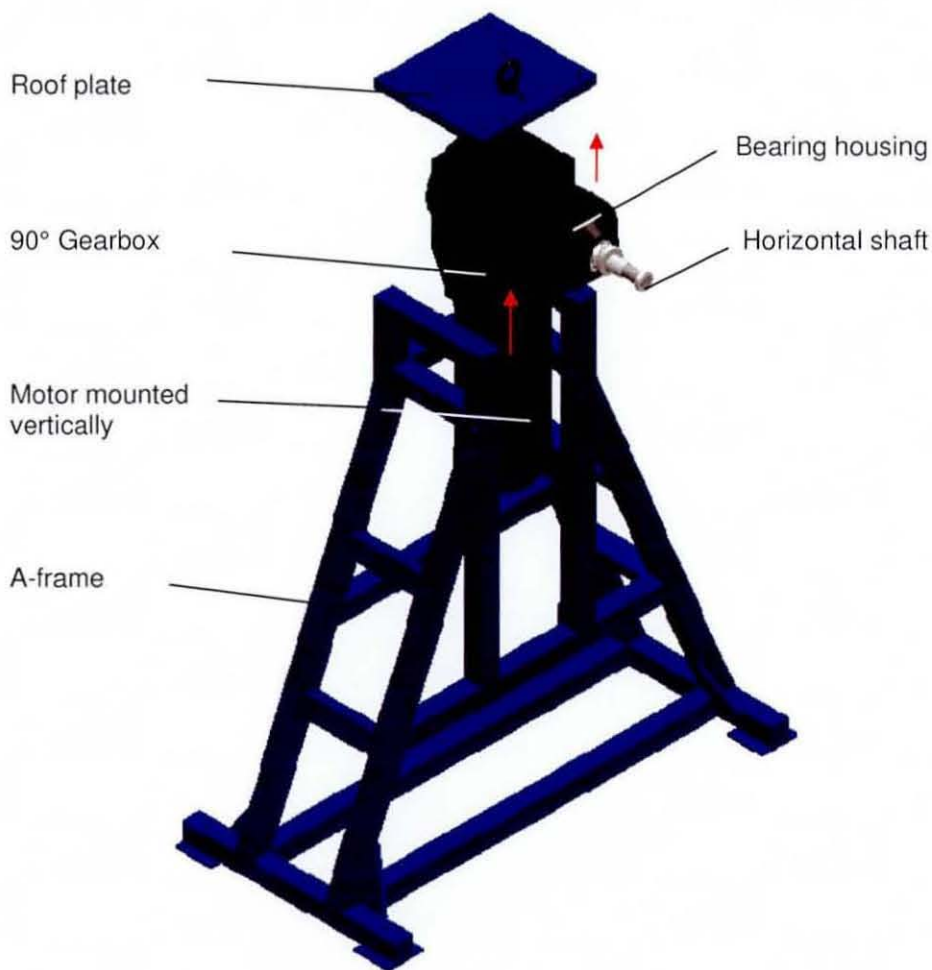


Figure 6.16: The motor assembly mounted in the A-frame.

The A-frame was manufactured from 5mm thick square (50x50mm) steel struts, to ensure a stable configuration with minimal deflection of the critical components under operation. In addition, the A-frame was bolted to the floor at each foot via 8mm bolts. A thick rubber layer was added between the feet and the floor, which served as a working area as well to dampen machine vibrations. As mentioned in the previous section, the drive arm was counter balanced to minimise the off-centre load on the system, therefore further reducing the vibration, while improving the accuracy and repeatability of the entire system. The IC-unit and racket was not counter balanced in an attempt to keep its weight to a minimum, allowing simulation of the different gripping conditions.



In order to determine the motor specifications, calculations were performed for both 'single' and multiple revolution concepts to compare the requirements for accelerating the assembly up to the required racket head speed of  $50\text{m.s}^{-1}$  as stipulated in the PDS (§6.3.3). The torque needed to achieve this in a 'single' revolution was calculated as  $128.9\text{Nm}$ , but only  $10.8\text{Nm}$  to achieve the same speed in  $\sim 10$  revolutions, favouring the multi-revolution concept. This advantage was further magnified when comparing the torque requirements needed to brake the drive assembly fast enough for it not to hit the racket during impact. In contrast to the 'single' revolution concept where the entire assembly would be brought up to speed and the arm slowed down in a single revolution, the multi-revolution concept only needed to slow down the arm within its last revolution, resulting in less strain on the drive system and the mechanical components.

The final aspect of motor selection was based on the ratio between the inertia of the driving (motor and gearbox) and the driven system (drive arm and racket assemblies). If this ratio was higher than 10:1 the actuator would not be responsive enough for effective control over the driven system. This was even more critical for the braking of the drive arm, since the torque needed was higher than that needed to accelerate the entire assembly. As a result, a relatively low torque (rated  $19.0\text{Nm}$ , maximum  $100\text{Nm}$ ) 3-phase Lenze motor connected via a 3:1 Vögel gearbox was suggested as a solution, combined with a  $32.5\text{kW}$  brake chopper and external resistor unit to enhance the braking capabilities.

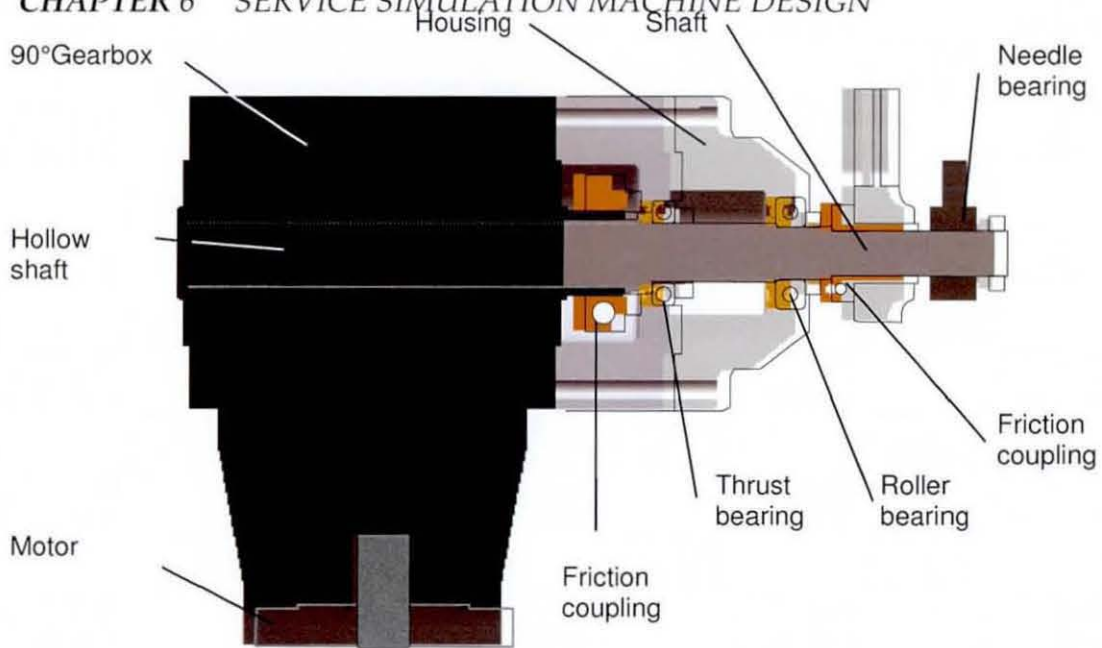


Figure 6.17: Detailed schematic of the robot driving mechanism.

To avoid the use of any keyways, which structurally weaken components, a gearbox was selected with a hollow shaft and a friction coupling, as shown in Figure 6.17. The absence of flexible couplings between the shaft and the motor necessitated very accurate bearing assembly alignment, which was achieved by turning the housing out of two concentric parts, which were bolted directly to the gearbox instead of to the A-frame. The entire drive system was then connected to the A-frame by suspending it underneath a sturdy roof plate. The plate can be fitted with heavy-duty eyebolts to assist in transportation and assembly.

#### 6.4.5 Ball presentation assembly

Balls are dropped into the path of the racket from a representative height in order to achieve a realistic downward velocity during a serve. Similar to real play, the ball has appreciable downward velocity before the impact, resulting in progression down the racket face during impact and a realistic replication of the interaction with the stringbed. To the knowledge of the author, this is a novel concept, which has not featured in any other test machine.

In order to utilise a single energy source (electricity) for all machine systems, solenoids were investigated as the main option for the dropper

actuator rather than pneumatic solutions. The two main criteria for the actuator were quick reaction time and, most importantly, consistency. The latter was therefore evaluated by testing an existing solenoid actuated dropping mechanism developed by the ITF. A high-speed camera system was used, as described later in §7.1.1, to capture and measure the distance travelled by the ball at a specified time (508ms) after the actuator had been triggered by an electric pulse. Results indicated a standard deviation of  $\pm 15\text{mm}$ , which was within the  $\pm 22\text{mm}$  specified by the PDS in §6.3.4, with most of the scatter believed to be a result of mechanical friction in the mechanism, rather than solenoid inconsistency. As a result, it was concluded that a solenoid should provide an adequate solution, providing care was taken to use a strong enough solenoid, which would not be affected by increased friction in the system.

The selection of a linear solenoid above a rotary solenoid was mainly due to the lower costs and familiarity with its limitations. Further, opting for a single rather than multiple solenoid solution was based on the assumption that fewer components means a lower probability of failure. The design concept for the dropper was developed by means of a two-dimensional model constructed and tested in Working model 2D, which was transferred to a three-dimensional model in Solid Edge for refining the manufacturing details (Figure 6.18).

In order to prevent multiple balls from dropping into the racket path due to the solenoid failing in the open position, a unique J-shaped 'trap door' was developed. The sequence in Figure 6.19 indicates how it allowed the balls to be fed individually, with each leg of the 'fork' blocking the next ball from being fed through, while the bottom 'foot' acted as a trap door for the ball resting upon it. Only when the trap door returns to its resting place does it allow the next ball to move into the dropping position.



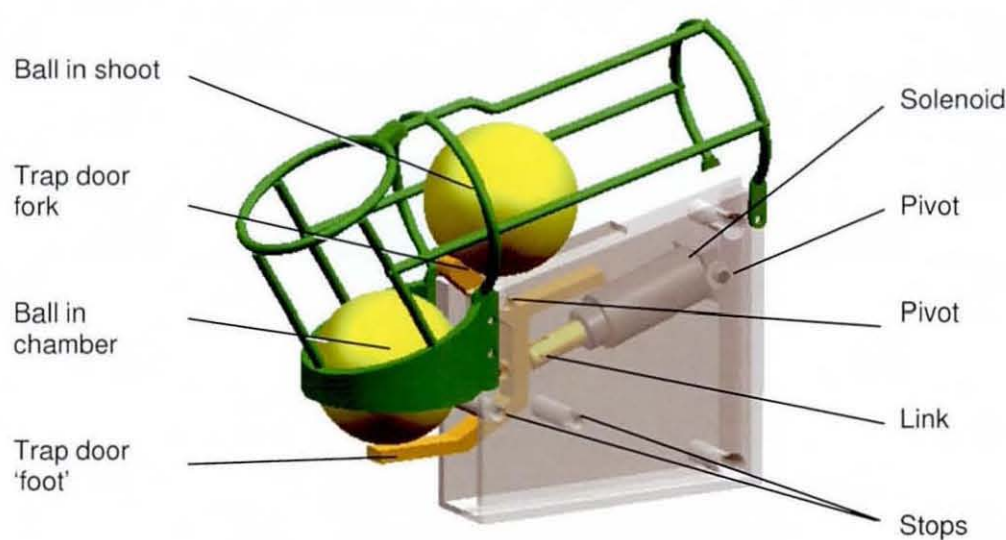


Figure 6.18: A 3D model of the ball drop mechanism.

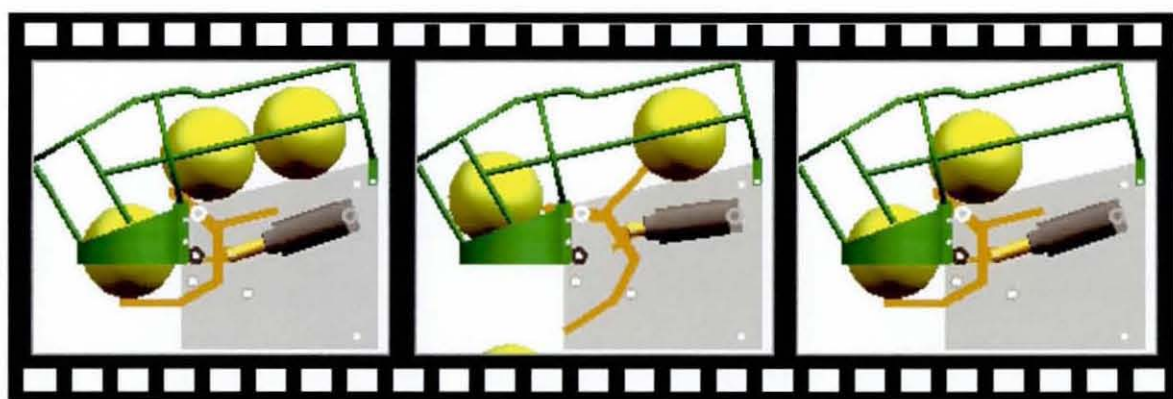


Figure 6.19: The functioning of the ball drop mechanism.

From the tests described in §7.1.1, a linear equation was determined, which was used to reverse calculate the time needed to reach a specific drop distance, and then used during operation to determine when the dropper should be activated to achieve the desired ball impact location on the racket face. In order to quantify dropper variability and calculate the real impact location on the racket surface, two lasers were mounted below the dropper as depicted in Figure 6.20.



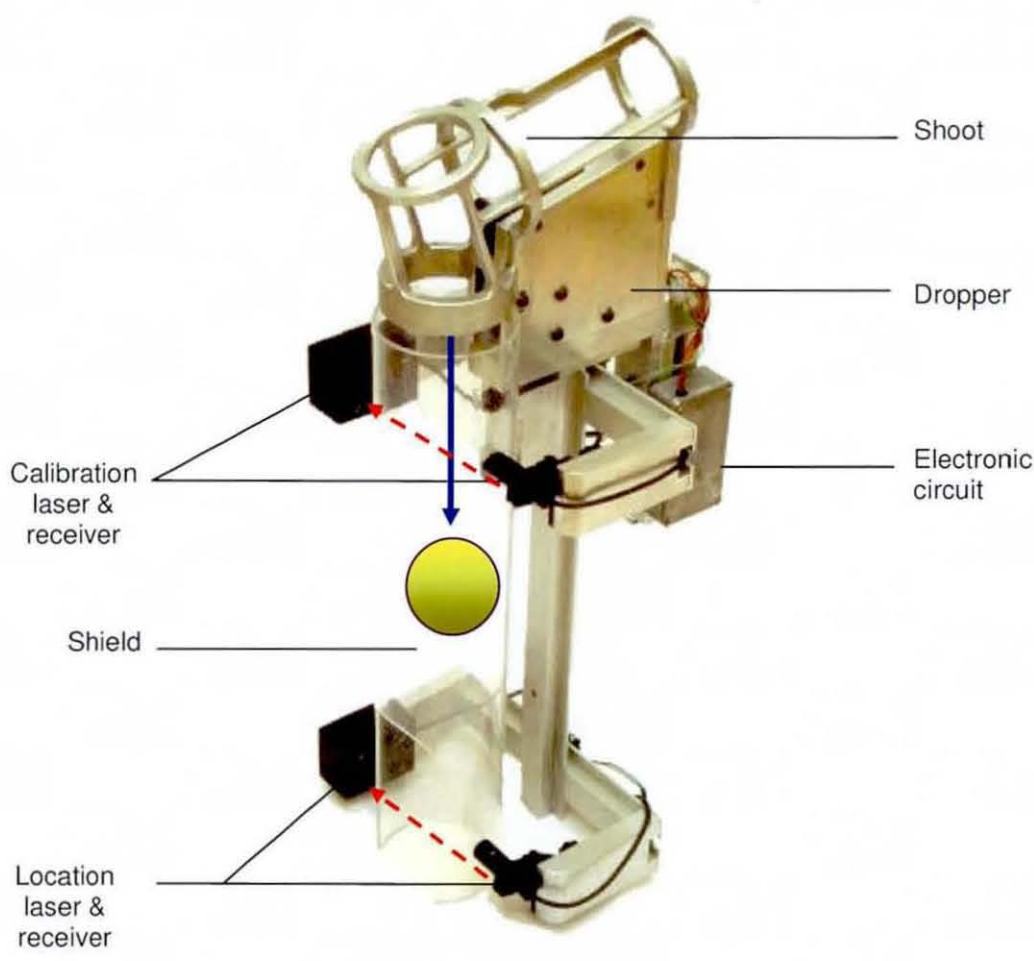


Figure 6.20: The ball delivery system.

As specified by the PDS, the machine needed to be able to map the rebound characteristics across the entire racket face, which meant the ball had to be able to travel across the full length of the string bed. Hence, since the test involved the racket reaching the desired speed in multiple revolutions, the ball had to enter the racket envelope at a sufficient vertical speed enabling it to travel across the face at the fastest possible impact speed ( $50\text{m.s}^{-1}$ ). Consequently, constant acceleration equations were used to calculate this minimum drop clearance ( $S_{clear}$ ) between the racket tip and the trap door:

$$S_{clear} = \frac{\left( \frac{S_{head}}{t_{rev}} - \frac{g \cdot t_{rev}}{2} \right)^2}{2 \cdot g} \tag{6.9}$$

with  $S_{head}$  being the length of the racket head,  $t_{rev}$  the duration of a rotation at the maximum impact speed and  $g$  gravitational acceleration. This yielded a minimum clearance of ~575mm. Including a ~10% tolerance, to ensure the ball does not hit the racket frame during a mistimed drop, resulted in a final clearance of ~680mm.

No tangible data exists on the height of ball toss during a serve but Brody *et al.* (2002) highlighted that, although a higher toss is more difficult to hit it would significantly increase the player's acceptance window due to the additional top spin generated by the ball moving further on the racket face. It was calculated that instead of hitting the ball at the apex of its trajectory, an overthrow of 457mm would increase the percentage of serves going in by 28%. It is therefore very probable that professionals would utilise this by attempting to toss the ball as high as possible, without sacrificing significant accuracy. The author was therefore confident that the selected clearance height for the machine was representative of a professional serve.

### 6.4.6 Data capture systems

In order to maintain the high tolerances specified by the machine's PDS, the most accurate data capturing systems possible were utilized to measure the racket and ball speeds. The motor/gearbox unit incorporated a standard resolver, which continuously provided the angular position of the shaft. The resolver's signal was fed to a Lenze 9327 servo drive, which converted it into an analogue signal, which is supplied to the MC216 Trio motion controller at 20.8kHz and converted into the drive arm's angular position and velocity. The Lenze drive and Trio controller formed the core of the control system and are described in more detail in §6.4.8. In order to measure the angular position and velocity of the racket, which was not the same as that of the drive arm during separation, a resolver was mounted to the IC-unit. The resolver had no internal datum index, i.e. it only indicated the number of encoder increments moved

from an external datum point at 2048 pulses per revolution. The datum, consisting of a magnetic proximity sensor detecting a steel pin inserted into an aluminium disc mounted on the shaft, was mounted to the A-frame, providing a consistent peak signal every time the shaft is in the same angular position. Similar to the encoder, the signal was converted by the Lenze drive and the Trio controller into the desired angular location and speed. Both racket and drive arm positions and velocities are continuously monitored by the system at the fastest possible sampling rate, as described in §6.4.8., to ensure the required accuracy.

The rebound ball velocity was measured by the ball cutting two ballistic laser light curtains, which were created by reflecting each beam three times between two mirrors as shown in Figure 6.21.

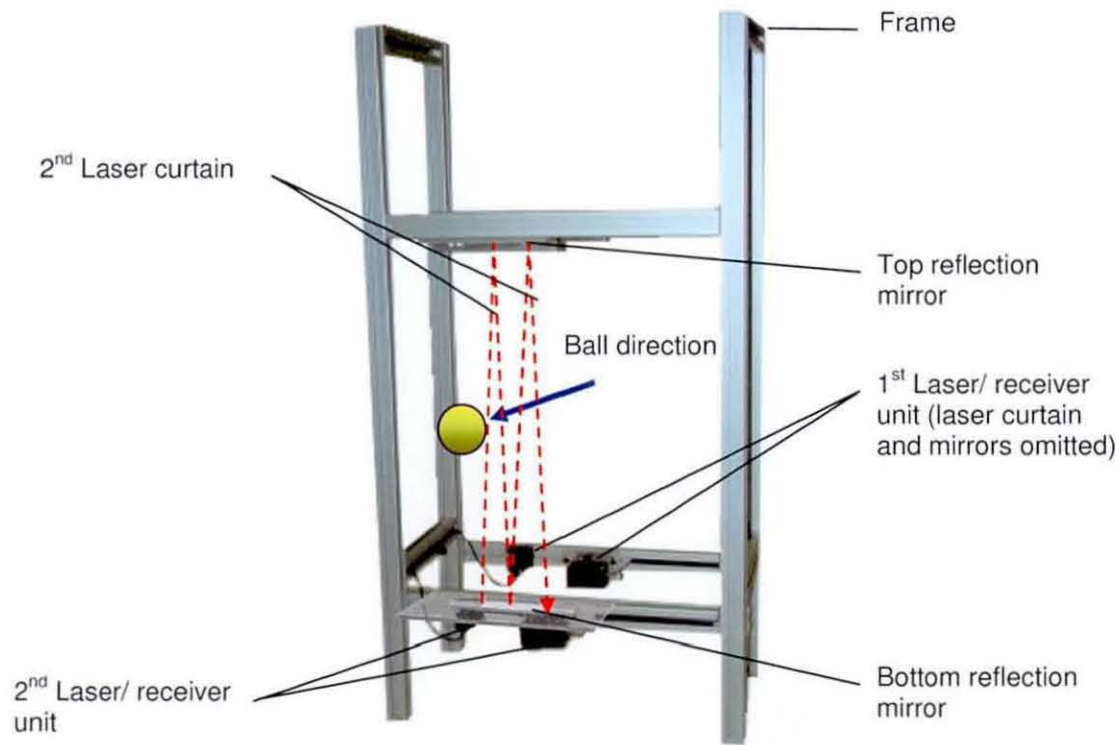


Figure 6.21: The laser unit measuring rebound ball speed.

Special highly reflective mirrors were used, in order to minimise stray light during reflection, resulting in a stronger and more reliable signal. The laser curtains were positioned a known distance (300mm) apart, measuring the



time for the ball to travel between the first and second beam, which was used by the PC software to calculate the ball velocity. The duration was measured by a timer interface card inside the PC, sampling at 1MHz, resulting in a maximum ball speed error of 0.02% at  $66.6\text{m.s}^{-1}$ , which was well below the tolerance specified by the PDS in §6.3.5. The entire unit was fitted onto a separate frame in order to isolate it from the cage's mechanical vibrations, which had previously caused the misalignment of the lasers and faulty measurements.

#### 6.4.7 Safety systems

The machine was enclosed in a durable extruded aluminum profile cage, fitted with 6mm polycarbonate panels to contain any moving parts from the operator (Figure 6.22), hence creating a safe operating environment. The enclosed space consisted of three functional sections allowing racket rotation (red), ball speed measurement (blue checked) and ball catching (green hatched). The only entrance to the cage was from the front via a large undivided slide door, which allowed an unobstructed view of the racket motion for photographic purposes.

Additional safety features included a double-function safety lock, which would not allow the user to operate the machine while being inside the cage, or allow opening of the door while the machine is still in motion. As soon as no motor rotation was detected by a sensor measuring the back-current from the motor, a built-in timer kept the door locked via a solenoid activated pin for an additional three minutes to ensure nothing else was moving inside the cage.



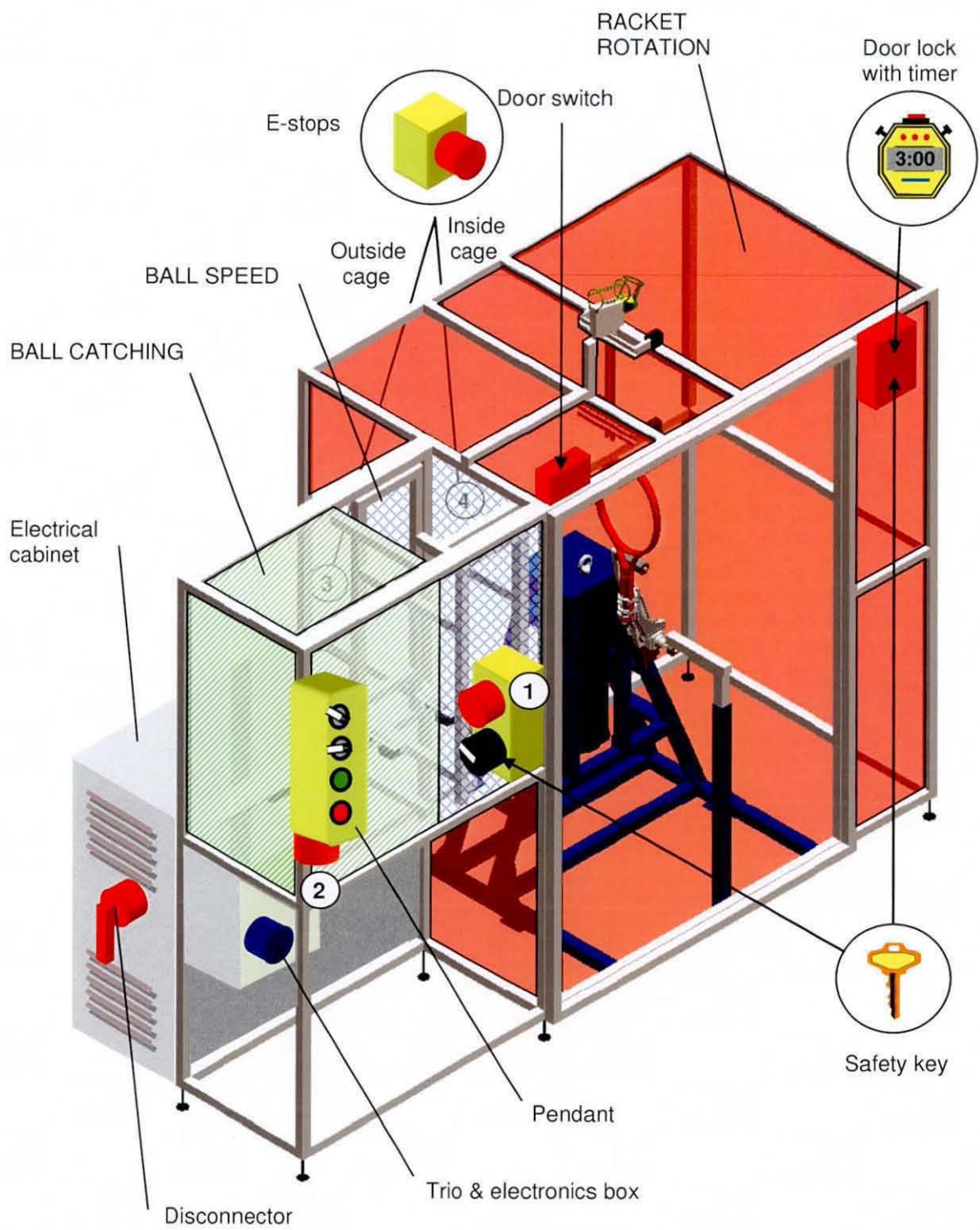


Figure 6.22: The robot's safety systems.

The cage was fitted with four emergency stop buttons (E-stops) distributed around the cage to allow access from all operating locations. Two buttons were fitted on the outside of the frame, while another was on the control pendant and the fourth inside the cage. The E-stops had an additional function in that they acted as a double-up security to the main switch for unlocking the cage door. The main switch cuts the power to the motor functions only with the correct mechanical key, which was the same key used to mechanically lock and unlock the cage door, preventing the machine from being operated with the operator inside the cage.

Special care had to be taken to ensure an accurate control system, which was not influenced by external signals. Hence, all power supplies, high voltage motor control systems and safety controls were enclosed and shielded in a ventilated steel cabinet behind the cage. It fed from a single 3-phase connection, which was physically locked and electrically connected via a disconnect. The remaining low voltage control components (including the Trio controller) were situated in a smaller steel cabinet in the front of the cage in order to screen it from the high voltage systems and allow easier access to the PC and operator.

### 6.4.8 Control systems

#### *Single vs. multiple revolutions*

As mentioned earlier, one of the initial considerations was to develop a machine which would be able to bring the racket up to speed in a single revolution rather than multiple revolutions, mainly since a single rotation would seem more realistic to the public and similar systems had been successfully implemented in other sports such as golf. Nevertheless, since impact dynamics are unaffected by how the racket reaches impact speed, the disadvantages of the multiple revolutions solution were outweighed by its advantages: ease of automation assisting the acquisition of sufficient number of impacts for statistically significant test result, lower power requirements, less



strain on components due to the lower accelerations and decelerations and higher consistency since it allowed sufficient time for the racket speed to stabilise during each operation stage.

#### *Basic control strategy*

The standard test procedure consisted of four distinct stages; the datum, acceleration, constant velocity and deceleration stages as depicted in Figure 6.23 (a)-(d).

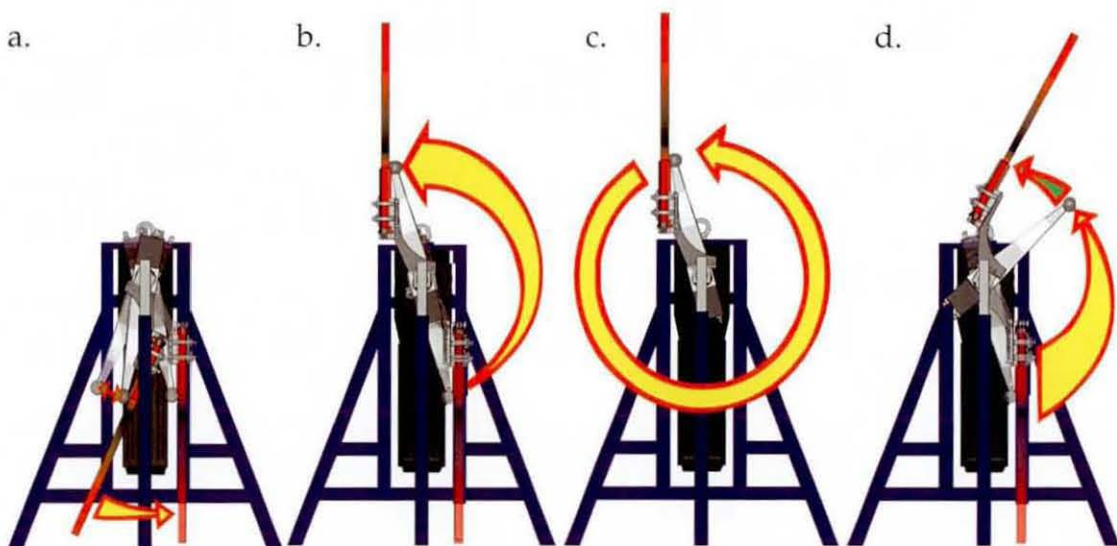


Figure 6.23: The different operations stages during a normal test procedure.

The next sections provide a condensed explanation of the machine controls, while more detailed user instructions are documented in the online help. Figure 6.24 clarifies the terminology used and where needed, detailed control diagrams are presented in Appendix B.

The basic principle of the machine is based on a novel concept, which has the racket rotating freely around the main shaft via an IC-unit. The combined assembly is driven to the desired speed by the drive arm through a foam-covered crossbar from behind the racket face.

Each test is started with the *datum* procedure, which locates the data for both the drive arm and the racket assembly, while assuming both are located in

the 'valley', with the drive arm behind the racket. During this stage the drive arm slowly moves  $44^\circ$  backwards and then forward until the racket reaches its bottom datum. The racket pauses in this position for a second to give the operator time to verify that the encoder index still corresponds to the racket's vertical position. The controller also sets the origin for the resolver and the encoder, with this location as the bottom-dead-centre (BDC) position at  $-180^\circ$ .

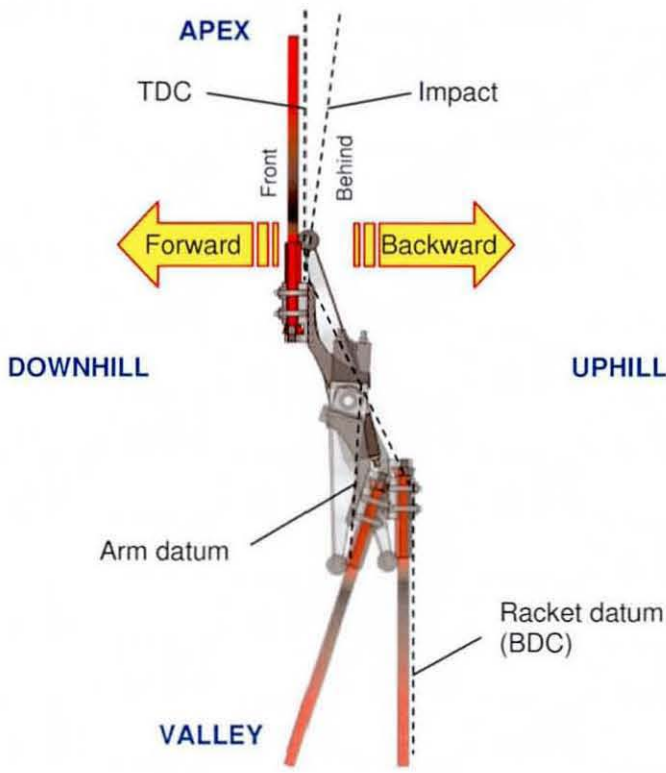


Figure 6.24: A diagrammatic clarifying the control terminology.

The next stage is *acceleration*, during which the drive arm accelerates the racket to the desired impact speed, which is then maintained throughout the *constant velocity* stage. The flexibility in the cross arm combined with the effect of gravity on the racket assembly causes a fluctuation in the racket speed at the beginning of the stage. The assembly is therefore allowed to rotate for five revolutions at the constant speed to ensure a constant racket motion. During the next revolution, the ball drop is activated by the Trio controller at a pre-calculated drive arm angle. The entire assembly continues at a constant velocity



until reaching the BDC before starting the *deceleration* stage, during which the drive arm is decelerated sufficiently to allow the racket unrestricted rotation until after the impact. The deceleration is set such that the drive arm reaches half its constant velocity before reaching top-dead-centre (TDC). Impact occurs just before TDC, at an angle calculated to achieve the desired impact location on the strings, with a higher impact location correlating to a smaller angle with the vertical. During the impact, which lasts about 5ms, the racket slows down to not less than 50% of its impact speed (§5.5), hence the gap between it and the drive arm is reduced considerably by the time the drive arm reaches TDC. On reaching the TDC the arm starts closing the remaining gap by entering a closed proportional speed loop, which accelerates the drive arm towards the racket assembly, decreasing its acceleration as the gap decreases, in order to minimise the relative velocity at contact between them. As soon as the gap is closed the drive arm re-enters the *acceleration* stage, with the test cycle repeating itself until the last impact is performed, or the test is terminated by the user.

Since the drive arm and the racket mechanism were not mechanically coupled, the motor drive cannot be used to reduce the racket speed while the crossbar is behind the racket. Therefore, other than letting the racket and IC-unit wind down on its own, the only more effective way to stop the unit is to use the drive arm to brake the assembly from the front. A reverse braking procedure was therefore developed, which brings the racket to a halt from the front without sacrificing the racket or any machine components. The drive arm is braked until it touches the racket from the front and is moving at the same speed as the racket utilising another proportional closed loop, in which deceleration of the arm decreases as the size of the gap with the front of the racket decreases. After contact with the racket is made, the arm decelerates slowly to maintain contact with the racket until it reaches a predefined angle, where the deceleration increases to a halt downhill from TDC. In this position the racket is lying on the cross arm and is then moved slowly to the racket's gravitational equilibrium in the valley, with the drive arm continuing in the

same direction but at a higher speed to move back into the start position behind the racket.

*Maintaining system integrity and accuracy*

Signals from all the instruments discussed are acquired via custom built circuitry, the Lenze drive, the Trio controller or the timer/counter (TC) card inside the controlling PC. The Trio controller and the interface software developed combine all this information with the safety systems to provide a fully automated multi-impact testing system (Figure 6.25), able to accurately map the desired rebound characteristics down the racket face.

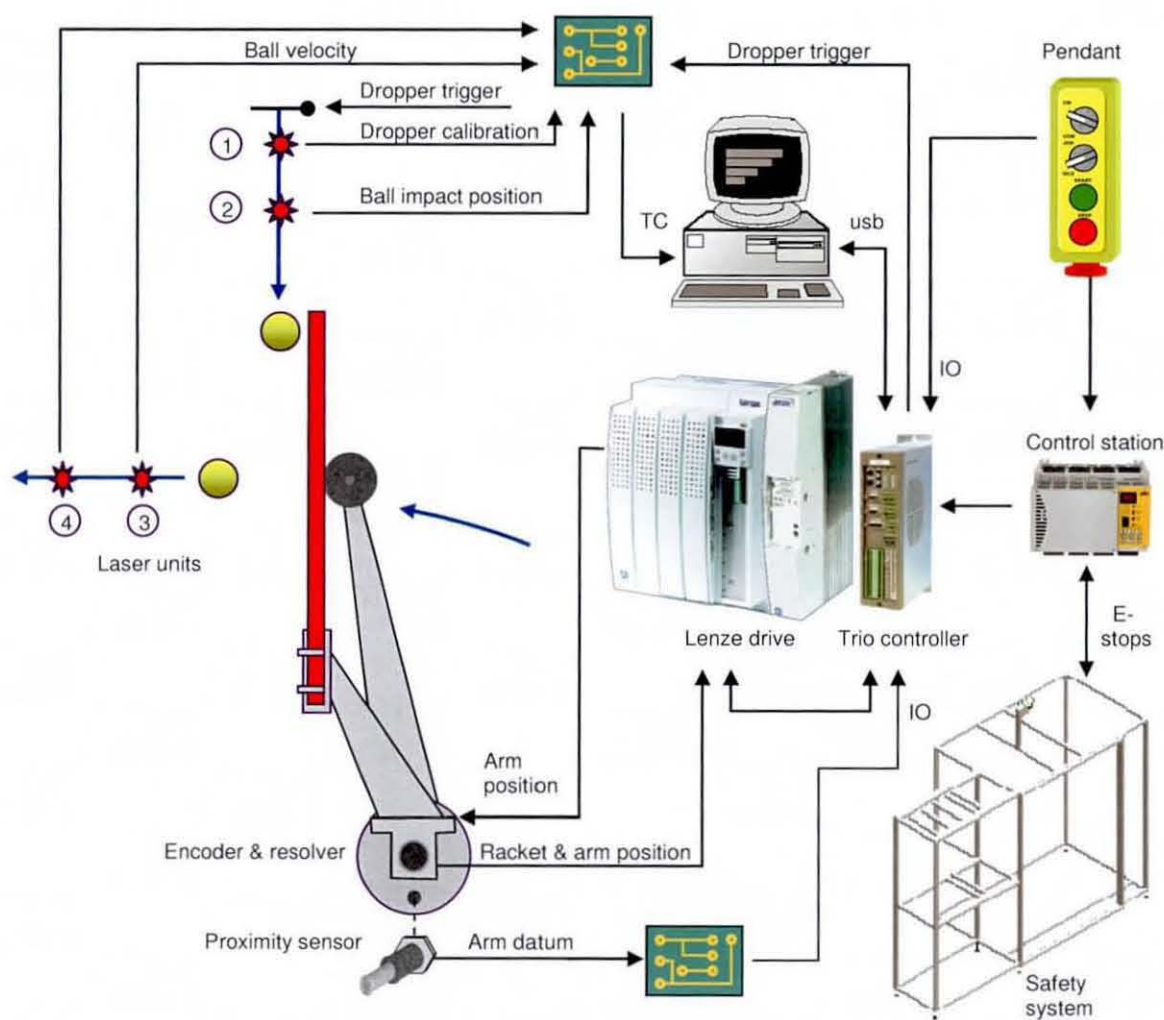


Figure 6.25: A diagrammatic representation the control systems.



To ensure the high accuracy demanded by the PDS, *proactive error detection* is performed by prompting the operator to perform a datum set-up routine at the start of every day's testing. The routine involves detecting and checking the encoder and resolver's datum locations, as well as the size of the maximum gap which can be opened between the racket and the drive arm before it touches the front of the racket. The foam covering the cross bar gradually compresses with time, therefore decreasing in diameter and increasing the maximum gap size. The latter is a parameter used in the closed loop during reverse braking of the racket, so regular monitoring is required.

The timed ball drop is triggered by the Trio controller via an output port, which drives the solenoid through a hardware-timed constant duration pulse. The hardware provides a consistent 500ms duration pulse to the ball dropper ensuring the ball has left the dropper before the solenoid closes again, letting the next ball through. The accuracy of the dropper is checked by two *laser based optical triggers* (Figure 6.20). The first laser (calibration laser), located immediately below the drop mechanism is used for calibrating the dropper timing, while the second laser (location laser) is located as close to the 'hitting zone' as possible, hence providing an accurate estimation of the real impact location.

The Lenze 9327 servo drive can be programmed and controlled directly via PC based software but this would be very cumbersome and make the control dependent on the PC's operating performance and the operating system's task allocation, which is unreliable for motion control and therefore not good practice. An intermediate industrial controller, the *MC216 Trio motion controller*, was therefore employed for programming and specific control of the Lenze drive. In addition to the motion control functions, the Trio also has input/output (IO) ports, which are used for detecting and triggering external events. The Trio is connected to the PC via a universal serial bus (USB) connection for high-speed uploading and downloading of test parameters but

apart from the parameters the Trio functions independently and in parallel with the PC interface. This is imperative to the system integrity needed to adhere to the high accuracy, consistency and safety requirements specified by the PDS.

Trio programs are composed as text files with motion and IO commands, which the Trio converts into appropriate analogue signals to and from the Lenze drive, digital signals on the IO ports or information available for upload by the PC interface. A fundamental difference to normal PC programming is that multiple Trio programs can truly be executed simultaneously ensuring equal resource distribution; even multiple instances of the same program can be executed. Programs can be executed at different speeds, with commands in normal programs being executed at 1ms and those of specially designated fast programs at 0.33ms. Since a maximum of three fast programs are allowed at once, only the programs needed for emergency detection and high-speed measurements are executed as fast programs. Five programs were used to control the motion, as illustrated in Figure 6.26, while detailed flow diagrams for each of the five programs are presented in Appendix B with a description of each in Appendix C. As discussed earlier, to ensure high reliability all critical error detection, such as motion errors, E-stops and control panel stops, are managed by the Trio rather than the PC. All safety equipment used on the machine has double redundancy components and is wired to the Trio's inputs, which are monitored by a continuous loop in the POWERUP program. Similarly, motion errors on the Trio set an error constant in the software, which is monitored in the same loop.

The *PC interface* is an executable program, written in Visual Basic, which provides the operator with a user-friendly interface for controlling the test machine. The program runs in parallel with the Trio programs and primarily serves as an input for test parameters and conversely to calculate and output the measured results. This is achieved principally by downloading variables to the Trio program through the USB connection when needed and continuously



monitoring and displaying useful indicators to the user. Once testing commences, the machine's fundamental control is handled by the Trio controller and can be carried out without connection to the PC. More detail on the interface screens are presented in Appendix C and flow diagrams assisting in the explanation of its control strategy are provided in Appendix B.



*Inputs:* User inputs are entered via a *Setup* screen, of which two examples are shown in Figure 6.27, while system inputs are measured via the three timers on the counter/timer board (Figure 6.28).

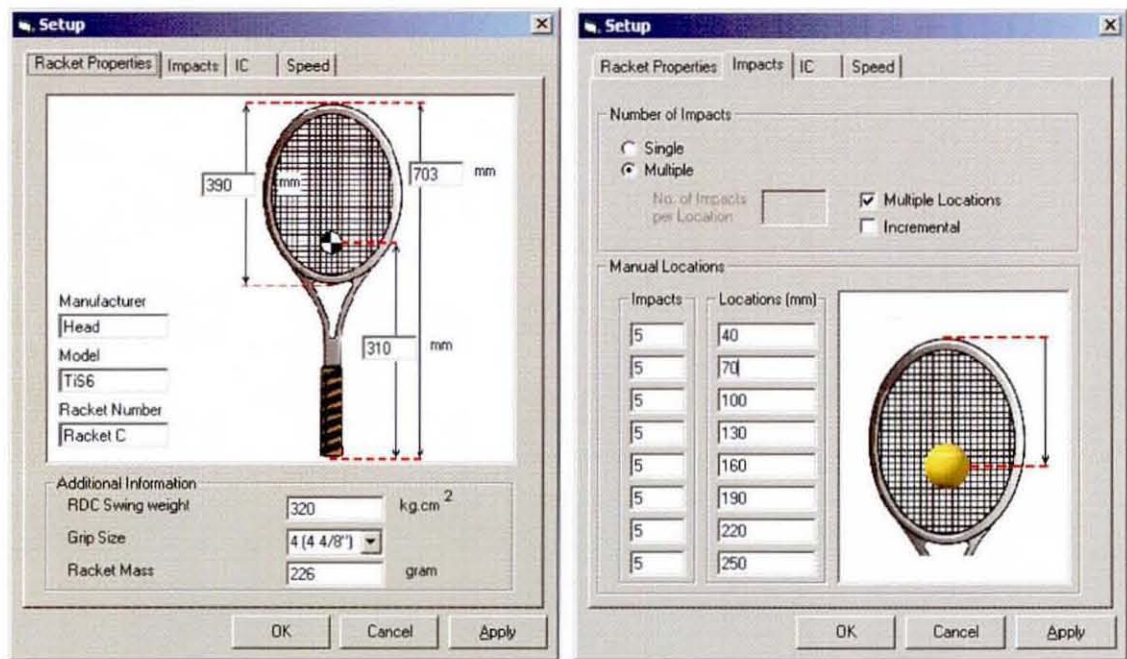


Figure 6.27: PC main interface screen during test operation.

The first timer (T1) measures the time from the output signal to the ball dropper to the calibration laser, triggering the second timer (T2), which measures the time to the start of the location laser signal. The third timer (T3) measures the time for the ball to move from the first ball speed laser to the second (Figure 6.21).

*Outputs:* During operation, information such as racket velocity, impact number and distance, and the test stage is indicated in the *Main interface* screen (Figure 6.29), while after each impact the racket's speed before and after impact, the ball speed, the real impact location and a 'racket power' indicator are displayed. In order to measure the racket's pre- and post-impact speeds, the racket speed during the impact is recorded by the Trio, then uploaded and analysed by the PC interface. The typical speed profile, as shown in Figure 6.30,

is analyzed for various relevant parameters. The signal appeared as if its been clipped and attempts to improve it with the help of the drive suppliers were fruitless, so it was used as is.

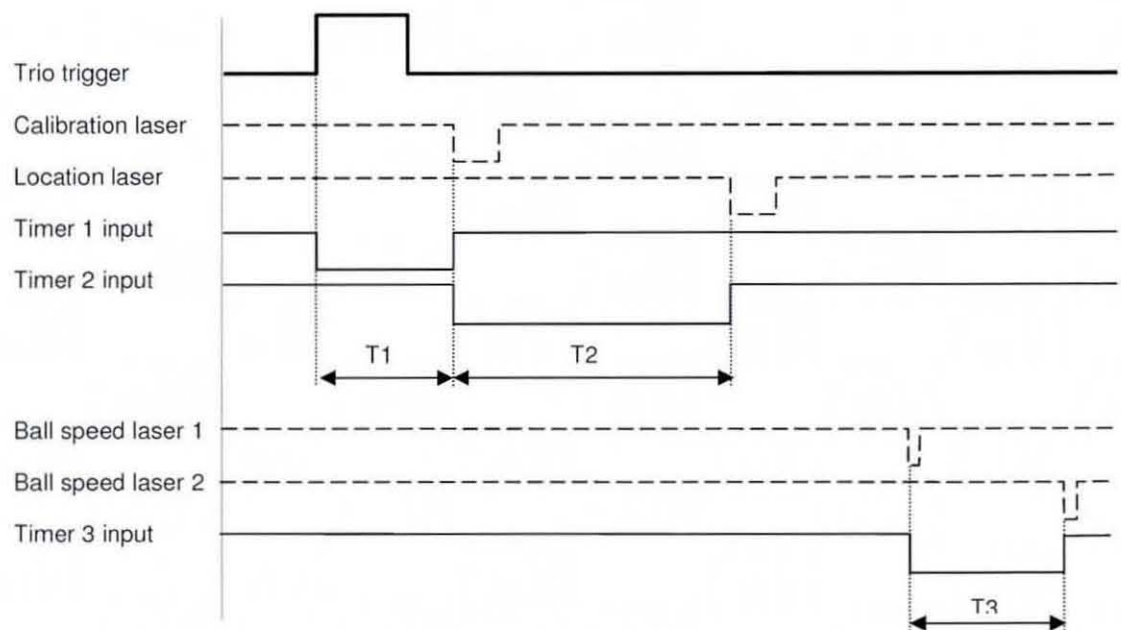


Figure 6.28: Input signals to the IO timer card (not to scale).

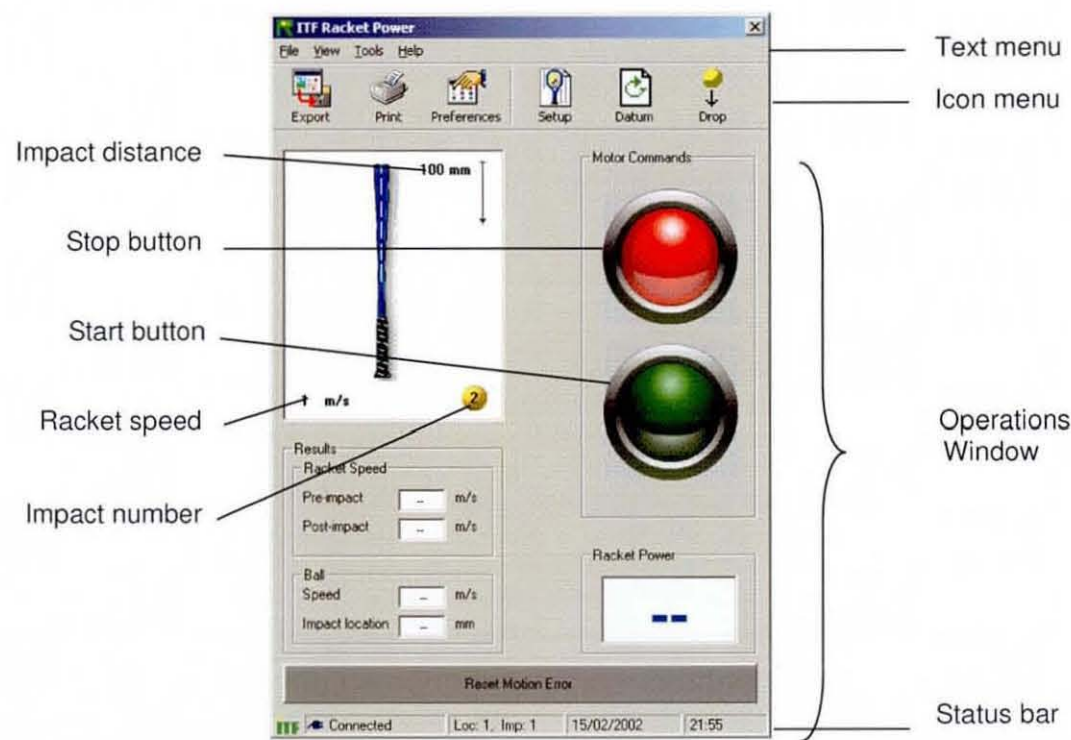


Figure 6.29: PC main interface screen during test operation.



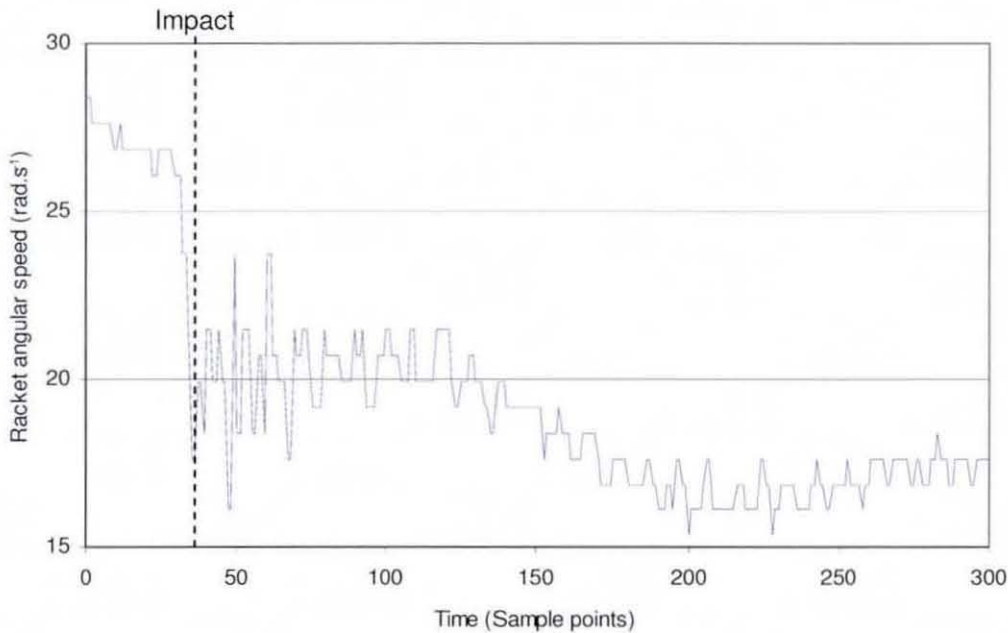


Figure 6.30: The measured speed profile for a typical impact.

For the racket, only the pre- and post-impact speeds were required by the PDS but recording the entire impact would allow for any further parameters to be calculated if needed. The impact instance was determined by searching for a drop of more than  $3.1\text{rad.s}^{-1}$  in racket angular speed between two consecutive data points, which equated to about  $2.1\text{m.s}^{-1}$  at a 700mm radius. The pre-impact speed is calculated as the average of the five sample points before impact and the post-impact speed as the average of the speed from the remaining data samples after the impact. The performance indicator calculated and displayed for the commissioning phase was the  $\text{COR}_s$ .

### 6.5 Summary

A novel tennis serve simulation machine (Figure 6.31) was developed to replicate human performance and, in so doing, allow the investigation of a tennis racket's performance. Specifications for the machine were derived, documented in the PDS, and met by the incorporation of some distinctive design features.

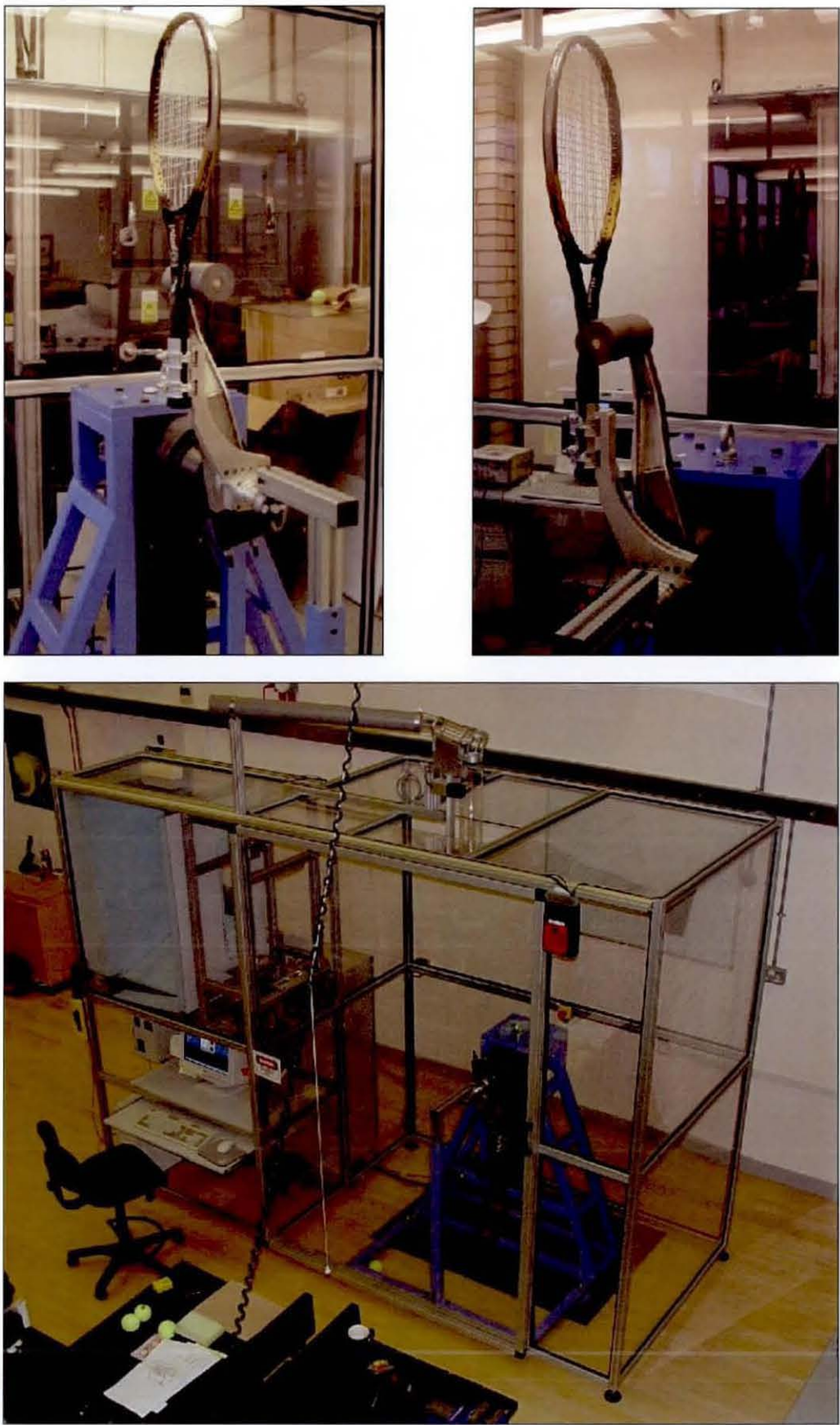


Figure 6.31: Photos of the developed serve simulation machine.

The machine consisted of a unique drive and gripping mechanism, allowing testing of the effects of various feasible boundary conditions. The design was simple, with a rigid structure and control paradigms, which should guarantee repeatable performance at representative head speeds unmatched by motion realistic test robots at the time. The machine also reproduced more realistic serve impact conditions than current robots by introducing realistic vertical ball speeds during the impact. This was also the first fully automated test robot, able to measure the racket performance across the entire racket face with the press of a single button.

The following chapter will describe the commissioning of the machine and the stringent validation of its performance and adherence to the PDS.



## Chapter 7

### Machine commissioning and evaluation

The objective of the chapter is to confirm that the developed test machine (called MΨO) fulfils its requirements and can therefore be successfully employed to investigate racket performance. As a help, the machine design is clustered into functional themes critical to the machine's performance and assessed in the subsequent sections.

#### 7.1 Ball systems

##### 7.1.1 Ball timing and consistency

To facilitate the ball drop timing so that it results in an impact at a specific location on the racket face, the ball path versus time was mapped for the expected impact region. Using the range of standard racket lengths specified by the PDS, the envelope was determined to be between 600-1000mm from the ball's resting position in the dropper. Consequently, the consistency of the mechanism was tested at ~800mm, which roughly represented the distance to the GC of the average racket face. This was performed using the Sensicam, a long duration flash shutter camera, with the shutter speed set at 70μs (Figure 7.1). To obtain a picture of the ball only (without the racket) and eliminate all other interferences, balls were dropped manually via the *Drop* button on MΨO program's *Main* screen without the machine running. The same output used to trigger the dropper was used to trigger the delayed shutter opening on the



Sensicam, which captured a digital image of the ball on a calibrated background (Figure 7.2).

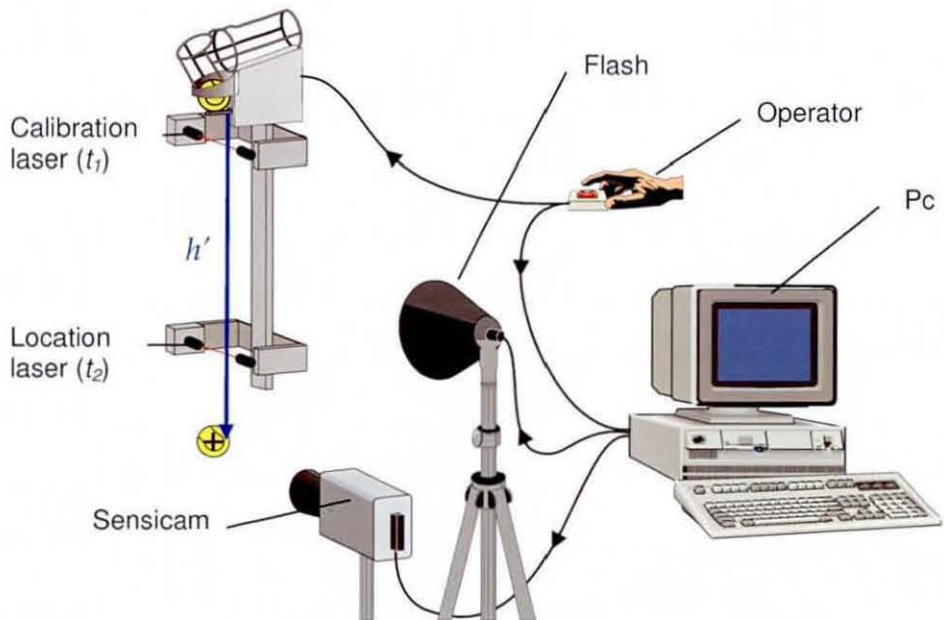


Figure 7.1: Diagrammatic explanation of dropper calibration set-up.

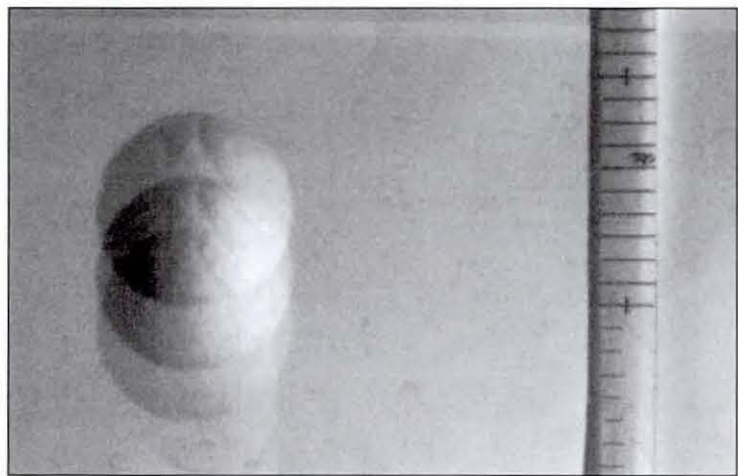


Figure 7.2: A zoomed image showing the calibration background for digitizing the ball position.

The images were then digitized and the distance from the edge of the dropper to the centre of the ball determined. The resulting drop distance was measured with a standard deviation of  $\pm 2.3\text{mm}$  and a maximum variation of 10mm, which was sufficiently accurate according to the PDS. The map in Figure 7.3 of the time  $t_{imp}'$  (in ms) needed to achieve a desired drop distance  $h'$  (in mm),

appeared to be linear but was nevertheless fitted with a second-order polynomial, for higher accuracy:

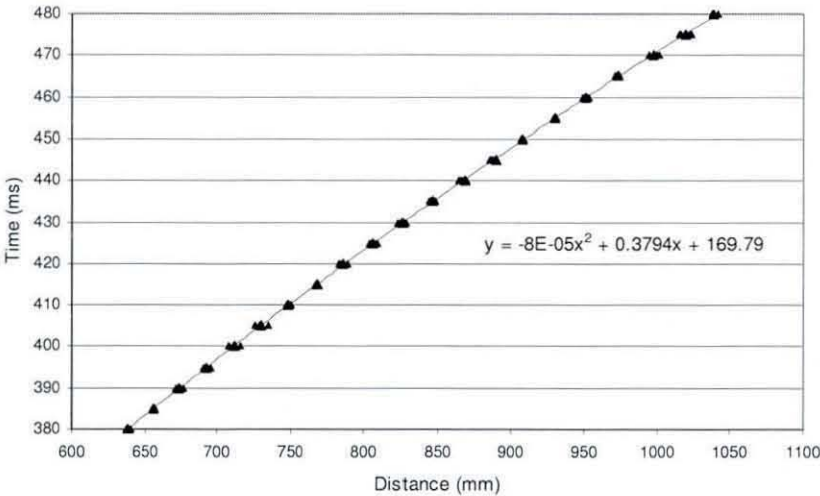


Figure 7.3: Mapping of the predicted time needed for the ball to travel from the drop trigger to an impact location versus the distance travelled

$$t_{imp}' = -8 \cdot 10^{-5} h'^2 + 0.3794 \cdot h' + 169.79 \quad (7.1)$$

Equation 7.1 is used to calculate the timing needed during each impact for the ball to travel to the intended impact location. Using the racket’s angular speed, the angular position is calculated at which the Trio should trigger the dropper.

In order to increase the accuracy of the impact locations during operation, which was dependent on the ball as well as the racket timing, inconsistencies were corrected by measuring the actual timing of the ball as close to the racket as possible and correlating it with the known racket timing. Since the Trio constantly measures the racket orientation it can calculate when the racket is in the contact position, therefore an additional timer was started on the Trio when the signal to the dropper was switched on and stopped as soon as the racket was in the impact position. This provided the most accurate indication of the real impact time, and is combined with the time measured by the location laser,

which provides the best indication of the real ball location at the same time. Since the robot will be used to map the velocity profile across the face of the racket, rather than measure the velocity at a discrete point, this reverse calculation of the real impact point would not affect the results, providing the error in impact location still resulted in sufficient impacts along the racket face to produce statistically significant results. The parallel measurement was performed by an integrated laser/receiver unit (Figure 7.1 and Figure 6.20). The location laser was positioned immediately above the racket envelope to measure the time needed for the ball to travel to the laser ( $t_1+t_2$  in Figure 6.28) from the instant the trigger was sent to the dropper. The remaining time needed for the ball to travel from the location laser to any impact location in the racket envelope ( $t_4$ ) is mapped by subtracting the time taken to travel to the location laser from the total time ( $t_{imp}'$ ) to the impact location measured by the Trio timer. According to basic mechanics the relation between the real distance travelled from the location laser to the impact  $h$  (in mm) and  $t_4$  (in ms) is a second-order polynomial, for which the constants were determined from inverse of Equation 7.1:

$$h = 0.0047 \cdot t_4^2 + 2.8627 \cdot t_4 + 406.12 \quad (7.2)$$

The accuracy of the actual location measurement during operation was determined using the Sensicam system, with a similar set-up as for the dropper calibration but performed during operation, with the signal to the dropper also triggering the Sensicam. The Sensicam was programmed to record an image of the ball at predetermined intervals from the predicted impact time onwards. The ball was measured to move about 20mm on the string surface before leaving it, therefore the centre of the 'footprint' was taken as the actual location and compared to the location calculated from the laser measurement. Testing indicated that adding a 2ms delay to the calibration Equation 7.1 resulted in an exact prediction of the impact location. This delay incorporated the ball movement on the strings and other small time delays between the systems. As a



final system assessment, the timing from all individual lasers was double-checked with an oscilloscope.

In the export file containing the impact results, both the desired and calculated impact locations are documented. If the correlation is not to the user's satisfaction the dropper timing can be recalibrated. This is performed by dropping balls while monitoring the time taken to travel to the calibration laser, positioned immediately underneath the dropper ( $t_1$ ). The balls are dropped manually via the *Drop* button on MYO program's *Main* screen, and the time displayed in its main window in a special *Utilities* mode (Appendix A). The dropper can also be calibrated during normal operation but it is more cumbersome and prone to interference, therefore the manual method is recommended. If the time ( $t_1$ ) is found to be consistently different from the standard (141.83ms) it means there has been a constant shift in the system behaviour, such as increased mechanical friction, causing the error. This is not critical and can be adjusted by changing a variable in the interface's initialisation (*MYO.INI*) file. If the error is not consistent the dropper needs to be repaired.

It was anticipated that balls in different states of wear might have an influence on the dropper's accuracy, hence the timing of three different tennis balls were measured; cores, new balls and fluffed-up (old) balls. These balls were considered to be representative of the range of balls likely to be used for testing. The Sensicam was used to measure the drop distances 508ms after the dropper was triggered. The average distance measured for cores were 1.207m, 1.189m for new balls and 1.188m for fluffed-up balls. The difference between cores and normal balls was significant but the difference between the new and old balls was negligible relative to the dropper variation. Nevertheless, it is recommended to use standard balls for not more than 100 impacts (from §4.2) as a precaution to ensure rebound consistency and prevent blockages in the dropping mechanism.



High-speed Sensicam footage was used to monitor the ball trajectory and its effect on ball speed accuracy. It was observed that if the racket is in the vertical position during the start of the impact the ball leaves the racket face on a downward trajectory, resulting in an incorrect ball rebound speed measurement, since the laser only measures the horizontal speed component. Considering the ball stays on the racket surface for  $\sim 5\text{ms}$ , by the time it leaves the face, the racket has moved past the vertical, propelling the ball at  $\sim 11^\circ$  to the horizontal (Figure 7.4).

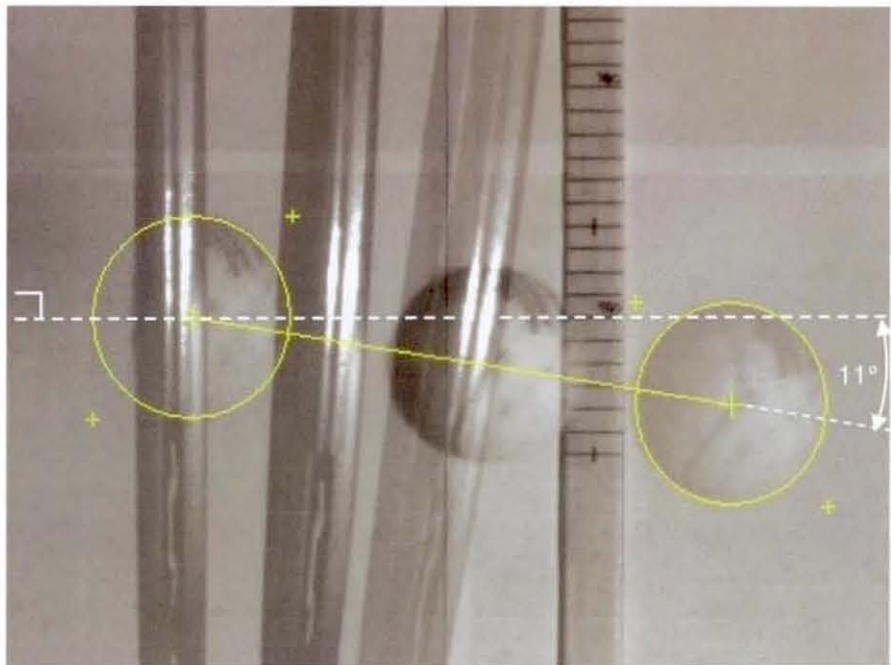


Figure 7.4: A high-speed image from the Sensicam depicting the ball on a downward trajectory of  $\sim 11^\circ$  after impact.

This is similar to a real serve, during which it is intentional to assist the ball in bouncing before the service line but it is not desired for the test machine. The dropper was therefore moved further backwards, to 92mm behind the racket's upright location, such that the ball would impact the racket before it reaches the vertical position (Figure 7.5). The same tests were performed at a racket speed of  $\sim 30\text{m.s}^{-1}$  measuring the racket angle at the onset of the impact at  $\sim 11^\circ$  before the vertical. The angle varies for impact locations along the face though and is therefore accounted for in the calculation of the timing for each

location. This dropper position was chosen as a good compromise between a realistic ball angle and accuracy of the speed measurement but, if desired, could be changed to compensate for the different racket speeds. If the distance is changed, the corresponding parameter in the MYO.INI file should be updated to adjust the calculation of the impact location.

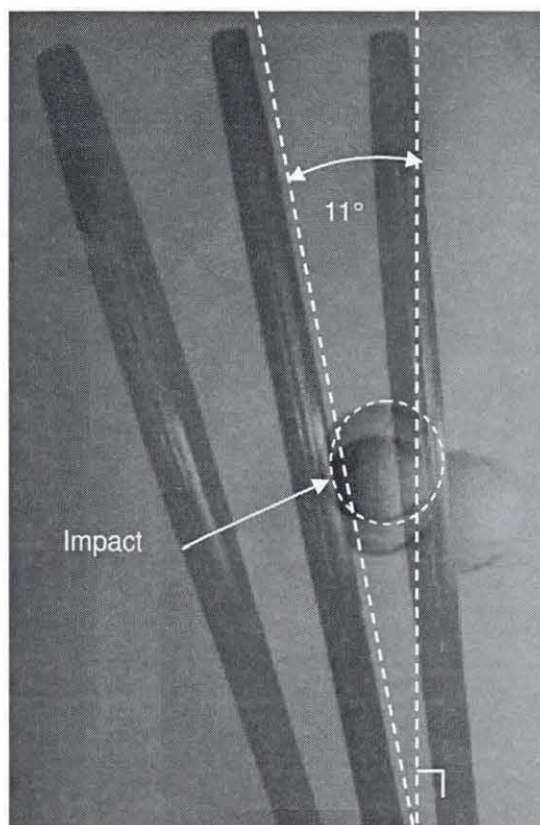


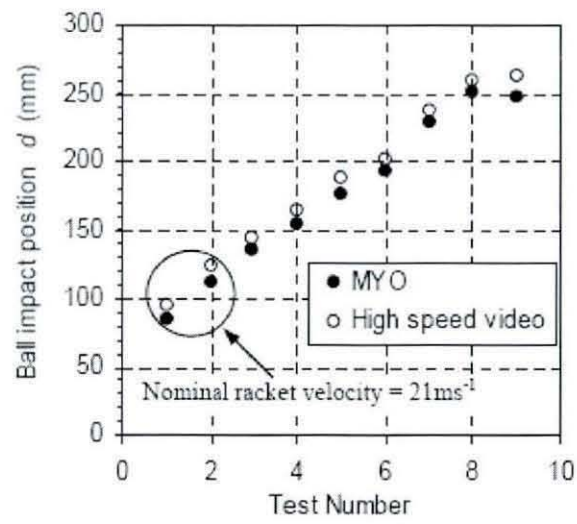
Figure 7.5: A high-speed image from the Sensicam depicting the onset of the impact, with the racket angle at  $\sim 11^\circ$  before TDC.

After commissioning, the machine's performance was also evaluated by an independent study performed by an ITF investigator (Goodwill 2003). A Phantom v4 high-speed video camera (at 1000 fps) was used to film the machine during operation. Two markers were fixed to the racket frame, at discrete locations along the longitudinal axis, in order to allow digitisation of the racket motion. Ten images before impact were digitised and the racket velocity calculated. The racket velocity after impact was not determined from the high speed video images due to the excessive racket oscillation after the impact. During the evaluation the machine was tested at head speeds up to

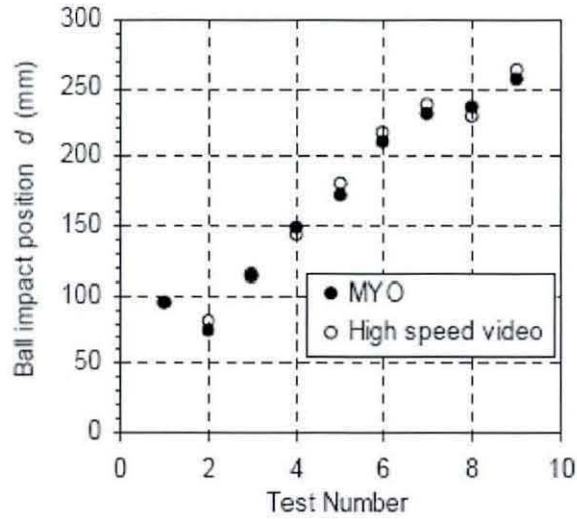
50m.s<sup>-1</sup>, but the range of speeds selected for comparative testing were considerably lower, at nominal speeds of 22 - 35m.s<sup>-1</sup>, due to the sheer intensity of testing at higher speeds, which often resulted in racket failures.

The results from the impact location measurements shown in Figure 7.6 indicated that at 22m.s<sup>-1</sup> the MΨO software underestimates the ball impact location by approximately 10mm, while the results at 35m.s<sup>-1</sup> are virtually identical (3mm) to the high-speed measurements. The investigator mentioned the vertical movement of the ball on the racket face complicating the measurement of the impact location using the high-speed video footage, and although a visual method should be more accurate, this degree of uncertainty justifies use of the laser method in the machine design, as an acceptable compromise between accuracy, simplicity and automation.





(a) 22 ms<sup>-1</sup>



(b) 35 ms<sup>-1</sup>

Figure 7.6: Comparing ball impact locations measured by the machine with that measured with the high-speed camera.

The trajectory of the rebounding ball was measured at 2.5° – 4.0° with the horizontal and the racket is itself measured to move through 10° during impact. The investigator shared the author’s opinion that the vertical ball speed provides a realistic representation of an actual serve.

7.1.2 Ball speed measurement

As mentioned in §6.4.6, the machine’s ball speed measurement involved the ball cutting two laser beams positioned with a known separation. The



lasers' signals were combined by hardware into a continuous signal ( $t_3$  in Figure 6.28), of which the duration was measured by a counter card in the computer. In order to avoid error readings from the measurements of balls not travelling in the racket's X-Z plane, as a result of a misaligned racket or non-uniform ball, a laser curtain was implemented, which reflected the existing beam three times between two mirrors before being detected by the receiver. With every reflection, the intensity of the beam is reduced, weakening the signal, so the standard grade mirrors used were replaced with more reflective industrial mirrors, which reflected up 97%, as opposed to the standard 93%. The mirror curtain introduced another disadvantage in that the total reflected beam length is directly related to the number of times the beam is reflected, which magnified any laser misalignment. This considerably decreased the beam's chances of hitting a relatively small active area of the receiver, which was only ~4mm in diameter.

The system functioned reliably at moderate impact speeds but developed problems during commissioning at higher impact speeds. Investigations revealed that the higher speeds caused larger vibrations of the robot cage, which caused a momentary misalignment of the lasers. This was interpreted by the system as a ball cutting the lasers and therefore restarted the counters, causing an error in the ball speed measurement. The consistency was therefore improved by replacing the original ball catching mechanism, which consisted of polyamide flaps suspended from the cage's roof in a number of rows to slow the ball down. These were very effective for stopping the ball but transferred the impact directly to the frame, causing excessive vibrations of the lasers, which were mounted directly into the frame. The flaps were replaced with thick high-quality industrial foam, which considerably decreased the vibrations, but not entirely, so the lasers were removed from the frame and mounted on their own isolated rigid frame, as described in §6.4.6, which resulted in a significant improvement in the reliability of the ball speed measurement.

An additional factor affecting the consistency of the measurements was the influence of magnetic noise from the robot and its environment on the relatively low 5V inputs to the counter card in the PC. Particularly large spikes were experienced from the ball dropper, which operated via a high-powered 24V solenoid, as well as the power surges caused by the motor itself. This was solved by separating and screening cables from different systems, as well as electrically isolating most hardware components. The combined effect of all improvements virtually eliminated faulty readings at the commissioned impact speeds.

Results from the independent study (Goodwill, 2003) evaluating the M $\Psi$ O's post-impact ball speed measurement (Figure 7.7) revealed consistently lower values ( $0.4\text{m.s}^{-1}$ ) than the high-speed camera measurements. This was established to result from the ball slowing down before entering the machine's measurement zone. In order to prevent collision with the racket, the zone is located just outside the racket's rotational envelope, which is positioned approximately 1.5m away from the TDC racket position, while the high-speed measurement was performed on the ball immediately after leaving the racket face over a distance of about 700mm.

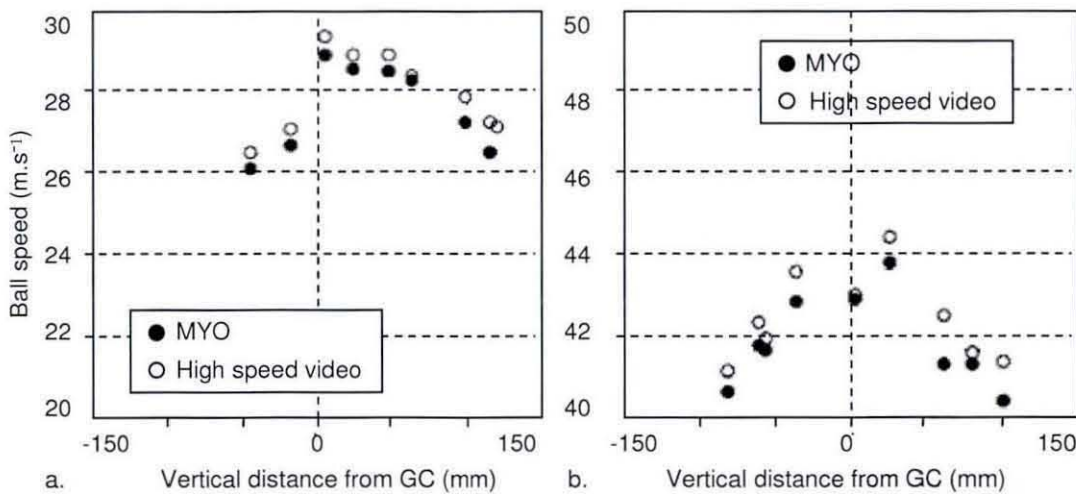


Figure 7.7: Comparing ball post-impact velocity measured by the machine with that measured by the high-speed camera at (a)  $22\text{m.s}^{-1}$  and (b)  $35\text{m.s}^{-1}$ .



## 7.2 Racket systems

### 7.2.1 Racket speed prediction

During the braking stage of the operation, the racket is released at the BDC to continue rotating unassisted until after the impact. During this period the racket loses rotational speed due to gravity, friction and air resistance, which means the real impact speed is lower than the constant set speed before separation. At a constant velocity of  $21\text{m.s}^{-1}$ , racket B lost  $1.98\text{m.s}^{-1}$  ( $\sigma=0.53\text{m.s}^{-1}$ ) from the set speed and  $1.45\text{m.s}^{-1}$  ( $\sigma=0.20\text{m.s}^{-1}$ ) at  $30\text{m.s}^{-1}$ . This is a significant drop in speed but consistent enough not to affect the functionality of the system greatly, since the real racket speed from the IC-unit encoder is used to calculate the performance parameters, instead of the set speed.

Consistencies measured by the independent study (Goodwill 2003) were somewhat conflicting, indicating lower consistencies measured with the MΨO. Figure 7.8 presents the pre-impact racket speed measurements from the MΨO and the high-speed camera measurements at nominal racket speeds of  $22\text{m.s}^{-1}$  and  $35\text{m.s}^{-1}$ , with the largest difference between the two systems measured as  $1\text{m.s}^{-1}$ . The racket speed measured by the high-speed camera was consistent with  $\sigma=0.2\text{m.s}^{-1}$ , while the MΨO measurement was less consistent with  $\sigma=1.0\text{m.s}^{-1}$ . The uncertainty in the speeds calculated from the high-speed video data was determined from the scatter in the data at approximately  $0.3\text{m.s}^{-1}$ , therefore the higher variation was assumed by the investigator to be an inconsistency in the machine measurement but it could also be that the machine measurement is more precise, specifically sensitive to inconsistencies in racket speed. The machine measurement is a direct measure from the racket encoder, while the high-speed video value is an average calculated over 10 frames. This is equal to 10ms, during which the racket has travelled between 220 – 350mm and could have changed speed significantly.

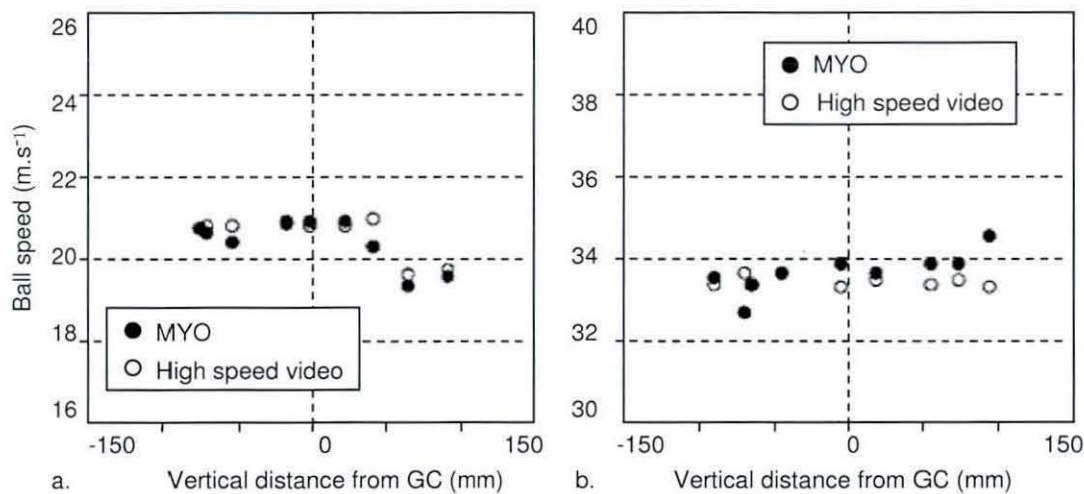


Figure 7.8: Comparing racket impact velocity measured by the machine with that measured with the high-speed camera at (a) 22m.s<sup>-1</sup> and (b) 35m.s<sup>-1</sup>.

The study also investigated the effect of different racket properties on the resulting impact speed by calculating and measuring the effect of gravity and air resistance on a TiS6 racket, and an ITF reference racket, which had a considerably higher MOI and smaller head size. The calculations revealed that for both rackets the decrease in racket speed due to gravity and air resistance were of a similar magnitude. It also indicated an insignificant difference of about 0.2m.s<sup>-1</sup> between the rackets, which is considerably smaller than the scatter in the machine's racket speed measurements ( $\sigma=1.0\text{m.s}^{-1}$ ). Theoretically, the decrease in speed could be determined more accurately through further investigations, although it was deemed unnecessary since only a few trial runs are usually needed for each racket to empirically realize the desired impact speed for the particular racket.

Another critical parameter for the machine's performance was the relation between the racket speed before and after impact, which is dependent on racket COR and the impact velocity. Determining the maximum possible loss in racket velocity would ensure the drive arm always braked fast enough to prevent a high-speed collision between it and the racket during, or after, the impact. A maximum reduction of ~50% in racket speed was estimated from the player tests described in §5.3. Calculations based on this assumption predicted that a



gap of at least  $40^\circ$  between the drive arm and the racket at impact should ensure no collision between them after the impact. This was validated by monitoring the reduction in racket velocity during the impacts across the racket face of low inertia rackets, which should be the most critical.

### 7.2.2 Maximum racket speed

Considerations for machine component and racket failures during the preliminary commissioning stages compelled the machine to be operated at the lowest possible impact speed. As the reliability of systems was improved the impact speeds were increased up to the  $50\text{m.s}^{-1}$ , as required by the design criteria. Unfortunately rackets are not designed for these operating conditions and started breaking regularly under the increasing impact loads. The failures occurred just above the gripping mechanism and this was partly attributed to the temporary IC-unit used during commissioning, which was more rigid than the original unit designed in §6.4.3. Failures occurred predominantly due to an extreme bending moment immediately above the grip, especially while testing the more modern light-weight rackets which have very thin walls because of the specific design intent to reduce weight. The findings again emphasised the complex hand/grip interaction of professional players. Previous research into common elbow injuries infer that a firm grip is maintained during the swing phase to affectively accelerate the racket, while it is relaxed during the impact without affecting the ball speed but minimising the impact on the arm. This could be why professionals rarely suffer from tennis elbow, which is linked to impact and vibrations transferred to the arm. During play, the arm and hand act as a perfect active dampening system, protecting the player from injury and rackets against mechanical failures, which was the intent of the original more flexible IC-unit which still needs to be tested and evaluated during future research.

With the safety measures incorporated into the system, the racket failures were harmless to the operator but were feared to be damaging to the robot's structural integrity. The machine was therefore only tested at speeds up to  $36\text{m.s}^{-1}$  during the remainder of the commissioning phase.

### 7.2.3 Minimum racket speed

During the constant speed stage, the machine possessed a minimum constant racket speed, where the effect of gravity on the racket assembly is large enough to separate the racket from the drive arm while moving "down-hill". This caused a variable racket speed during rotation, which complicated timing calculations, as well as introducing unnecessary collisions between the arm and the racket, shortening the lifespan of the components. The minimum speed was established at 175rpm, by monitoring the racket speed for several rackets and determining the threshold speed resulting in a smooth constant speed profile for the racket axis. This was coded into the software as the lowest set speed limit allowed by the machine under normal operation.

### 7.2.4 Control loops

In order to deal with the possible separation scenarios between the drive arm and the racket mechanism, two control loops were programmed (§6.4.8). The first allows the drive arm to catch up with the racket from the back after separation, while the braking loop closes the gap between the drive arm and the racket mechanism from the front of the racket during the braking procedure. During commissioning, the efficiency and reliability of the loops were fine-tuned with the assistance of a high-speed camera and dedicated monitoring of the component speeds by the Trio controller.

Initial attempts to use the direct speed measure from the encoders as inputs to the control loop were not optimal due to the spiky nature of the controller's standard speed measurement when monitored at the highest

possible sample rate, which is needed for a reliable control loop. As a substitute, moving averages of both axes' speeds were calculated in the high-speed loop of the Trio's POWERUP program (Appendix C). Figure 7.9 shows the difference between the filtered signal and the raw measured signal. The averaged speeds were used in both control loops and for exporting of velocities displayed in the visual *Graph* screen (Appendix C). As indicated in Figure 7.10 it is clear that after the impact the arm following the averaged signal responds quicker to close the gap between the racket and the arm than for the raw signal.

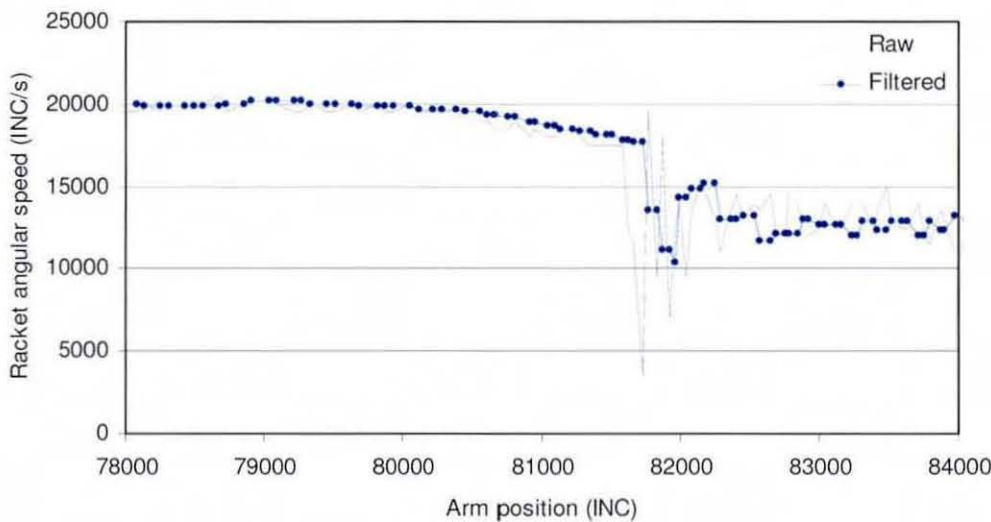


Figure 7.9: Velocity profiles of the drive arm and racket axis, demonstrating the effectiveness of the optimum control parameters.



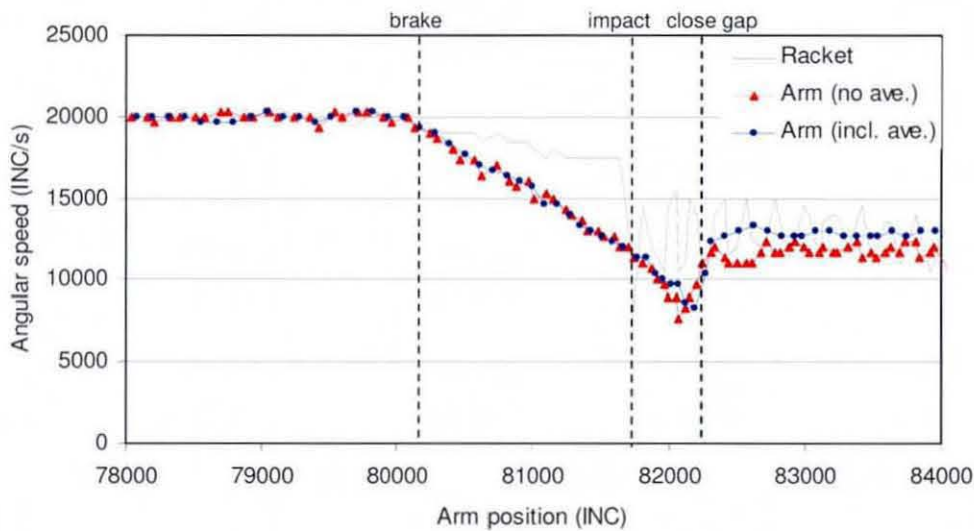


Figure 7.10: Velocity profiles indicating the difference between the direct velocities measured and the moving average calculated for implementation.

Both of the control loops are differential speed loops, with two parameters determining the response thereof; the differential constant and the motor's acceleration or deceleration constant. Initial parameters were developed with the use of a high-speed camera system, while further refinement of the parameters was performed by comparing measured profiles from both axes (Figure 7.10). The parameters were adjusted empirically in order to achieve the smoothest fit of the drive arm speed profile to the racket speed profile, resulting in a very stable system. During the commissioning phase, all speed measurements were performed using the Trio's internal units (INC) and in order to convert them into more familiar units a nominal impact radius of 700mm was used. This represented the radius to the GC of an average racket and was selected for calculating and comparing all head speed measurements until a more suitable method was found. The maximum angular speeds at which tests were performed therefore related to a head speed of  $\sim 30\text{m.s}^{-1}$ , which was not the maximum speed possible with the machine but no timing problems were anticipated at higher speeds.



### 7.2.5 Influence of the gripping condition

During most of the commissioning phase the machine was operated with a simple temporary IC-unit, as opposed to the more adaptive design presented in §6.4.3. The IC-unit is a very critical machine component, both structurally and functionally, therefore a more robust unit was used during the initial phases to minimise the risk of machine component failures, while its lack of compliance would also insure the racket's speed measurements, which were still being evaluated, were not being affected by relative motion between the racket and the unit. During the following stage, the preliminary unit was evaluated in order to determine its effect on the racket performance, which would assist in finding the optimum unit for permanent use in the machine. The tests performed during the independent evaluation (Goodwill, 2003), comprising of comparative rebound ball cannon tests, which provided the advantage of isolating the effect of the unit, not possible with the MPO itself. Tests were performed on two rackets; an ITF development racket (mass = 347g, swingweight = 335kg.cm<sup>2</sup>, balance 322mm), which is a typical tour racket, and a Ti.S6 (mass = 246g, swingweight = 301kg.cm<sup>2</sup>, balance 380mm), a recreational racket, the similar to those used during the main research.

The firsts set of tests was performed on the freely suspended development racket, with and without the preliminary IC-unit attached to it. The unit weighed 852g, with an inertia of ~24kg.cm<sup>2</sup> about the shaft axis, which was lighter than the 946g proposed by Casolo & Ruggieri (1991) to have the equivalent effect on the racket as the added inertia from the human hand and arm. Impacts were performed on different locations along the racket face as presented in Figure 7.11 (a)-(c). The results indicated that the unit had no significant influence on the ball rebound speed close the tip but that the influence increased for impacts closer to the throat, with the largest difference measured for the impact closest to the throat.

In order to relate the results from the ball-cannon to that achievable with the M $\Psi$ O, the ball speeds were transformed from a moving ball/stationary racket, to that of a stationary ball/moving racket frame of reference, as described in Appendix A. Since the results for the impact location closest to the throat had indicated the biggest difference for the ball-cannon setup (Figure 7.11c), only results for this location were compared in Figure 7.12, indicating no significant difference in the rebound ball speed, with or without the temporary IC-unit.

These comparative ball-cannon tests were only performed for the ITF development racket with a relatively low fundamental frequency and needed to be confirmed for lighter and stiffer rackets, which are more likely to be affected by gripping conditions. Therefore, rebound speeds from the ball-cannon tests for both freely suspended rackets were compared to their 'clamped' rebound speeds measured with the M $\Psi$ O. To do so, the measurements were normalised to the same impact speed via the translation of reference frames. The results are shown in Figure 7.13.

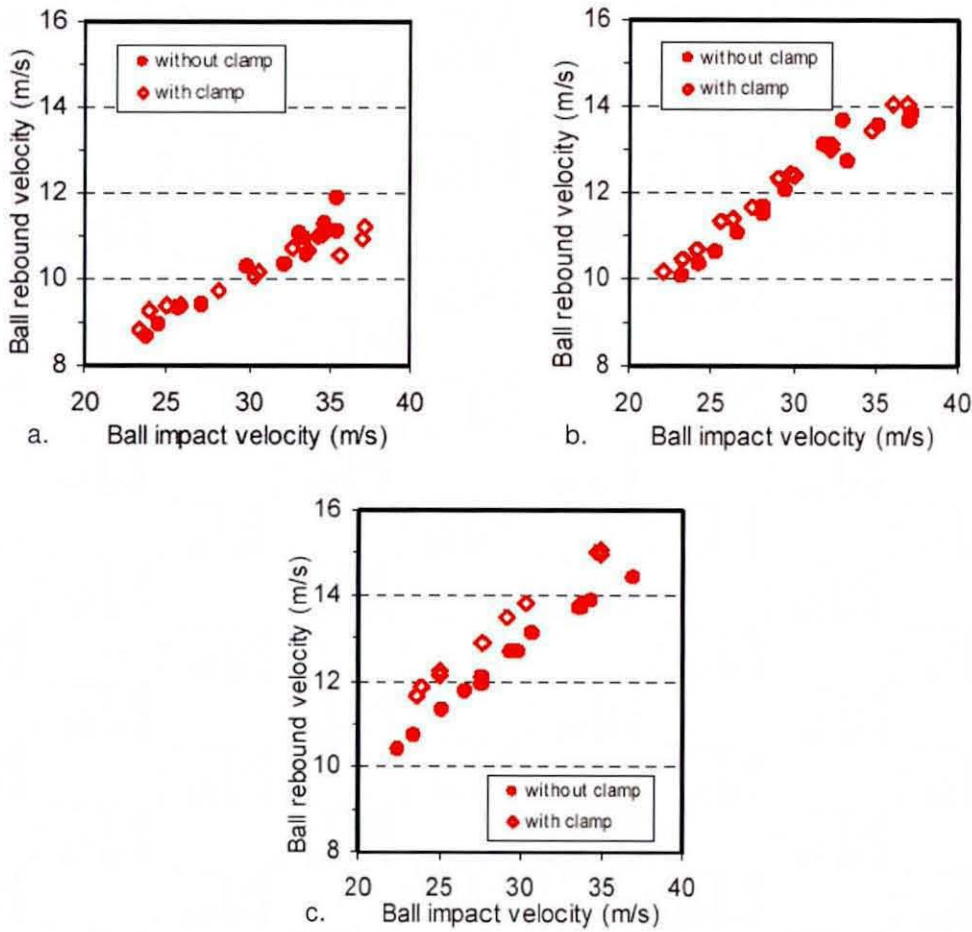


Figure 7.11: The ball-cannon rebound ball velocity vs. impact velocity, at discrete impact locations from the CG (a) 33mm, (b) -7mm and (c) -47mm.

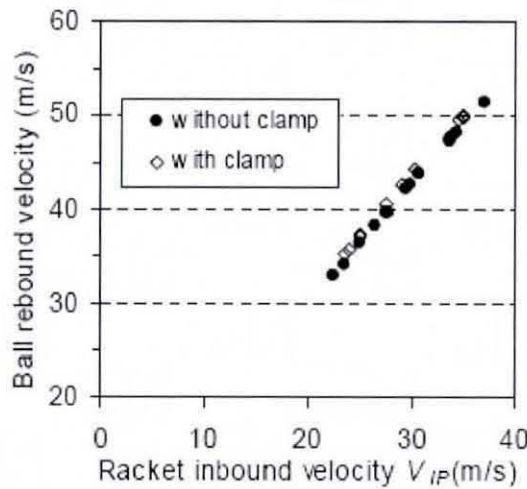


Figure 7.12: The transformed ball rebound velocities sampled by the ball-cannon versus the impact velocity (47mm below the GC).



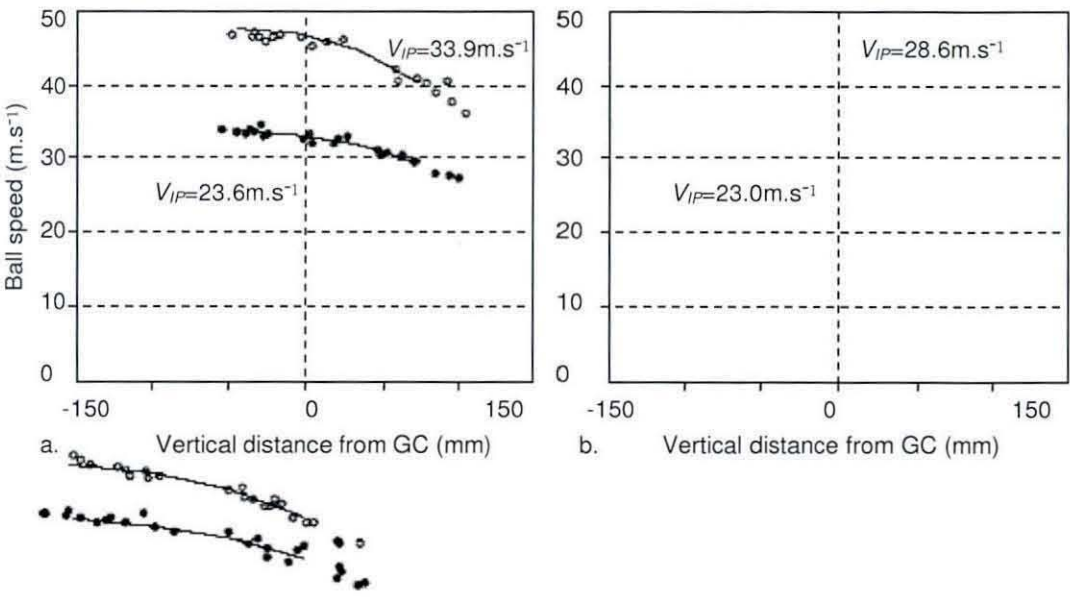


Figure 7.13: A normalised comparison of results obtained from MΨO (data points) and ball-cannon (solid line) tests the (a) ITF development racket and the (b) Head Ti.S6

The results revealed very similar values for measurements with and without the IC-unit, which was accepted by the independent investigators as sufficient evidence to prove the MΨO test was equivalent to the ball cannon test and that the provisional IC-unit had no significant influence on the ball rebound characteristics.

### 7.3 Initial racket performance testing

In order to demonstrate that the machine could be used effectively to investigate racket performance, three parameters were mapped for the control group of test rackets; the rebound ball speed, COR and ACOR. The rackets used were the same weighted Ti.S6 rackets (Rackets A-D) used during the ball-cannon and player testing described in Chapters 4 and 5, which also allowed a



comparison between these different test methods. The rackets were tested at an average nominal head speed of  $19.5\text{m.s}^{-1}$  measured about a radius of 700mm. A fear of racket failures at such a late stage of the research prompted the performance parameters to be compared at these relatively low impact speeds. For the same reason, rackets were not mapped across the entire racket face, since impacts close to the racket tip resulted in excessive bending moments in the racket grips. Lightweight rackets, in particular, were shown during the ball cannon testing in Chapter 4 to be relatively fragile. The rackets were clamped tightly in the provisional IC-unit via their standard grip material, while the unit was fixed in its neutral horizontal (130mm) and vertical (165mm) position. No additional mass was attached to the unit to provide the best possible simulation of the freely suspended condition. In order to compensate for the variance in the real impact speed, the measurements were all normalised to an average head speed of  $19.5\text{m.s}^{-1}$  at the nominal radius, by changing the frame of reference.

The rebound ball speeds presented in Figure 7.14, indicated a small but noticeable difference in maximum speed of about  $2\text{m.s}^{-1}$  (~7%) for the range of rackets measured, with the average peak location for all four rackets at about -10mm.

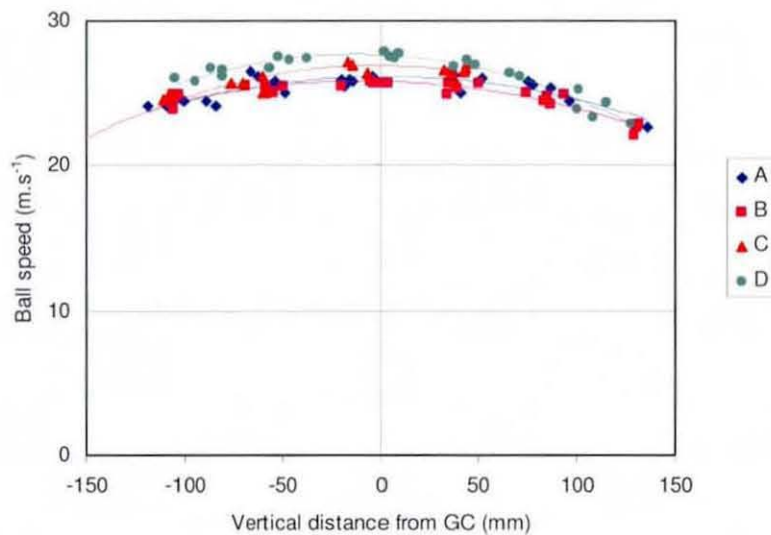


Figure 7.14: The rebound ball speed measured across the racket face of four Head Ti.S6 rackets adjusted to different moments of inertia (normalised for  $19.5\text{m.s}^{-1}$  at a nominal radius of  $700\text{mm}$ ).

This was virtually identical to the  $-12\text{mm}$  predicted in Figure 5.18, which was obtained by combining the average angular speeds and ICR locations from the play tests (§5.3) with the rebound characteristic from the freely suspended tests in §4.3.1. Comparing the maximum ball speeds with that predicted in §5.4 (Figure 5.18) by first transforming the results to an impact speed of  $19.5\text{m.s}^{-1}$ , yielded a peak ball speeds of  $\sim 10\%$  lower than the measured with the M $\Psi$ O.

Next, the M $\Psi$ O's  $\text{COR}_s$  and  $\text{ACOR}_s$  results were calculated and presented in Figure 7.15 and Figure 7.16 respectively.

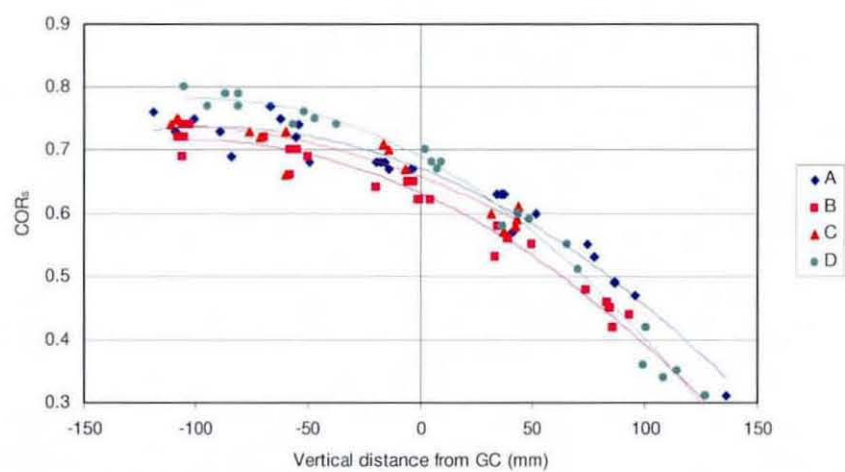


Figure 7.15: The COR<sub>s</sub> measured across the racket face of four Head Ti.S6 rackets with adjusted moments of inertia.

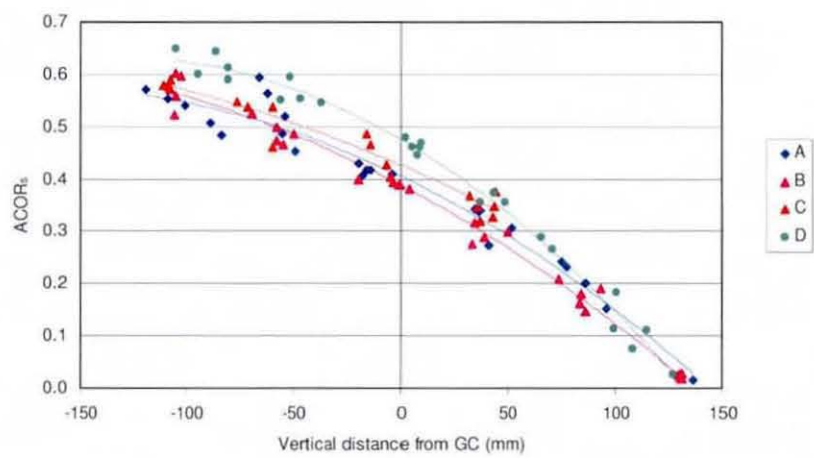


Figure 7.16: The ACOR<sub>s</sub> measured across the racket face of four Head Ti.S6 rackets with adjusted moments of inertia.

There was a noticeable increase (~8%) in COR<sub>s</sub>, for the 12% increase in racket swingweight, although, the COR<sub>s</sub> should theoretically be the same for all four rackets, since by definition it is independent of mass and MOI. The results for the ACOR<sub>s</sub> in Figure 7.16 displayed an increase of ~7%, which agrees with standard theory.

Compared to the stationary racket rebound tests performed in §4.3 (Figure 4.15 and Figure 4.17), the MΨO's peak COR<sub>s</sub> results for all the rackets are about 11% lower while the ACOR<sub>s</sub> is about ~16% higher. This is believed to be a result



of the additional constraint added by the inertia and clamping of preliminary IC-unit. If the added constraint is sufficiently rigid and close enough to the impact for the impulse to return to the ball while it is still on the face, it would increase the balls speed and therefore the ACOR<sub>s</sub>, while the additional inertia at the same time would prevent the racket from slowing down as much after the impact, which would decrease the COR<sub>s</sub>. This conjecture is substantiated by the ~10% increase in the maximum rebound ball speed when compared to that from the freely suspended results calculated in §5.4, as mentioned previously in this section. The conjecture was supported further by the shift in the location of the peaks of both the COR<sub>s</sub> and ACOR<sub>s</sub> measurements towards the throat. For impact locations approaching the constraint, the increase in racket stiffness shortens the distance the impulse wave needs to travel in order to reach the ball in time to increase the ball speed. It is therefore postulated that for the stiffer, light-weight rackets the added inertia from the temporary IC-unit would have a significant effect on the COR<sub>s</sub> and ACOR<sub>s</sub> measurements close to the throat, when compared to freely suspended testing.

It is suspected that the ITF investigation (Goodwill, 2003) did not indicate an effect of this magnitude, since the investigator only directly compared ball-cannon measurements with and without the MΨO clamp for the heavier, more flexible reference racket, which should be less sensitive to changes in the gripping condition. The comparison of the Ti.S6 racket using the MΨO only measured a relatively small area of the racket face, and only as low as 47mm below the GC, which is still relatively far from the racket throat where the difference with the MΨO results became apparent.

The increase in the MΨO's rebound ball speeds, compared to the freely suspended results, is believed to be representative of a real serve, since the mass and inertia of the IC-unit have been shown to be representative of a real human hand and arm. Although, substituting the rigid unit with the more compliant version developed in §6.4.3 should provide even more realistic results.



In order to further demonstrate the effective use of the machine to investigate racket performance, the test results for rackets tested at different impact speeds were requested from the ITF. Results for two unknown rackets with very similar properties were provided, showing mappings at impact speeds of 25, 30 and 35m.s<sup>-1</sup>, as presented in Figure 7.17.

According to the literature, there should be a small but noticeable decrease in COR<sub>s</sub> and ACOR<sub>s</sub> for a significant increase in impact speed (Goodwill and Haake 2004, Brody 1997). This is clear from the results, with the biggest difference between the impact speeds being for Racket K, Figure 7.17b, with a significantly higher COR<sub>s</sub> at the lowest impact speed of 25m.s<sup>-1</sup>. In order to explain this comparatively large difference, the racket properties presented in Table 7.1, were investigated in more detail.

Nr	Mass [g]	MOI [kg.cm <sup>2</sup> ]	Balance [mm]	Frame stiffness	Stringbed stiffness	String tension [N]	Length [mm]	Head length [mm]	Head width [mm]	Head size [cm <sup>2</sup> ]
J.	300	307	330	61	65	267	680	340	260	632
K.	308	321	334	58	75	267	690	340	260	613

Table 7.1: The properties measured for each test racket on the Babolat RDC.

Racket K had almost identical properties to Racket J, with a slightly higher mass, MOI and balance, and noticeably lower frame stiffness, while the only significantly difference was its higher stringbed stiffness. By definition the COR<sub>s</sub> is independent of mass, MOI and balance, while frame and string deformation should be strain rate dependent, possibly lowering the COR<sub>s</sub> at higher impact speeds. The higher stringbed stiffness will have the opposite effect though, since the dwell time is less influenced by impact speed at high string tensions (Brody 1987), meaning Racket J would display the biggest difference in COR<sub>s</sub>. Therefore, the larger difference in COR<sub>s</sub> for Racket K is attributed to its lower frame stiffness, which would considerably increase frame bending under high impact speeds, hence increasing the energy losses to the frame, resulting in a significant decrease in COR<sub>s</sub>.

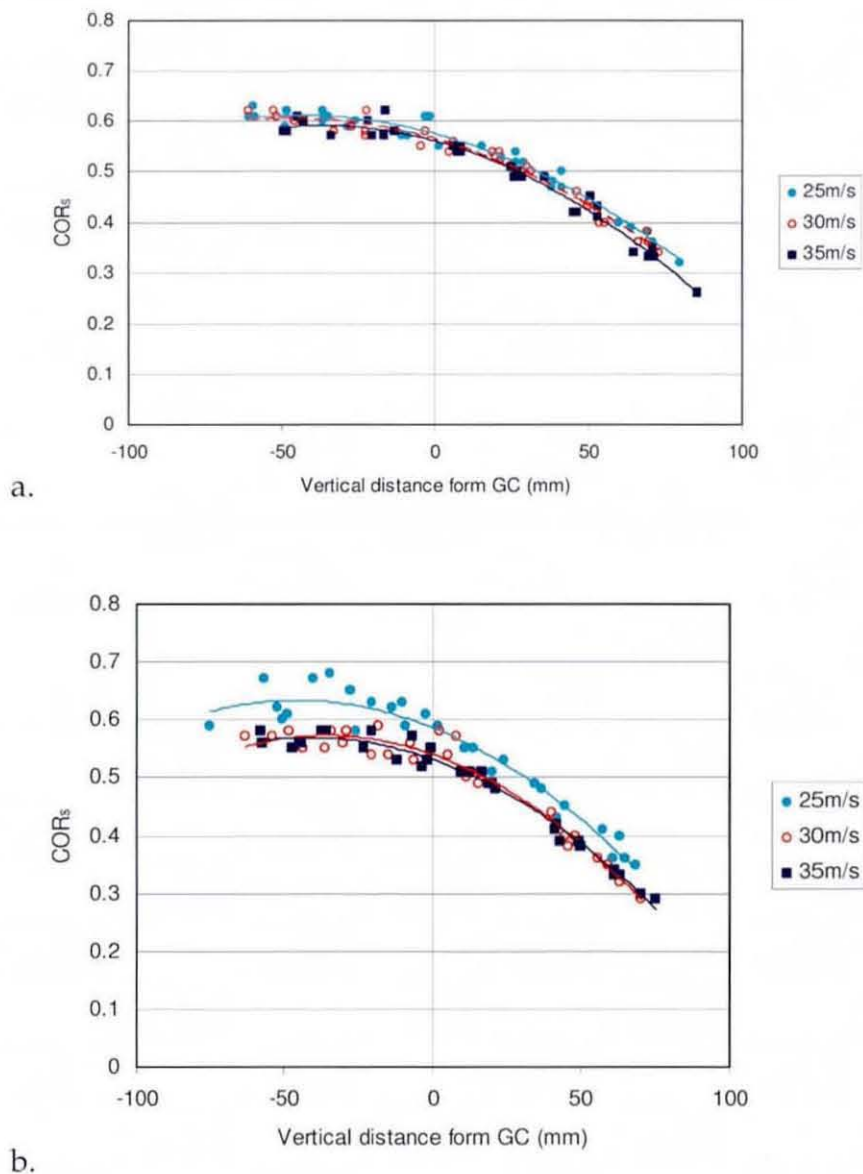


Figure 7.17: The COR<sub>s</sub> measured for two unknown racket models at different nominal impact speeds; (a.) Racket J, (b.) Racket K.

In conclusion, the MΨO's performance testing indicated its use as a research tool for investigating racket rebound characteristics. Results were shown to compare well with the rebound measurements performed with the more commonly used ball-cannon, providing the impact and clamping conditions are the same. The small differences between the freely suspended ball-cannon and MΨO results are believed to be a result of the machine's more realistic gripping unit, although combining further player testing with experimental MΨO results using the original adaptable version of the IC-unit,

are needed to find the optimum compliance providing the most realistic representation of a serve. The machine has been shown to be unique and provide results with acceptable accuracies and performance, with the main advantages over conventional methods being the realistic racket and ball presentation during the impact and the facility for automation. Throughout the commissioning process, areas of improvement or further investigation have been identified and will be discussed in the next section.

### 7.4 Machine modifications

During the ITF's commissioning of the machine, some improvements were made to enhance stability and functionality.

#### *Impact location speed normalisation*

As mentioned in §6.4.8, the impact speed for the machine was specified as the speed at a constant radius in order to have a standard for comparing results between rackets. As a research tool though, the ITF developed the need for comparing results with other similar test methods, which often had different impact frames of reference. A feature was therefore added to the software, which gave the operator the option to perform the tests at the same impact speed across the racket face, instead of having to normalise all the results afterwards.

#### *Flexible IC-unit*

In an attempt to eliminate racket failures at high impact speeds and to investigate another gripping mechanism, a more flexible IC-unit was developed. The flexibility was achieved by means of four spring-loaded clamp screws as indicated in Figure 7.18 at the cost of a weight increase of about 0.2kg. The unit has been used successfully by the ITF, proving that increased compliance in the gripping unit is needed to decrease racket failures. This unit



was claimed not to influence the rebound results but no supporting data was provided.

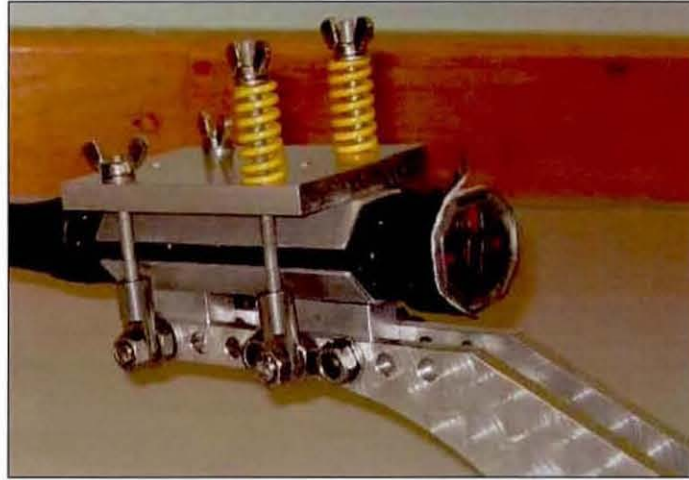


Figure 7.18: The modified IC-unit adding flexibility to the grip.

## 7.5 Proposed machine improvements

Based on the experience gained during the commissioning procedure, the following improvements to the machine are proposed.

### ***Ball speed measurement accuracy***

The accuracy of the post impact ball speed measurement had been verified during commissioning but the ITF investigators pointed out that this velocity is not measured immediately after impact. With the current set-up it is not possible to move the measurement closer to the impact region since it would have to be within the racket's rotational envelope. A possible solution is to extrapolate the current measurement to the racket face, since the ball deceleration should be predictable using standard ball flight models. If a more direct measure is desired it might be possible to move the lasers closer to the impact region. This would necessitate the laser arrangement being converted to a horizontal arrangement, rather than current vertical arrangement, or having a much bigger curtain stretch from the roof to the floor of the cage. Both these solutions would introduce various complications, such as laser misalignment,



racket interference and the lasers obstructing the view of other possible test equipment such as high-speed cameras. Consequently extrapolating the current ball speed measurement is proposed as the simplest and most reliable solution.

### *Ball speed measurement reliability*

During commissioning there were some reliability issues with the ball speed measurements. This was mainly related to interfering signals triggering the timers at the wrong instance and impact vibrations causing misalignment of the laser beams, which resulted in a false trigger. Although most of these problems were eliminated during commissioning, the system could be made more tolerant of changes in the environment such as, a significant change in ambient light affecting the photo detector sensitivity, an increase in racket speed or new equipment with high electrical emissions operating in the vicinity of the machine. The best solution against mechanical vibrations would be to completely isolate the speed measurement unit from the cage, such that no vibrations can be transmitted to it. To improve the sensitivity of the laser unit the most effective solution would be to create the laser curtain with a number of individual lasers, with a photo detector each, rather than the current reflected laser curtain. These individual laser beam would provides a signal when any of them are cut by the ball.

### *Racket speed prediction*

The most significant and unfortunate inherent disadvantage of the machine design is the fact that the racket does not impact the ball at the set impact velocity. This is a result of the racket not being driven during the last half rotation, during which time it is slowed down by gravity and air resistance. This was highlighted by the ITF investigators as one of the machine's few shortcomings, since the set speed resulting in the desired impact speeds needs to be determined empirically for different rackets and impact speeds. This loss in speed is smaller at higher speeds, since the gravitational deceleration is

smaller in comparison, which means operating the machine at relatively high speeds improves the situation but for a more effective solution the ITF proposal is viewed as a step in the right direction. Their approach entailed determining the relation between set speed and real head speed for different racket properties, which could be programmed into the MPO software.

A related drawback in the current system, the inconsistency in the impact speed, had also been indicated as a concern. The variation of  $1\text{m.s}^{-1}$  at lower speeds is perceived as too high, since investigations indicated most impact parameters to be dependent on the racket speed. The main reason for the variance is assumed to be the fluctuation in racket speeds during the acceleration and constant speed stages. A relatively small change in loading could result in separation between the drive arm's cross bar and the racket, which are both highly elastic. This introduced a bouncing motion between the two components, which only settled down after a few rotations of the drive arm moving at a relatively high constant speed. Therefore, proposed changes to improve the racket speed accuracy included operating the machine at relatively high speeds, changing the machine drive's control parameters or increasing the number of rotations of the machine during the 'constant' speed stage.

### ***Ball dropper consistency***

Although any ball dropper inconsistency should be accounted for by measuring the actual impact location, a more consistent dropper would increase test effectiveness. The major cause of existing inconsistencies is believed to be the variability of the solenoid combined with mechanical friction. The selection of a linear solenoid, as opposed to a rotational solenoid, as the dropper actuator was strongly influenced by the author's familiarity with linear solenoids. Having a single actuator was also favoured, since it would reduce components and simplify control. In retrospect, it might have been beneficial to use a rotational solenoid, since the dropper action is mainly a rotation of the 'trap



door', which was problematic with the power and stroke limitations of the linear solenoid.

### *Gripping issues*

Throughout the literature there are inconsistencies regarding the influence of different gripping conditions on racket performance. Hence, one of the main motivations for the features of the current machine was to allow the testing of different gripping conditions. With the current design, two issues relating to the gripping arose; the first is the failure of rackets at high speeds and the second is that the set-up does not seem to satisfactorily represent the free-free condition. Both of these are believed to be a result of the rigid clamping used during the commissioning phase, which was needed in order to ensure the structural integrity of the machine. Since confidence in the machine's performance has been established, experimentation with the more adaptive IC-unit can commence, in order to eliminate these restrictions.

The effect of the human hand and arm on the racket rebound characteristics is still mostly unexplored, mainly due to the inability of traditional measurement systems to accurately measure parameters during play, without disturbing the players. The accuracy and size of such motion acquisition devices have improved considerably over the last few years, opening new ways of investigation. It is therefore proposed that similar testing to that performed in Chapter 5 could be combined with more accurate ball speed measurement systems, such as the EDH radar and Hawkeye camera, in order to resolve the effect of the arm and hand on the racket performance during play, which should be used to determine the most realistic gripping mechanism to ensure the best machine performance.

## Chapter 8

### Conclusions and Recommendations

The research was initiated by the ITF, with the ultimate goal of developing a racket 'power' standard, which could be implemented as a new regulation. The aim of the regulation is to focus on slowing down the serve in the game of tennis, which is believed to have changed the nature of the game over the last decade and has the potential to change it even further in future, to the point where tennis may lose its popularity as a spectator sport. The research included a thorough investigation of the available literature on the subject resulting in a publication, which for the first time tied all the research together while exploring similarities, and inconsistencies and highlighting gaps for further research. This was followed by a series of racket rebound and player tests, in order to determine the specifications needed to develop a test machine, which could be used to investigate racket rebound characteristics.

#### 8.1 Ball cannon tests

##### 8.1.1 Racket rebound measurements for modern rackets

The rebound tests performed on the set of test rackets provided the expected properties for these rackets at representative serve speeds. The rackets used included very modern rackets, with very stiff and lightweight frame constructions, for which insufficient data was available. This was especially important, with the focus of the research aimed at the influence of modern technology on the game. Maximum  $COR_f$  and  $ACOR_f$  values of 0.50 and 0.89,



were noticeably higher than those previously measured by researchers. The results also confirmed common theories such as the racket's COR being independent of the racket inertial properties, while it is not the case for its ACOR. An increase of 21% in MOI resulted in an increase of 23.6% in the maximum ACOR. To the author's knowledge, no data had been published on the accuracies of current test methods, therefore the rebound results from the ball cannon tests were used to determine the desired accuracies to be achieved by the test machine. The ball cannon yielded ball impact speeds with a standard deviation of  $1.8\text{m.s}^{-1}$  for all impacts, and a standard deviation of  $0.35\text{m.s}^{-1}$  for the ball speed measurements at discrete impact locations, while the maximum tolerance calculated for the impact location was  $\pm 5\text{mm}$  in the horizontal and  $\pm 22\text{mm}$  in the vertical direction. The rebound measurements for the individual test rackets also provided an important comparison later during the machine's commissioning.

### 8.1.2 Grip compliance

Due to the racket failures during the rebound tests on the rigidly clamped and head clamped racket, it was apparent that it would not be possible to test current lightweight rackets under these 'abnormal' gripping conditions and at representative serve speeds. Modern racket designs are optimised with the intent of withstanding impacts during play, whilst being extremely light. When subjected to abnormal constraints by different clamping conditions, atypical stresses are exerted on the frame, leading to failure. After conferring with other researchers, the same phenomenon was found to have occurred but it had not been documented before. These failures would later significantly affect the design of the test machine, since similar failures had to be avoided, while still providing sufficient adaptability to enable further investigation of the gripping condition's effect on racket rebound characteristics. During follow-up research, this ability to simulate a wide range of gripping conditions will allow the

evaluation of various gripping mechanisms, in order to find the most realistic representation to be used in the final test standard.

### 8.2 Player motion tests

#### 8.2.1 Racket head speed

During player tests, the 3-dimensional racket motion was recorded for the serve. The method used was considerably more comprehensive than conventional methods at the time, allowing an in-depth analysis previously not possible. The rackets were fitted with active markers, which were tracked by special strategically placed motion cameras with an accuracy of up to 0.1mm and at 800Hz. A typical velocity profile was analysed to provide the desired motion profile to be achieved by the developed test machine. Features of interest included the maximum head speed, the state of the racket's angular acceleration just before impact and the deceleration rate of the racket during the impact.

The maximum head speed recorded for the males tested varied between 31-42m.s<sup>-1</sup> and between 27-31m.s<sup>-1</sup> for the females. For the machine to fulfil its ultimate goal, which is to implement a fair racket performance standard. Therefore the relation between racket MOI and the maximum achievable head speed during play should be used to determine the head speed at which a particular racket should be tested. As a result, the influence of racket MOI on the maximum head speed was determined during a serve, for the first time. This was achieved by selecting the lightest racket on the market at the time and adding mass in the form of lead tape in the racket throat area. In so doing, the MOI was increased incrementally to cover the range of commercially available rackets at the time. An average decrease in head speed of 5.8% for the impact location was measured for a 21% increase in MOI. The constants for a linear and an inversely proportional equation describing this relation were calculated,



which needs further investigation in order to select the preferred candidate for future testing.

Results did not indicate a deceleration in the head speed before the impact, as suggested by the literature but rather a peak or a constant speed at the onset of the impact. This was believed to be a result of the higher sample rate used for the measurements. The results did indicate though that the racket was not driven through the impact, which considerably simplified the design of the test machine.

The racket deceleration for the hand held racket during play was measured at up to  $\sim 5000\text{m.s}^{-2}$ , resulting in loss of almost 50% of maximum head speed during an impact of about 5ms. This was useful during the development of the machine, in order to avoid a collision between the separating components during the impact.

### 8.2.2 Location of the ICR

Having established that a constant racket angular speed is sufficient to reproduce the serve conditions, the location of the ICR needed to be determined from the player tests. To the knowledge of the author, the identification of the ICR during real serve conditions was the first work ever published on this subject. The results revealed that skilled players displayed a very consistent ICR location, independent of the racket properties, and that the locations for individual players were in the same region relative to the racket. The average ICR location for the players was determined at between 34-122mm below and 1-111mm behind the racket butt in the racket frame of reference. This provided the dimensions needed for developing the machine's IC-unit, which was designed to be adjustable over a sensible range for the ICR, thus allowing investigation of its influence on racket performance.

### 8.2.3 Impact location

During player testing, the impact location of the ball on the strings during serve was also determined and, for the first time, the relationships with common performance measurements obtained from other static and dynamic tests were determined and documented for the same set of rackets. The racket's stringing surface was covered with ink, which rubbed off during contact with the ball, leaving an imprint of the average impact location after the set of serves. Impact locations were found to be extremely consistent for the level of players tested. For first and second team university players a variation of only ~50mm in both the vertical and horizontal directions was recorded. The average impact location was located 30mm above the face centre and 15mm towards the inside of the racket face. The fact that the resulting impacts were so close to the racket centre-line for all players led to the omission of racket polar rotation in the machine design, simplifying it to a single axis rotation mechanism. A combination of the results for the same set of test rackets subjected to static vibration measurements, ball-cannon tests and player tests, provided exclusive tangible evidence for describing the relationship between the rebound measurements from these different conventional test methods. The vertical location of the 'sweet spot' used by the players was located near the location of the upper node for the fundamental vibration mode, which provides a significant link for sensibly translating a racket's laboratory measurements to its performance on court.

### 8.3 Developed machine

A unique machine (called M $\Psi$ O) was developed to test and investigate the influence of different racket and swing parameters on racket performance. The machine uses a distinctive drive arm mechanism which is decoupled from the racket at impact, thus allowing the gripping condition to be varied from the



## CHAPTER 8 CONCLUSIONS AND RECOMMENDATIONS

virtually free gripping condition to the fully clamped condition. The machine is the first of its kind to have high enough adaptability and accuracy to allow a thorough investigation of racket parameters at representative serve speeds under realistic serve conditions. Balls were presented to the racket face with an appreciable vertical speed, in order to realistically simulate the vertical movement across the racket face during a serve.

Since its commissioning, the MΨO has since been successfully employed by the ITF for investigating various racket performance parameters, during which time some minor changes were made in collaboration with the author. The machine's accuracy and consistency were tested in an independent investigation, performed by an ITF investigator in 2003, who reported the design to be satisfactory for the purpose it was developed. The machine provides a unique compromise between realism and accuracy, which should assist its acceptance by most stakeholders such as the manufacturers, tennis players and the general public.

### 8.3.1 Proposed machine alterations

The design specifications demanded a machine which could swing rackets at the same speed as the fastest recorded serve, which was estimated at  $\sim 50\text{m.s}^{-1}$ , using an  $\text{ACOR}_t$  value of 0.4. This was the peak value measured during the freely suspended testing described in §4.3.2, for Racket G which represented a typical tour racket, as used by professionals to achieve these record serve speeds. Operating the MΨO at these impact speeds with the rigid IC-unit used during the commissioning stage resulted in numerous racket failures to the extent that both the author and the ITF investigators opted to perform the majority of the remaining performance testing at lower impact speeds ranging between about  $20\text{-}35\text{m.s}^{-1}$ .

The rigid IC-unit used during the evaluation was a temporary solution introduced to assist the development and commissioning of the MΨO. The unit

## *CHAPTER 8 CONCLUSIONS AND RECOMMENDATIONS*

has a representative mass and inertia of a real human hand and arm, but its rigidity had been shown to cause racket failures, and influence the COR<sub>s</sub> and ACOR<sub>s</sub> measurements for the light-weight rackets when compared to freely suspended results. The unit should be replaced with the adaptive version originally intended for testing, which allows adaptability of the gripping compliance. Using the MPO for its intended purpose, the influence of various gripping variables on the racket rebound characteristics should be investigated, as described in the following section, in order to find the most realistic gripping condition.

The consistency of the ball dropping mechanism was critical to the machine's accuracy; hence a minimalist approach was taken in its design, which included the incorporation of a single solenoid as the actuator for three functions. This unique design was very effective but sensitive to the inconsistencies and limitations of available linear solenoids and could therefore be improved by replacing the linear solenoid with a rotary solenoid, which should be more suited to the natural rotary motion of the trapdoor. Another consideration could be to add another solenoid to replace the blocking function, which would reduce the forces acting on the trapdoor, hence improving the accuracy of the mechanism. A secondary advantage of reducing the solenoid's power requirements would be to reduce the magnetic noise from the current high-powered solenoid, which is one main cause of interference with the ball speed measurements. Alternatively, other more powerful forms of actuation, such as pneumatics or hydraulics, could also be considered for the consistency.

Another critical measurement contributing to the machine's accuracy is the ball speed measurement. The current system is still relatively sensitive to mechanical vibrations causing false triggers at high-speed impacts, for which the most effective solution would be to separate the measurement unit completely from the main cage, in order to eliminate the transfer of any vibrations. Another disadvantage of the unit, pointed out by the ITF

investigator was that the current measurement unit placed outside the racket's hitting envelope allows the ball to slow down noticeably from immediately after the impact to the location of the light gates, resulting in ~1% lower ball speeds. The easiest solution would be to extrapolate the speed measurement using common flight models and experimental validation, while a more extensive solution would be to replace the vertical laser curtains with horizontal curtains, which could be placed on either side of the racket without interfering with the racket envelope.

### 8.4 Proposed machine test protocol

Concluding this research, the following test protocol is proposed in order to effectively use the MPO to establish a sensible and realistic 'power' factor, which could be implemented to contain the speed of the serve in the modern game.

The first objective of future research should be to find the optimal gripping condition to be incorporated in the test machine. The gripping mechanism should be functional for repeated testing and produce results representative of a real serve. Currently the machine has been tested with two different gripping configurations; a lightweight rigid construction and a heavier more compliant one. The temporary rigid construction has been shown to have some influence on the racket's rebound performance, when compared to the freely suspended ball cannon tests and tends to break rackets at high impact speeds, while the heavier construction is more forgiving but the influence of its higher mass has not been determined. These units should be substituted with the original mechanism developed in §6.4.3, which was designed to allow adaptability of the grip force, grip compliance and added inertia, enabling a wide range of conditions to be tested and compared to that of a real human grip during a serve.

## CHAPTER 8 CONCLUSIONS AND RECOMMENDATIONS

To this end, a benchmark would have to be determined against which the proposed racket performance indicators could be correlated. A set of player tests similar to those performed in Chapter 5 is therefore proposed, during which the racket speed before and after impact are measured, but with the addition of an accurate measurement of the ball speed. A motion tracking system, such as the CODA, or accelerometers could be used to measure the racket speeds, while newly developed ball tracking systems, such as the EDH radar or Hawkeye camera system, could be used to accurately determine the ball speed immediately after leaving the racket face. The impact location for each impact can be determined by the method used in §5.4 or via the more extensive capacitance method employed by Hennig & Schnabel (1998). Measuring these parameters for a group of skilled players (preferably tour players) subjected to a similar test protocol used in §5.3 while serving with a carefully selected range of rackets would provide realistic rebound data, which should be used as a benchmark for comparing the M<sub>YO</sub>'s gripping configurations. As indicated during the machine's commissioning, the maximum values and peak locations for at least the ball rebound speeds, ACOR and COR measurements should be compared at the same impact speeds. For tests at different impact speeds, the results should be converted to a nominal impact speed by adjusting the speed of the reference planes, similar to the method used for transferring from the global to the racket reference frame, as described in Appendix A.

The rebound results from the play test should also establish a speed ranking for all the rackets, which will be used to evaluate the potential 'power' definitions to be tested with the machine. The rebound parameters for the same set of rackets should therefore be mapped in the M<sub>YO</sub> at the appropriate impact speed calculated from its relationship to the MOI of each racket, as determined in Chapter 5. The rackets should all be ranked according to the



## *CHAPTER 8 CONCLUSIONS AND RECOMMENDATIONS*

different 'power' indicators, with the indicator providing the closest match to the ranking from the player testing forming the basis of the final test standard.

The selected indicator should be measured for all ITF approved rackets expected to produce high serve speeds in order to recommend an upper limit to which all newly submitted rackets should adhere before they can be used in official tournaments.

It is hoped that as a result the new knowledge gained from this research and the use of the developed test machine will contribute to the research community's understanding of racket performance in general, as well as provide a tool for regulating the modern game of tennis in such a way that the future of the sport would be protected.

# Appendix A

## Rebound definitions

## A.1. Deriving the COR

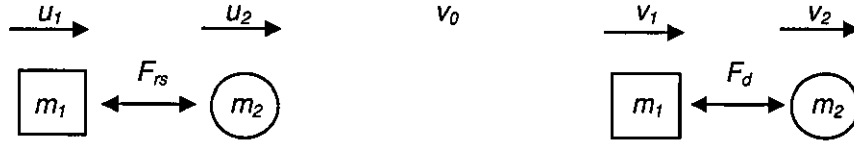


Figure A.1: Diagram illustrating the collision between two moving bodies

For two colliding bodies as shown in Figure A.1, the coefficient of restitution is given by Equation A.1 as the ratio between the reaction impulses during the deformation and restoration stages of the impact:

$$COR = \frac{\int_{t_0}^t F_{rs} dt}{\int_0^{t_0} F_d dt} \quad (A.1)$$

During the transition from the deformation to restoration, at  $t=t_0$ , both masses have the same velocity  $v_0$  and since the impulse integral  $\int F dt = m \cdot \Delta v$ , the COR for  $m_1$  can be written as:

$$COR = \frac{m_1 (-v_1 - (-v_0))}{m_1 (-v_0 - (-u_1))} = \frac{v_0 - v_1}{u_1 - v_0} \quad (A.2)$$

Equally, the COR for  $m_2$  is given as:

$$COR = \frac{v_2 - v_0}{v_0 - u_2} \quad (A.3)$$

Rewriting Equations (A.2) and (A.3) in terms of  $v_0$  gave:

$$v_0 = \frac{v_2 + u_2 \cdot COR}{1 + COR} = \frac{v_1 + u_1 \cdot COR}{1 + COR} \quad (A.4)$$

which reveals COR as:

$$COR = \frac{v_2 - v_1}{u_1 - u_2} \quad (A.5)$$

the ratio of the relative velocity after the impact to the relative velocity before the impact.

## A.2. Changing reference frames

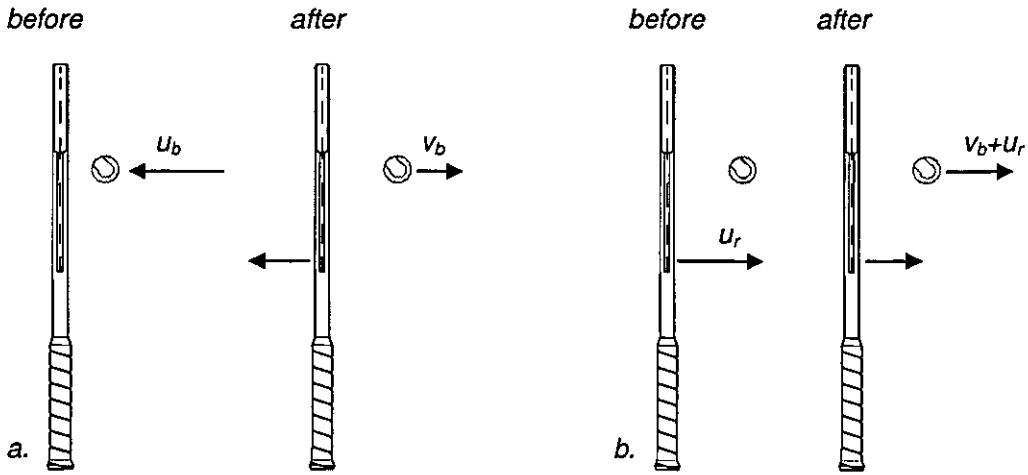


Figure A.2: Impact conditions for (a) a moving ball/stationary racket set-up and (b) a moving racket/stationary ball set-up.

For the moving ball/stationary racket scenario illustrated in Figure A.2(a), the racket speed  $u_r$  equal to zero, Equation 3.4 is rewritten as:

$$ACOR' = \frac{v_b}{u_b} \quad (A.6)$$

If one wants to use the results to predict the ball rebound speed for the moving racket/stationary ball scenario as illustrated in Figure A.2(b), the frame of reference needs to be changed from the global frame to that of the racket. This means the equivalent in relation to the racket frame is given by subtracting the



racket speed ( $u_r$ ) from the ball inbound speed before the impact, which is zero, and adding to the ball speed after the impact, yielding:

$$ACOR'' = \frac{v_b + u_r}{u_r} \quad (A.7)$$

with  $u_r$  in Figure A.2(b) being equal to  $u_b$  in Figure A.2(a) giving:

$$ACOR'' = \frac{v_b}{u_b} + 1 \quad (A.8)$$

$$ACOR'' = ACOR' + 1 \quad (A.9)$$

### A.3. Relating ACOR to COR

In order to relate ACOR to COR for the stationary racket/moving ball test set-up Figure A.1 and Equation A.5 is adapted by setting the initial racket speed  $u_1=0$  and the initial ball speed  $u_2=-u_b$  as demonstrated in Figure A.3 and Equation A.10.



Figure A.3: The collision between a moving and stationary body.

$$v_r = v_b - u_b \cdot COR \quad (A.10)$$

while the conservation of linear momentum for the impact yields:

$$-m_b u_b = m_r v_r + m_b v_b \quad (A.11)$$

Combining Equations A.10 and A.11 gives:

$$-m_b u_b = m_r (v_b - u_b \cdot COR) \quad (A.12)$$

which can be rewritten in terms of  $v_b$ :

$$v_b = \frac{u_b (m_r \cdot COR - m_b)}{m_r + m_b} \quad (\text{A.13})$$

Rewriting Equation A.6 yields:

$$ACOR = \frac{v_b}{u_b} \quad (\text{A.14})$$

and substituting Equation A.12 provides the relation between the ACOR and the COR as:

$$ACOR = \frac{m_r \cdot COR - m_b}{m_r + m_b} \quad (\text{A.15})$$

#### A.4. Deriving the effective mass

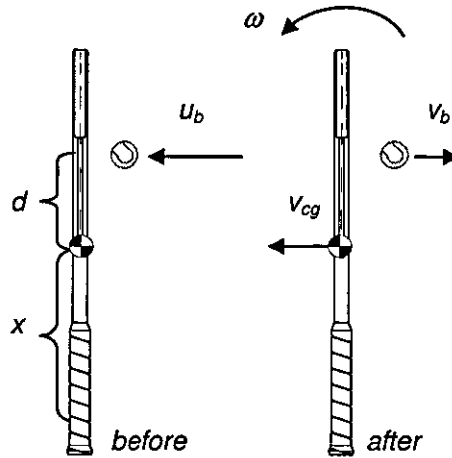


Figure A.4: Impact conditions for a moving ball/stationary racket set-up.

Considering the impact scenario in Figure A.4 the conservation laws for linear and angular momentum as well as kinetic energy are given by:

$$m_b u_b = m_r v_{cg} - m_b v_b \quad (\text{A.16})$$

$$m_b u_b d = I_{cg} \varpi - m_b v_b d \quad (\text{A.17})$$

$$\frac{1}{2} m_b u_b^2 = \frac{1}{2} m_b v_b^2 + \frac{1}{2} m_r v_{cg}^2 + \frac{1}{2} I_{cg} \varpi^2 \quad (\text{A.18})$$

Equations A.16 and A.17 can be rewritten as:

$$v_{cg} = (u_b + v_b) m_b / m_r \quad (\text{A.19})$$

$$\varpi = (u_b + v_b) m_b d / I_{cg} \quad (\text{A.20})$$

Substituting Equations A.19 and A.20 into A.18 yields:

$$u_b^2 = v_b^2 + m_b \left( 1/m_r + d^2/I_{cg} \right) (u_b + v_b)^2 \quad (\text{A.21})$$

At the 'dead spot' the ball mass is equal to the effective racket mass ( $m_e$ ) and the  $v_b=0$ , thus Equation A.21 can be rewritten as:

$$1/m_e = \left( 1/m_r + d^2/I_{cg} \right) \quad (\text{A.22})$$

giving the effective mass as:

$$m_e = 1 / \left( 1/m_r + d^2/I_{cg} \right) \quad (\text{A.23})$$

## A.5. Deriving the COP location

From Figure A.4, the COP is location on a distance  $s$  from the CG, where the recoil speed of a conjugate point on the grip, located  $b$  from the CG has a zero recoil resulting speed, where the rotational and translational velocity components cancel each other out, hence:

$$\varpi = v_{cg} / b \quad (\text{A.24})$$

Substituting Equation A.24 into Equation A.20 yields:

$$v_{cg} = (u_b + v_b)m_b d \cdot b / I_{cg} \quad (\text{A.25})$$

and combining with Equation A.19 gives:

$$(u_b + v_b)m_b / m_r = (u_b + v_b)m_b d \cdot b / I_{cg} \quad (\text{A.26})$$

which can be simplified to give the location of the COP as:

$$d = I_{cg} / (bm_b) \quad (\text{A.27})$$



# Appendix B

## Control flow diagrams

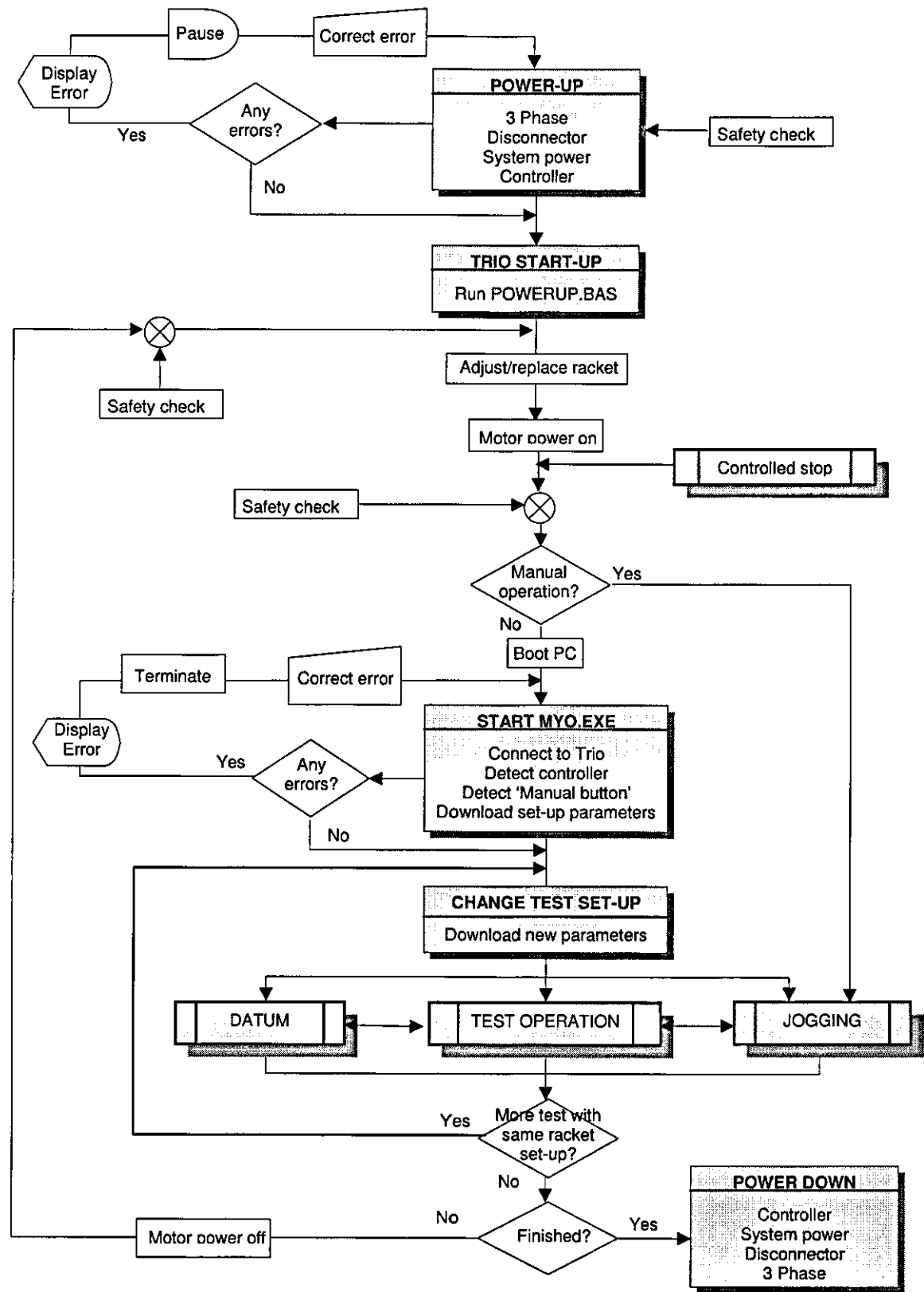


Figure B.1: General operating procedure

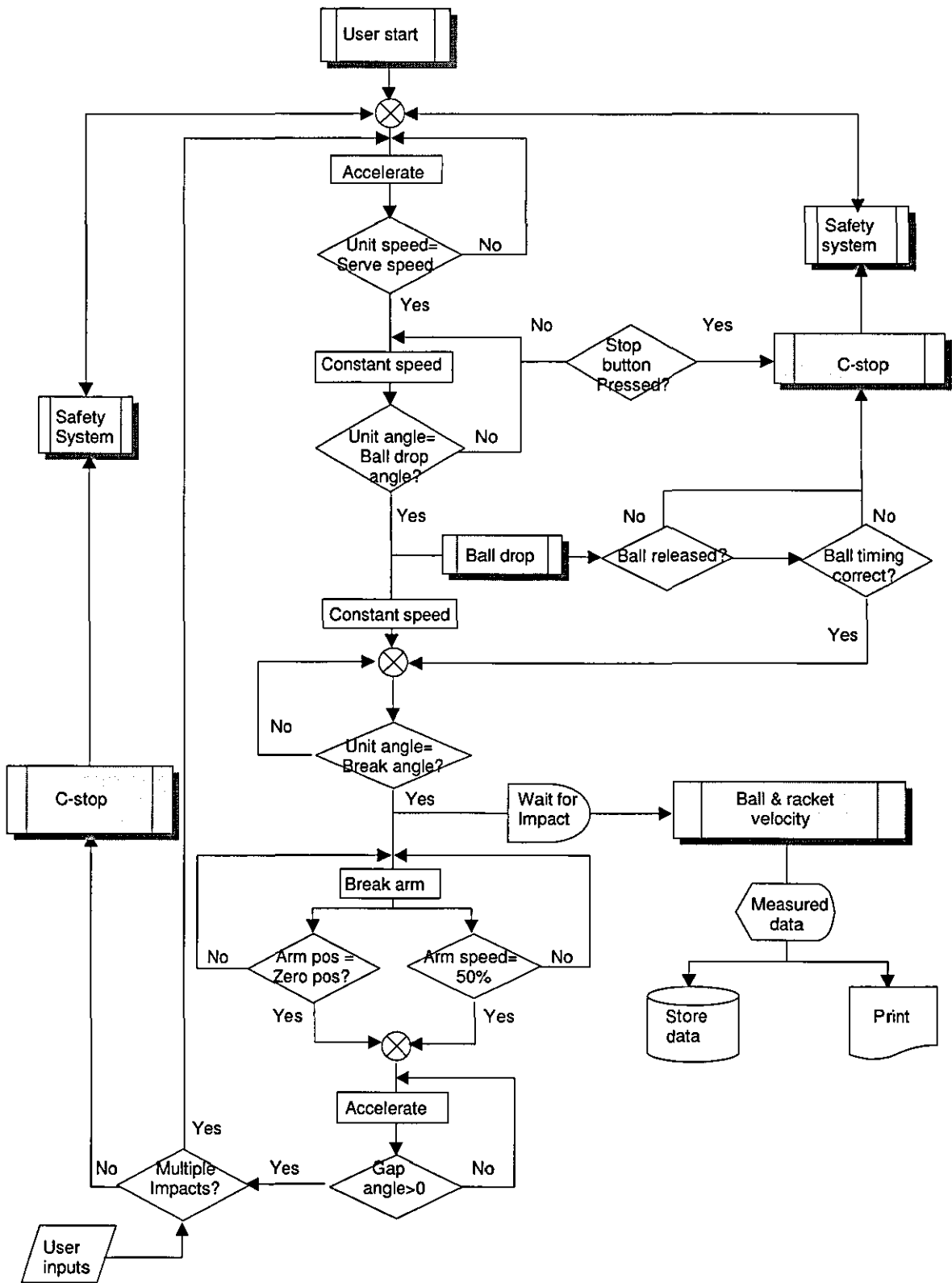


Figure B.2: Overview of the testing procedure.

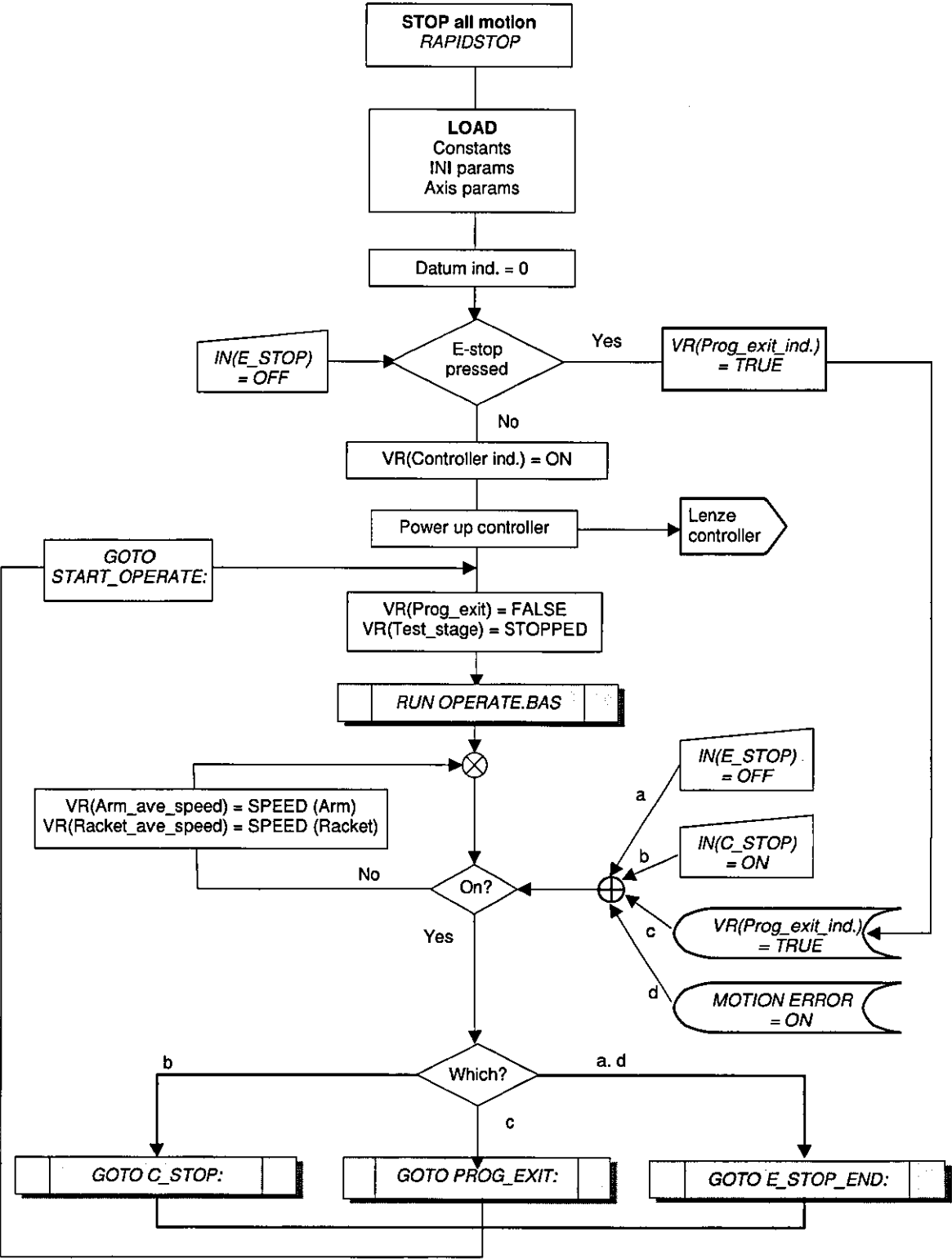


Figure B.3: The main control structure of the Trio controller (POWERUP.BAS).



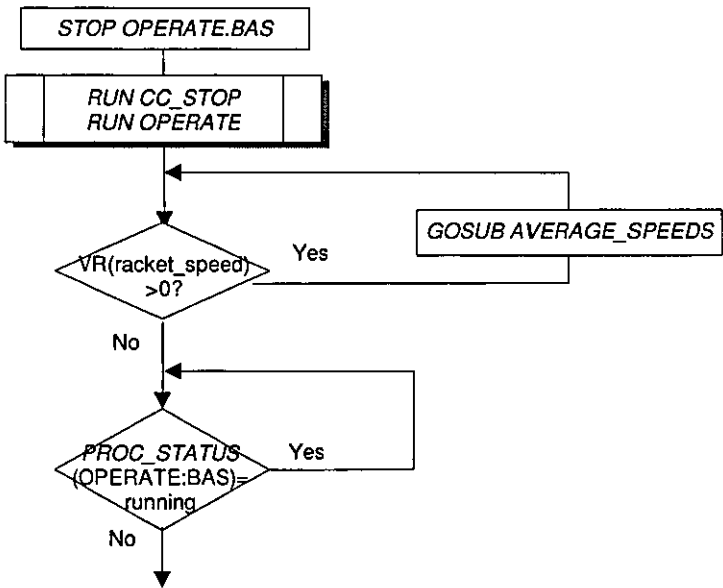


Figure B.4: The routine handling the c-stop procedure (POWERUP, c\_stop:).

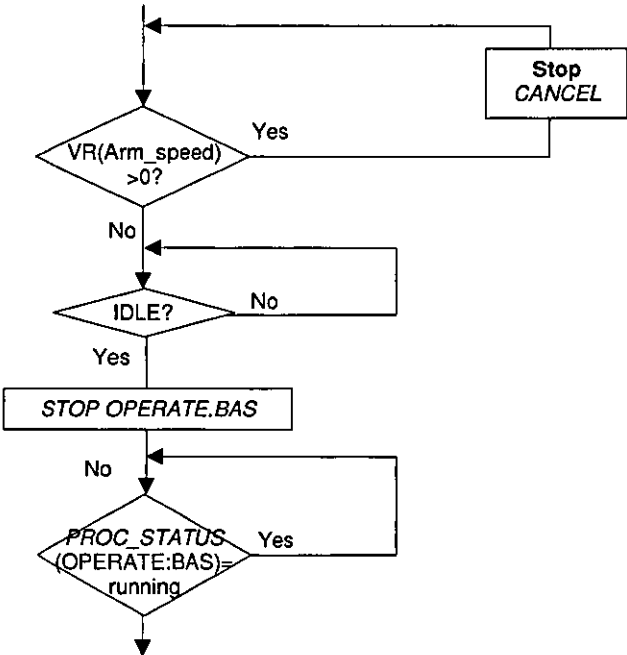


Figure B.5: Routine for exiting the jog mode (POWERUP, prog\_exit:).



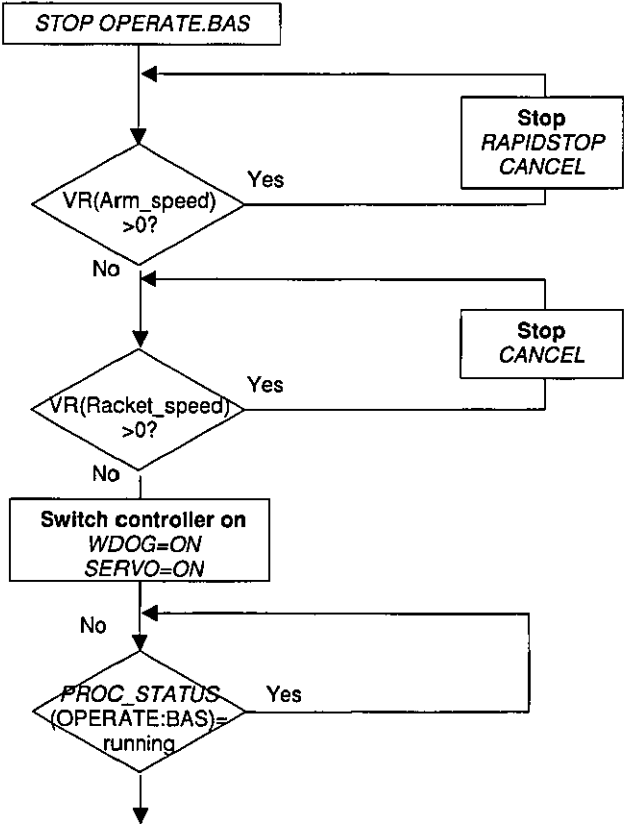


Figure B.6: The routine handling E-stops (OPERATE, E\_stop\_exit:).

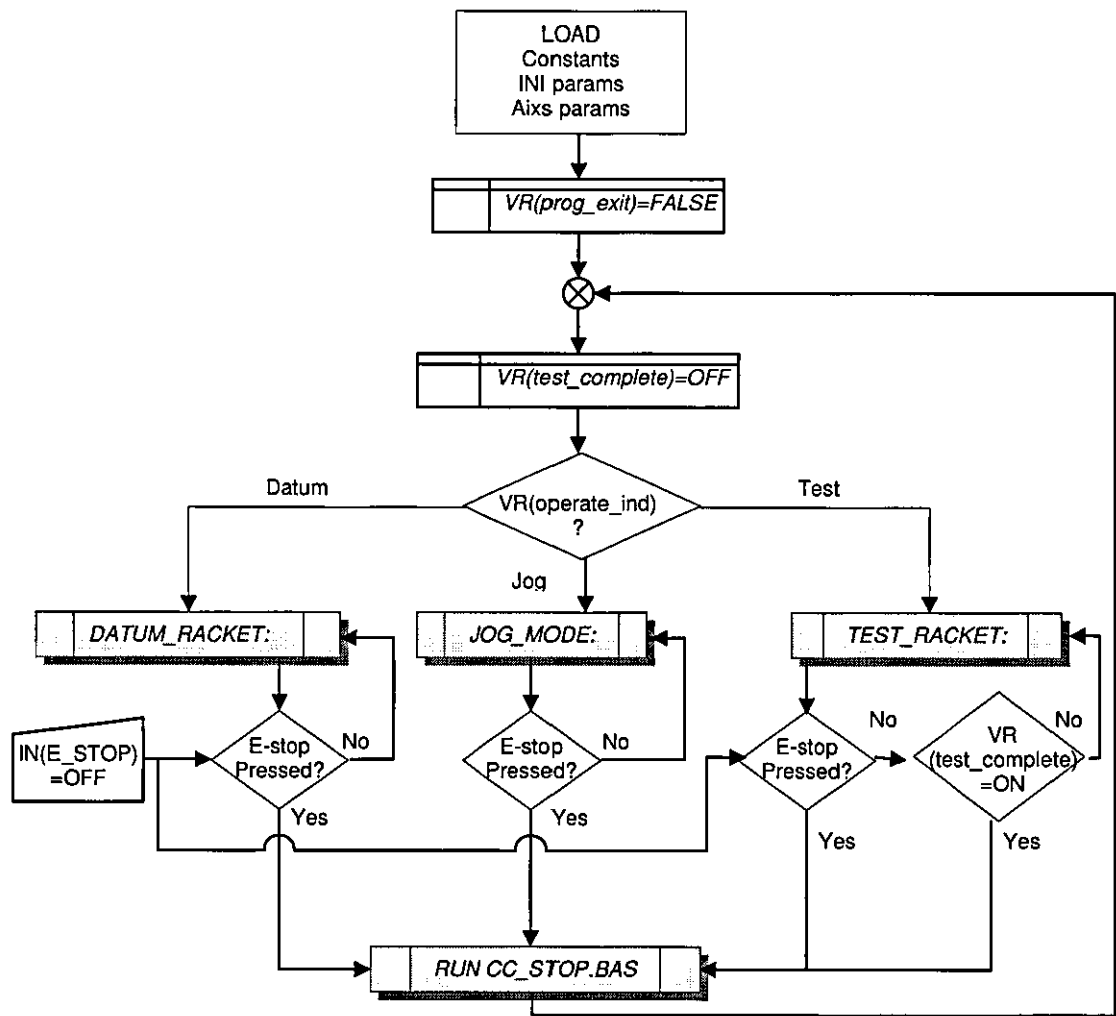


Figure B.7: The main operating procedure on the Trio controller (OPERATE.BAS).



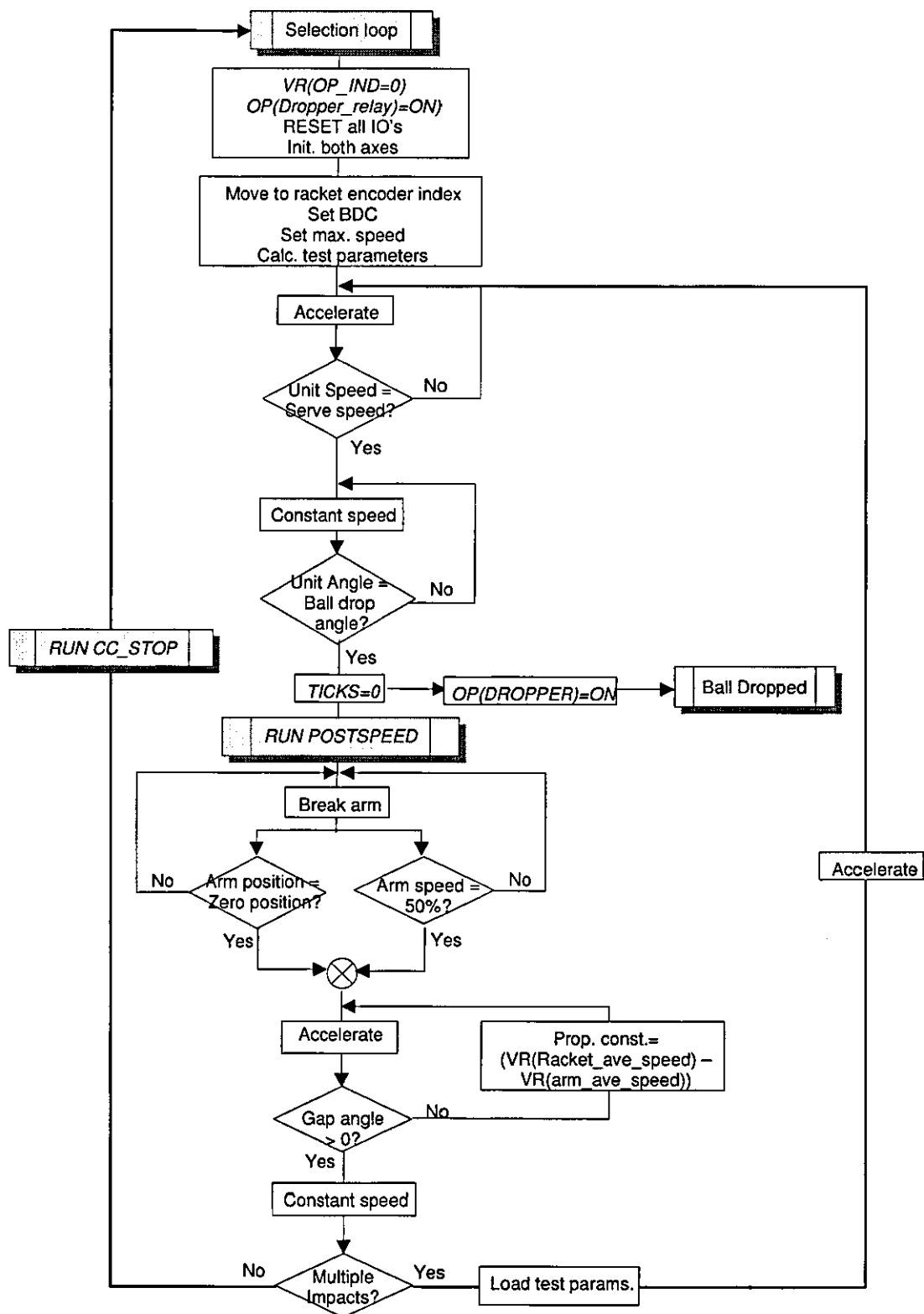


Figure B.8: The test operation procedure (Test\_racket:).

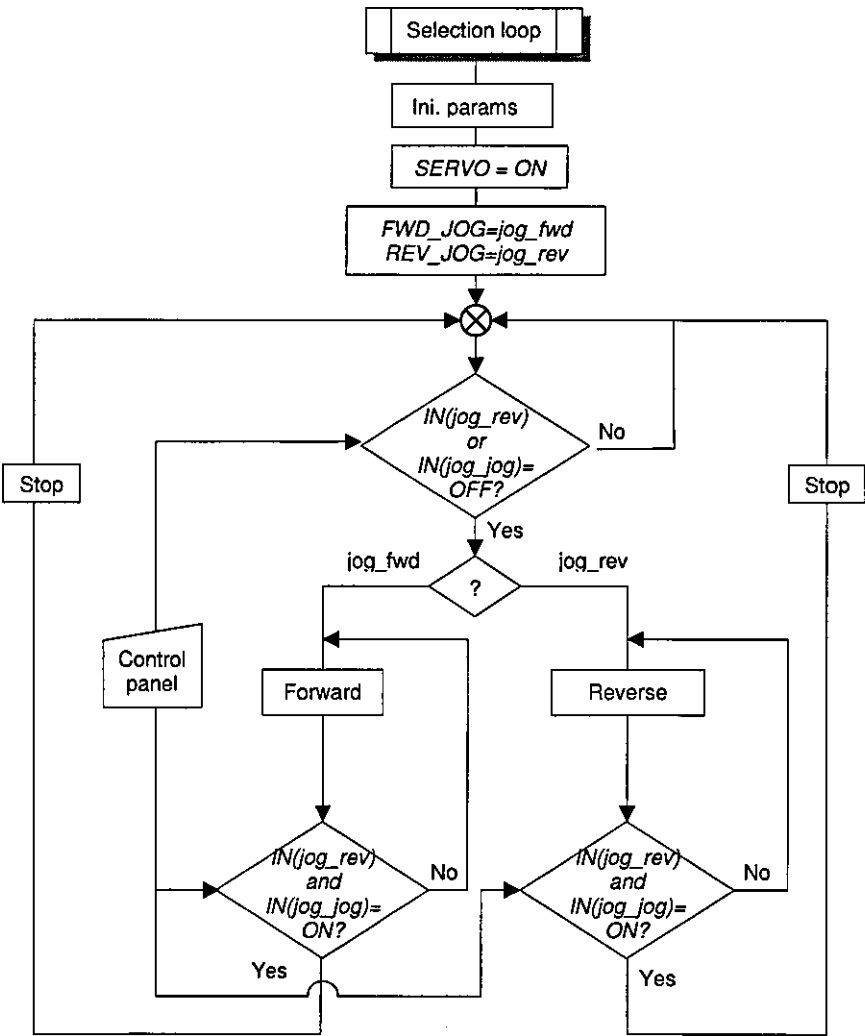


Figure B.9: The jogging procedure of the Trio controller (Jog\_mode:).

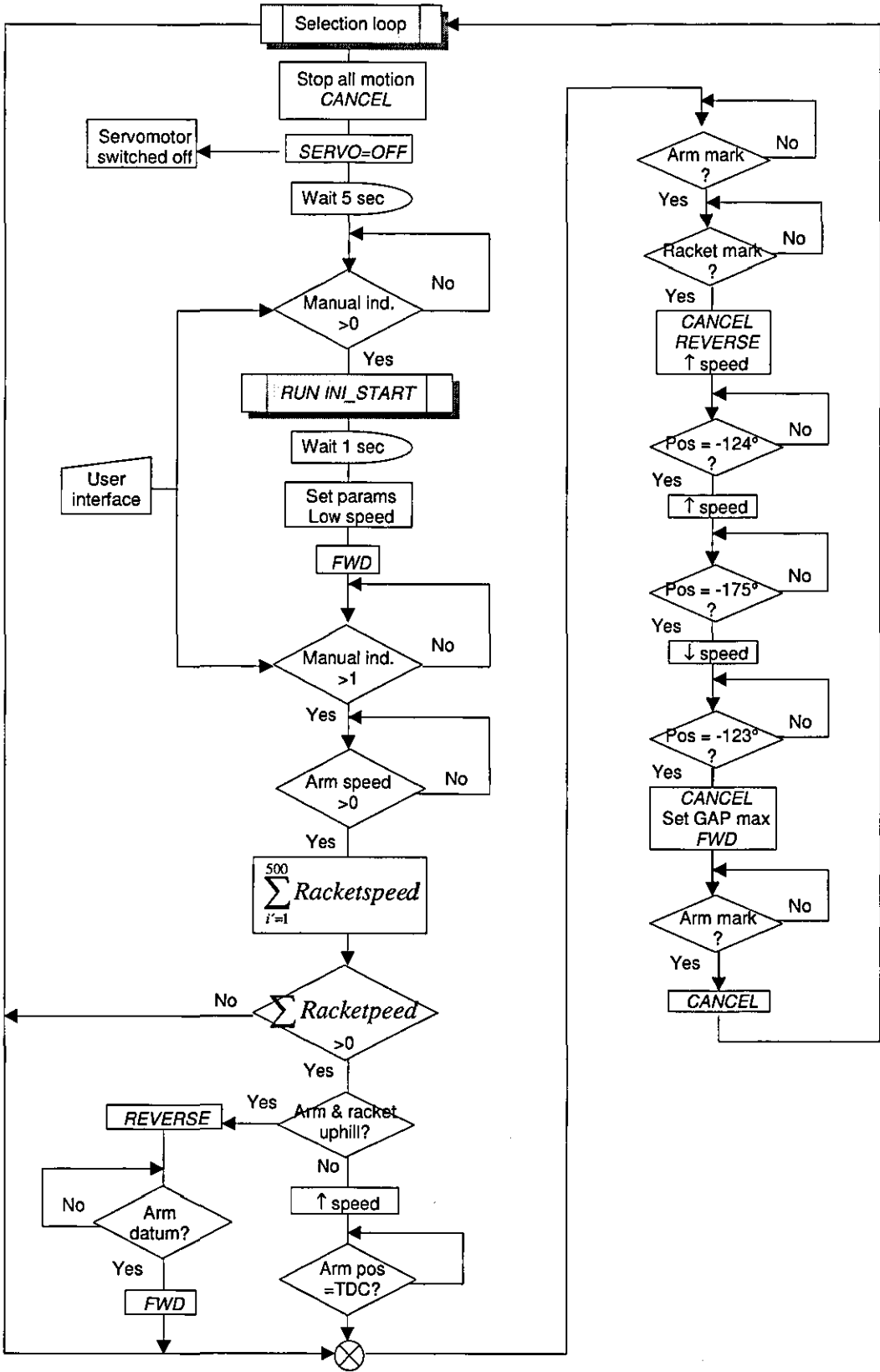


Figure B.10: The datum operation procedure (Datum\_racket:).

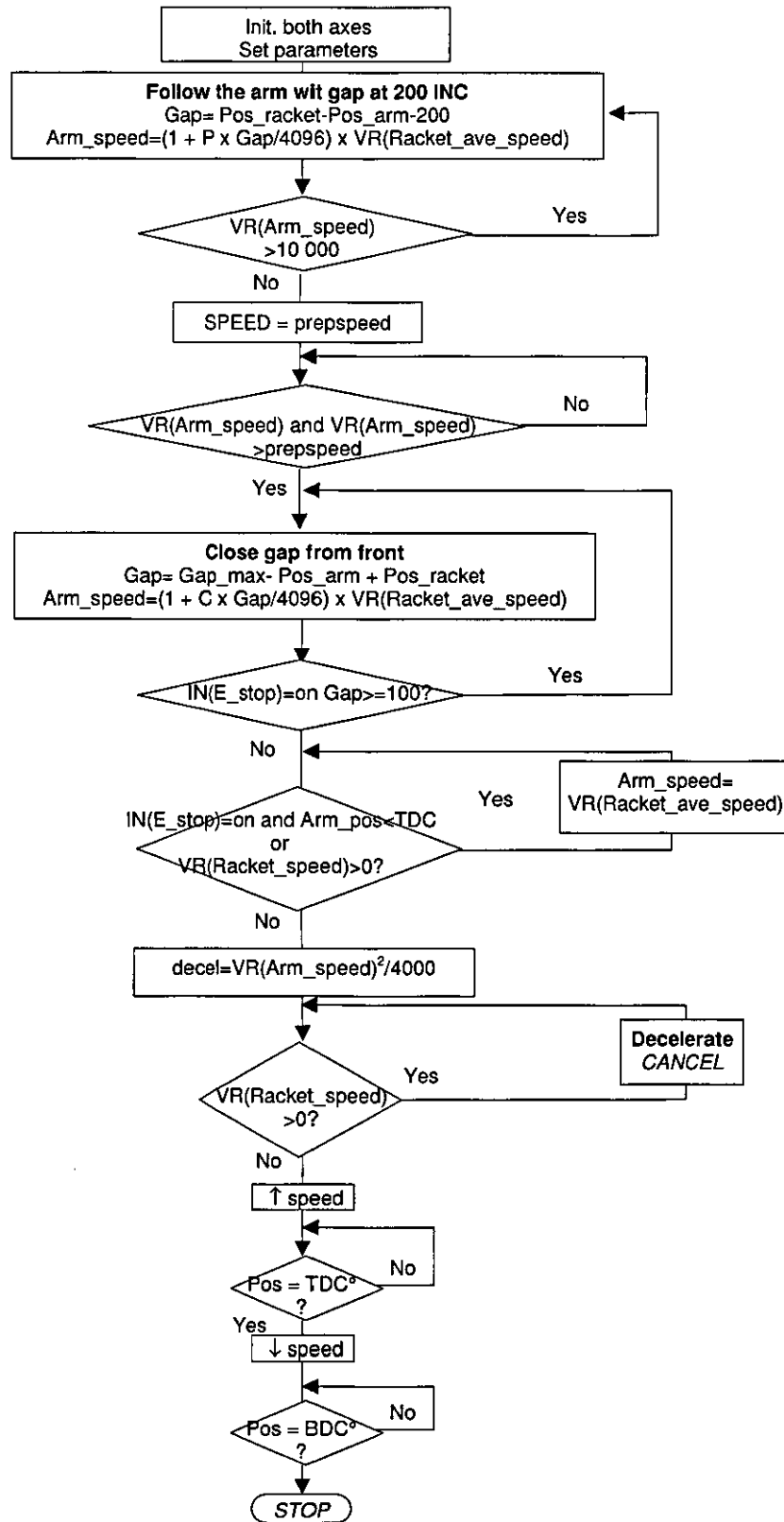


Figure B.11: The datum operation procedure (CC\_STOP.BAS).



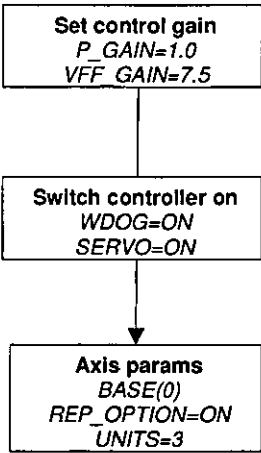


Figure B.12: Trio program starting the controller (INI\_START.BAS).

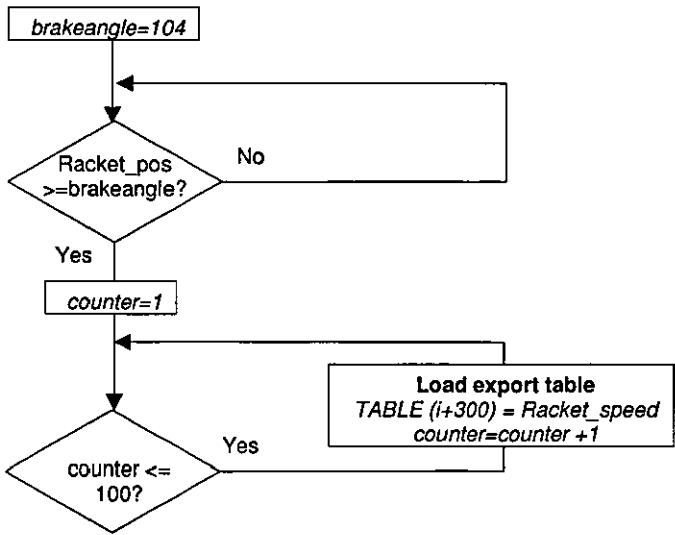


Figure B.13: Trio program recording racket speed during impact (POSTSPEED.BAS).

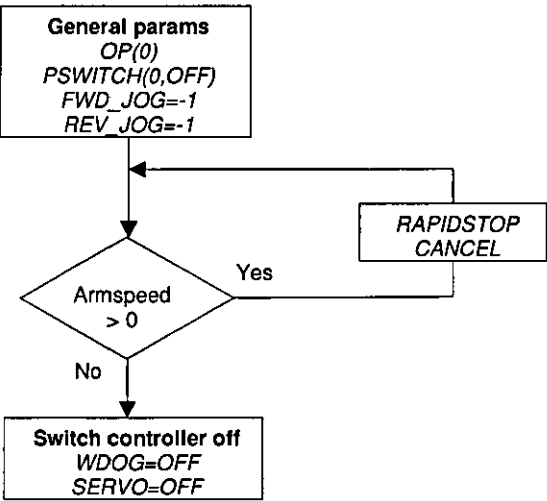


Figure B.14: Trio programming stopping all motion (INI\_STOP.BAS).

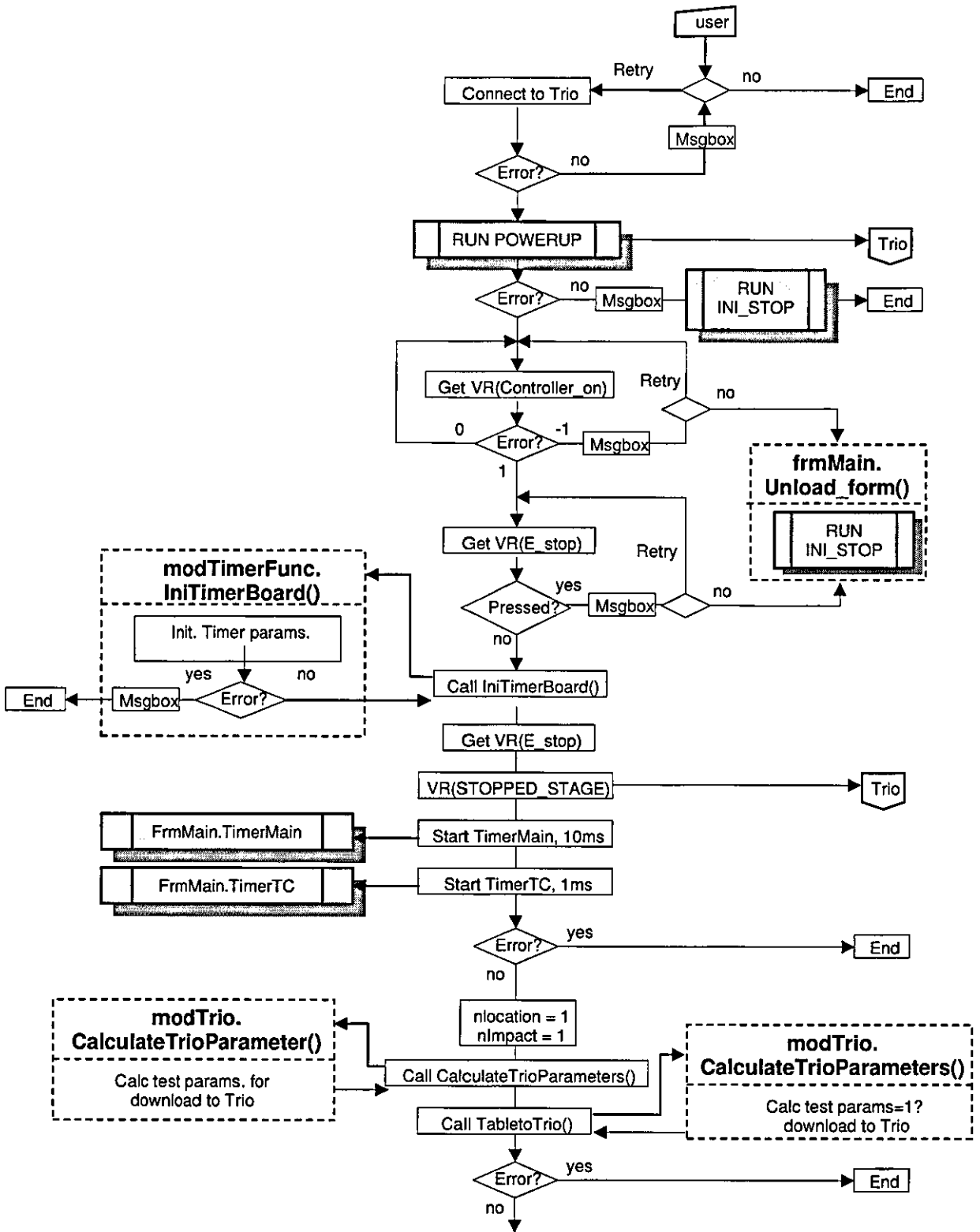


Figure B.15: The frmMain.Load function.

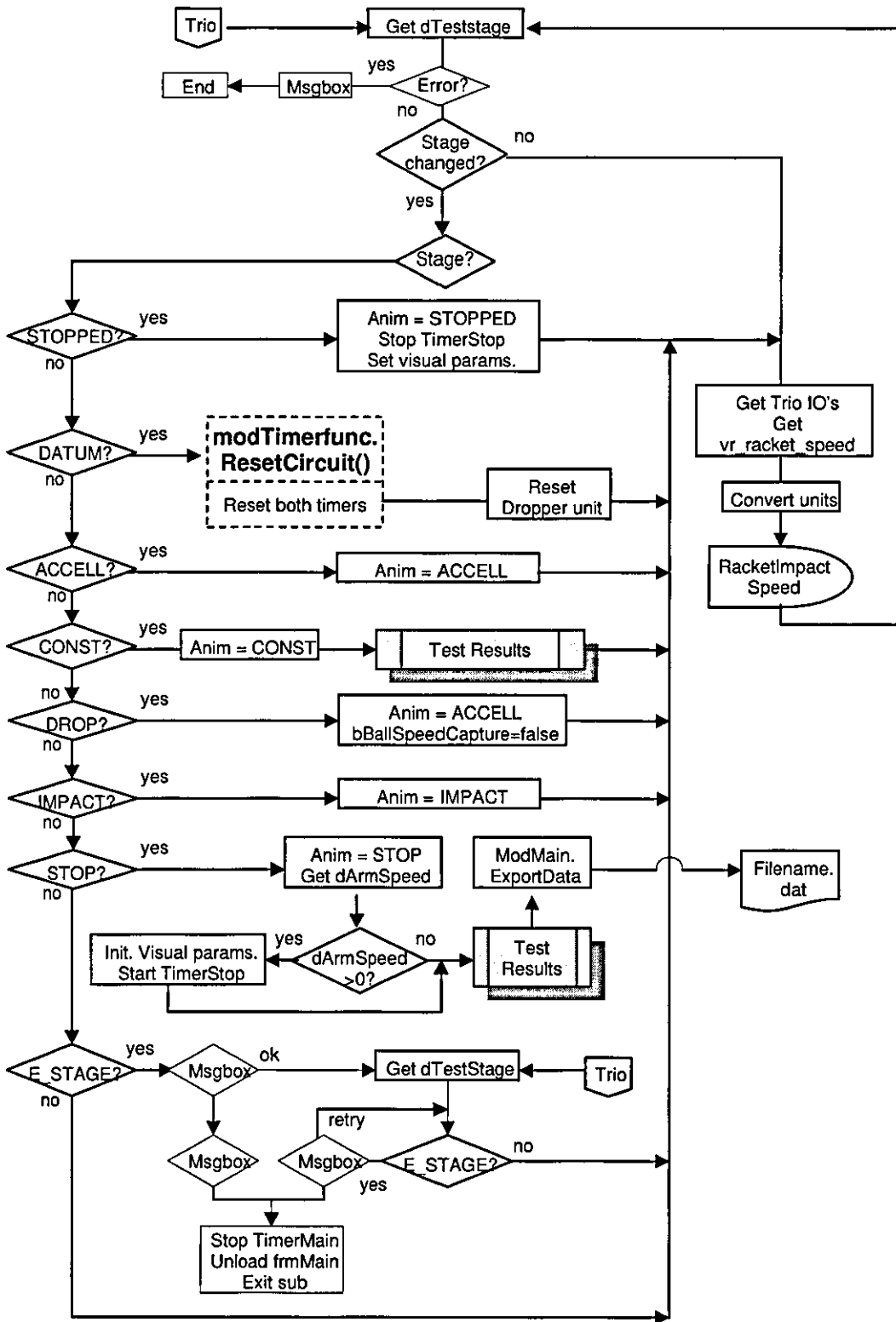


Figure B.16: The TimerMain\_Timer function.



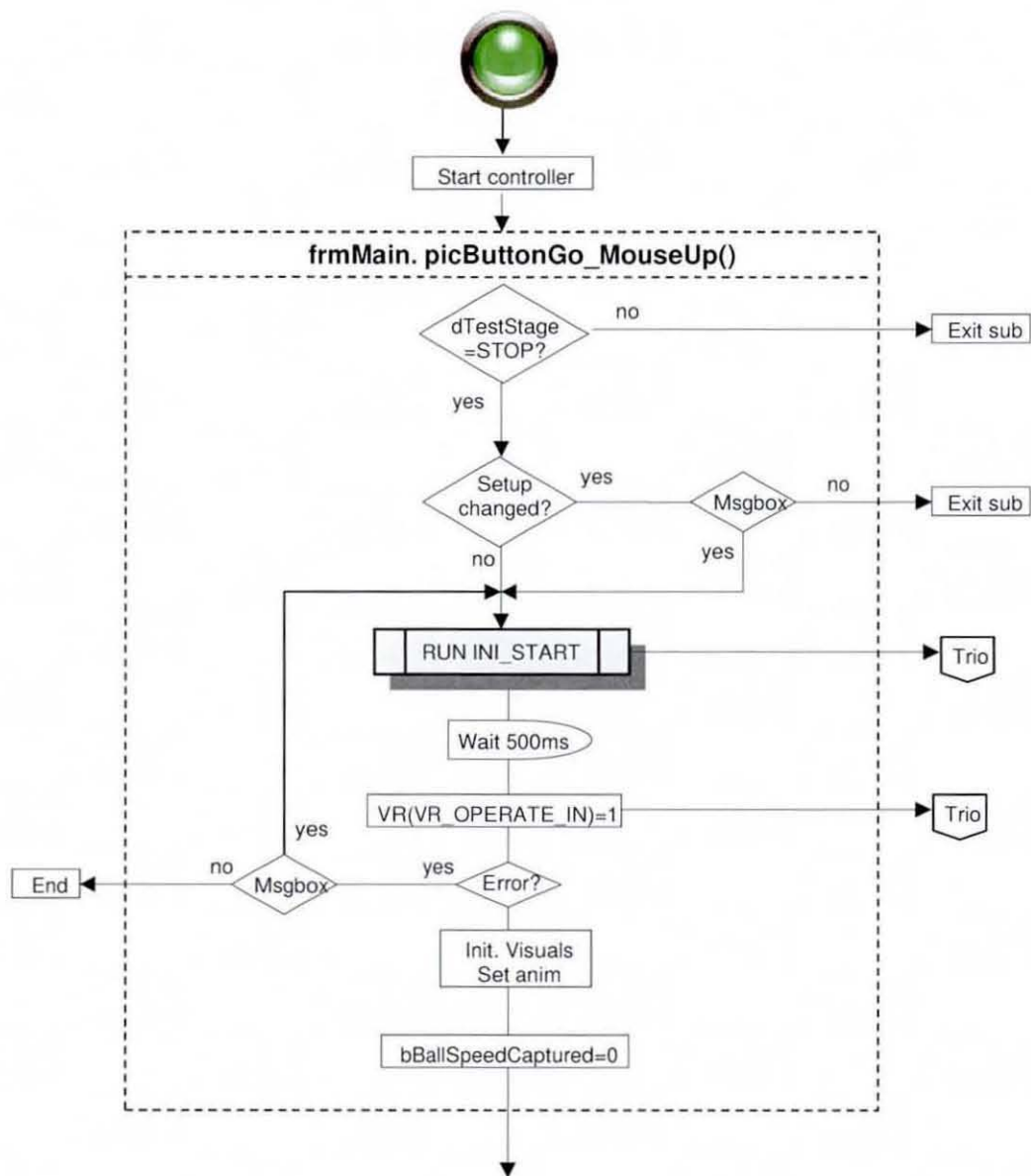


Figure B.17: Start testing operation.

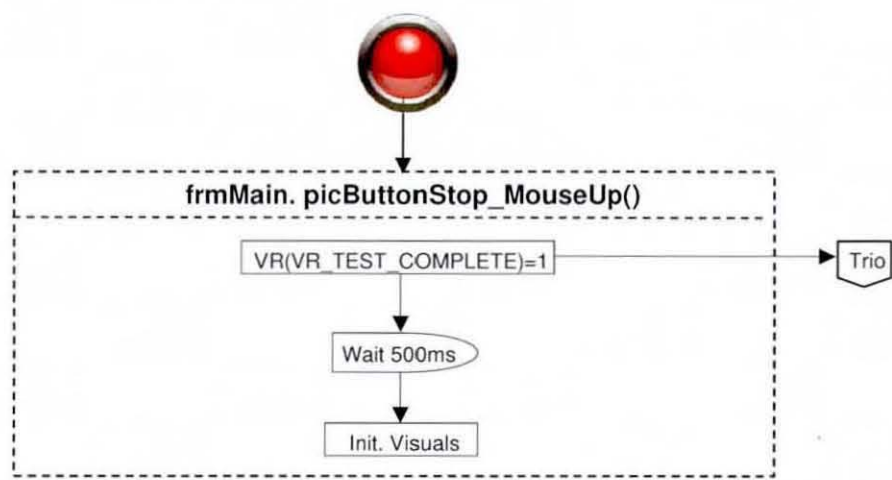


Figure B.18: Finish testing.

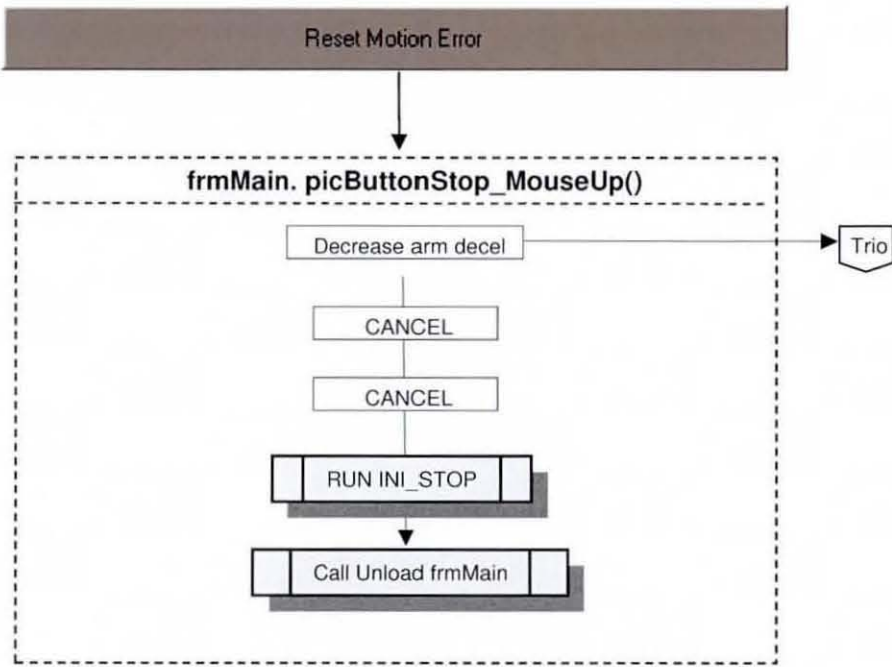


Figure B.19: Reset the machine when a motion error occurs.

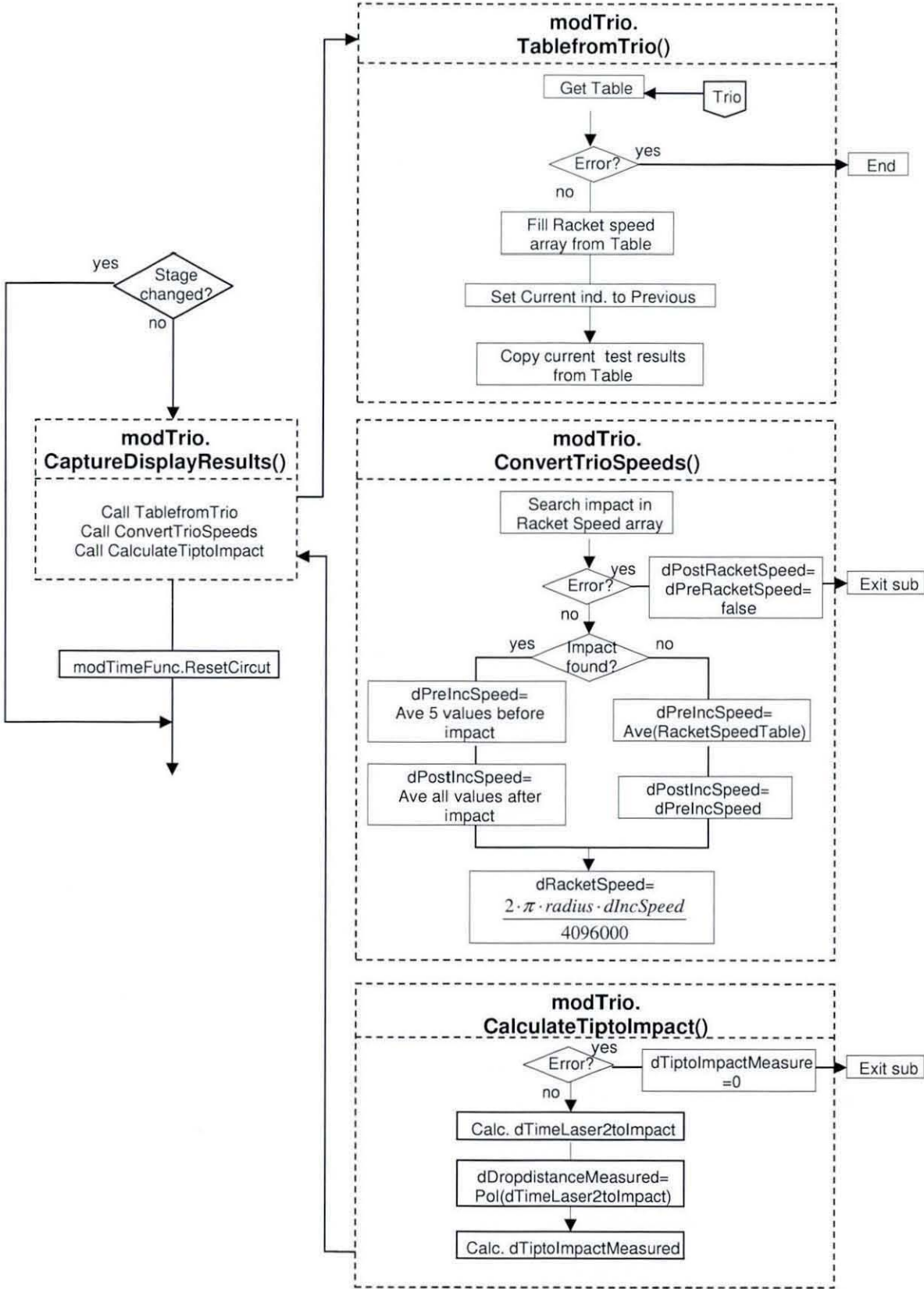


Figure B.20: Manipulating the test results.

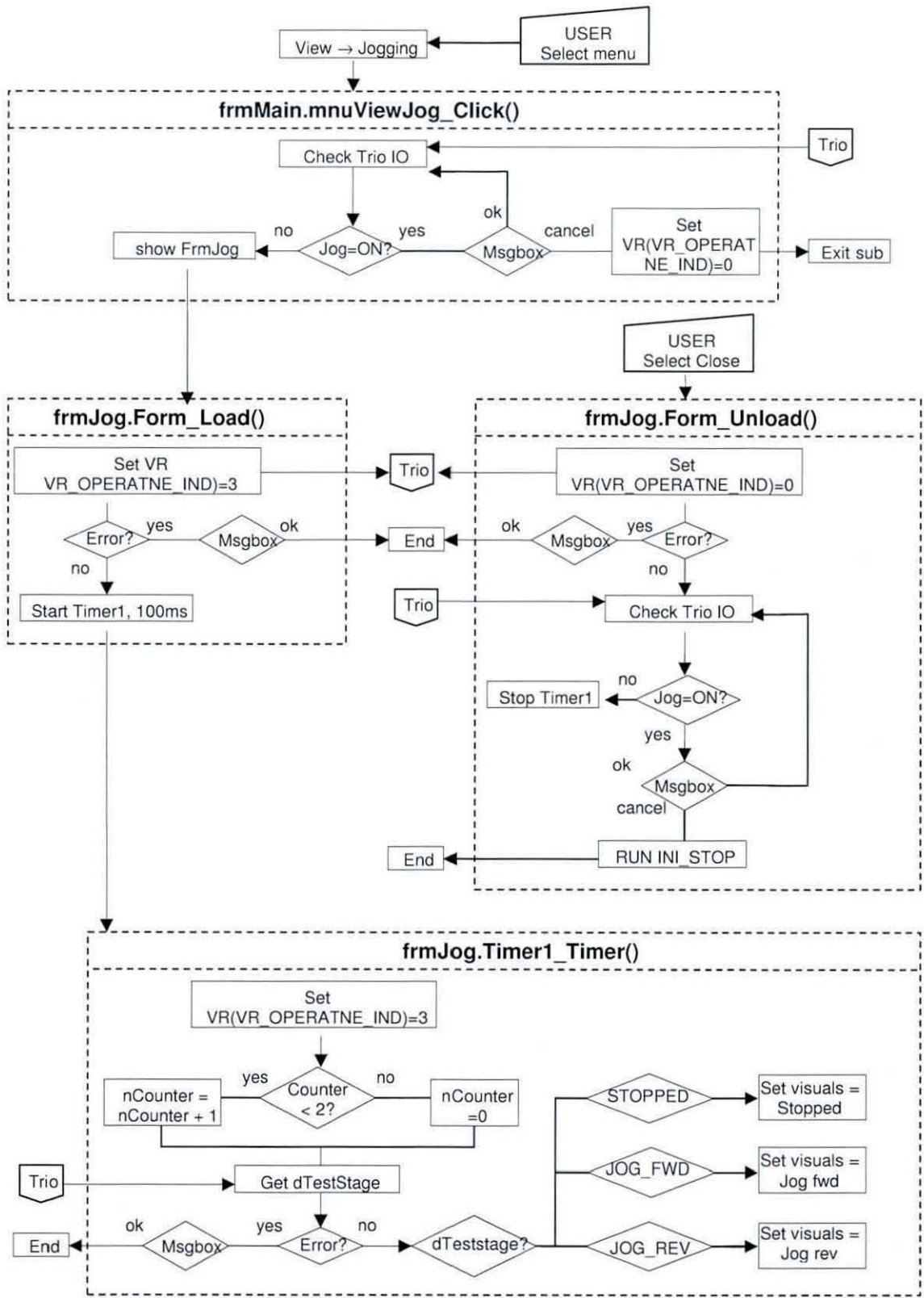


Figure B.21: The jogging operation function.



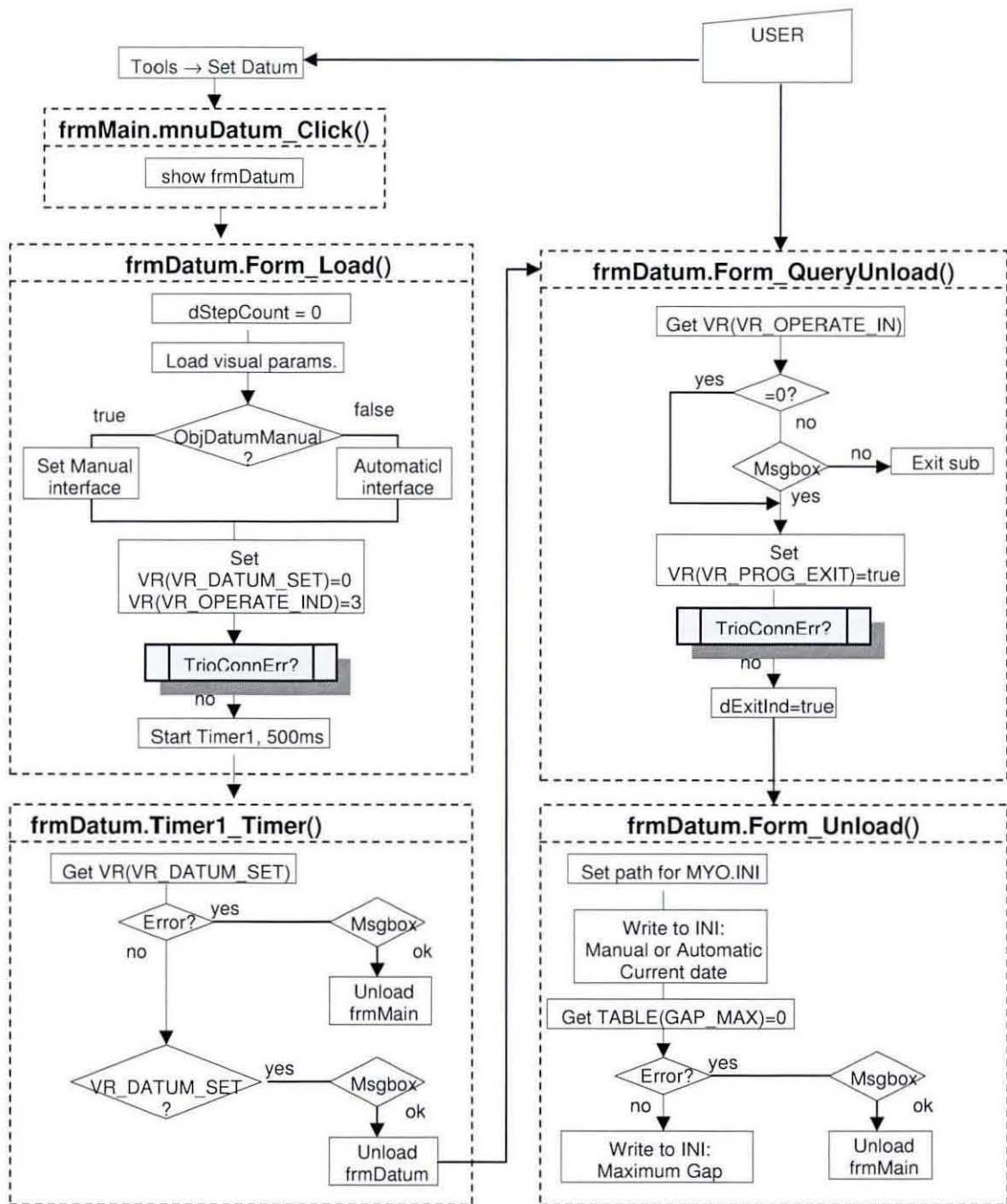


Figure B.22: The datum operation function.

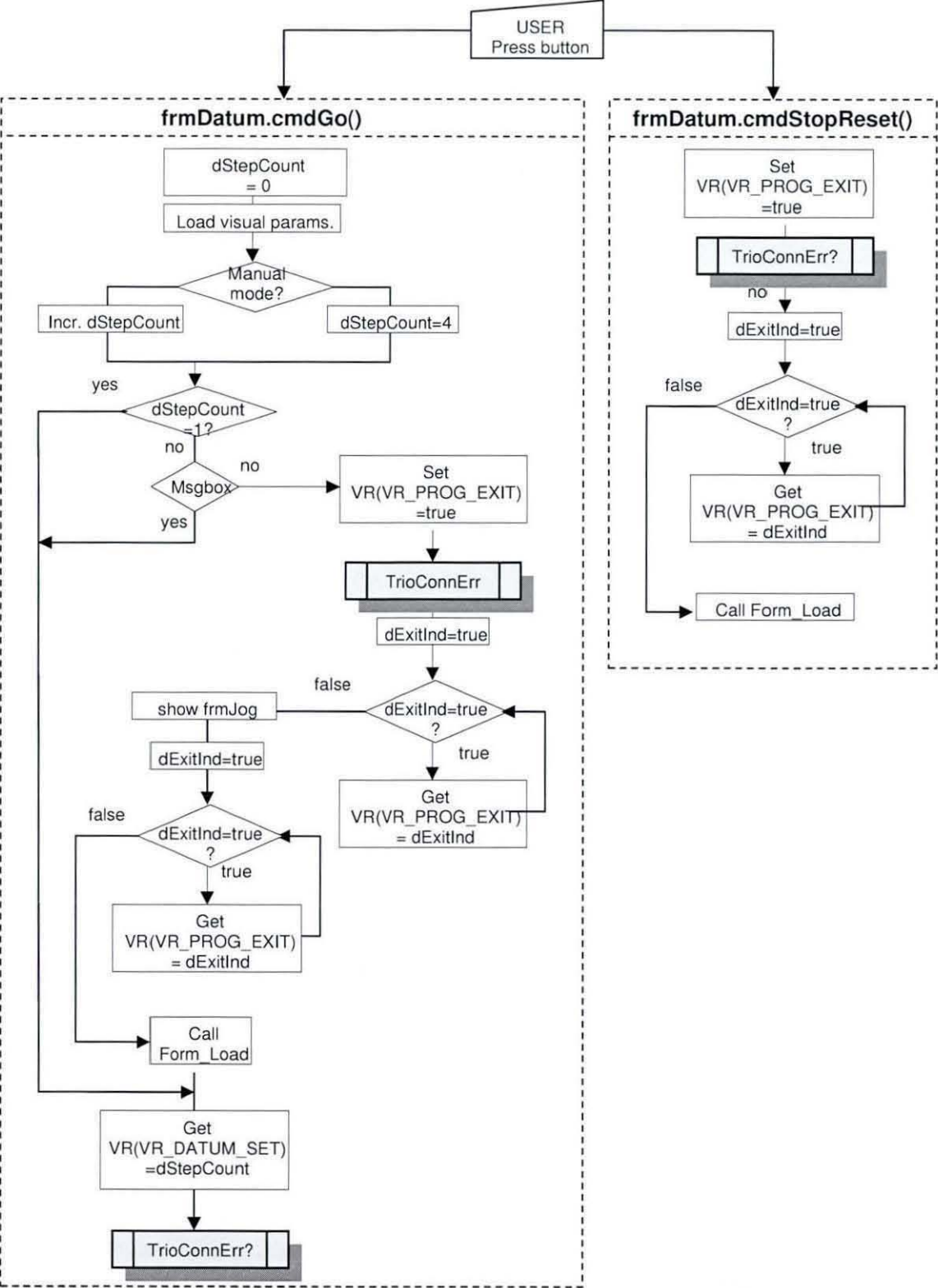


Figure B.23: Go and Stop/Reset button functions in frmDatum.

# Appendix C

## Machine control detail

### C.1. Trio controller programs

**POWERUP:** This is the first program loaded when power to the controller is switched on. It loads default constants and parameters and then starts the **OPERATE** program after which it continues into a continuous loop, constantly calculating a moving average velocity for both the drive arm and the racket. This produces a smoother velocity profile used in some closed loop control functions. The average velocity is calculated during each loop in the program, computing the average of the current value and those measured during the previous two loops. The program is executed as a fast program, hence the highest speed, ensuring the most accurate average velocity possible. During each loop the program also checks for motion errors or emergency and controlled stops. In case of such an event, the program exits the loop and performs the appropriate shut down procedure demanded by the particular event, as well as terminating the **OPERATE** program. After completion of the particular shutdown procedure, the **POWERUP** program resumes at a point in the program where the **OPERATE** program is restarted and the loop is re-entered.

**OPERATE:** Since all variables are treated as local to each program, the program starts by reloading default constants and parameters. It then enters a continuous selection loop until an operating mode variable is received from the PC. The user can select one of three operation modes using the PC interface; *Test operation*, *Datum routine* or *Jogging*. On selection of the operation mode, the program will execute the selected operation until the user exits the mode, in which case it will return back to the loop and wait for the next operating mode selection.

*Test operation (Test\_racket):* The operation commences with loading initial parameters and variables from the table downloaded via the PC set-up



interface, after which it starts the testing by driving the machine through the individual test stages, as described earlier in the section. In addition to constantly controlling all motions, the program also monitors and coordinates various inputs and outputs. During the *datum* stage it detects the racket's encoder index, and sets the correct data for both axes. Subsequently, it calculates the test parameters as dictated by the specific operating parameters and continues controlling the motion of the drive arm through the *acceleration*, *constant* and *deceleration* stages. During the acceleration stage, the trigger is activated for the output to the ball dropper, at the pre-calculated drive arm angle. Simultaneously a timer on the Trio is activated, which is read when the racket reaches the impact angle. This is used to accurately predict the actual impact position of the ball on the racket face by correlating the time with the time measured by the impact laser, hence compensating for dropper inconsistencies. After impact a proportional control loop in the program guides the arm to smoothly close the gap and catch up with the racket, using the average racket speed calculated in the POWERUP program. On contact, the acceleration stage is restarted, unless the final test was performed or testing was terminated by the user. The latter can be performed via the control panel, E-stops or the PC interface as described later in this section.

*Datum routine (Datum\_racket):* The purpose of the routine is to find the datum positions for the racket and arm after power-up, hence setting the correct origin for each axis. This is necessary, since all axes data are reset during power-down. The routine also detects the maximum gap which can be opened between the crossbar and the racket and saves it as a variable used by the control loop during the controlled stop procedure. The datum routine can also be performed at any time to check the accuracy of the system in order to ensure the high level of accuracy demanded by the PDS. The routine commences by stopping all motion and disconnecting the power to the motor. This results in both the drive arm and the racket assembly falling down to their natural gravitational equilibrium, if not already there. After an adequate break, power

to the motor is switched back on and the drive arm slowly moves forward while the racket speed is monitored. If the racket also moves, the routine knows the crossbar is behind the racket, rather than in front. Since the measured racket speed is rather spiky, often implying movement when there is none, the measured value is summed over 500 program cycles and the total used to indicate movement. In case of the standard scenario where the drive arm is located behind the racket, the drive arm changes direction and moves through its external datum, changes direction again and moves until it reaches the racket's internal datum. This position is then set as the BDC position for both the racket and the drive arm. In the second scenario, the crossbar is located in front of the racket, and therefore, the speed is increased for a full rotation, until it is behind the racket. When the arm reaches the racket's internal datum it is slowed down and continues as for the standard scenario. Subsequently, the procedure measures the maximum gap by moving the drive arm backwards through more than a full rotation, speeding up at first and slowing down towards the end in order to speed up the process without sacrificing accuracy. The drive arm stops, with the racket resting on top and behind it, with the difference in angle from the previous contact in front of the crossbar indicating the maximum gap possible between the two. The drive arm then moves back to the BDC position and exits the routine. If needed, the operator can select the *Jogging* mode at any stage during the routine to manually move the drive arm with the control pendant (Figure C.1) into a desired position.

*Jogging (Jog\_mode):* The jogging mode is activated via the user interface. During this mode the controller acts on inputs from two switches on the control pendant, *Direction* ["CW/CCW"] and *Jogging* ["JOG/IDLE"]. The pendant is hard-wired to inputs on the Trio, which interprets the signals and sets the jog motions accordingly via the developed programs. This method provides a robust method for controlling the machine under special circumstances, such as calibration, general malfunctioning or PC control/connection errors. During the jog mode, the machine moves at the default machine settings, i.e. a preset jog



speed. Therefore, to ensure safe operation, on entering the jogging mode with the *Jogging* switch set to “JOG”, it prompts the operator to switch it to “IDLE” before resuming the routine. Consequently, switching the *Jogging* button to “JOG” will move it in the direction selected by the *Direction* switch (“CW” = clockwise and “CCW” = counter clockwise). When attempting to exit the jogging mode while the arm is jogging, the program prompts the operator to switch it to “IDLE” first, before returning back to the operation selection loop. These user prompts are relayed back to the user interface via set variables, which are continuously monitored by the PC interface.

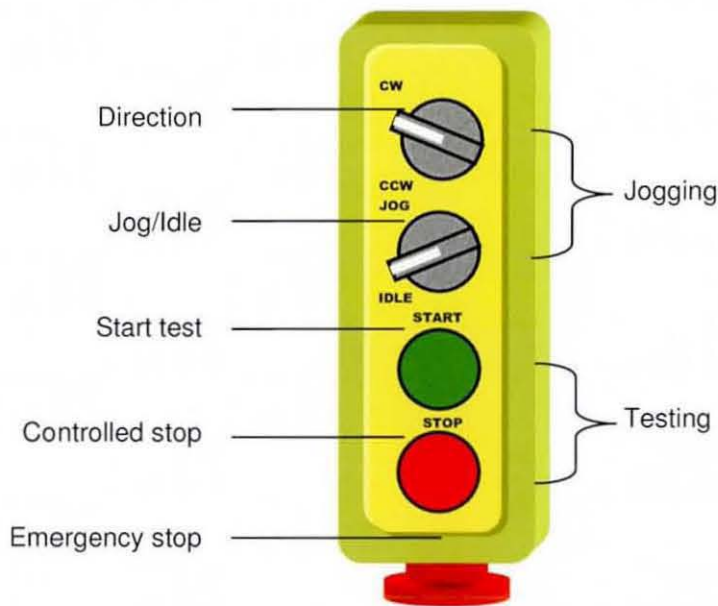


Figure C.1: The control pendant for manually controlling the robot.

**INI\_START:** This small program is executed by the OPERATE program during the *Datum routine*, to switch the controller power back on.

**POSTSPEED:** The program is executed during the *Test operation* procedure by the OPERATE program, the instance the ball drop angle is reached. The program records the velocity of the drive arm and the racket for 100 sample points (i.e. 100ms) from the moment the side arm starts braking. These values are loaded into the variable table, which is uploaded to the PC after each impact for determining the resulting impact speeds.

**CC\_STOP:** This small program is executed by the POWERUP and OPERATE programs to safely stop the machine after the final test has been performed or when a controlled stop was selected by the user. First both axes are initialised and parameters set, after which a differential control loop is entered, during which the drive arm follows the racket until it has reached a safe velocity to start the braking procedure. As soon as the safe speed is reached a second loop is entered decelerating the drive arm in order to catch the racket from the front. The procedure brings the drive arm and racket to a rest just before BDC. Leaving the racket at its gravitational equilibrium, the arm continues for a full rotation to get behind the racket, similar to the last stage of the *datum* routine described earlier. In this location the machine is ready to continue a terminated test sequence or to start a new sequence.

### C.2. Pc interface detail

*Start-up:* During software start-up the initialisation constants and default (previous) test parameters are loaded from the MYO.INI file. The software then attempts to establish the USB connection with the Trio and in case of no connection enters a loop prompting the operator to ensure a proper connection. Once connection is established, it starts the POWERUP program on the Trio and initiates the timer/counter board. The Trio's 1kHz counter is sufficient for most synchronised events except for the post-impact ball speed of up to  $66.6\text{m.s}^{-1}$ , which requires an additional dedicated high-speed timer/counter in the PC. An Amplicon PCI215 timer/counter card, sampling at up to 10MHz, was used for this purpose. Consequently, all inputs from the laser units were detected via the same card, to guarantee system accuracy and uniform design integrity. After initialising the timer card the Trio variables are calculated from the default set-up parameters and downloaded as a table into the Trio memory. Finally, the *Main* interface screen (Figure C.2) is loaded, which contains a text menu for performing all possible tasks, an icon menu for more common tasks, an



operations window for performing standard tests and providing visual feedback and a status bar with additional information.

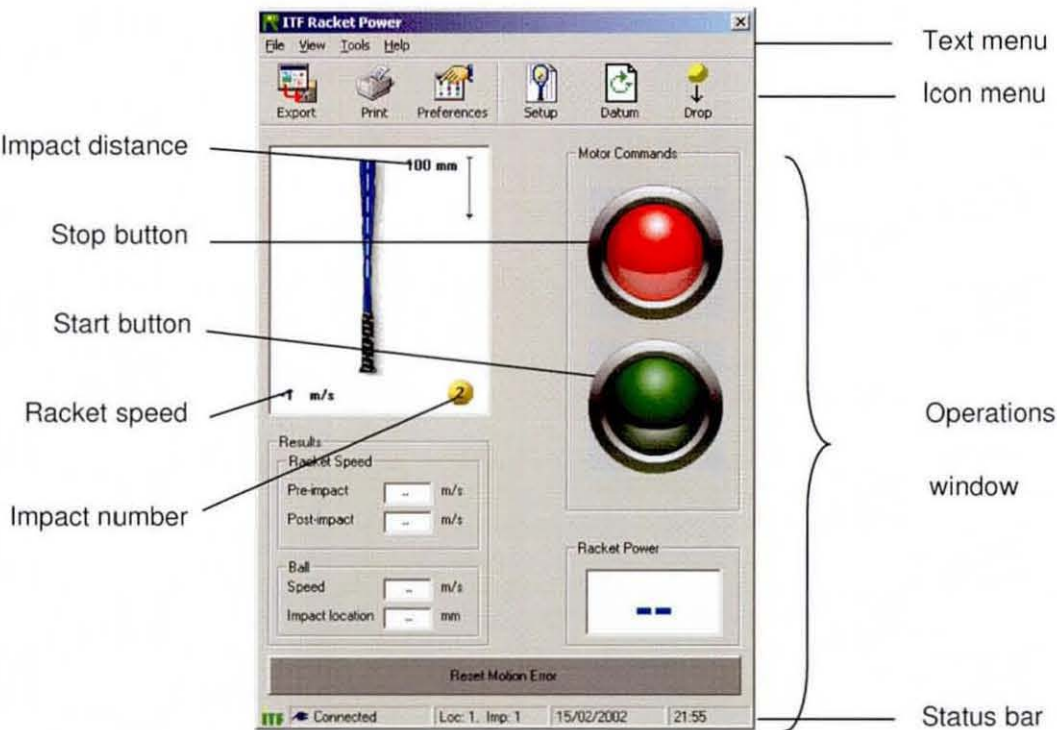


Figure C.2: PC main interface screen during test operation.

*Test operation:* If the default test set-up is invalid for the current test, the parameters can be changed using the *Setup* screen (Figure C.3) via “Setup” option from the “Tool” menu bar (henceforth denoted as Tools→Setup) on the *Main* interface screen. The screen consists of four tab strips, for setting different parameters; Racket Properties, Impacts, IC and Speed. Upon closing the *Setup* screen (described in the next section), the new variables are calculated and saved as the default to the INI file as well as downloaded to the Trio, ready for test operation. Only when all safety checks have been passed, can the test be started by pressing the *Start* button. This downloads an operation variable to the Trio, which is continuously monitoring the value of the variable via a selection loop in the OPERATE program in order to proceed to the correct procedure. The test procedure will perform a sequence of impacts as specified

in the setup until the last impact is performed, or it is terminated by the user. Throughout the test the main interface provides the user with impact data, which is calculated and stored in memory after each impact and can be exported to a data file after the test series is completed (File→Export). The software also uses a timer to continuously check the state of the Trio for the racket speed and to know which stage of the test the controller is performing.

The *Racket Properties* strip on the *Setup* screen consists of racket details such as the model, physical dimensions, mass and swing weight (RDC). These parameters are used to determine other test parameters such as the racket speed and variables for achieving the desired impact locations. The latter is determined by calculating distances in relation to the ball dropper using the racket dimensions and impact information, which in turn is combined with the dropper calibration curve to determine the correct ball timing variables.

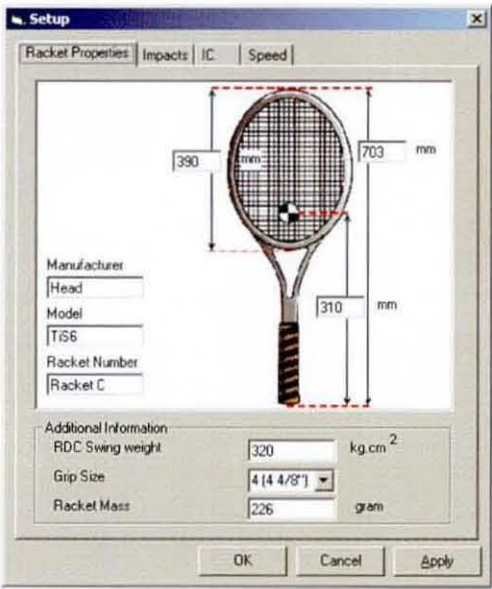


Figure C.3: The Setup screen's Racket Properties strip.

With the *Impacts* strip (Figure C.4) different impact test configurations can be specified, such as single (a) and multiple (b) impacts. For both, a distance from the racket tip can be entered. In order to further automate the test procedure such that it could perform tests across the length of the racket face,

two multiple impact location configurations can be specified; the first (c) specifies the first and last location and how many locations in between, with the software calculating the individual discrete locations, while with the second method (d) each location can be specified manually.

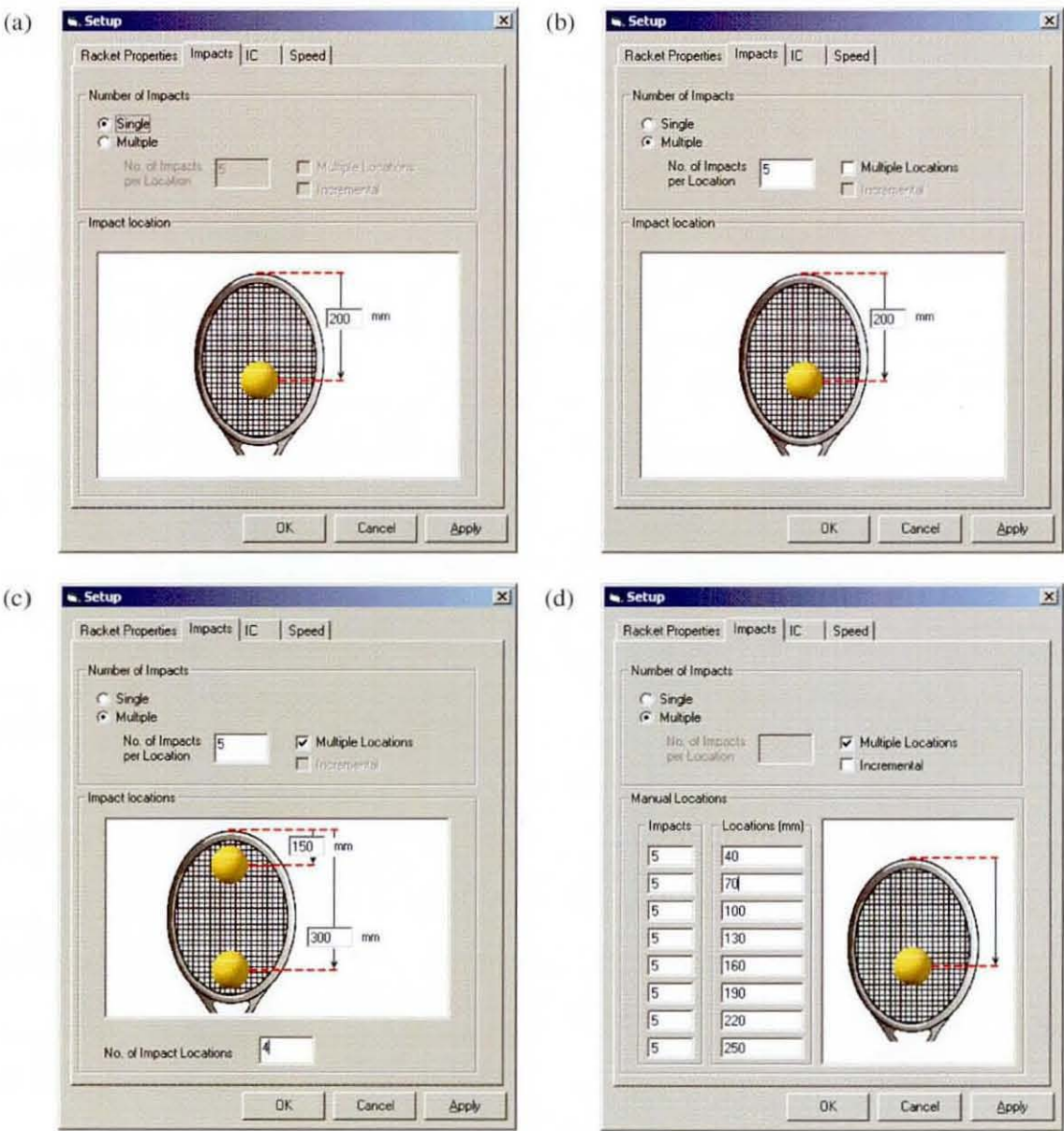


Figure C.4: The Impacts strip for specifying different impact sequences.

The IC strip (Figure C.5) is used to specify the IC-unit's horizontal and vertical dimensions, which is measured from the axis centre to the racket butt. For the manual setup (a), both the horizontal and vertical dimensions are



measured and entered manually, while the automatic setup (b) assumes the calibrated IC-unit is used and calculates the horizontal distance by specifying the index hole used (as marked on the unit) and the horizontal distance from the indicated edge of the butt center, which is easier to measure accurately than the manual procedure.

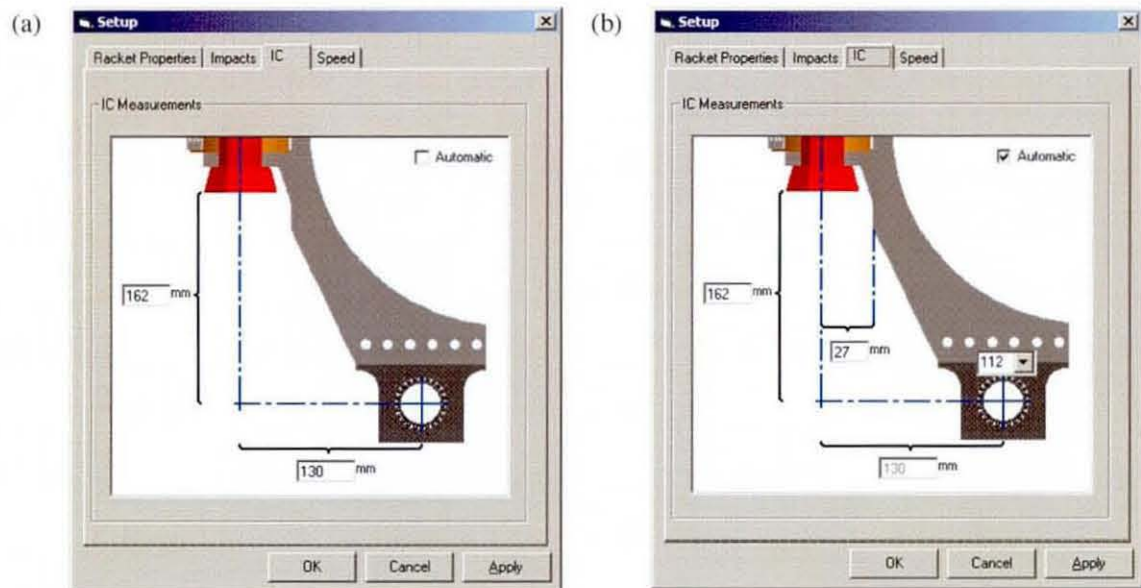


Figure C.5: The IC strip for entering the dimensions of the IC unit.

The *Speed* strip (Figure C.6) is used to specify or calculate the impact speed of discrete points on the racket, which would allow for investigating different power factor definitions. Since, these definitions had not been determined by the end of the research, only the *Constant Speed* option was made functional. For this option the impact speed at a given radius is entered which is specified in the MYO.INI file under “SpeedRadius” constant as 700mm. Depending on the power factor and what needs to be tested, this can be changed and if needed the software can be altered to specify different speeds at different impact locations or to allow different impact speeds to be calculated as a function of the racket properties. The additional proposed options included on the strip are *Linear integration*, which would vary the impact speed for racket with different MOI properties, or *Constant Energy*, which would use an energy relationship to



calculated the impact speed from the energy needed to get the racket up to speed.

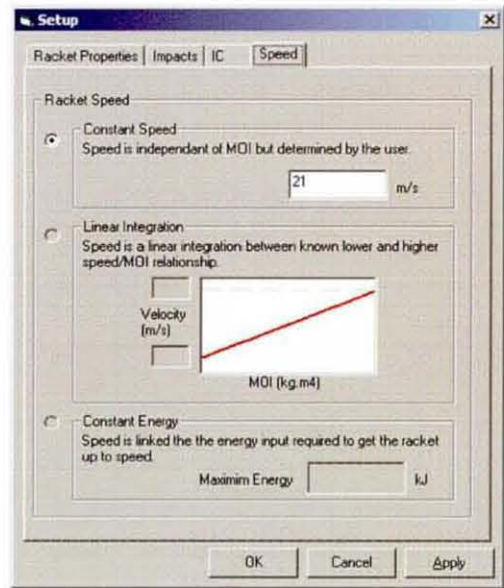


Figure C.6: The Speed strip for determining the desired racket speed.

At any stage during normal operation a graphic window (Figure C.7) can be opened (View→Graph) to provide the user with speed profiles of the drive arm and the racket, which can be captured and exported to a data file.

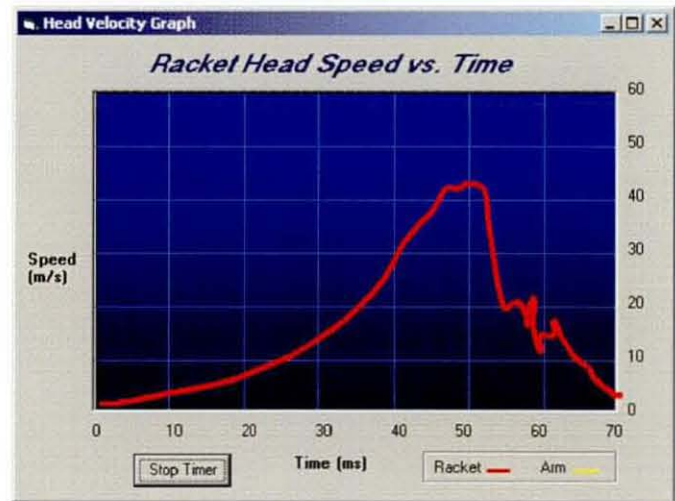


Figure C.7: The real-time racket head and drive arm speed graph.

In order to provide the user with real time speed profiles the graph data is sampled at a lower rate (100Hz) than that used for calculating the power

parameters. The speed for each axis is continuously measured via a software timer in the software, which has a limited sample rate as well as the USB connection to the Trio and is therefore intended as a visual aid rather than for calculating research parameters.

An additional function which considerably improves the usability and accuracy of the machine is the ability to manually activate the ball dropper, either to test the dropper accuracy or to manually feed a ball into the dropper chamber. Pressing the “Drop” button on the *Main* screen drops the ball in the chamber or if no ball is loaded, loads the next ball in the feeder mechanism into the chamber. The button sends a command to the Trio, which in turn switches an IO-port and activates PC timer. This mode can be used to calibrate the dropper more accurately without possible interference for the running machine.

*Datum*: The Datum routine (Appendix A), which respectively sets the datum for both axes, is initialised via the menu Tools→Set Datum and opens a control screen. As indicated in Figure C.8, there are two modes for the datum routine; Manual and Automatic, with the previously used mode being saved as the default for the next operation.

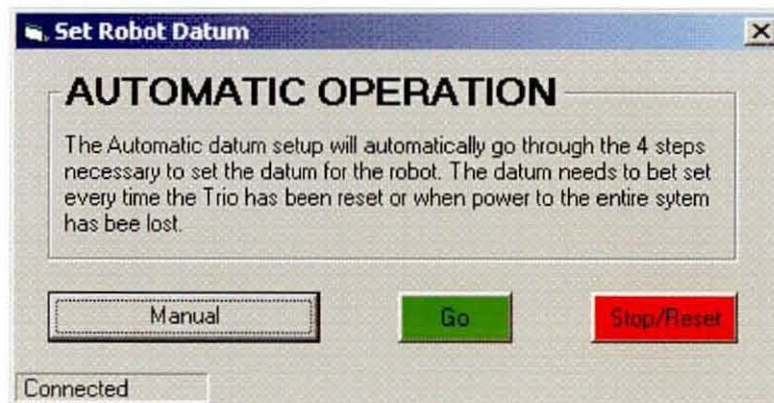


Figure C.8: The Datum interface screen.

The routine consists of four steps, which are performed continuously during the Automatic mode or step-by-step during the Manual mode, waiting for user interaction before continuing to the next step. In most cases the

Automatic mode will suffice but for some situations it might be preferable to use the Manual mode. One such example is when the arm is not in the optimum start position, in which case using the Manual mode in conjunction with the Jogging mode (described in the next paragraph) could be more efficient. At any stage during the operation the user can switch between Manual and Automatic mode. The routine is started by pressing the “Go” button and stopped via the “Stop/Reset” button. In the Manual mode the routine pauses at the end of each step and needs to be started again with the “Go” button.

*Jogging:* The Jogging routine is activated via the menu View→Jogging, which initialises the jogging loop in the Trio (Appendix A) and opens an interface screen (Figure C.9), which portrays the jogging state to the user. Jogging is controlled via the pendant, which is hardwired to the Trio inputs, while the display only provides a visual indication of the robot motion.



Figure C.9: The Jogging interface screen portraying the jogging motion.

### C.3. Stop procedures

There are five ways to terminate the test prematurely, depending on the level of urgency:

- Termination via the *Main* user interface is performed by pushing the red *Stop* button, which will complete the current impact and thereafter terminate the testing. The interface software sends a variable to the Trio



controller, which is detected at the end of the operation loop in the OPERATE program. The arm is brought to a halt, similar to the last impact in a standard sequence, catching the racket from the front and stopping it in the BDC position. The program is redirected to the operation selection loop, ready to restart at the sequence from the impact where it was terminated.

- If the Trio gets stuck in a program loop or code error loop, the “Reset Motion Error” bar on the *Main* screen sends direct control commands to the Trio, to slowly bring the drive arm to a halt without utilizing the Trio programs which might be malfunctioning.
- The red *C-Stop* button on the pendant is wired to a Trio input and detected by the main loop in the POWERUP program, resulting in an immediate controlled stop. The test is aborted immediately and the racket driven to a safe speed after which it is stopped from the front by the drive arm in a controlled way, without sacrificing any components.
- The E-stop buttons are the quickest but most severe and less preferred way to abort a test, only to be used in a real emergency, in which case it should be the first button to press. All E-stops are connected in series to a Trio input and also detected by the operation loop in the OPERATE program, which redirects it to a shutdown procedure, which brings the drive arm to a halt as fast as the motor is capable. In the process, the dowel crossbar might be sacrificed and excessive strain is put on the system, hence the use in emergency situations only.
- The final termination procedure perform when a motion error during operation. During a controller motion error the Trio sets an internal variable, which can be interrogated at any time. This is also performed by operation loop in the OPERATE program and redirected to the same shutdown procedure used when pressing an E-stop button.



C.4. Error detection and machine calibration

All motion errors are detected by the PC interface and will force the operator to exit the program and fix the problem before continuing testing.

In order to assist with general system error detection, the *Main* interface screen can be extended via the main menu (Tools→Utilities→Show) to show additional parameters and system variables measured during the test operation (Figure C.10). More information on all the different parameters is documented in the software’s online help (Help→Contents).

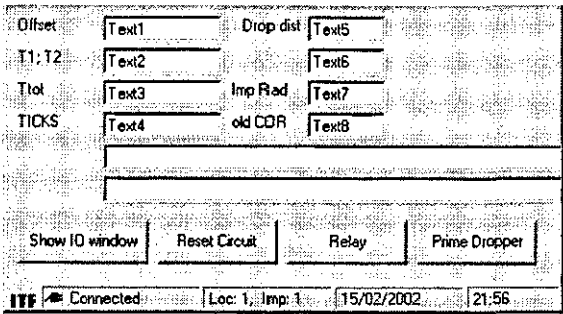


Figure C.10: The extended main screen menu for advanced system error detection.

C.5. Documentation

For additional information and help, a comprehensive Windows help file can be accessed via the in the *Main* user interface (Help→Contents). This contains help on standard operating procedures, machine assembly, error detection and details of components and their suppliers.

## References

- Arthur, C. (1992) Anyone for slower tennis. *New Scientist*, 2 May, p. 24-28
- Anderson, M.B. (1979) Comparison of Muscle Patterning in the Overarm Throw and Tennis Serve. *Research Quarterly*, 50(4), p. 541-553
- Bahamonde, R.E. (1989) Kinetic analysis of the serving arm during the performance of the tennis serve. *Journal of Biomechanics*, 22(10), p. 983
- Baker, J.A. & Putnam, C.A. (1979) Tennis Racquet and Ball Responses During Impact Under Clamped and Free-standing Conditions. *Research Quarterly*, 50(2), p. 164-170
- Bartlett, R.M., Piller, J. & Miller, S. (1994) A three-dimensional analysis of the tennis serves of National (British) and County standard male players. In: *Science and Racket Sports* (eds, Reilly, T. *et al.*), E & FN Spon, p. 98-102
- Beercheck, R.C. (1991) Sporting goods win with high-tech materials. *Machine Design*, June, p. 62-66
- Bernstein, A.D. (1977) Listening to the Coefficient of Restitution. *American Journal of Physics*, 45(1), p. 41-44
- Bowyer, S., Caine, M.P. and Mitchell, S.R. (2002) The effect of ball size upon play, player reception, muscle fatigue and soreness amongst recreational players. In: *The Engineering of Sport 4* (eds, Ujihashi, S. & Haake, S.J.), Oxford: Blackwell Science, p. 861-484
- Brannigan, M. & Adali, S. (1981) Mathematical modelling and simulation of a tennis racquet. *Medicine and Science in Sports and Exercise*, 1, p. 44-53
- Brody, H. (1979) Physics of the tennis racquet. *American Journal of Physics*, 47(6), p. 482-487
- Brody, H. (1981) Physics of the tennis racquet II: The "sweet spot". *American Journal of Physics*, 49(9), p. 816-819
- Brody, H. (1987) Tennis science for tennis players. Pennsylvania: University of Pennsylvania Press.
- Brody, H. (1989) Vibration Damping of Tennis Racquets. *International Journal of Sport Biomechanics*, 5, p. 451-456
- Brody, H. (1995) How Would a Physicist Design a Tennis Racket? *Physics Today*, 48, p. 26-31
- Brody, H. (1996a) A modest proposal to Improve Tennis. *TennisPro*, January - February: p. 8-9

## REFERENCES MACHINE CONTROL DETAIL

- Brody, H. (1996b) The Modern Tennis Racket. *The Engineering of Sport*, p. 79-82
- Brody, H. (1998) Improving your serve. In: *The Engineering of Sport* (ed, Haake, S.J.), Sheffield: UK, p. 311-316
- Brody, H. (1997) The physics of tennis III. The ball-racket interaction. *American Journal of Physics*, 65(10), p. 981-987
- Brody, H., Cross, R. & Lindsey, C. (2002) *The Physics and Technology of Tennis*, Solana Beach, California: RacquetTech Publishing.
- Broer, M. (1973) *The efficiency of human movement*, Philadelphia: W.B. Saunders.
- Buckley, J.P. and Kerwin, D.G. (1988) The role of the biceps and triceps brachii during tennis serving. *Ergonomics*, 31(11), p. 1621-1629
- Bunn, J.W. (1955) *Scientific principles of coaching*, New York: Prentice-Hall.
- Casolo, F. & Ruggieri, G. (1991) Dynamic analysis of the ball-racket impact in the game of tennis. *Meccanica*, 26, p. 67-73
- Charnwood (2003) *CODA mpx30 User Guide*. Charnwood, UK: Charnwood Dynamics Ltd.
- Clerici, G. (1976) *Tennis*. (translated from de Michele E.), London: Octopus Books Ltd., p. 1-59
- Coe, A.O. (2000) The balance Between Technology and Tradition in Tennis, In: *Tennis Science and Technology* (eds, Haake S.J. & Coe, A.O.), Oxford: Blackwell Science, p. 3-40
- Cochran, A. & Stobbs, J. (1999) *Search for the perfect swing*. 5<sup>th</sup> Edition, Chicago: Illinois: Triumph Books
- Cohen, D.B., Mont, M.A. Campbell, K.R., Vogelstein, B.N. & Loewy, J.W. (1994) Upper Extremity Physical Factors Affecting Tennis Serve Velocity. *American Journal of Sports Medicine*, 22(6), p. 746-750
- Cottey, R. (2002) The modelling of spin generation with particular emphasis on racket ball games. Loughborough University: PhD Thesis
- Cross, R.C. (2003a) Properties of tennis equipment: balls that bite, rackets that don't vibrate and strings don't make any difference. In: *Tennis Science and Technology 2* (ed, by S. Miller), London: ITF Licensing Ltd., p. 17-29
- Cross, R.C. (1997) The dead spot of a tennis racket. *American Journal of Physics*, 65(8): p. 754-764
- Cross, R.C. (1998a) The sweet spots of a tennis racquet, *Sports Engineering*, Blackwell Science, 1, p. 63-78
- Cross, R.C. (1998b) Optimizing the performance of a tennis racket. Unpublished report submitted to the Journal of Sports Sciences, p. 1-25
- Cross, R.C. (1999) Impact of a ball with a bat or racket, *American Journal of Physics*, 67, p. 692-702

## REFERENCES MACHINE CONTROL DETAIL

- Cross, R.C. (2000b) Dynamic properties of tennis strings. In: *Tennis Science and Technology 2* (ed, Miller, S.), London: ITF Licensing Ltd., p.119-126
- Cross, R.C. (2000c) Effects of friction between the ball and strings in tennis. *Sports Engineering*. Blackwell Science, 3: p. 85-97
- Cross, R.C. (2000d) Flexible beam analysis of the effects of string tension and frame stiffness on racket performance. *Sports Engineering*. Blackwell Science, 3: p.111-122
- Cross, R.C. (2001) Customising a tennis racket by adding weight. *Sports Engineering*, 4(1), p. 1-14
- Daish, C.B. (1972) *The Physics of Ball Games*, London: The English Universities Press Ltd., p. 180
- Domininghaus, H. (1992) *Die kunststoffe und ihre eigenschaften*, 4<sup>th</sup> Edition, Düsseldorf: VDI Verlag GmbH, p. 873
- Easterling, K.E. (1993) *Advanced materials for Sports Equipment*, London: Chapman & Hall, ISBN 0-412-40120-7
- Elliott, B.C., Blanksby, B.A., & Ellis, R. (1980) Vibration and rebound velocity characteristics of conventional and oversized tennis racquets. *Research Quarterly for Exercise and Sport*, 51(4), p. 608-615
- Elliott, B.C. (1982a) Tennis: The Influence of Grip Tightness on Reaction Impulse and Rebound Velocity. *Medicine and Science in Sports and Exercise*, 14(5), p. 348-352
- Elliott, B.C. (1982b) The influence of tennis racquet flexibility and string tension on rebound velocity following a dynamic impact. *Research Quarterly for Exercise and Sport*, 53(4), p. 277-281
- Elliott, B. (1983) Spin and the Power Serve in Tennis. *Journal of Human and Movement studies*, 9: p. 97-104
- Elliott, B. & Wood, G. (1983) The Biomechanics of the Foot-up and Foot-back Tennis Service Techniques. *The Australian Journal of Sport Sciences*, (2), p. 3-5
- Elliott, M.B. (1986) 3-Dimensional Cinematographic Analysis of the tennis serve. *International Journal of Sport Biomechanics*, 2(4), p. 260-271
- Elliott, B.C., Marshall, R.N. & Noffal, G.J. (1995) Contributions of Upper Limb Segment Rotations During the Power Serve in Tennis. *Journal. of Applied Biomechanics*, 11, p. 433-442
- Fisher, A. (1977) Super Racket - is this the Shape of Things to Come in Tennis? *Popular Science*, p. 44,46,150
- Goodwill S.R. & Haake S.J. (2000), Modelling the impact between a tennis ball and racket using rigid body dynamics, In: *Tennis Science and Technology* (eds, Haake S.J. & Coe, A.O.), Oxford: Blackwell Science, p. 49-56



## REFERENCES MACHINE CONTROL DETAIL

- Goodwill S.R. & Haake S.J. (2002a), Why were 'spaghetti string' rackets banned in the game of tennis? In: *Engineering in Sport 4* (ed, S Ujihashi & S.J. Haake) Oxford: Blackwell Science, p. 231-237
- Goodwill S.R. & Haake S.J. (2002b), A model of ball impacts on a tennis racket. In: *Engineering in Sport 4* (ed, S Ujihashi & S.J. Haake) Oxford: Blackwell Science, p. 215-222
- Goodwill S.R. & Haake S.J. (2003), Modelling of an impact between a tennis ball and racket, In: *Tennis Science and Technology 2* (ed, Miller, S.), London: ITF Licensing Ltd., p. 79-86
- Goodwill S.R. & Haake S.J. (2004), Effect of string tension on the impact between a tennis ball and racket, *Engineering of Sport 5* (eds, Hubbard, M., Mehta, R.D. & Pallis, J.M.) USA: Central Plains Book Mfg., p. 3-9
- Golf laboratories website (2004) *Hitting machine specifications*, Accessed: October 2004, [http://www.golf laboratories.com/robot\\_sales.html](http://www.golf laboratories.com/robot_sales.html)
- Grabiner, M., Groppel J. & Campbell, K. (1983) Resultant tennis ball velocity as a function of off-centre impact and grip firmness. *Medicine and Science in Sports and Exercise*, 15(6), p. 542-544
- Graff, K.F. (1975) *Wave motion in elastic solids*, Oxford University Press, Oxford, p. 649
- Groppel, J.L., Shin, I., Spotts, J. & Hill, B. (1987) The effects of string type and tension on impact in mid-sized and oversized tennis racquets. *International Journal of Sports Biomechanics*, 3, p. 40-46.
- Haake, S. J., Rose, P. & Kotze, J. (2000a) Reaction time testing and grand slam tie-break data. In: *Tennis Science and Technology* (eds, Haake S.J. & Coe, A.O.), Oxford: Blackwell Science, p. 269-275
- Haake, S.J., Chadwick, S.G., Dignall, R.J., Goodwill, S.R. & Rose, P. (2000b) Engineering Tennis - Slowing the game down. *Sports Engineering*, Oxford: Blackwell Science, 3(2), p. 131-143
- Haake, S.J., Chadwick, S.G., Dignall, R.J., Goodwill, S.R. & Rose, P. (2000b) Slowing the Game with Bigger Balls. *RacquetTech*, November, p. 12-20
- Hatze, H. (1976) Forces and duration of impact, and grip tightness during the tennis stroke. *Medicine and Science in Sports*, 8(2), p. 88-95
- Hatze, H. (1992a) The Effectiveness of Grip Bands in Reducing Racquet Vibration Transfer and Slipping. *Medicine and Science in Sports and Exercise*, 24(20), p. 226-230
- Hatze, H. (1992b) Objective Biomechanical Determination of Tennis Racquet Properties. *International Journal of Sport Biomechanics*, 8, p. 175-287
- Hatze, H. (1993) The Relationship Between the Coefficient of Restitution and Energy Losses in Tennis Racquets. *Journal of Applied Biomechanics*, 9, p. 124-142
- Haake, S.J. (2002) A brief history of tennis regulation. Keynote 1 in: *Engineering in Sport* (eds, Ujihashi, S. & Haake, S.J.), Oxford: Blackwell Science, p. 15-24
- Haines, R.C., Curtis, M. E., Mullaney, F. M. & Ramsden, G. (1983) The design, development and manufacture of a new and unique tennis racket. *Proc Instn Mech Engrs*, 197B, p. 71-79

## REFERENCES MACHINE CONTROL DETAIL

- Head, H. (1976) Tennis Racket, U.S. Patent 3999756, 28 December 1976.
- Head brochure (1995) *The new Pyramid Power technology – It will change your game*, Head Sport AG, Wuhrkopfweg 1, A-6921, Kennelbach, Austria.
- Head brochure (2001) *Smarter racket. Better game*, Head Sport AG, Wuhrkopfweg 1, A-6921, Kennelbach, Austria.
- Hennig, E.M. & Schnabel, G. (1998) A method to determine ball impact location and its movement across the strings of a tennis racket. In: *XVI International Symposium on Biomechanics in Sport* (Riehle, H.J. & Vieten, M.M.), Konstanz, Germany: UVK – Universitätsverlag Konstanz, p. 178-181
- ITF (2004) ITF Rules of Tennis 2004. In: Annual General Meeting of ITF. United Kingdom: Wilton, Wright & Son Limited.
- Jenkins, M. (2003) *Sports Equipment*. UK: Woodhead, ISBN 0-8493-1766-5
- Johnson, J. (1957) Tennis Serve of Advanced Women Players. *Research Quarterly*, 28(2), p. 123-131
- Johnson, M.L. (1976) High Velocity Serve. *Athletic Journal*, 56, p. 44-46
- Jorgenson, T.P. (1999) *The physics of Golf*. 2<sup>nd</sup> Edition, New York: Springer-Verlag.
- Kanemitsu, Y. (2003) The relationship between racket properties and player preference. In: *Tennis Science and Technology 2* (ed, Miller, S.), London: ITF Licensing Ltd., p. 41-48
- Kawazoe, Y. (1993) Coefficient of Restitution between a Ball and a Tennis Racket. *Theoretical & Applied Mechanics*, 42, p. 197-208
- Knudson, D.V. & White S.C. (1989) Hand Forces and Impact Effectiveness in the Tennis Forehand. *Journal of Human Movement Studies*, 17(1), p. 1-7
- Koenig, K., Dillard, J.S., Nance, D.K. & Shafer, D.B. (2004) The effects of support conditions on baseball bat performance testing. In: *Engineering of Sport 5* (eds, Hubbard, M., Mehta, R.D. & Pallis, J.M.) USA: Central Plains Book Mfg., p. 139-144
- Kotze, J., Mitchell, S.R. & Rothberg, S.J. (2000) The role of the racket in high-speed tennis serves. *Sports Engineering*, 3, p. 67-84
- Kotze J., Lammer, H. Cottey, R. and Zirngibl, W. (2003) The effect of active piezo fibre rackets on tennis elbow. In: *Tennis Science and Technology 2* (ed, Miller, S.), London: ITF Licensing Ltd., p. 55-60
- Kotze, J. and Mitchell, S.R., (2002) A tennis serve impact simulation machine. In: *The Engineering of Sport 4* (eds, S. Ujihashi and S.J. Haake), Oxford: Blackwell Science, p. 477-484
- Kramer, S. (1999) Simplifying the Science of Golf (Playing with fire). *Golf Magazine*, March, 41 (3). p. 108, 111, 113, 115
- Kuebler, S. (2000) *Book of Tennis racket from the beginning in the 16<sup>th</sup> century until about 1990*. Singen, Germany: Kuebler GmbH. ISBN 3-9802903-9-5

## REFERENCES MACHINE CONTROL DETAIL

- Lammer, H. & Kotze, J. (2003) Materials and Tennis Rackets. In: *Materials in Sports Equipment* (ed. Jenkins, M.), UK: Woodhead, ISBN 0-8493-1766-5, p. 222-248
- Leigh, C.L. & Lu, W. (1992) Dynamics of the Interactions Between Ball, Strings, and Racquet in Tennis. *International Journal of Sport Biomechanics*, 8, p. 181-206
- Lindsey, C. (1997), Racquet selection charts: Power and Maneuverability, *RacquetTECH*, June, p. 5, 8
- Lindsey, C. (1997) Hole-y Wars, *RacquetTECH*, September, p.10, 19, 20
- Lindsey, C. (2000a) Spring 2000 Racket Intros. *RacquetTECH*, January, p. 6
- Lindsey, C. (2000b) Reinventing the Wheel: Wilson's New Rollers 2.6 Overdrive. *RacquetTECH*, July
- Lindsey, C. (2000c) 'Head's Intelligence Technology - The Shocking Details', *RacquetTECH*, November, p. 6, 8, 9, 27
- Lindsey, C. (2001) 'Völkl's Catapult Reinvents the Stringbed', In *RacquetTECH*, August, p. 20-23
- Liu, Y. (1983) Mechanical analysis of racquet and ball during impact. *Medicine and Science in Sports and Exercise*, 15(5) p. 388-392
- Lo, K.C, Wang, L.H, Lin, H.T & Su, F.C. (2003) Momentum transfer of upper extremity segments during the tennis flat serve. *Tennis Science and Technology 2* (ed, Miller, S.), London: ITF Licensing Ltd, p. 185-191
- May, M. (2000), Changing the Game - The Athletic Arms Race, in *Scientific American*, Quarterly. p. 74-79
- Meriam, J.L. and Kraige, L.G. (1998) Engineering Mechanics: Dynamics. 4<sup>th</sup> Edition. New York: John Wiley & Sons, Inc., p. 725
- Ming, A., Kawano, T., Xu, B. & Kajitani, M. (1998) A golf swing robot to simulate human skill-the introduction of learning control. In *The Engineering of Sport* (ed, Haake, S.J.), Oxford: Blackwell Science, p. 283-290
- Ming, A., Teshima, T., Takayama, T., Kajitani, M. and Shimojo, M. (2002) Motion control of a new golf swing robot for hitting a ball. In: *The Engineering of Sport 4* (eds, Ujihashi, S & Haake, S.J), Oxford: Blackwell Science, p. 450-455
- Miller, S. (2003) Speed is of the essence. In: *Tennis Science and Technology 2* (ed, Miller, S.), London: ITF Licensing Ltd, p. 3-12
- Missavage, R., Baker, J. & Putnam, C. (1984) Theoretical modelling of grip firmness during ball-racquet impact. *Research Quarterly for Exercise and Sport*, 55(3), p. 254-260
- Mitchell, S.R., Jones, R., and King, M. (2000a) Head speed vs. racket inertia in the tennis serve. *Sports Engineering*, 3(2), p. 99-110

## REFERENCES MACHINE CONTROL DETAIL

- Mitchell, S.R., Jones, R., and Kotze, J. (2000b) The influence of racket moment of inertia during the tennis serve 3-Dimensional analysis. In: *Tennis Science and Technology* (eds, Haake S.J. & Coe, A.O.), Oxford: Blackwell Science, p. 57-65
- Miura, K. and Naruo, T. (1998) Accelerating and decelerating phases of the wrist motion of the golf swing, In: *The Engineering of Sport* (edited by S. Haake), Oxford: Blackwell Science, p. 455-463
- Miyamae website (2004) *ShotroboIV: One step closer to you swing*, Accessed: October 2004, <http://www.miyamae.co.jp/english/golf/business/robo4-e.html>
- Miyamoto, H. & Kawato, M. (1998) A tennis serve and upswing learning robot based on bi-directional theory. *Neural Networks*, 11, p. 1331-1344
- Miyashita, T.S., Tsunoda, T., Sakurai, S., Nishizono, H. & Mizuno, T. (1980) Muscular activities in the tennis serve and overhand throwing. *Scandinavian Journal of Sports Science*, 2(2) p. 52-58
- Nakagawa, N., Sekiguchi, Y., Okada, N. & Monden, H. (2002) Influence of tennis-ball slide on ball-spin during impact, In: *The Engineering of Sport 4* (eds, S. Ujihashi and S.J. Haake), Oxford: Blackwell Science, p. 46-51
- Pallis, J.M. Yandell, J., Pandya, S., Mehta, R., Roetert, P. & Iskander, N. (1999) NASA Tennis Research Project, Copyright © Cislunar Aerospace, ucdavis website, Accessed March 2000, <http://wings.ucdavis.edu/Tennis/Project>
- Papadopoulos, C., Emmanouilidou, M. & Prassas, S. (2000) Kinematic analysis of the service stroke in tennis. In: *Tennis Science and Technology* (eds, Haake S.J. & Coe, A.O.), Oxford: Blackwell Science, p. 383-387
- Plagenhoef, S. (1970) *Fundamentals of Tennis*. Englewood Cliffs, New Jersey: Prentice-Hall.
- Plagenhoef, S. (1971) *Patterns of Human Motion: A Cinematographical Analysis*. Englewood Cliffs, New Jersey: Prentice-Hall.
- Polich, C. (1996) Tennis Rackets. In: *Sport and Fitness Equipment Design* (eds, Kreighbaum, E. F and Smith, M.A.) Champaign, IL: Human Kinetics, p. 85-95
- R&A (2004) *The rules of golf and the rules of amateur status 2004-2007*, © The Royal and Ancient Golf Club of St Andrews and the United States Golf Association, <http://www.randa.org>
- Racquet Research (2000) *June 2000 rankings*, Accessed June 2000, <http://www.racquetresearch.com>
- Robertson, M. (1974) *The Encyclopedia of Tennis*. New York: The Viking Press, Inc., p. 14-29
- Shigley, J.E. & Mischke, C.R. (1989) *Mechanical Engineering Design*. New York: McGraw & Hill
- Springings, E., Marshall, R., Elliott, B. & Jennings, L. (1994) A three-dimensional kinematic method for determining the effectiveness of arm segment rotations in producing racquet-head speed. *Journal of Biomechanics*, 27(3) p. 245-254



## REFERENCES MACHINE CONTROL DETAIL

- Suzuki, S. & Inooka, H. (1997) Golf Swing Robot Emulating a Human motion. *IEEE International Workshop on Robot and Human Communication*, IEEE Publications, p.28-33
- Suzuki, S. & Inooka, H. (1998) A new golf-swing robot model utilizing shaft elasticity. *Journal of Sound and Vibration*, Academic Press, 217(1), p. 17-31
- Suzuki, S. & Inooka, H. (1999) A new golf-swing robot model emulating golfer's skill. *Sport Engineering*, (ed, Haake, S.J.) Oxford: Blackwell Science, 2, p. 13-22
- Suzuki, S. & Ozaki, Y. (2003) Three dimensional analysis of a new golf-swing robot emulating skillful golfers. In: *The Engineering of Sport 4* (eds, S. Ujihashi and S.J. Haake), Oxford: Blackwell Science, p. 450-455
- Stanbridge, K., Mitchell, S.R. & Jones, R. (2003) The effect of tennis racket properties on forehand stroke performance amongst children. In: *Tennis Science and Technology 2* (ed, Miller, S.), London: ITF Licensing Ltd, p. 31-40
- Stanbridge, K.J., Mitchell, S.R. & Jones, R. (2004) Design and development of sports equipment for children. In: *Engineering of Sport 5* (eds, Hubbard, M., Mehta, R.D. & Pallis, J.M.) USA: Central Plains Book Mfg., p. 291-297
- Stronge, W.J. (2000) *Impact mechanics*, Cambridge, UK: Cambridge Press
- Thornhill, P.M., Baker J.S., & Cooper, S.M. (1993), Interaction between tennis string type and tension and the subsequent effect upon ball rebound velocity. *Journal of Human Movement Studies*, 24, p. 157-167
- Tilmanis, G.A. (1975) *Advanced tennis*. Philadelphia: Lea and Febiger
- USGA website (2004) *Rules of Golf*, Accessed september 2004, <http://www.usga.org/playing/rules/books/rules/>
- Van der Meer, D. & Kibler, W.B. (2000) The biomedical fundamentals, the commonalities, and the preference of tennis strokes. In: *Tennis Science and Technology* (eds, Haake S.J. & Coe, A.O.), Oxford: Blackwell Science, p. 355-360
- Van Gheluwe, B. & Hebbelinck, M. (1985) The Kinematics of the Service Movement in Tennis: A Three-Dimensional Cinematographical Approach. In: *Biomechanics IX-B* (eds, Winter, D.A. et al.) Champaign, IL: Human Kinetics, p. 521-526
- Van Gheluwe, B., De Ruyscher, I. & Craenhals, J. (1987) Pronation and Endorotation of the Racket Arm in a Tennis Serve. In: *Biomechanics X-B*, (ed, Jonasson, B.), International series on Biomechanics Vol.6B, Champaign, IL: Human Kinetics, p. 521-526.
- Völkl website (1999), *Hot Spot Series - The secret is in the racquet head*, Copyright Volkl Sport America, Accessed August 1999, <http://www.volkl.com/tennis/hot.spot.line.html>.
- Watanabe, T.I.Y. & Miyashita M. (1979) Tennis: The Effects of Grip Firmness on Ball Velocity after Impact. *Medicine and Science in Sports and Exercise*, 11(4), p. 359-361
- Wang, L.H., Wu, C.C., Su, F.C., Lo, K.C. & Wu, H.W. (2000) The biomedical fundamentals, the commonalities, and the preference of tennis strokes. In: *Tennis Science and Technology* (eds, Haake S.J. & Coe, A.O.), Oxford: Blackwell Science, p. 395-400

## REFERENCES MACHINE CONTROL DETAIL

Wilson brochure (1992), *Tennis 1992*, Wilson Sporting Good Co Ltd, the Harlequin Centre, Southall Lane, Southall UB2 5LY, UK.

Wilson, J.F. and Davis J.S. (1995) Tennis Racket Shock Mitigation Experiments. *Journal of Biomechanical Engineering*, 117, p. 479-484

Wilson website (1999), *Wilson: Hyper Carbon Technology*, Accessed August 1999, <http://www.wilsonsports.com/tennis/hyper-tech.html>

Yonex website (1999), *Yonex: tennis*, Torrance, California, Accessed August 1999, [http://www.yonex.com/new-yonex/tennis/yonex\\_tennis\\_home.htm](http://www.yonex.com/new-yonex/tennis/yonex_tennis_home.htm)

